XXIII INTERNATIONAL WORKSHOP ON OPTICAL WAVE AND WAVEGUIDE THEORY AND NUMERICAL MODELLING

O

W

T

N

M

2

0

1

5

CITY UNIVERSITY LONDON

17 – 18 APRIL 2015

ABSTRACT BOOK

XXIII INTERNATIONAL WORKSHOP ON OPTICAL WAVE AND WAVEGUIDE THEORY AND NUMERICAL MODELLING

ORGANISERS

TECHNICAL COMMITTEE

- Trevor Benson, University of Nottingham, UK
- Jiri Ctyroky, Institute of Electronics and Photonics, Czech Republic
- Manfred Hammer, University of Paderborn, Germany
- Andrei V. Lavrinenko, COM-DTU, Lyngby Kgs., Denmark
- John Love, Australian National University, Canberra, Australia
- Andrea Melloni, DEI-Politecnico di Milano, Italy
- Olivier Parriaux, Lyon University at Saint Etienne, France
- Reinhold Pregla, FernUniversität Hagen, Germany
- Ivan Richter, Czech Technical University, Prague, Czech Republic
- Christoph Wächter, Fraunhofer IOF, Jena, Germany
- Anne-Laure Fehrembach, Institut Fresnel, Aix-Marseille University
- Arti Agrawal, City University London, UK

LOCAL ORGANISING COMMITTEE

- Arti Agrawal, City University London
- B.M.A. Rahman, City University London
- Tong Sun, City University London
- Gregory Wurtz, King's College London
- Roy Taylor, Imperial College London
- Annibal Fernandez, University College London
- Richard De La Rue, University of Glasgow
- Trevor Benson, University of Nottingham
- Jean Sebastien Bouillard, University of Hull
- Alexey Krasavin, King's College London
- Yuri Kivshar, Australian National University

WEBSITE

www.city.ac.uk/owtnm-2015

OWTMN 2015

XXIII INTERNATIONAL WORKSHOP ON OPTICAL WAVE AND WAVEGUIDE THEORY AND NUMERICAL MODELLING

16th-18th April

London, United Kingdom

City University London

Preface

The 23rd edition of the International Workshop on Optical Wave & Waveguide Theory and Numerical Modelling (OWTNM) is organized at the City University, London, United Kingdom, from April 16th to April 18th 2015. This annual workshop has been successfully organized since 1992 as a forum for enthusiastic scientists in the field of optics to exchange ideas and discuss problems related to optical theory, computational modelling, and novel device concepts. Since 1992 the content of the workshop has evolved to incorporate the latest topical subjects relevant to our community, including metamaterials and plasmonics.

The OWTNM 2015 encompasses 100 scientific contributions, including 10 keynotes and invited talks, distributed over 8 oral and 2 poster sessions. The organization benefits from the financial support of 11 companies and institutions advertised throughout the workshop on displays, booths, and in this book of abstracts. Adhering to a tradition of the OWTNM series, a special journal issue of Optical and Quantum Electronics will be organized on the occasion of the workshop.

The organizers are looking forward for that new edition to be as successful as its predecessors in a setting that we hope will be stimulating for both experienced and younger researchers.

London, March 2015
The local organizing committee

We thank our partners:

- City University London
  www.city.ac.uk
- City Graduate School, London
  www.city.ac.uk/citygraduateschool
- Princeton Instruments
  www.princetoninstruments.com
- CST Microwave
  www.cst.com
- Lumerical
  www.lumerical.com
- Institute of Physics Computational Physics Group for funding
  www.iop.org/activity/groups/subject/comp/
- Institute of Physics Optical Group for funding
  www.iop.org/activity/groups/subject/opt/
- Institute of Physics Quantum Electronics and Photonics Group for funding
  www.iop.org/activity/groups/subject/qep/
- Light Tec
  www.lighttec.fr/rsoft.html
- Fraunhofer UK
  www.fraunhofer.co.uk
- Comsol
  www.comsol.com
- Optical Society of America
  www.osa.org
- Artech House
  www.artechhouse.co.uk

Imaging and Spectroscopy Reimagined!

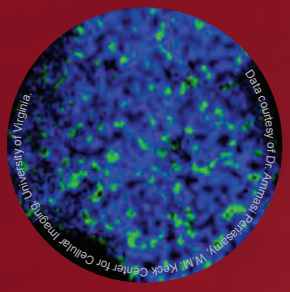

Microspectroscopy • Biomedical Imaging
Plasmonics • LIBS • Raman Hyperspectral Imaging
Carbon Nanotube Research • Singlet Oxygen
Detection Combustion • FLIM
• Small Animal Imaging
• Quantum Imaging

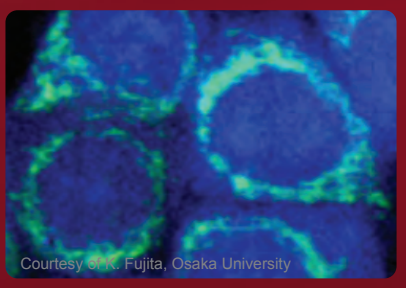

Princeton Instruments

Learn how our innovative products can facilitate your research.
Visit **www.princetoninstruments.com**
or call **+1 609-587-9797**

XXIII International Workshop on

Optical Wave & waveguide Theory and Numerical Modelling

City University London, April 17-18, 2015

Thursday, April 16, 2014

Activity	Time start	Time end	Activity	Details
Women in Optics	11.30	15.00	Workshop and lunch	IoP Optical Group, IEEE Photonics Society **Venue**: DLG 03/08, Rhind Building, St. John Street
Student tutorials	15.00	18.00	Simulation workshop	Conducted by Lumerical **Venue**: D518 Rhind Building, St. John Street
Registration	18.00	20.00	Spot Registration	**Venue**: DLG 03/08 Rhind Building, St. John Street
Welcome reception	18.00	20.00	Networking	Wine reception **Venue**: DLG 03/08 Rhind Building, St. John Street

Friday 17 April 2015

Activity	Time start	Time end	Session name and Venue
Registration	08.30		Centenary Building Entrance, Spencer Street
Welcome	09.00	09.15	Birley Lecture theatre, Centenary Bldg
Session1	09.15	11.05	**Metamaterials** (Birley Lecture theatre, Centenary Bldg)
Coffee break	11.05	11.30	DLG 03/08, Rhind Building
Session2	11.30	13.10	**Plasmonics** (Birley Lecture theatre, Centenary Bldg)
Lunch & posters1	13.10	14.30	**Posters 1** DLG 03/08, Rhind Building
Session3	14.30	16.35	**Modelling of Active and Passive Waveguide Devices** (Birley Lecture theatre, Centenary Bldg)
Coffee break	16.35	16.55	DLG 03/08, Rhind Building
Session4	16.55	18.05	**Optical Sensors** (Birley Lecture theatre, Centenary Bldg)
Gala Dinner	**19.00**	**22.00**	**HMS President**

Saturday, April 18, 2014

Activity	Time start	Time end	Session name and Venue
Registration	8.45		Centernary Building Entrance, Spencer Street
Session5	9.15	10.25	**Modelling of Resonators and Photonic Devices** (Birley Lecture theatre, Centenary Bldg)
Coffee break	10.25	10.50	DLG 03/08, Rhind Building
Session6	10.50	12.30	**Photonic Crystals and Nanostructures** (Birley Lecture theatre, Centenary Bldg)
Lunch & posters2	12.30	14.00	**Posters 2** DLG 03/08, Rhind Building
Session7	14.00	15.25	**Modelling methods for Photonics** (Birley Lecture theatre, Centenary Bldg)
Coffee break	15.25	15.50	DLG 03/08, Rhind Building
Session8	15.50	16.45	**Multiphysics effects in active and functional devices**
Closing remarks	**16.45**	**17.00**	**Student paper prizes; vote of thanks**

CST STUDIO SUITE 2015

From Components to Systems. Simulate, Optimize, Synthesize.

From the first steps to the finishing touches, CST STUDIO SUITE® is there for you in your design process. Its tools allow engineers to develop and simulate devices large and small across the frequency spectrum. The powerful solvers in CST STUDIO SUITE 2015 are supplemented by a range of new synthesis and optimization tools, which are integrated directly into the simulation workflow. These can suggest potential starting points for component design, allow these components to be combined into systems, and finally analyze and fine-tune the complete systems.
Even the most complex systems are built up from simple elements. Integrate synthesis into your design process and develop your ideas.

Choose CST STUDIO SUITE – Complete Technology for EM Simulation.

XXIII International Workshop on

Optical Wave & waveguide Theory and Numerical Modelling

City University London, April 17-18, 2015

Thursday, April 16, 2014

Activity	Time start	Time end	Activity	Details
Women in Optics workshop	11.30am	3pm	Workshop and lunch	Sponsors: IoP Optical Group, IEEE Photonics Society
Student tutorials	15.00	18.00	Simulation workshop	Conducted by Lumerical
Registration	18.00	20.00	Registration	http://www.city.ac.uk/owtnm-2015/registration
Welcome reception	18.00	20.00	Networking	Wine reception

Friday 17 April 2015

Activity	Time start	Time end	Activity	Details
Registration	08.30			
Welcome	09.00	09.15		
Session 1	**09.15**	**11.05**	**Talks**	**Metamaterials**
Page 19	09.15	09.55	Keynote 1 40 mins	*All-dielectric nanophotonics: Magnetic response, Fano resonances, functional metasurfaces, and nonlinear effects.* Professor Yuri Kivshar, Australian National University
	09.55	10.20	Invited 25 mins	*Chiral and bianisotropic metamaterials for Thz polarization control* Professor Maria Kafesaki, FORTH-IESL
	10.20	10.35	Contrib 1 15 mins	*Optical Grating or Lattice Resonances on Silver Strip and Wire Gratings* Alexander I. Nosich, Volodymyr Byelobrov, Tatiana L. Zinenko, Denys M. Natarov and Olga V. Shapoval
	10.35	10.50	Contrib 2 15 mins	*Modelling coherent nonlinearities in nanostructured plasmonic metamaterials* Giuseppe Marino, Paulina Segovia, Alexey Krasavin, Pavel Ginzburg, Nicolas Olivier, Gregory A. Wurtz and Anatoly V. Zayats
	10.50	11.05	Contib 3 15 mins	*Phase Matching and Frequency Mixing of Contra-propagating Electromagnetic Pulses in the Waveguide Tampered by Carbon Nanoforest.* Alexander Popov, Sergey Myslivets, Alexander Kildishev and Alexander Korotkevich
Coffee break	11.05	11.30		

Session 2	11.30	13.10	Talks	Plasmonics
Page 25	11.30	11.55	Invited 25 mins	*Active and reconfigurable CMOS-compatible functional complex plasmonic metasurfaces* Professor Harald Giessen, University of Stuttgart
	11.55	12.10	Contrib 1	*Comparing plasmonic waveguides: a comprehensive figure of merit* Alexey Krasavin and Anatoly Zayats
	12.10	12.25	Contrib 2 15 mins	*Modelling Optical Bistability with Hybrid Silicon-Plasmonic Resonators.* Odysseas Tsilipakos, Thomas Christopoulos, Georgios Sinatkas and Emmanouil Kriezis
	12.25	12.40	Contrib 3 15 mins	*Graphene Plasmonics for Efficient Energy Transfer* Vasilios D. Karanikolas, Cristian A. Marocico and A. Louise Bradley
	12.40	12.55	Contrib 4 15 mins	*Vertical mode expansion method for transmission of light through an arbitrary aperture in a metallic film* Hualiang Shi and Ya Yan Lu
	12.55	13.10	Contrib 5 15 mins	*Transparent conductive oxides as near-IR plasmonic materials: the case of metal-doped ZnO derivatives*. Alessandra Catellani, Alice Ruini and Arrigo Calzolari
Lunch & posters1	13.10	14.30	Posters 1	
Session 3	**14.30**	**16.35**	**Talks**	**Modelling of Active and Passive Waveguide Devices**
Page 33	14.30	15.10	Keynote 2 40 mins	*The Extraordinary World of Optical Waveguides* Professor Sir David Payne, University of Southampton
	15.10	15.35	Invited 25 mins	*The essential elements of low loss in hollow optical fibres.* Professor Jonathan Knight, University of Bath
	15.35	15.50	Contrib 1 15 mins	*Planar waves that climb dielectric steps* Manfred Hammer, Andre Hildebrandt and Jens Förstner
	15.50	16.05	Contrib 2 15 mins	*Inverse scattering designs of mode-selective waveguide couplers* Alexander May and Michalis Zervas
	16.05	16.20	Contrib 3 15 mins	*Beneficial Impact of Multi-order Dispersion Engineering in Designing a Flat-top Wide-band Supercontinuum Source* Sudip Chatterjee, Saba Khan and Partha Roy Chaudhuri
	16.20	16.35	Contrib 4 15 mins	*Modeling of single-mode regime in active large mode area photonic crystal fibers under severe heat load* Enrico Coscelli, Federica Poli, Lorenzo Rosa, Annamaria Cucinotta and Stefano Selleri
Coffee break	16.35	16.55		

Session 4	16.55	18.05	Talks	Optical Sensors
Page 41	16.55	17.20	Invited 25 mins	*Optical Fibre Sensor Systems for Safety and Security applications in industry.* Professor K.T.V. Grattan, City University London
	17.20	17.35	Contrib 1 15 mins	*Multichannel Photonic Crystal Fiber Surface Plasmon Resonance Based Sensor* Shaimaa Azzam, Mohamed Hameed and Salah Obayya
	17.35	17.50	Contrib 2 15 mins	*Highly sensitive D shaped PCF sensor based on SPR for near IR* Jitendra Dash and Rajan Jha
	17.50	18.05	Contrib 3 15 mins	*Numerical Analysis of a Hollow-Core Coaxial Fiber Biosensor* Tamara Monti and Gabriele Gradoni
Gala Dinner	**19.00**	**22.00**		**HMS President**

Saturday, April 18, 2014

Activity	Time start	Time end	Activity	Details
Registration	08.45			
Session 5	**09.15**	**10.25**	**Talks**	**Modelling of Resonators and Photonic Devices**
Page 47	09.15	09.40	Invited 25mins	*Modal approach for absorptive and dispersive resonators.* Professor Philippe Lalanne, Institut d'Optique d'Aquitaine
	09.40	09.55	Contrib 1 15 mins	*Extraordinary Angular Tolerance of Cavity Resonator Integrated Grating Filters* Nadege Rassem, Anne-Laure Fehrembach and Evgueni Popov
	09.55	10.10	Contrib 2 15 mins	Threshold Preservation of PT-Resonant Structures in Realistic-Dispersive Medium Sendy Phang, Ana Vukovic, Stephen Creagh, Phillip Sewell, Trevor Benson and Gabriele Gradoni
	10.10	10.25	Contrib 3 15 mins	*Generation of Higher Dimensional Modal Entanglement* Divya Bharadwaj, Krishna Thyagarajan, Michal Karpinski and Konrad Banaszek
Coffee break	10.25	10.50		

Session 6	10.50	12.30	Talks	Photonic Crystals and

				Nanostructures
Page 53	10.50	11.15	Invited 25 mins	*Photonic control of thermal radiation leading to radiative cooling.* Professor Shanhui Fan, Stanford University
	11.15	11.30	Contrib 1 15 mins	*Simulation of high-speed nanophotonic modulators based on electrical and two-photon absorption injection* Simeon Kaunga-Nyirenda, Hasula Dias, Steve Bull, Jun Lim, Gaetano Bellanca and Eric Larkins
	11.30	11.45	Contrib 2 15 mins	*Interrogating Nanoparticles with Focused Doughnut Pulses* Tim Raybould, Vassili A. Fedotov, Nikitas Papasimakis, Ian Youngs and Nikolay Zheludev
	11.45	12.00	Contrib 3 15 mins	*Rigorous retrieval of linear and nonlinear parameters in graphene waveguides* Alexandros Pitilakis, Dimitrios Chatzidimitriou and Emmanouil Kriezis
	12.00	12.15	Contrib 4 15 mins	*Rod-type Photonic Crystals For Colloidal Quantum Dot Light Coupling* Yasir Noori
	12.15	12.30	Contrib 5 15 mins	*Photonic and Plasmonic Quasicrystals* Faris Mohammed and Alex Quandt
Lunch & posters2	12.30	14.00	Posters 2	
Session 7	**14.00**	**15.25**	**Talks**	**Modelling methods for Photonics**
Page 61	14.00	14.25	Invited 25 mins	*Simulation of photonic nanostructures – mixing nonlinear material theories with Maxwell solvers.* Professor Jens Förstner, University of Paderborn
	14.25	14.40	Contrib 1 15 mins	*Modelling the coupling of electromagnetic waves to cylindrical waveguides with the Method of Lines* Stefan Helfert
	14.40	14.55	Contrib 2 15 mins	*Computing 3-D Diffraction by Finite Difference Split-Step Nonparaxial Method* Debjani Bhattacharya and Anurag Sharma
	14.55	15.10	Contrib 3 15 mins	*Modified Finite Element Frequency Domain Using Gradient Smoothing Technique* Khaled Atia, Ahmed Heikal and Salah Obayya
	15.10	15.25	Contrib 4 15 mins	*Reduced Basis Method for Fast Online Solution of Scattering Problems* Sven Burger, Martin Hammerschmidt, Sven Herrmann, Jan Pomplun and Frank Schmidt
Coffee break	15.25	15.50		
Session 8	**15.50**	**17.00**	**Talks**	**Multiphysics effects in active and functional devices**

Page 67	15.50	16.15	Invited 25 mins	*Fundamental aspects of linear slow light systems.* Professor Luc Thevenaz, EPFL Switzerland
	16.15	16.30	Contrib 1 15 mins	*Laser gain compact model for photonic integrated circuit (PIC) simulation* Vighen Pacradouni, Jackson Klein, Valentina Donzella and James Pond
	16.30	16.45	Contrib 2 15 mins	*Diffraction properties of a tailored parity-time (PT) symmetric grating* Nicolas Rivolta and Bjorn Maes
Closing remarks	16.45	17.00		Student paper prizes; vote of thanks.

In order	List of posters	Session: Day 1
1	98 Title: Equiangular Spiral Micro-Structured Waveguides in Lithium Niobate Authors: Huseyin Karakuzu, Mykhaylo Dubov, Sonia Boscolo, Yousaf O. Azabi and Arti Agrawal	Day 1
2	58 Title: Mid-infrared supercontinuum generation using dispersion-engineered Ge11.5As24Se64.5 chalcogenide rib-waveguide Authors: Mohammad Karim and Azizur Rahman	Day 1
3	55 Title: Effect of SPR on the attenuation coefficient of an Ormocomp nanowire Authors: Charusluk Viphavakit, Sakoolkan Boonruang, Christos Themistos, Michael Komodromos, Waleed S. Mohammed and B.M. Azizur Rahman	Day 1
4	99 Title: Counter-propagating Airy beams interactions in nonlinear media Authors: Delphine Wolfersberger, Noemi Wiersma, Nicolas Marsal and Marc Sciamanna	Day 1
5	89 Title: Fast Finite Element Time Domain with Perforated Mesh Authors: S M Raiyan Kabir and B. M. A. Rahman	Day 1
6	17 Title: Analysis of a Plasmonic Pole-Absorber Illuminated from a Specific Direction Authors: Junji Yamauchi, Shintaro Ohki and Hisamatsu Nakano	Day 1
7	38 Title: Gain-Equalization of 3-mode groups using dual-core EDFA Authors: Ankita Gaur and Vipul Rastogi	Day 1
8	56 Title: Mode mixing in anisotropic metamaterial waveguides Authors: Andres Barbosa, Greg Wurtz and Anatoly Zayats	Day 1
9	36 Title: Mimicking photon propagation through 2-D array by a 1-D array Authors: Krishna Thyagarajan and Surajit Paul	Day 1
10	37 Title: Graphene based Surface Plasmon Resonance Gas sensor for Terahertz Authors: Rajan Jha and Amrita Purkayastha	Day 1
11	9 Title: Multi-path propagation in waveguide media: Fading emulation assuming large RC network models with pre-equalization using fractional order models Authors: Sillas Hadjiloucas, Hashem Alyami and Victor Becerra	Day 1
12	50 Title: Full-vector modeling of thermally-driven gain competition in Yb-doped large-mode-area photonic-crystal fiber Authors: Lorenzo Rosa, Enrico Coscelli, Federica Poli, Annamaria	Day 1

	Cucinotta and Stefano Selleri	
13	18 Title: Counter-circular-polarization Characteristics of a Quarter-wave Plate Using a Triangular Hole Array in a Metallic Plate Authors: Junji Yamauchi, Yuhei Takagi and Hisamatsu Nakano	Day 1
14	15 Title: A Polarization Converter Using a Curvilinearly Tapered Waveguide Authors: Yuta Nito, Shunya Fujimura, Junji Yamauchi and Hisamatsu Nakano	Day 1
15	93 Title: Power Budget Analysis for Waveguide-Enhanced Raman Spectroscopy Authors: Zilong Wang, Michalis Zervas, Philip Bartlett and James Wilkinson	Day 1
16	65 Title: Characteristics of Twist Induced Phase Deviation through a Distinct Dual-mode-fiber in a Sagnac Loop Authors: Saba Khan, Sudip Chatterjee and Partha Roy Chaudhuri	Day 1
17	68 Title: Detection of Low Magnetic Field using Fiber Optic Cantilever Technique Authors: Somarpita Pradhan and Partha Roy Chaudhuri	Day 1
18	16 Title: Wavelength Characteristics of a Waveguide Polarization Converter with Sidewall-Roughness Authors: Junji Yamauchi, Takumi Takada and Hisamatsu Nakano	Day 1
19	79 Title: Purcell effect of asymmetric dipole source distributions in nanowire resonators Authors: Konstantin Filonenko, Jost Adam, Lars Duggen and Morten Willatzen	Day 1
20	100 Title: Optimization of textured Si solar cell with array of hut-like micro pillars Authors: Francisco Jose Cabrera España, Arti Agrawal and B. M. A. Rahman	Day 1
21	60 Title: Accurate and efficient arrayed waveguide grating simulations for InP membranes Authors: Bernardo Gargallo, Yuqing Jiao, Pascual Muñoz, Jos van der Tol and Xaveer Leijtens	Day 1
22	77 Title: Optimization of an Integrated Mach-Zehnder interferometer using the Fisher Information Authors: Nevena Raicevic, Aleksandra Maluckov and Jovana Petrovic	Day 1
23	39 Title: Fiber based Plasmonic Sensor using Graphene oxide encapsulated Au-nanoparticles Authors: Jeeban Nayak and Rajan Jha	Day 1

24	14 Title: Travelling Wave Model Approach for Longitudinal Multimode Dynamics in Multi-Section Lasers Authors: Antonio Perez-Serrano, Mariafernanda Vilera, Julien Javaloyes, Jose Manuel G. Tijero, Ignacio Esquivias and Salvador Balle	Day 1
25	20 Title: Transmission Spectra in a Multilayer Photonic Structure Authors: Eudenilson Albuquerque, U. L. Fulco and M. S. Vasconcelos	Day 1
26	90 Title: Dynamics of decelerating pulses at a dielectric layer Authors: Alexander Nerukh, Denis Zolotariov, Olga Kuryzheva and Trevor Benson	Day 1
27	71 Title: A Switchable Figure Eight Fiber Laser Based on Inter-Modal Beating By Means of Non-Adiabatic Microfiber Authors: Ali Jasim	Day 1
28	11 Title: Effect of Filling the Surface Texture with Metamaterial on Spoof Surface Plasmon Dispersion Authors: Tatjana Gric, Jaromir Pistora and Michael Cada	Day 1
29	76 Title: Effect of wavelength and graphene layers on the SPR sensitivity Authors: Kaushalkumar Bhavsar and Radhakrishna Prabhu	Day 1
30	8 Title: Modelling of Polarization and Wavelength Insensitive Single Mode Al2O3 Rib Waveguides for Active and Passive Applications Authors: Mustafa Demirtaş, Ayberk Özden and Feridun Ay	Day 1
31	102 Title: Advanced bifurcation analysis of a laser diode with phase-conjugate optical feedback Authors: Marc Sciamanna, Emeric Mercier, Andreas Karsaklian Dal Bosco, Martin Virte, Lionel Weicker and Delphine Wolfersberger	Day 1
32	78 Title: Investigation of Confinement Losses in Photonic Crystal Fibre Authors: Jincy Johny, Radhakrishna Prabhu and Wai Keung Fung	Day 1
33.	69 Title: Modelling the optical properties of mixed ionic and electronic conductors (MIECs) with reversible ion intercalation Authors: Francesco Morichetti, Lea Luken, Frank Berkemeier, Guido Schmitz, Hans-Dieter Wiemhofer and Andrea Melloni	Day 1

In order	List of posters	Session: Day 2
1	53 Title: Diffraction Suppression and Soliton Formation in Binary Plasmonic Lattices Authors: Yao Kou and Jens Förstner	Day 2
2	63 Title: Efficient Optical Modeling of Graphene Authors: Roberto Armenta, Jens Niegemann, James Pond and Adam Reid	Day 2
3	75 Title: Analysis of modal spectrum and associated thresholds of a silver-strip plasmonic nanolaser as a novel light emitter Authors: Olga V. Shapoval and Alexander I. Nosich	Day 2
4	32 Title: Numerical Investigation of a Fiber Grating Coupler on SOI for SDM Authors: Benjamin Wohlfeil, Sven Burger, Frank Schmidt, Christos Stamatiadis, Lars Zimmermann and Klaus Petermann	Day 2
5	72 Title: Numerical Investigation of the Photon-Extraction Efficiency for InGaAs/GaAs Quantum Dots in Microlens-Mirror Structures Authors: Benjamin Wohlfeil, Sven Burger, Frank Schmidt, Sven Rodt and Stephan Reitzenstein	Day 2
6	46 Title: Modified Grating for High Absorption Enhancement Thin Film Solar Cell Authors: Muhammad Muhammad, Mohamed Hameed and Salah Obayya	Day 2
7	45 Title: Semi-vectorial Sinc-Galerkin Method with Domain Decomposition for Optical Waveguides Analysis Authors: Amgad A. El-Mohsen, Ahmed Heikal and Salah Obayya	Day 2
8	84 Title: Optimization of Gold Nanorod Arrays for SERS analysis of CTCs Authors: Jonathan Calderón, Maria Isabel Gómez and Daniel Hill	Day 2
9	57 Title: Acousto-optical Interaction in Ge-doped Silica Planar Optical Waveguide Authors: Mohammed Moseeur Rahman and B. M. A. Rahman	Day 2
10	29 Title: Modelling of microbending loss in optical fibres Authors: Xianqing Jin, Dominic O'Brien and Frank Payne	Day 2
11	54 Title: 1D Glass Bragg grating analysis for integrated Raman pump	Day 2

	filtering in the visible Authors: Alain Morand and Pierre Benech	
12	81 Title: Design Methodology for Metal Clad Polarizer in SOI Waveguides Authors: Shivani Sital and Enakshi Khular Sharma	Day 2
13	82 Title: Design of compact polarization splitter using silicon nanowiresAuthors: Sasan Soudi and B. M. A Rahman	Day 2
14	96 Title: Tunable Mid-IR Fiber-Optic Parametric Sources Authors: Satyapratap Singh, Viswatosh Mishra and Shailendra Varshney	Day 2
15	70 Title: Photon control by multi-periodic binary grating waveguides: A coupled-mode theory approach Authors: Jost Adam, Hannes Lüder and Martina Gerken	Day 2
16	30 Title: Coupled Electromagnetic –Thermal Model for Plasmonic Waveguides Authors: Ahmed Elkalsh, Ana Vukovic, Trevor Benson and Phillip Sewell	Day 2
17	67 Title: Modelling Multiphysics Effects in Optical Components Authors: Alon Grinenko	Day 2
18	97 Title: PIC Tunable Double Outputs Coupler in MDM system Authors: Weifeng Jiang, Xiaohan Sun, Na Dong, Chao Pan, Ningfeng Bai and Xu Liu	Day 2
19	44 Title: Surface Plasmon Resonance Liquid Crystal Photonic Crystal Fiber Temperature Sensor Authors: Mohamed Hameed, Shaimaa Azzam and Salah Obayya	Day 2
20	59 Title: Efficient O – band superluminescent diode with wide optical bandwidth and high power Authors: Mohammed Zahed Mustafa Khan, Hala H. Alhashim, Tien Khee Ng and Boon Ooi	Day 2
21	61 Title: Coupling mechanisms and field confinement in a hybrid plasmonic-photonic crystal resonator for enhanced optical trapping Authors: Mina Mossayebi, Alberto Parini, Amanda J. Wright, Eric Larkins, Gaetano Bellanca and Mike Somekh	Day 2
22	4 Title: Vertical Mode Expansion Method for Scattering of Light by	Day 2

	Nanocylinders Authors: Xun Lu and Ya Yan Lu	
23	85 Title: Floquet Bloch Analysis of Hill's Equation with Analytically Solvable Potentials Authors: Stuart Caffrey and Gregory Morozov	Day 2
24	83 Title: Nano-Porous Silicon Waveguides for Optical Sensors Authors: Tanya Hutter, Stephen R. Elliott and Nikos Bamiedakis	Day 2
25	27 Title: Square-Lattice Index-Guiding Microstructured Optical Fibers: An Analytical Field Model Authors: Dinesh Kumar Sharma, Anurag Sharma and Suarabh Mani Tripathi	Day 2
26	34 Title: Approximate Modal Analysis of Dielectric-loaded Surface Plasmon Polariton Waveguide on Metal Strip of Finite Width Authors: Kanchan Gehlot and Anurag Sharma	Day 2
27	21 Title: Plasmon-polaritons in Photonic Crystals Authors: Umberto Fulco, Eudenilson Albuquerque and Luciano Da Silva	Day 2
28	74 Title: WGM Microrod Laser Fabricated by pulsed CO2 Laser Micromilling Authors: Shahab Bakhtiari Gorajoobi, Ganapathy Senthil Murugan and Michalis Zervas	Day 2
29	94 Title: Lasing Threshold of Plasmon Mode of Silver Nanowire Grating Embedded in a Partially Active Dielectric Slab Authors: Volodymyr Byelobrov	Day 2
30	73 Title: Finite Element and FDTD Characterizations of Light Propagation through Lossy Insect Ommatidia Authors: M. Enayet Rahman and B.M. Azizur Rahman	Day 2
31	47 Title: In-fibre whispering gallery mode microresonator: a two-sphere coupled system Authors: Kyriaki Kosma, Kay Schuster, Jens Kobelke, George Nikolopoulos and Stavros Pissadakis	Day 2

SESSION 1

Metamaterials

All-dielectric nanophotonics: Magnetic response, Fano resonances, functional metasurfaces, and nonlinear effects

Yuri S. Kivshar
Nonlinear Physics Center, Australian National University, Canberra ACT 0200, Australia
ysk124@physics.anu.edu.au

This talk will review a new, rapidly developing field of all-dielectric nanophotonics and discuss many novel interesting physical effects including "magnetic light" and engineering of magnetic response, magnetic Fano resonances, resonant magnetoelectric effects, all-dielectric metasurfaces, and enhanced nonlinear effects.\

Metamaterials are artificial electromagnetic media structured on the subwavelength scale; they were suggested initially for the realization of negative refractive index and superlensing applications, but very soon they became a paradigm for engineering electromagnetic space by means of transformation optics. The research agenda is now focusing on the realization of *metadevices* that can be defined as metamaterial-based devices with novel functionalities achieved by structuring of functional matter on the subwavelength scale [1]. However, up to now, a majority of such structures included metallic elements and thus suffers from high dissipative losses at optical frequencies, dramatically limiting their performance. One of the canonical examples is a split-ring resonator, an inductive metallic ring with a gap that is a building block of many metamaterials. Thus, the big question now is: How to remove metallic components from metamaterials but maintain electric and magnetic responses enabling low loss metadevices at the nanoscale?

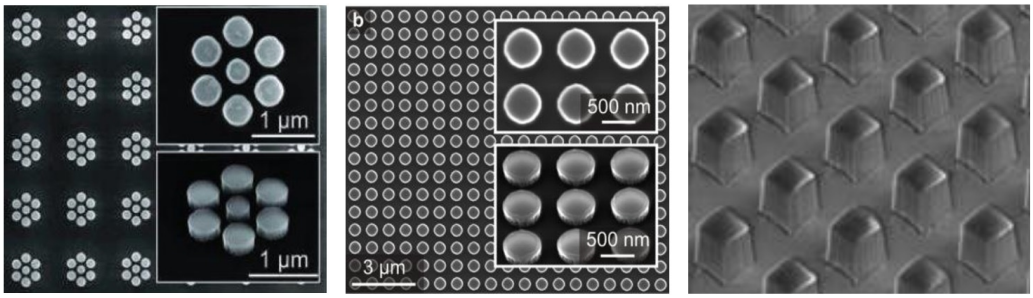

Figure 1. Examples of all-dielectric metasurfaces with optically resonant electric and magnetic responses: nanoantenna oligomers, regular square array of silicon nanoparticles, and magnetic metasurface.

Recent developments in the physics of metamaterials stipulated a birth of a new branch of nanophotonics dealing with optically-induced magnetic response of high-refractive-index dielectrics rather than metallic components. Unique advantages of dielectric nanostructures over metallic plasmonic structures are their low dissipative losses that provide new and competitive alternatives for many types of metadevices including nanoantennas and optical metasurfaces.

This talk will overview the recent developments of this research direction in nanophotonics exploring the electric and magnetic responses of dielectric nanoparticles due to Mie resonances. Optically resonant dielectric nanoscale structures are the best candidates for the emerging field of metadevices with unique functionalities well beyond the capabilities of currently existing devices.

References

[1] N. Zheludev & Yu.S. Kivshar, *From metamaterials to metadevices*, *Nature Mat.* **11**, 917 (2012).

Chiral and bianisotropic metamaterials for THz polarization control

M. Kafesaki*, G. Kenanakis, C. M. Soukoulis, E. N. Economou
Foundation for Research and Technology Hellas (FORTH), Institute of Electronic Structure and Laser (IESL), Crete, Greece, and University of Crete, Department of Materials Science and Technology, Greece
*kafesaki@iesl.forth.gr

A variety of THz chiral metamaterial structures is discussed and demonstrated. The structures show strong chiral response, both passive and dynamically (optically) controllable, offering thus unique possibilities for passive and active THz polarization control.

Introduction

Chiral metamaterials, due to their strong chiral response, can provide a unique vehicle for the control of wave polarization. Such a control is particularly important in the THz region where most of the natural materials do not show strong response (therefore they are not offered for the creation of THz manipulation components), given the great application-potential of the THz waves, especially in security and sensing.

Structures and results

Here we discuss our recent work on THz chiral metamaterials, both passive and dynamically controllable. The passive structures studied, which are shown in Fig. 1, have been fabricated on flexible substrates using UV lithography and show strong chiral response; this strong response is translated to large optical activity, large circular dichroism and negative refractive index for both left- and right-handed circularly polarized waves [1]. The dynamically controllable structures have been obtained by incorporating in the passive structures photoconducting Si which is transformed from an insulating to a conducting state by photoexcitation, altering thus the metamaterial response. Using this approach strong switchable chirality is demonstrated [2].

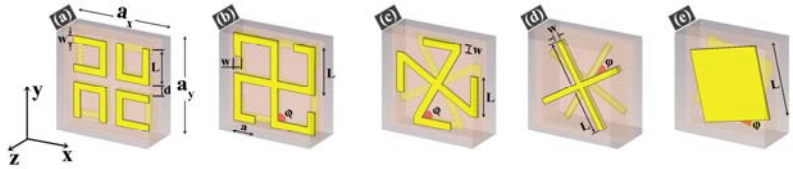

Fig. 1. The THz planar chiral designs studied in the present work.

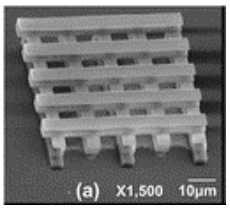

Fig. 2. A three-dimensional bianisotripic structure showing asymmetric transmission.

Additional polarization control capabilities to those obtained by the bi-isotropic chiral structures shown in Fig.1 can be obtained by properly designed anisotropic structures. Such a structure is shown in Fig. 2. Employing the structure of Fig. 2, which is fabricated by direct laser writing, we demonstrated polarization dependent asymmetric transmission response for linearly polarized waves [3]. Such a response offers additional potential for polarization control, as it facilitates polarization isolation applications.

References

[1] G. Kenanakis et. al., *Flexible chiral metamaterials in the terahertz regime: a comparative study of various designs*, Opt. Mat. Express 2, 1702 (2012).
[2] G. Kenanakis et. al., *Optically controllable THz chiral metamaterials*, Opt. Express 22, 12149 (2014).
[3] G. Kenanakis et. al., *Three-dimensional infrared metamaterial with asymmetric transmission*, ACS Photonics 2, 287 (2015).

Optical Grating or Lattice Resonances on Silver Strip and Wire Gratings

A. I. Nosich*, V. O. Byelobrov, T. L. Zinenko, D. M. Natarov, O. V. Shapoval
Laboratory of Micro and Nano Optics, Institute of Radio-Physics and Electronics NASU, Kharkiv, Ukraine
*anosich@yahoo.com

Abstract This is a mini-review of the nature and the history of discovery of the high-quality natural modes existing on periodic arrays of many sub-wavelength scatterers.

Summary

In the optical range, metal nanoparticles display localized shape-dependent surface-plasmon (LSP) resonances. For a circular wire in free space single LSP peak is observed in the H-polarization case near the wavelength λ^P where dielectric permittivity $\mathrm{Re}\,\varepsilon_{met}(\lambda^P) = -1$ that is 330 nm for silver. For a rectangular-section silver strip, several LSP resonances appear if standing waves are formed along the strip sides. Their Q-factors are low, about $|\mathrm{Re}\,\varepsilon_{met}(\lambda^P)|/\mathrm{Im}\,\varepsilon_{met}(\lambda^P)$. In the E-polarization case there are no LSP-like modes and associated resonances.

Besides, if many nanostrips or nanowires are placed periodically, they show the presence of absolutely different resonances with much larger Q-factors, which grow with the number of elements and take certain limiting values for infinite gratings. These are the resonances on the grating (or lattice) modes (GMs) sitting very close to Rayleigh anomalies.

It is interesting to compare the characteristics of the nanogratings made of comparable silver wires and silver strips, in the two alternative polarization regimes. Such comparison is shown in Fig. 1 for wires of the radius 48.85 nm and strips of the cross-section 50 nm x 150 nm and the period 800 nm.

As one can see in panel (a), in the H-case each nanograting displays a broad Lorentz-shape LSP-resonance at the corresponding wavelength. Besides of that, each grating produces two super-narrow GM-resonances at the wavelengths slightly up-shifted from the Rayleigh anomalies. Note that the LSP-mode wavelengths are very different however the GM ones agree well.

In the case of the E-polarization depicted in panel (b), no resonances are visible at all although the GM poles exist for all gratings in both polarizations [1]. The reason that they are not seen is in the Q-factors of GM poles, which in the E-case are $|\varepsilon_{met}|^2$ times lower than in the H-case that is a factor varying from 25 at 400 nm to 1100 at 800 nm. This “invisibility” of the optical GM-poles in the E-polarization scattering regime has been apparently hindering correct identification of their nature.

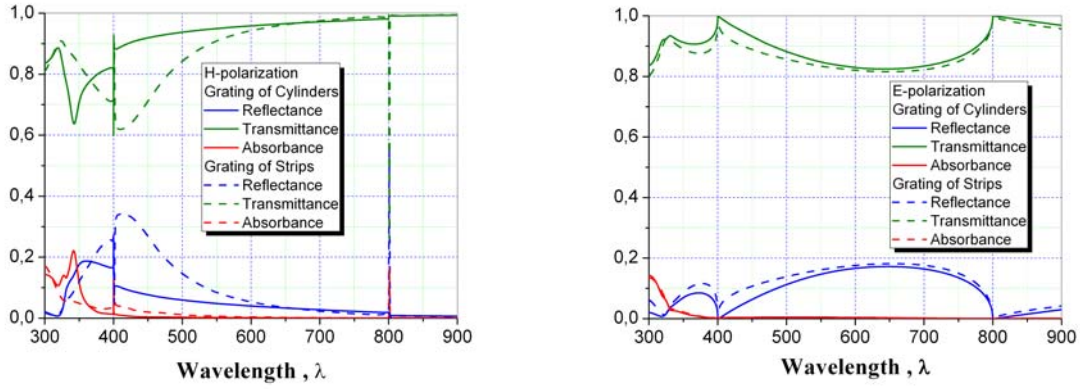

Fig. 1. Power fractions vs. wavelength, for two types of silver gratings and two polarizations

Conclusion The optical GM resonances are more promising for applications than usual LSP ones.

Reference

[1] V. O. Byelobrov, T. L. Zinenko, A. I. Nosich, *IEEE Antennas Propagat. Mag.*, vol. 57, 2015.

Modelling coherent nonlinearities in nanostructured plasmonic metamaterials

Giuseppe Marino[1,*], Paulina Segovia[1], Alexey Krasavin[1], Pavel Gingzburg[1,2], Nicolas Olivier[1], Gregory A. Wurtz[1], Anatoly, V. Zayats[1]
[1]*Department of Physics, King's College London, London WC2R 2LS, United Kingdom*
[2]*School of Electrical Engineering, Tel Aviv University, Ramat Aviv, Tel Aviv 69978, Israel*
*giuseppe.marino@kcl.ac.uk

Introduction

Second harmonic generation (SHG) from noble metal nanostructures has been extensively studied due to the unique optical properties offered by both localized surface plasmons and their hybridization in complex nanostructured systems to enhance the efficiency [1,2,3].
.

Summary

We have developed a full-vectorial numerical model to study SHG at gold nanorod-based plasmonic metamaterials. Our frequency-domain (FD) implementation of the hydrodynamic model of the metal permittivity for bound and conduction electrons allowed to achieve a full description of the nonlinear susceptibility followed by scattering of the local electromagnetic fields. We show that the nanorod-based hyperbolic metamaterial with the epsilon-near-zero frequency tuneable across the visible and near-IR frequency range, exhibits a set of SHG resonances enabling a multi-resonant coherent response both at the fundamental and harmonic frequencies (Fig.1).

Results

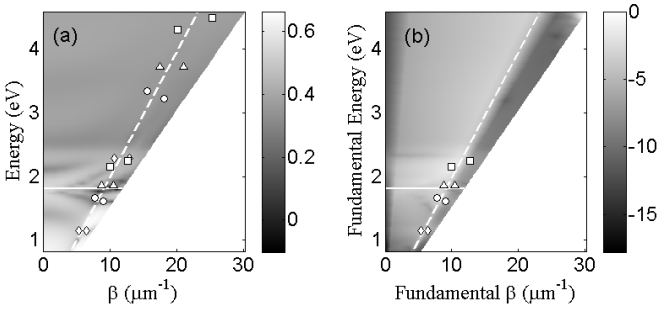

Fig. 1. (a) Reflectance and (b) Transmitted SH power in $\log_{10}$ scale obtained using FD based on the hydrodynamic model.

Conclusion

The developed FD method facilitated modelling of second-harmonic generation processes in metamaterials in elliptic and hyperbolic regimes and allows the tailoring SHG conversion efficiency in metamaterials.

References

[1] G. A. Wurtz, R. Pollard, W. Hendren, G. P. Wiederrecht, D. J. Gosztola, V. A. Podolskiy, and A.V. Zayats, Nature Nanotech. 6, 107-111 (2011)

[2] P. Gingzburg, A. Krasavin, Y. Sonnefraud, A. Murphy, R. J. Pollard, S. A. Maier,

and A.V. Zayats, Phys Rev. B 86, 085422 (2012)

[3] P. Ginzburg, A. V. Krasavin, G. A. Wurtz, and A.V. Zayats, ACS Photonics 2, 8−13 (2015).

Phase Matching and Frequency Mixing of Contra-propagating Electromagnetic Pulses in the Waveguide Tampered by Carbon Nanoforest

A. K. Popov [1,*], S. A. Myslivets [2,3], A. V. Kildishev [1], A. O. Korotkevich [4]

[1] *Purdue University, West Lafayette, IN 47907, USA*
[2] *Institute of Physics, SB of the Russian Academy of Sciences, 660036 Krasnoyarsk, Russian Federation*
[3] *Siberian Federal University, 660041 Krasnoyarsk, Russian Federation*
[4] *University of New Mexico, Albuquerque, NM 87131, USA*
[*] *popov@upurdue.edu*

We show that particular spatial distributions of carbon nanotubes enables extraordinary nonlinear-optical propagation processes commonly attributed to negative-index metamaterials. The possibility of great enhancement of frequency conversion is demonstrated with numerical simulations.

Metamaterials (MM) are artificially designed and engineered materials, which can have properties unattainable in nature. Usually, MM rely on advances in nanotechnology to build tiny metallic nanostructures smaller than the wavelength of light. These nanostructures modify the electromagnetic (EM) properties of MM, sometimes creating seemingly impossible optical effects. Negative-index MM (NIMs) are most intriguing EM materials that support backward EM waves (BEMW). Phase velocity and energy flux (group velocity) become *contra-directed* in NIMs. The appearance of BEMW is commonly associated with simultaneously negative electric permittivity ($\epsilon < 0$) and magnetic permeability ($\mu < 0$) at the corresponding frequencies and, consequently, with negative refractive index $n = -\sqrt{\mu\epsilon}$. Counter-intuitive backwardness of EMW is in strict contrast with the electrodynamics of ordinary, positive-index materials. The possibility of huge enhancement of nonlinear-optical frequency conversion processes has been predicted through three-wave mixing in NIMs if one of the coupled electromagnetic waves falls in the negative-index frequency domain. Among them are second harmonic generation, optical parametric amplification and frequency-shifted nonlinear reflectivity [1, 2]. Current mainstream in fabricating bulk NIM slabs relies on engineering of LC nanocircuits - plasmonic mesoatoms with negative electromagnetic response. Extraordinary coherent nonlinear optical frequency-converting propagation processes predicted in NIMs have been realized (simulated) so far only in the microwave. This paper proposes a different paradigm which employs spatial dispersion [3, 4] to realize outlined processes. We show that metamaterial slabs made of carbon nanotubes may support coexistence of ordinary electromagnetic waves with co-directed phase velocity and energy flux ($\partial\omega/\partial k > 0$) and extraordinary optical modes with contra-directed phase and group velocities ($\partial\omega/\partial k < 0$). Numerical simulations of nonlinear optical frequency-mixing of contra-propagating ordinary short optical pulses and pulses with negative group velocity has shown the possibility of greatly enhanced energy exchange between the coupled waves in such MMs.

This work was supported in parts by the NSF (Grant ECCS-1346547), by the AFOSR (grant FA950-12-1-298), by the ARO (Grant W911NF-14-1-0619) and by the Russian Foundation for Basic Research (Grant RFBR 15-02-03959A). We thank I. S. Nefedov for inspiring inputs.

References

[1] I. V. Shadrivov, A. A. Zharov, and Yu. S. Kivshar, *Second-harmonic generation in nonlinear left-handed metamaterials,* J. Opt. Soc. Am. B**23**, 529-534 (2006).

[2] A. K. Popov and V. M. Shalaev, *Negative-index metamaterials: second harmonic generation, Manley-Rowe relations and parametric amplification,* Appl. Phys. B: Lasers and Opt. **84**, 131-137 (2006).

[3] V. M. Agranovich and Yu. N. Gartstein, *Spatial dispersion and negative refraction of light,* Physics-Uspekhi (UFN) **176**, 1051-1068 (2006).

[4] I. Nefedov and S. Tretyakov, *Ultrabroadband electromagnetically indefinite medium formed by aligned carbon nanotubes,* Pys. Rev. B **84**, 113410-4 (2011).

SESSION 2

Plasmonics

Active and reconfigurable CMOS-compatible functional complex plasmonic metasurfaces

H. Giessen[1]
[1] *4th Physics Institute and Research Center SCoPE, University of Stuttgart, Germany*
Email: giessen@physik.uni-stuttgart.de

Introduction

We demonstrate active mid-infrared plasmonics using the phase-change material germanium-antimony-telluride (GST) in combination with different complex plasmonic structures. GST is a truly phase changeable material which can be in a crystalline as well as in an amorphous phase.

Summary

Switching of GST from one phase into another can be accomplished by slow or rapid heating and cooling. The switching temperature is between 65 and 70 °C. This material is also well know from rewritable CDs and DVDs and hence available in excellent and CMOS compatible quality.

In order to demonstrate the versatility, we demonstrate a variety of different concepts. First, we are going to show tunable and switchable chirality. C4-symmetric resonant plasmonic nanoantennas are stacked above each other with CST sandwiched inbetween. Heating the GST above the phase transition temperature and cooling it back down allows for shifting the plasmonic resonances due to the change of refractive index from about 3 to about 6. The plasmonic resonances exhibiting strong circular dichroism (CD) are designed to be situated in the mid-infrared spectral region, where GST losses are low. Therefore, the CD resonances can be shifted by roughly 20% in wavelength. Biasing the structure with a reverse plasmonic chiral structure, it is possible over a dedicated wavelength band to switch chirality from right- to left-handed and vice versa.

In another concept, we devised a perfect absorber with near-diffraction limited pixel sizes that were able to absorb spectral bands in the mid-IR. These spectral bands were correlated to peak temperatures of a Planck distribution of a heated body. Also, using GST, the spectral response was tunable and could be shifted in order to carry out background correction. It was possible to operate the device at room and low temperature.

Conclusion

Combining complex plasmonic metamaterials and metasurfaces with function layers can result in active, switchable, and reconfigurable devices that offer functionality in the mid-IR spectral region for tunable chirality, chiral switching, as well as tunable and temperature-selective perfect absorption.

Acknowledgements

We acknowledge funding by ERC (Complexplas), Zeiss-foundation, DFG, BW-Stiftung, AvH Stiftung, and BMBF. Support and fine work by Xinghui Yin, Andreas Tittl, and Martin Schäferling regarding the measurements and simulations and Thomas Taubner, Ann-Kathrin Michel, and Matthias Wuttig (RWTH Aachen) for preparation of the GST layers is kindly acknowledged.

Comparing plasmonic waveguides: a comprehensive figure of merit

A. V. Krasavin[1,*], A. V. Zayats[1]
[1]*Department of Physics, King's College London, London WC2R 2LS, United Kingdom*
*alexey.krasavin@kcl.ac.uk

We will present a comprehensive figure of merit for passive plasmonic waveguides. For the first time the figure is derived in terms of ultimate global characteristics of the waveguide circuitry benchmarking its performance for on-chip data communication: bandwidth and power dissipation values per circuit unit area.

Introduction

Optical data lines with their high bandwidth propose a new paradigm for on-chip data communications. At the same time, the cross-sectional size of traditional optical waveguides where the signal is transferred by photons is inherently limited by the diffraction limit of light, which leads to the fundamental mismatch between the integration level of electronic and photonic circuits: nanometer vs. merely sub-micrometre levels.

Summary

Transferring the optical signal in the form of surface plasmon polaritons, which are electromagnetic waves coupled to free electron oscillations localised at a dielectric-metal interface, offers a unique solution for this problem. Following this approach, a huge variety of plasmonic waveguiding geometries has been proposed which cover the whole range of achievable mode sizes and signal propagation lengths. In these circumstances, a figure of merit (FOM) for quantitative characterisation of their performance is needed. For the first time, we will derive it on the basis of ultimate global characteristics of the waveguide circuitry, benchmarking its performance particularly for on-chip data communication through a ratio of bandwidth b to power dissipation p, both per circuit unit area. These parameters are linked to the local waveguide characteristics:

$$FOM = \frac{b}{p} = B \cdot \frac{L_{prop}}{d_{sep}} \cdot \left[\frac{L_{tot}(r)}{r} \right]_{\max},$$

where B is the bandwidth of an individual waveguide [1], L_{prop} is the propagation length along a straight waveguide, d_{sep} is a separation distance between two parallel waveguides [2,3], $\left[L_{tot}(r)/r \right]_{\max}$ is the optimal value of ratio of the propagation length of the mode in the curved section of the waveguide to the bending radius. Interestingly, the derived FOM provided a general validation of the local FOMs [2,3], underlining different characteristics of waveguide performance, e.g. transmission coefficient vs. propagation length along a curved section. Furthermore, it revealed previously overlooked importance of individual waveguide bandwidth.

Conclusion

The obtained figure of merit provided new insights in the performance of the main types of plasmonic waveguides and showed the ability to efficiently benchmark plasmonic circuitry on the basis of waveguides having hugely diverse characteristics as well as to optimise the particular designs.

References

[1] D. Yu. Fedyanin, A. V. Krasavin, A. V. Arsenin, A. V. Zayats, *Nano Lett.* **12**, 2459 (2012).

[2] A. V. Krasavin, A. V. Zayats, *Opt. Lett.* **36**, 3127 (2011)

[3] A. V. Krasavin, A. V. Zayats, *Opt. Express* **18**, 11791 (2010).

Modelling Optical Bistability with Hybrid Silicon-Plasmonic Resonators

Odysseas Tsilipakos*, Thomas Christopoulos, Georgios Sinatkas, Emmanouil E. Kriezis
Department of Electrical and Computer Engineering, Aristotle University of Thessaloniki, Greece
* otsilipa@auth.gr

Optical bistability with hybrid silicon-plasmonic resonators is studied with a theoretical framework combining perturbation theory, coupled mode theory and the finite element method. Each physical system is designed so as to exhibit minimum power threshold and maximum extinction ratio between bistable states.

Introduction

Nonlinear phenomena based on the third-order susceptibility or free-carrier effects can be a favorable approach towards designing functional plasmonic components featuring fast response and all-optical operation. When combined with resonant structures, nonlinearity can lead to optical bistability, offering a route towards memory or switching elements. Importantly, the intensity build-up in the resonator leads to reduced power requirements compared to non-resonant approaches.

Results

Figure 1(a) depicts a travelling-wave (disk) resonator comprising a $\chi^{(3)}$ nonlinear polymer (DDMEBT) side-coupled to an access waveguide. The physical implementation is based on the nonlinear conductor-gap-silicon (NLCGS) hybrid plasmonic waveguide [1] which allows for nanonscale confinement and at the same time low propagation loss, thus favoring the manifestation of optical bistability. By conducting rigorous 3D simulations we find that R=1 μm minimizes the power required for bistability and g=225 nm results in critical disk-waveguide coupling maximizing the extinction ratio (ER) between bistable states [2]. The corresponding hysteresis loop is depicted in Fig. 1(b). Bistability manifests for optical powers just above 1W with the ER being theoretically infinite. Importantly, the instantaneous nature of $\chi^{(3)}$ nonlinearity permits the system to switch between states in less than 5 ps, rendering the proposed structure suitable for ultrafast memory/switching applications. Carrier-induced bistability with travelling- or standing-wave hybrid plasmonic resonators [Fig. 1(c)] is also examined since a Si layer is present in the structure giving rise to two-photon absorption. Such implementations lead to reduced power thresholds of few mW but are associated with ns response times due to the relatively slow process of carrier diffusion.

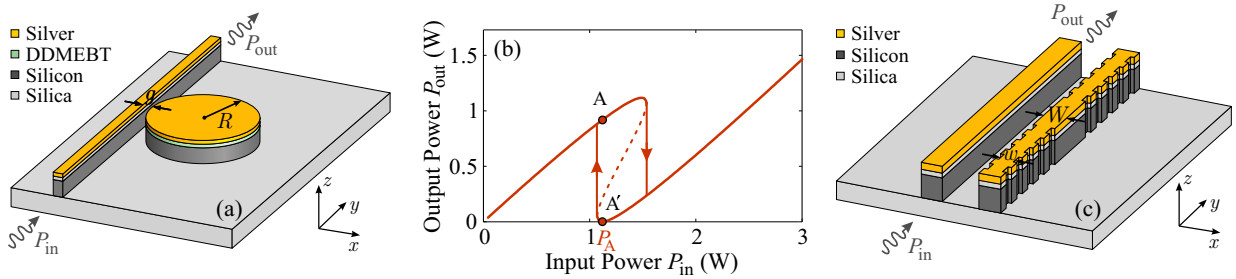

Fig. 1. (a) NLCGS-based disk resonator coupled to CGS access waveguide. (b) Bistability curve for a disk-waveguide system with R=1 μm and g=225 nm. For P_{in}=P_A=1.12 W the system exhibits bistable states with theoretically infinite ER. (c) Standing wave resonator with Bragg reflectors for carrier-induced bistability.

This work has been supported by the Research Committee of the Aristotle University of Thessaloniki through a postdoctoral research fellowship and by the European Union (European Social Fund) and Greek national funds through the Research Funding Program THALES (Project ANEMOS).

References

[1] A. Pitilakis, O. Tsilipakos and E. E. Kriezis, *ICTON 2012*, paper 6254436.

[2] O. Tsilipakos and E. E. Kriezis, *J. Opt. Soc. Am. B* **31**, 1968-1705, 2014.

Graphene Plasmonics for Efficient Energy Transfer

Vasileios D. Karanikolas[1], Cristian A. Marocico[1], A. Louise Bradley[1,*]
[1]*Semicondictor Photonics Group, School of Physics and CRANN, Trinity College Dublin, Ireland*
*bradlel@tcd.ie

We present a theoretical investigation of the energy transfer efficiency between a pair of quantum emitters in the presence of a graphene monolayer. At small distances an enhanced direct interaction between the quantum emitters dominates, while at larger separations efficient energy transfer occurs via the graphene plasmon mode.

Overview

Graphene is a 2D material with interesting plasmonic properties which can be tuned by varying the applied voltage [1]. Furthermore, it exhibits lower material losses compared to conventional plasmonic materials. An excited donor quantum emitter (QE) can relax through spontaneous emission (SE) or, if a second QE is present, by transferring its excitation to the second QE. These two processes are competitive thus an energy transfer (ET) efficiency is introduced. Both of these processes are strongly influenced through the interaction of the QEs with a graphene monolayer (GM). At small donor-acceptor distances the Förster contribution dominates and the characteristic distance, at which the ET efficiency is 50%, is enhanced from its free-space value of 20nm to 120nm. As the separation is increased the graphene plasmon (GP) contribution dominates.

Results

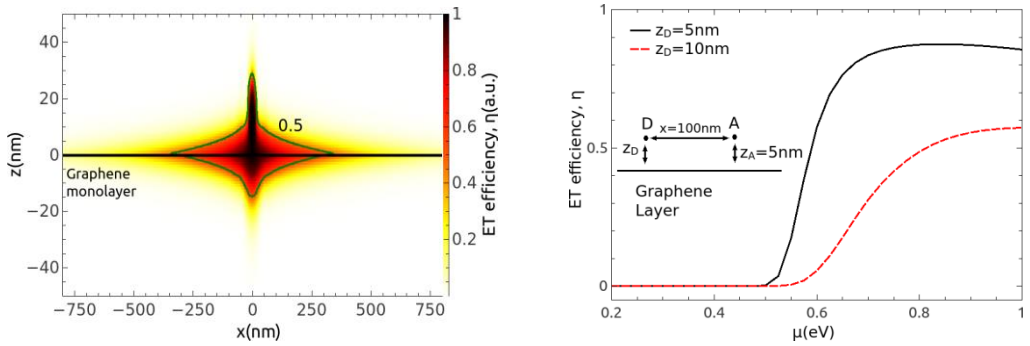

Fig. 1. (Right) ET efficiency of a QE emitter placed at r=(0,0,10nm) (Left) ET efficiency varying the chemical potential, μ, for different position of the donor-QE

We use QEs which they resemble real physical systems. Fig.1(Right) presents a contour plot of the ET efficiency for a donor placed at 10 nm above the GM, $\mathbf{r}_D = (0,0,10\text{nm})$, and varying the acceptor position in the xz-plane. Close to the GM and for separations up to 300nm we see that the ET efficiency has values above 50%. In panel Fig.1(Left) we present the tunability of the ET efficiency, for a fixed separation of the acceptor from the donor, 100nm and at two heights above the GM, z_D =5nm and z_D =10nm, with varying chemical potential, μ. For values of μ below 0.5eV the GP interaction is switched-off and thus the ET efficiency is small. Above values of μ =0.5eV the excitation of the GP mode leads to efficient ET between donor and acceptor.

Conclusion

Graphene plasmons greatly enhance the ET range and efficiency between a pair of QEs. Furthermore, the energy transfer characteristics can be tuned via the chemical potential.

References

[1] F. J. Garcia de Abajo ACS Photonics, 2014, 1(3), pp 135-152

Vertical mode expansion method for transmission of light through an arbitrary aperture in a metallic film

Hualiang Shi [1,*], Ya Yan Lu [1]

[1] *Department of Mathematics, City University of Hong Kong, Kowloon, Hong Kong, China*
[*] *shi.hualiang@my.cityu.edu.hk*

Applications of a vertical mode expansion method (VMEM) with horizontal boundary integral equations, are presented for the study of transmission of light through a subwavelength cylindrical aperture in a metallic film, where the aperture has an arbitrary cross section with a smooth boundary.

Method

The VMEM [1] is a recently developed method for multiply-layered structures. A metallic film which is parallel to the xy plane with a cylindrical aperture can be considered as a multiply-layered structure. We denote the 3D cylindrical region corresponding to the aperture as S_1, and the region outside as S_0. The common boundary of cross sections of S_0 and S_1 is Γ. By VMEM, the difference between the total electromagnetic filed and "1D" solution in S_l with $l \in \{0, 1\}$ is expanded in vertical modes which consist of $\phi_j(z)$ and $V_j(x, y)$, where $\phi_j(z)$ satisfies an eigenvalue equation in z direction and $V_j(x, y)$ satisfies 2D Helmholtz equation in the cross-section of S_l. The vertical modes are calculated by a Chebyshev pseudospectral method with the truncation of z by perfectly matched layers. With the help of boundary integral operators on Γ, we construct matrix approximations of the Neumann-to-Dirichlet maps which map $\partial_\nu V_j$ to V_j on Γ, then $\partial_\nu V$ are solved from a linear system established on the boundary of the cylinder by matching E_z, H_z, E_τ, H_τ, where ν and τ are the unit normal and tangential vectors on Γ in the xy plane.

Results

We calculate the transmission of light through a C-shaped aperture in a silver film with thickness $120nm$.

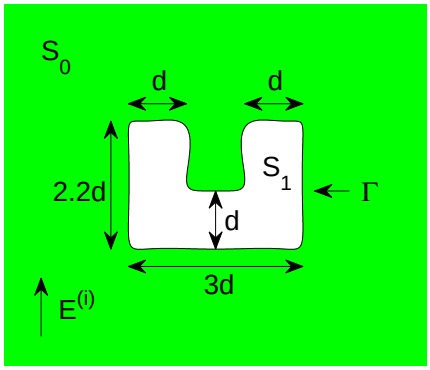

Fig.1. The aperture ($d = 100nm$) in xy plane.

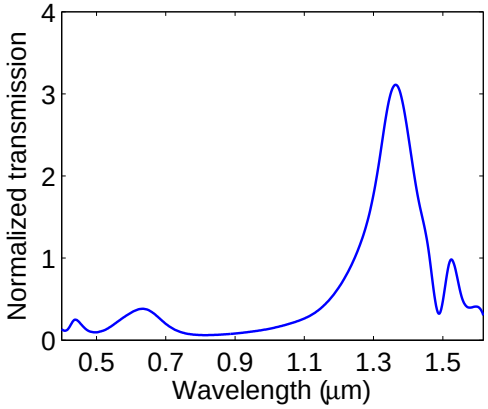

Fig.2. Normalized transmission for the left aperture.

References

[1] X. Lu, H. Shi, and Y. Y. Lu, *Vertical mode expansion method for transmission of light through a single circular hole in a slab,* J. Opt. Soc. Am. A, vol. 31, pp. 293-300, February 2014.

Transparent conductive oxides as near-IR plasmonic materials: the case of metal-doped ZnO derivatives

Alessandra Catellani[1,2], Alice Ruini[1,3], and Arrigo Calzolari[1*]

1. CNR-NANO Istituto Nanoscienze, Centro S3, Modena IT

2. CNR-IMEM, Parma IT

3. Dipartimento di Fisica Informatica e Matematics, Univerità di Modena e Reggio Emilia, Modena, IT

*arrigo.calzolari@nano.cnr.it

We present a fully first principles study of the plasmonic properties of metal-doped ZnO derivatives, proposed as plasmonic materials for energy conversion applications and telecommunications.

Introduction

Noble metals such as gold and silver are conventionally used as the primary plasmonic building blocks in the fields of the telecommunications and energy conversion [1]. However, metals are plagued by large losses, especially in the UV–vis and IR spectral ranges, arising in part from interband electronic transitions and in part from dissipative scattering events. These losses are detrimental to the performance of plasmonic devices. As an alternative, transparent conductive oxides (TCOs) can exhibit a high conductivity and very small losses at the infrared and longer wavelengths: the necessary requirements for good plasmonic materials [2].

Summary

Here we present a first principles investigation of the optical and plasmonic properties of metal-doped ZnO systems, based on density functional theory, within the Random-Phase-Approximation. We first demonstrate the TCO character of metal-doped ZnO crystals, and their bulk plasmon properties. Then, we show the formation of SPP resonances at Al:ZnO/ZnO interfaces, and their dependence on doping dosage. Finally, we study the plasmon properties of In-doped nanowires.

Results

Our results [3-4] predict realistic values for the plasma frequency and the free electron density as a function of the metal (Al, In) doping, in agreement with recent experimental results. These systems present tunable plasmonic activity in the near-IR range and in particular at wavelength relevant for energy conversion devices and telecommunications (1,5 μm) [4]. In-doped ZnO wires result to be stable highly doped 1D materials, maintaining good plasmon properties.

Conclusion

Our results reveal the microscopic mechanisms that regulate the plasmonic behavior in ZnO derivatives, and complement the newest experimental findings in confirming that TCOs are very promising materials for plasmonic applications, also at the nanoscale.

References

[1] Murray, W. A.; Barnes, W. L. *Plasmonic Materials*. Adv. Mater. 2007, 19, 3771.
[2] Naik, G. V.; et al. *Alternative Plasmonic Materials: beyond gold and silver.* Adv. Mater. 2013, 25, 3264
[3] Bazzani, M.; Neroni, A.; Calzolari, A.; Catellani, A. *Optoelectronic properties of Al:ZnO: Critical dosage for an optimal transparent conductive oxide.* Appl. Phys. Lett. 2011, 98, 121907
[4] Calzolari, A.; Ruini, A.; Catellani, A. *Transparent Conductive Oxides as Near-IR Plasmonic Materials: The Case of Al-Doped ZnO Derivatives.* ACS Photonics 2014, 1, 703–709.

SESSION 3

Modelling of Active and Passive Waveguide Devices

The Extraordinary World of Optical Waveguides

David N Payne
Director
Optoelectronics Research Centre
The University of Southampton
Southampton SO17 1BJ
E-mail: dnp@orc.soton.ac.uk

ABSTRACT

The great success of optical fibre waveguides in telecommunications has generated numerous applications in a number of related fields, such as sensing, biophotonics and high-power lasers. The topic remains extraordinarily buoyant and new materials, structures and applications emerge unabated. The talk will review recent developments and explore future possibilities.

TELECOMMUNICATIONS

Following in the footsteps of Marconi and the revolution of wireless, the internet is perhaps the most important and life-changing invention of the 20th century. It too required the invention of a new global communication medium capable of carrying vast quantities of information across trans-oceanic distances, reliably, cheaply and efficiently. This turned out to be the unpredictable, unlikely and extraordinary role of optical waveguides (fibres) made from the two most common elements of the earth's crust, silicon and oxygen (silica).

In recognition of the huge impact of his invention, Charles Kao was awarded the Nobel Prize for Physics in 2009, while Charles Townes, who provided the laser, was similarly honoured in 1964.

As with all new and disruptive concepts, the optical internet has proven a rich source of innovation, from the optical amplifier that compensates for losses in long spans of fibre, through new forms of digital communications appropriate to light as a carrier, to new materials and lasers. Perhaps even to quantum technologies for the future.

But is the innovation over? The demand for capacity continues unabated, fuelled by demand for faster connections and a new age of creativity at home – You Tube, Twitter, Facebook – as well as an insatiable demand for high quality videos. You Tube alone consumes more bandwidth today than the entire internet in year 2000 and projections show that a capacity crunch looms in both the internet optical backbone and the wireless final drop in the next decade or so. Yet we are still on the first hardware iteration of the optical infrastructure, so is there an internet 2.0 and is it man enough to support the internet of things?

FIBRE LASERS

Incredibly, the same fibre waveguides that carry tiny internet signals when doped with rare-earths can generate more than 20 kilowatts of power, sufficient to cut through inch-thick steel. For the first time, we have a low-cost gain medium that can be produced in lengths of hundreds of kilometres. By analogy with the internet, this leads to the radical concept of fibre laser circuits consisting of thousands of lasing strands combined together into a single, controllable beam of immense power.

The exquisite control of the laser offered by the waveguide environment makes coherent beam combination a possibility for very large numbers of fibre amplifiers fed from a common seed laser, perhaps to power levels in the megawatt regime. As with a radar antenna, coherent combination in a phased-array configuration with active phase control of the individual beams allows control of the spatial beam profile, as well as a degree of beam steering and adaptive optics. In the ICAN project we are currently investigating the possibility of using coherently combined femtosecond fibre sources to drive Wakefield accelerators for particle colliders in an initiative led by G. Mourou and T. Tajima. The high average powers required makes the high efficiency of fibres a necessity. Although many thousands, perhaps millions, of fibre channels will have to be combined, the manufacturability, scalability and reliability of active fibre technology makes this a realistic proposition over the next few decades.

Whether by beam combination or the intrinsic control and flexibility of an individual laser, high-power fibre sources are truly revolutionary in the performance they offer and the applications they enable in science and industry.

The essential elements of low loss in hollow optical fibres

Jonathan C. Knight[1,*] Walter Belardi, Fei Yu
[1]*Department of Physics, University of Bath, Bath, BA2 7AY, United Kingdom*
*j.c.knight@bath.ac.uk

Improving on the performance of state-of-the-art optical fibers represents a massive design challenge. We describe how to form microstructured hollow core fibers with low attenuation, low dispersion and high damage thresholds.

Background

In many ways, hollow-core fibers represent a "holy grail" of optical fiber design, in which the fiber performance is uncoupled from the limitations of the material used to form it. Microstructured cladding material has long been recognized as an effective means to trap light in a hollow core. However, the physics of such structures is complex and sometimes poorly understood. We have recently re-evaluated the role played by some of the structural elements in widely-used fiber designs, and come up with simplified fiber designs with record-breaking properties.

Summary

In our simplified designs for microstructured hollow-core fibers, the structure of the fiber core is pre-eminent. The size, shape and thickness of the core wall is fundamental to determining the properties of the final fiber. It is almost invariably better to optimise these parameters than to be concerned with the semi-infinite cladding material which lies beyond the core wall. We describe the required structural features and the resulting fiber characteristics.

Results

The basic feature of a low loss hollow core microstructure fiber is that it be anti-resonant [1]. Introducing an inverted core wall curvature reduces the interaction between the core-guided mode and the "glassy" cladding modes and extends the low-loss spectral window. The core size should be large to reduce attenuation, nonlinearity, dispersion and to increase the damage threshold. This can lead to bending loss which can be addressed by forming the core walls using non-touching circles of glass [2]. Leakage loss is then limited by coupling to "airy" cladding modes and this can be reduced by modifying the structure outside of the core wall [3].

Conclusions

Simple designs can nonetheless achieve high performance in hollow core fibers. These fibers already outperform standard fibers in many ways and have great potential for further improvement.

References

[1] F. Yu, W. J. Wadsworth, J. C. Knight, *Low loss silica hollow core fibers for 3 - 4 μm spectral region*, Opt. Express **20** 10 11153 (2012)

[2] W. Belardi and J. C. Knight, *Hollow antiresonant fibers with low bending loss*, Opt. Express **22** 8 10091 (2014)

[3] W. Belardi and J. C. Knight, *Hollow antiresonant fibers with reduced attenuation* Opt. Letters **39** 7 1853 (2014)

Planar waves that climb dielectric steps

Manfred Hammer*, Andre Hildebrandt, Jens Förstner

Theoretical Electrical Engineering, University of Paderborn, Germany
*manfred.hammer@uni-paderborn.de

Oblique semi-guided light propagation across linear folds of slab waveguides is being considered. Exploiting a Fabry-Perot-like resonance effect, we observe virtually full transmission of laterally plane waves, and of laterally wide semi-guided beams, through step configurations consisting of two sharp 90° waveguide corners.

Incidence of semi-guided waves on folded slab waveguides at oblique angles

Sheets of slab waveguides with sharp corners are investigated. Referring to the schematic in part (a) of the figure, we consider the propagation of vertically (x) guided, laterally (y, z) unguided plane waves at oblique angles of incidence θ, relative to discontinuity along the y-axis. Following a line of arguments resembling Snell's law, one finds that radiation losses vanish beyond a certain critical angle of incidence. One can thus realize lossless propagation through 90° corner configurations, where the remaining guided waves are still subject to pronounced reflection and polarization conversion. For the Si / SiO_2-like parameters as given for the figure, simulations with a rigorous quasi-analytic solver [1] predict extremal levels of 74% transmittance and 26% reflectance for a 90° corner at $\theta = 41°$.

Full transmission across resonant step configurations

A system of two corners can be viewed as a structure akin to a Fabry-Perot-interferometer, where the corners work as partial reflectors. By adjusting the height of the vertical waveguide segment one identifies step-like configurations that transmit the semi-guided plane waves without radiation losses, and virtually without reflections, at specific angles of incidence. For the example shown in the figure, our simulations predict levels of transmittance $T = 1\%$ and reflectance $R = 12\%$ at normal incidence $\theta = 0°$ (b), and numerically perfect performance $T > 99\%$, $R < 1\%$ at $\theta = 68°$ (c).

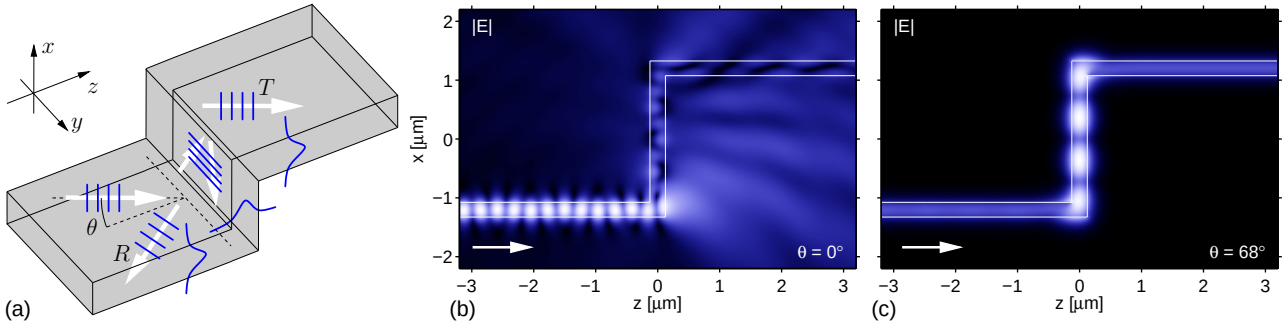

Oblique incidence of semi-guided waves on a step configuration at angle θ, schematic (a), and cross-section views of the optical electric field (absolute value $|\boldsymbol{E}|$), for normal incidence (b), and at angle $\theta = 68°$ (c). Parameters: refractive indices 3.4 (cores) : 1.45 (cladding), slab thickness $0.25\,\mu m$, vertical slab distance $2.15\,\mu m$, incidence of TE polarized waves at vacuum wavelength $1.55\,\mu m$.

Semi-guided beams

Simulations of laterally confined wave bundles, with in-plane wide Gaussian profiles, show that the effect survives in a true 3-D framework. The vQUEP solver [1] has been extended accordingly.

References

[1] M. Hammer. Oblique incidence of semi-guided waves on rectangular slab waveguide discontinuities: A vectorial QUEP solver. *Optics Communications*, 338:447–456, 2015.

Inverse scattering designs of mode-selective waveguide couplers

Alexander R. May*, Michalis N. Zervas
Optoelectronics Research Centre, University of Southampton, SO17 2BJ, United Kingdom
*arm103@orc.soton.ac.uk

We describe the design of arbitrary mode-selective waveguide couplers through application of the Darboux transform of inverse scattering theory. We demonstrate that contrary to recent SUSY designs, it is not necessary to use complex refractive index profiles to achieve this.

Introduction

We have previously discussed the design of multimode waveguides with prescribed mode effective indices through the use of the Darboux transformation [1] of inverse scattering in the context of group velocity equalization [2]. In this work, we discuss the design of waveguides suitable for building mode-selective waveguide couplers (MSC) for mode-division muxing/demuxing. We design appropriate trunk/partner waveguide pairs with phase matched propagation constants. The strength of this technique is the ability to phase-match any arbitrary combination of modes using real refractive index (RI) profiles. This is contrary to recently published works, involving supersymmetric (SUSY) transformations [3], which utilize complex RIs, involving gain and loss, and can mux/demux *only one mode* at a time.

Results

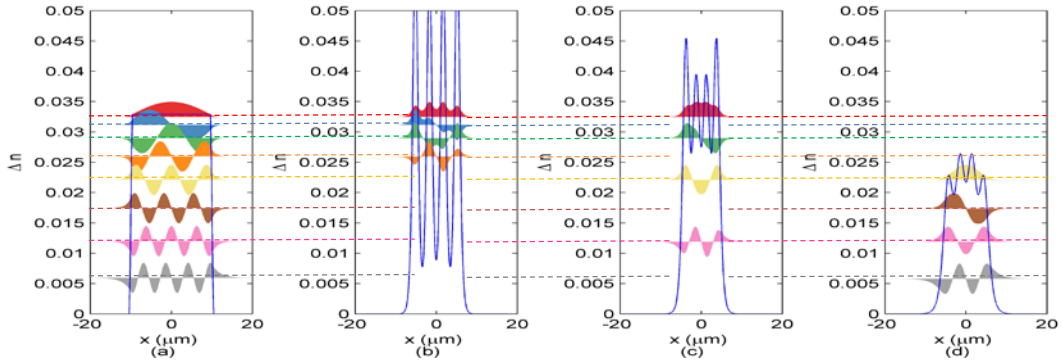

Fig. 1. RI profile of (a) multimode step-index trunk waveguide, and partner waveguides for (b) four lowest-order, (c) four alternate-order and (d) four highest-order modes @ λ=1.55μm, $n_{cladding}$ =1.444

Fig. 1 shows an example of a multimode step-index trunk waveguide (a) and the corresponding partner waveguides matching the four lowest-order (b), alternate-order (c), or four highest-order (d) modes, obtained by the use of the inverse scattering algorithm based on Darboux transformations. Such trunk/partner waveguide designs can be coupled optically and provide a scalable and potentially versatile method of mode discrimination and/or multiplexing technology in an era of ever-increasing demand upon high-capacity optical communication systems. Coupler designs will be presented at the conference.

References

[1] D. W. Mills and L. S. Tamil, "Synthesis of Guided Wave Optical Interconnects," *IEEE J. Quantum Electron.*, vol. 29, no. 11, pp. 2825–2834, 1993.

[2] A. R. May and M. N. Zervas, "Group velocity equalisation in multimode waveguides using inverse scattering designs," in *Sixth International Conference on Optical, Optoelectronic and Photonic Materials and Applications (ICOOPMA '14)*, 2014.

[3] M. Heinrich, M.-A. Miri, S. Stützer, R. El-Ganainy, S. Nolte, A. Szameit, and D. N. Christodoulides, "Supersymmetric mode converters," *Nat. Commun.*, vol. 5, p. 3698, 2014.

Beneficial Impact of Multi-order Dispersion Engineering in Designing a Flat-top Wide-band Supercontinuum Source

Sudip Kr. Chatterjee[1], Saba N. Khan[1], Partha Roy Chaudhuri[1,*]
[1]*Deaprtment of Physics, Indian Institute of Technology, Kharagpur, India*
**roycp@phy.iitkgp.ernet.in*

Abstract: We numerically demonstrate that accurately engineered multi-order dispersion parameters controlling the nonlinear dynamics of ultra-short pulse in a tailored Binary Multi-clad Microstructured Fiber can generate *single-pulse, flat-top, record bandwidth supercontinuum spectrum with high-spectral content.*

Optical Wave Breaking (OWB) assisted flat-top Supercontinuum generation (SCG) in all-normal dispersion (ANDi) regime (first proposed by Heidt et.al. in 2009) has been the key interest for researchers in recent years due to its well-known applications in time- resolve spectroscopy, comb-generation, dense wavelength- division multiplexing (DWDM) etc [1,2]. Recent work in visible and near-IR spectral region has described the impact of β_2 in designing wide-band SC spectra with temporarily compressible single cycle pulse. In this contribution we investigated the impact of higher order dispersion in order to transfer more energy to the spectral wings that minimize the spectral fluctuation. At first, we describe our model equations (GNLSE) and define some characteristic parameters (pulse-slopes at trailing/leading edge, spectral flatness or SF) to qualitatively interpret the temporal and spectral properties of a propagated pulse (T_w=75 fs). Next we revisit and optimize different steps that are involved in the development of a SCG under ANDi regime. Finally, we provide an original interpretation of how various dispersion parameters (β_2, β_3, β_4) may individually modulate the evolution (temporal and spectral domains) of the continuum. Our fine understanding of the high-power, ultra-short pulse propagation dynamics leads us to propose simple design rules that enable one to procure a record bandwidth, coherent, flat-top, SCG with high-spectral content. The desired dispersion profile is then extracted through a new host Binary Multi-clad Microstructured Fiber (BMMF) structure to obtain a record two-octave spanning SC band with fluctuation <5 dB. The glass material of the proposed structure is chosen to be Lead-silicate glass (SF6/SF57-LLF1) because of its high linear (1.76-1.8) and nonlinear refractive indices (2.2-4.1×$10^{-19}$$m^2$/W), high index contrast (Δn~0.14) and wide transparency window (500-3000 nm). Noteworthy, a rigorous full vector analysis of BMMF has been carried out to obtain the modal, dispersion and nonlinear characteristics.

Fig.1. shows the result of single-shot numerical SCG simulation for a 75fs pump-pulse at an operating wavelength of λ_p=1.55 μm after propagating 10 cm of host BMMF/SIF. An extremely flat and smooth spectral profile (SF-0.92) with bandwidth upto ~1300 nm is achievable with BMMF: B with moderate pump power of 20kW owing to the appropriate HOD parameters associated with the designed structure. The other BMMF/SIF fails to meet the dispersion requisite (BMMF :A- small β_4, BMMF :C- large β_i i=5,6.., SIF- large β_i i=3,4,5..) and thus yield a less-flattened, narrow band SCG. Next, commercially available SF57 glass possessing two-times higher nonlinearity and good thermal, chemical and mechanical stability with lead–silicate glass counterpart LLF1 is utilized to generate a record two-octave spanning (902-2580 nm) supercontinuum source. The optimized spectra is found to be perfectly coherent by estimating the first-order coherence function $|g_{12}^{(1)}|$ over the entire bandwidth. The vector-mode analysis scheme, SCG modeling and optimization recipe with more results would be discussed in the conference.

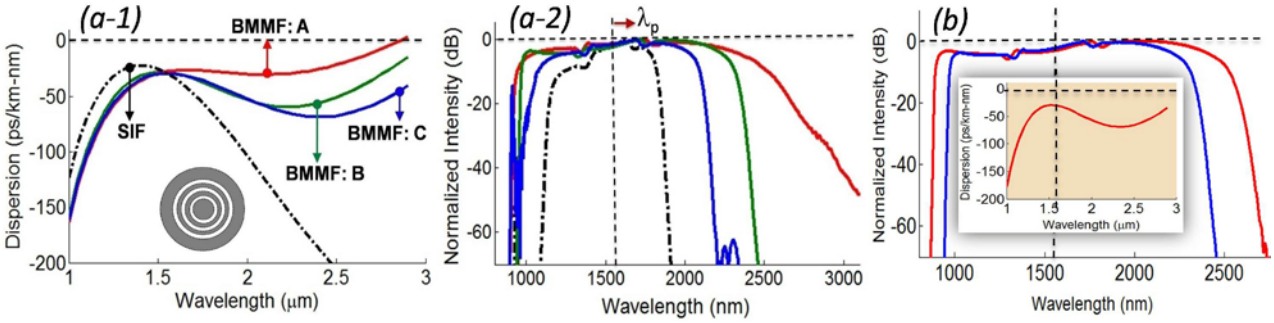

Fig.1.(a) Dispersion characteristics of selected SF6/LLF1 based fiber geometry (SIF, BMMF:A, BMMF:B, BMMF:C) with the corresponding optimized SC spectrum. (b) Optimized SCG in a host SF57/LLF1 BMMF

References

[1] J. Dudley and R. Taylor, "Supercontinuum generation in optical fibers," (Cambridge University Press, 2010).
[2] A. M. Heidt, "Pulse preserving flat-top Supercontinuum generation in all-normal dispersion photonic crystal fibers", JOSA B **27**, 550-559 (2009).

Modeling of single-mode regime in active large mode area photonic crystal fibers under severe heat load

E. Coscelli F. Poli L. Rosa A. Cucinotta S. Selleri

Information Engineering Department, University of Parma, Parma, Italy
enrico.coscelli@unipr.it

A computationally efficient model is proposed to analyze the single-mode regime of active large mode area photonic crystal fibers, significantly affected by thermal effects. Results show the model effectiveness in describing how heating conditions influence the guiding properties of fibers with different refractive index profiles.

Thermal effects in LMA PCFs

Active fiber core heating has recently been appointed as one of the most important causes of performance degradation in high-power systems [1]. In fact, fiber guiding properties are altered by the refractive index increase, due to the generated transverse thermal gradient. Since the impact of these effects scales with the mode field, it is significant in Large Mode Area (LMA) Photonic Crystal Fibers (PCFs) [2]. In this paper an efficient model is proposed to investigate the Single-Mode (SM) regime of LMA PCFs under severe heat load, which depends on the properties of the Fundamental Mode (FM) and the first Higher-Order Mode (HOM). Simulations demonstrate that the developed model can be successfully applied to different PCFs, regardless of the cross-geometry and the guiding mechanism.

SM regime model under head load

To obtain the temperature distribution in LMA PCFs, the fiber cross-section is approximated with four concentric layers, as shown in Fig. 1(left), each characterized by its own isotropic thermal conductivity, corresponding to core, inner cladding, air-cladding, and outer cladding. The steady-state heat equation is solved, assuming a certain heat power density generated in the core due to the quantum defect. The obtained temperature profile is used to evaluate the refractive index change related to the thermo-optic effect, then the full-vector modal solver based on the finite element method [3] is applied to calculate the guided mode field distribution. Two conditions, that is FM overlap integral higher than 0.8 and overlap difference between FM and HOM higher than 0.3, define the PCF SM regime, which can be studied for different heat load values. The developed model has been successfully applied to index-guiding PCFs, like large pitch or symmetry-reduced fibers, shown in Fig. 1(center) and 1(right), as well as to PCF which exploit more complicated guiding mechanisms, like distributed modal filtering fibers. Simulation results will be shown at presentation time.

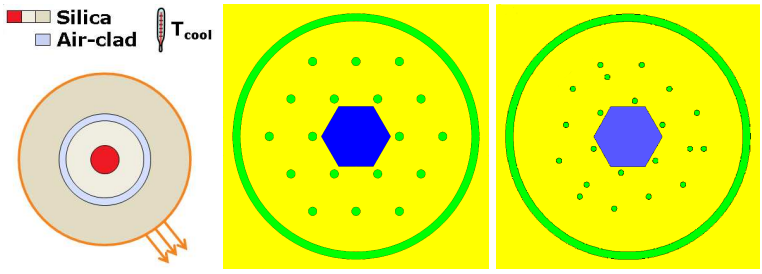

Fig. 1. (Left) Four-layer PCF cross-section, (center) large pitch and (right) reduced-symmetry fiber.

References

[1] A. V. Smith, J. J. Smith, *Mode instability in high power fiber amplifiers,* Opt. Exp. 19, 10180-10192, 2011.
[2] F. Jansen, F. Stutzki, H.-J. Otto, T. Eidam, A. Liem, C. Jauregui, J. Limpert, A. Tünnermann, *Thermally induced waveguide changes in active fibers,* Opt. Exp. 20, 3997-4008, 2012.
[3] F. Poli, A. Cucinotta, S. Selleri, *Photonic Crystal Fibers. Properties and Applications,* Springer, 2007

SESSION 4

Optical Sensors

Optical Fibre Sensor Systems for Safety and Security applications in industry

K T V Grattan[1,2*], T Sun[2]
[1]*City Graduate School, City University London, London, United Kingdom*
[2]*School of Mathematics, Computer Science and Engineering, City University London, London, United Kingdom*
*k.t.v.grattan@city.ac.uk

Optical fibre sensor systems have matured over recent years to the point where a number of applications in industry are seen which have a positive impact on safety and security needs. This paper provides an overview of such recent work and emphasizes the 'niche' areas where optical fibre systems designed by the authors are well suited to a range of safety and security needs and in so doing, show very good performance.

Introduction

There has been enormous growth in fibre optic sensor technology with new applications opening up and the technology maturing. Discussion of the underpinning technology of optical fibre sensors have been published previously by the authors (and is not further reproduced here). However to deal with the breadth of potential applications and for the different requirements, a wide range of different technological approaches to fibre optic sensors for a variety of measurands has been proposed in the literature. There is of course 'no right answer' when it comes to designing an optical fibre sensor but what is critically important is that there are effective sensors available.

Summary and Results

In this paper, several applications are considered showing the breadth of situations where such measurements are important, the need for clarity on issues such as compatibility with use in extreme environments or on human subjects and indeed the importance on making such measurements in aerospace applications such as in measurements under radiation environments. All this shows the tremendous breadth that must be reflected effectively in the system design, to achieve the required degree of ruggedness or biocompatibility, for example, and thus which underpins effective design.

OFS systems will be discussed for a number of key areas including Structural Health (SHM) applications where over the past few decades, the deterioration of civil infrastructure, such as buildings, bridges and roadways have demonstrated the need for high-performance sensing systems that can be used effectively to monitor changes in structures, often occurring over many years. In addition areas such as Food Process and Storage applications can benefit e.g. in monitoring the loss of moisture due to transportation and storage. Biomedical applications, such as the monitoring of breathing during imaging and surgical procedures where airflow monitoring has been widely applied to predict and detect respiratory disorders and failures, such as hypopnoea and apnoea are being developed. Ecological and environmental applications are broad and growing in scope and Agricultural applications, for example monitoring moisture level can allow better interpretation of the behaviour of different crops under sub-optimal environments. In Mineral Processing applications, soil moisture content measurement is important as is Fuel Quality applications where combustion of biomass for heat and power production is expanding due to the search for renewable alternatives to fossil fuels. In addition, Aerospace applications involve humidity sensors to perform *in situ* measurements and finally, the measurement of RH is important for human comfort such as in air-condition monitoring and for achieving controlled hygienic conditions.

Acknowledgements

The Royal Academy of Engineering and the George Daniels Educational Trust

Multichannel Photonic Crystal Fiber Surface Plasmon Resonance Based Sensor

Shaimaa I. H. Azzam[1,2], Mohamed Farhat O. Hameed[1,2], S. S. A. Obayya[1*]

[1]*Centre for Photonics and Smart Materials, Zewail City of Science and Technology, Egypt.*

[2]*Faculty of Engineering, Mansoura University, Mansoura, Egypt.*

sobayya@zewailcity.edu.eg

This work introduces a numerical analysis for an optical sensor that is based on photonic crystal fiber (PCF) coated with a metal layer to excite a surface plasmon resonance (SPR). The novelty in this design is the simple structural birefringence introduced in the core of the PCF which can enable the sensing with up to four channels simultaneously.

Basic Principles

Multichannel sensors are always preferred due to their ability to either greatly enhance the accuracy of sensing or to perform multiple analytes sensing at the same time. Problems with multichannel sensors have always been their complex structures that make their fabrication quite challenging. To introduce the structural birefringence, multichannel sensors normally use either air holes with different sizes or rely on shapes for the air holes other than the simple circular holes, e.g. the elliptical air holes, and hence enable modal distinction [1]. The proposed design is very simple based on PCF with a silica background and six similar air holes that can support light guidance. The analyte is contained in two large slots with their surfaces metalized to enable the excitation of the SPR modes. Birefringence is then introduced via a simple engineering of the positions of the air holes maintaining the structure simplicity and achieving comparable sensitivities to those reported in the literature [1] of more than 2000 RIU/nm sensitivity. Additionally, the suggested sensor offers sensing with up to four distinct modes of the sensor as shown in Fig.1. Further optimization of the proposed SPR-PCF sensor is expected to enhance the reported sensitivities and increase the separation of the different modes leading to more efficient sensing capabilities.

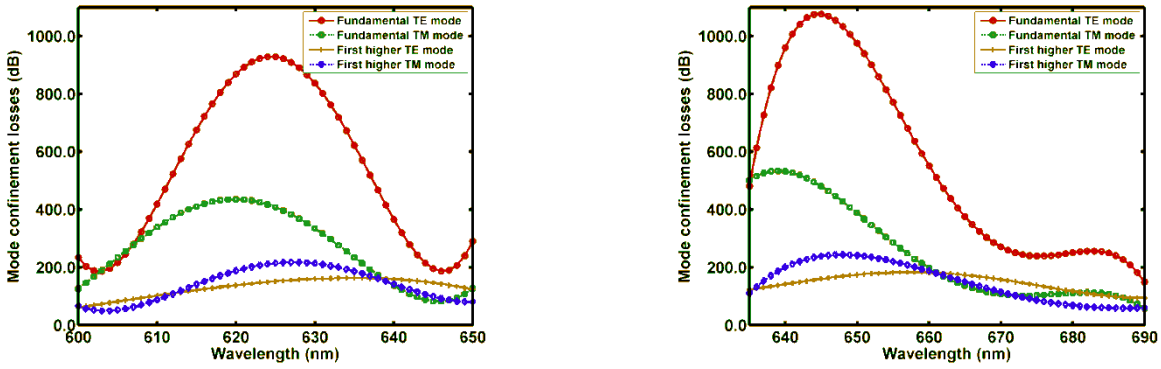

Fig. 1. Loss spectra of two fundamental and the first two higher order modes of the PCF when the analyte refractive index is changed from (a) 1.33 to (b) 1.34.

References

[1] E.K. Akowuah, T. Gorman, H. Ademgil, S. Haxha, G.K. Robinson, J.V. Oliver, "*Numerical Analysis of a Photonic Crystal Fiber for Biosensing Applications*," *Quantum Electronics, IEEE Journal of*, *48*(11), 1403-1410.

Highly sensitive D shaped PCF sensor based on SPR for near IR

Jitendra Narayan Dash and Rajan Jha*
Nanophotonics and Plasmonics Laboratory, School of Basic science, IIT Bhubaneswar, India
*rjha@iitbbs.ac.in ; rajaniitd@gmail.com

We propose a D-shaped photonic crystal fiber (PCF) based surface plasmon resonance (SPR) sensor using indium tin oxide (ITO) as a plasmonic metal. An optimized thickness of 70 nm is considered to be deposited on the flat surface to give R.I sensitivity of 5000 nm/RIU.

Introduction

Surface plasmon is the collective oscillation of electrons at the metal dielectric interface. In near IR ITO act as a plasmon active metal [1] and it has no band to band transition unlike other plasmon active metals.

Summary

The cross-section of the proposed structure is shown in Fig 1(a). The average diameter of the core is 35 μm while the total diameter of PCF is 335 μm. The air holes have diameter of 11.5 μm and a pitch of 23 μm. The D- shaped PCF can be fabricated by side polishing technique or by controlled etching process. The analyte can be easily placed on the flat surface of the proposed sensor and there is no need to fill the voids of PCF. The proximity of flat surface to the core of PCF helps in better coupling of light from core of the PCF to ITO- analyte interface. We used finite element based software to simulate the proposed structure.

Results

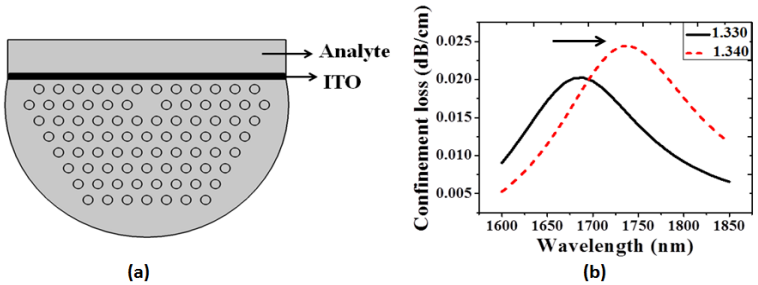

Fig. 1. (a) and (b) show the cross-section of the D- shaped PCF and shift of resonance peak respectively

When the R.I of analyte surrounding the D shaped PCF is increased from 1.330 to 1.340, the resonance peak shifts from 1690 nm to 1740 nm as can be seen in Fig.1(b). This shift occurs so as to satisfy the resonance condition at higher wavelength for the excitation of surface plasmon. From the shift of resonance peak, the wavelength sensitivity of the proposed sensor can be calculated to be 5000 nm/RIU.

Conclusion

A SPR sensor based on D-shaped PCF has been proposed. The resonance is observed in near IR and the wavelength sensitivity is found to be 5000 nm/RIU.

References

[1] J. N. Dash and R. Jha, "Surface plasmon resonance biosensor based on polymer photonic crystal fibers coated with conducting metal oxide," IEEE PTL. vol. 26, no.6, March 2014.

Numerical Analysis of a Hollow-Core Coaxial Fiber Biosensor

T. Monti[1,*], G. Gradoni[2]
[1]*National Center for Industrial Microwave Processing, University Of Nottingham, United Kingdom*
[2]*School of Mathematical Sciences, University Of Nottingham, United Kingdom*
*tamara.monti@nottingham.ac.uk

A multilayered coaxial fiber biosensor is investigated numerically. It is found that the results validate previous theoretical predictions achieved through the Transfer Matrix Method. In particular, we calculate the dispersion diagram of an optimized version of the biosensor.

Working principle

Recently, the Authors have proposed a hollow-core coaxial biosensor for selective and sensitive detection of proteins within a fluid compound [1]. It consists in a Bragg fiber with hollow core, and cladding made of layers alternating low and high refractive index materials. A particular manufacturing strategy, involving a fiber rolling procedure, can be exploited to obtain empty cladding layers. The empty part of the cladding, which can be filled by the analyte, corresponds to low-index layers *(n=1.33)*. The high-index cladding layers *(n=1.6)*, actually exposed to the fluid, are properly functionalized (unperturbed condition) so that they can selectively bind a target protein (perturbed condition). The very high sensitivity of Bragg-like structures to perturbations allows for detecting a relatively small quantity of target protein once the binding has occurred.

Theoretical analysis

The electromagnetic behavior of the structure has been investigated through the TMM formulation [2]. It is possible to find the stop-bands of the structure by applying the procedure described in [1], which takes into account the number of layers of the fiber. The procedure relies on an approximated condition that is accurate only for a large number of layers. The resulting confinement losses must then be evaluated in case of small number of layers.

Numerical validation

Based on the previously proposed design [1], a 20-layers hollow-core coaxial fiber (HCCF) sensor has been simulated through a commercial electromagnetic software (COMSOL Multiphysics©).
The values of the effective mode index, predicted by the theory and calculated exactly through the numerical simulations, are in good agreement.

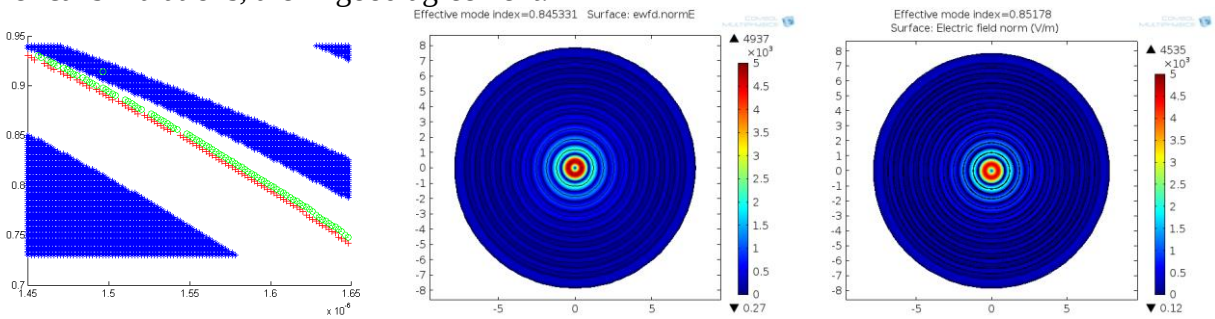

Fig. 1. Dispersion diagram from TMM formulation (left); transversal E field plot for the unperturbed and perturbed cases

Conclusion

We have shown, through an accurate FEM-based numerical analysis, the effectiveness of hollow-core coaxial fiber biosensors. Further work is ongoing towards the optimization of a recently proposed structure, based on both the theoretical and the numerical analysis.

References

[1] Monti, T.; Gradoni, G., *IEEE J. Select. Top. Quant. Electr.*, vol.20, is.2, pp.134-142, 2014
[2] Yeh, P.; Yariv, A.; Marom, E., *JOSA*, vol. 68, is. 9, pp. 1196-1201, 1978

SESSION 5

Modelling of Resonators and Photonic Devices

Modal approach for absorptive and dispersive resonators

J. Yang[1], P. Lalanne[1,*], C. Sauvan[2], J.P. Hugonin[2], M. Perrin[3]

[1]*Laboratoire Photonique Numérique et Nanosciences, Université Bordeaux, Institut d'Optique d'Aquitaine, CNRS, France*

[2]*Laboratoire Charles Fabry, Institut d'Optique, CNRS, Université Paris-Sud, France*

[3]*Laboratoire Ondes et Matière d'Aquitaine, Université Bordeaux, CNRS, 33405 Talence, France.*

*philippe.lalanne@institutoptique.fr

We propose an efficient and intuitive formalism (valid for lossy and dispersive resonators) to describe light scattering by a resonant metallic nanostructure. We apply it to various problems in quantum plasmonics, plasmonic sensing and spatial coherence in complex media.

Introduction

Micro-nanoresonators play an important role in the conversion of energy from localized fields to radiating waves and have many applications, especially in sensing, nonlinear nano-optics, or quantum optics. An interesting question is how to recover a diffracted field with the modes as building blocks. This can be done by expanding any diffracted field on the complete (?) basis of the eigenmodes. The coefficients in the expansion express the coupling between the sources and a given mode, revealing the conditions of excitation of this mode when varying incident parameters. The latter has a physical meaning of fundamental importance: once a mode is excited, it cannot transfer its energy to another mode. Such modes are usually referred to as normal modes in the literature.

Summary

However, normal-mode theories rely on the fact that energy dissipation in the system remains small enough. This key assumption may remain approximately valid for dielectric microresonators, but completely breaks down for metallic nanoresonators that confine light at a deep-subwavelength scale, for which radiative leakage and absorption and thus dispersion losses are generally large. Studying such systems with usual normal-mode theories does not give satisfying predictions.
In 2013, our group has made a significant step forward [1], by deriving analytical expressions for the coupling coefficients. The mathematical derivation that relies on reciprocity arguments is fully rigorous, the only hypothesis being on the completeness of resonance-mode basis used to expand the scattered field. Except for this hypothesis that is at least valid if the dispersion is weak, the derivation is mathematically sound. The same year, we have also proposed a simple and general numerical method [2] that allows us to compute and normalize the resonance modes with any Maxwell solver.

The talk will review some consequences of the formalism including

- LDOS modal theory (Purcell factor) [1]
- Modal theory of the spatial coherence in complex systems [3]
- Quantum formalism for the analysis of hybrid systems made of quantum emitters and plasmonic nanoresonators, which provides closed-form expressions for the hybrid-system optical response [4]
- An analytical treatment for complex-valued resonance shifts for plasmonic sensing [5]

Conclusion

Even if the proper limits for the validity of the approach are not yet established, we believe that the proposed analytical methods could certainly have their appeal as they focus on the most relevant concepts (the modes), as opposed to numerically complex but often confusing outputs of computational experiments.

References

[1] C. Sauvan, *et al*., Phys. Rev. Lett. **110**, 237401 (2013).

[2] Q. Bai, *et. al.,* Opt. Exp. **21**, 27371 (2013).

[3] C. Sauvan, *et al.*, Modal Representation of Spatial Coherence in Dissipative and Resonant Photonic Systems. Phys. Rev. A. **89**, 043825 (2014).

[4] J. Yang *et al.*, Analytical formalism for the interaction of two-level quantum systems with metal nanoresonators (submitted to PRX).

[5] J. Yang, H. Giessen and P. Lalanne, Closed-form expression for the frequency shifts of perturbed localized plasmon resonances (submitted to NL)**.**

Extraordinary Angular Tolerance of Cavity Resonator Integrated Grating Filters

N.Rassem[1,*], A-L.Fehrembach[1], E.Popov[1]
[1]*Université d'Aix-Marseille, CNRS, Centrale Marseille, Institut Fresnel UMR 7249, 13013 Marseille, France*
**nadege.rassem@fresnel.fr*

Cavity-Resonator-Integrated Guided-mode resonance Filter (CRIGF) is a promising structure which provides resonances with small spectral width (smaller than 1nm for optical wavelengths) and an extra-wide angular acceptance (several degrees). The extraordinary flattening of the dispersion curve is analyzed and explained as due to the intra-mode coupling imposed by the external Bragg resonators.

A CRIGF is composed with a grating coupler (Guided-Mode Resonance Filter - GMRF) surrounded by a Distributed Bragg Reflector (DBR) used to confine the excited guided mode [1, 2]. The angular acceptance of this structure is an order of magnitude greater than with classical gratings and our goal is to identify the phenomenon responsible for this extraordinary high angular acceptance. To begin, we plot on Fig 1 the reflectivity of the CRIGF with respect to the polar angle of incidence θ and the wavelength λ. The calculations are performed with a RCWA-based homemade code [3] (using the "super-cell technic). We observe a spot around λ=865nm and for θ between -2 and 2° where the reflectivity is maximum. The map in Fig.1 is very different from that obtained with an infinite grating, composed with the Bragg grating on top of the GMRF grating (not shown here). To explain this difference, we use an original approach based on the resolution of the homogeneous problem [4]. On one hand, we numerically calculated the dispersion curves for the CRIGF. We observed that the dispersion curve shows a flat part, where the resonance wavelength is quasi-independent of the angle of incidence, and that the flattening grows with the width (strength) of the Bragg reflector. On the other hand, we developed an approached model based on the coupled mode theory, which leads, again, to dispersion curves with a flat part. Moreover we deduce that the extraordinary flattening is due to an additional coupling of the waveguide modes of the GMRF provided by the Bragg grating, that does not occur in infinite gratings.

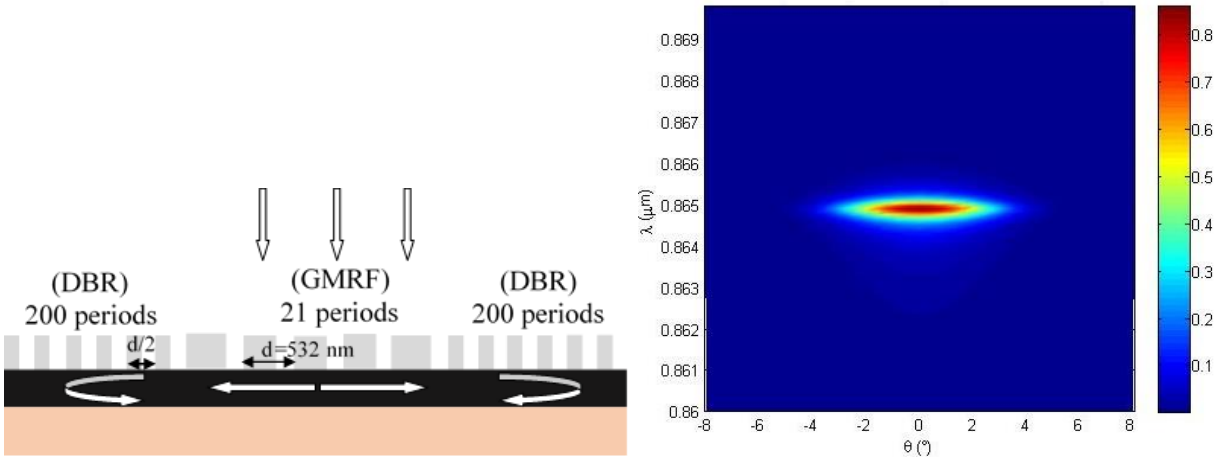

Fig. 1. Structure of the CRIGF and its R (θ, λ) map

References

[1]X. Buet, E. Daran, D. Belharet, F. Lozes-Dupuy, A. Monmayrant, and O. Gauthier-Lafaye, *"High angular tolerance and reflectivity with narrow bandwidth cavity-resonator-integrated guided-mode resonance filter,"* Opt. Expr., **20**, 9322-9327 (2012)

[2]K. Kintaka, T. Majima, K. Hatanaka, J. Inoue, and S. Ura, *"Polarization-independent guided-mode resonance filter with cross-integrated waveguide resonators,"* Opt. Lett., **37**, 3264-3266 (2012)

[3]Li, L. *"New formulation of the Fourier modal method for crossed surface-relief gratings"* J. Opt. Soc. Am. A, 1997, 14, 2758-2767

[4]N. Rassem, A.-L. Fehrembach, E. Popov *"Waveguide mode-in-the box with extra flat dispersion curve",* accepted for publication in J. Opt. Soc. Am. A.

Threshold Preservation of PT-Resonant Structures in Realistic-Dispersive Medium

S. Phang[1,*], A. Vukovic[1], S. Creagh[2], T. M. Benson[1], P. Sewell[1], G. Gradoni[2]
[1]*George Green Institute for Electromagnetics Research, Faculty of Engineering, University of Nottingham, UK*
[2]*School of Mathematical Sciences, University of Nottingham, Nottingham, UK*
*sendy.phang@nottingham.ac.uk

The impact of material dispersion in the performance of parity-time (PT) symmetric coupled microresonators is studied. The eigenfrequencies of the coupled PT-system are analysed for different dispersion parameter. We show that realistic dispersion preserves the PT-system with additional stabilising features.

Results and discussions

Photonic structures with balanced gain and loss, known as PT-symmetric structures, have been a subject of intensive investigation theoretically and experimentally, mainly due to the signature properties of the threshold point. Several applications exploiting the unique properties of PT-structures at the threshold point have been proposed such as, logical gate, memory, cloaking, and sensors. In this paper, we study the existence of the threshold point for PT-coupled microresonators and realistic dispersive material parameters that satisfies the Kramers-Kronig relationship.

The complex eigenfrequencies of PT-coupled microresonators are shown in Fig. 1 for three different dispersion parameters in the notation of [1], namely (A) non-dispersive, (B) weakly dispersive $\omega_\sigma \tau = 1$ and (C) $\omega_\sigma \tau = 212$ [2] for a realistic high dispersion. It can be seen that there is a distinct PT threshold in the case of non-dispersive (A) and highly dispersive (C) cases, but not in the case of weak dispersion (B). This is due to the fact that the gain/loss parameter alters the real part of refractive index of the material resulting in a structure that no longer satisfies the PT condition of $n = n^*$ in the case of weak dispersion, but is maintained in the case of high dispersion.

In the talk, we will discuss the implications of dispersion on the performance of PT-coupled microresonators and why the threshold point is preserved in the case of realistic material dispersion. Furthermore, it will be shown that practical dispersion only allows the PT-symmetric condition to be met at a single frequency which consequently also forbids multi-mode PT-symmetry breaking.

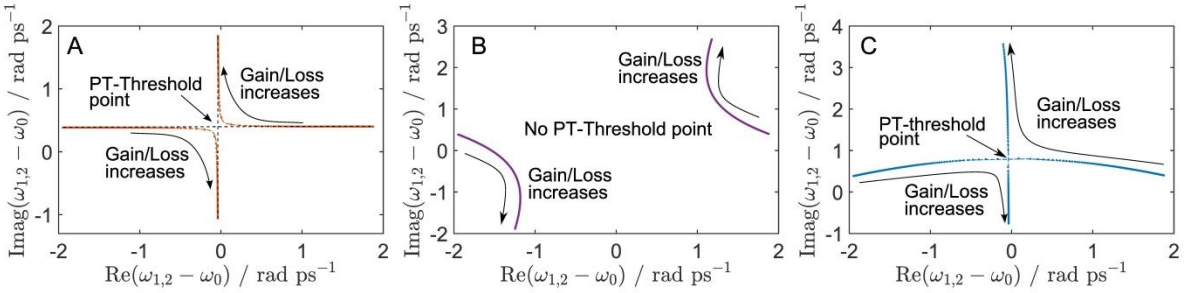

Fig. 1. Complex eigenfrequencies of PT-coupled microresonators for 3 different dispersion parameters, i.e. (A) non-dispersive, (B) small dispersion $\omega_0 \tau = 1$ and (C) realistic high dispersion. The structure is operated at a low *Q*-factor mode (7,2). Radius of each resonator $a = 0.54\mu m$, gap between resonators $g = 0.24\mu m$. For material model refer to [1].

References

1. S. Phang, A. Vukovic, H. Susanto, T. M. Benson, and P. Sewell, "Impact of dispersive and saturable gain/loss on bistability of nonlinear parity-time Bragg gratings.," Opt. Lett. **39**, 2603–6 (2014).
2. S. C. Hagness, R. M. Joseph, and A. Taflove, "Subpicosecond electrodynamics of distributed Bragg reflector microlasers: Results from finite difference time domain simulations," Radio Sci. **31**, 931–941 (1996).

Generation of Higher Dimensional Modal Entanglement

Divya Bharadwaj[1], K. Thyagarajan[1,*], Michal Karpinski[2] and Konrad Banaszek[3]
[1]*Department of Physics, IIT Delhi, New Delhi 110016, India*
[2]*Clarendon Laboratory, University of Oxford, Parks Road, Oxford, OX1 3PU, UK*
[3]*Faculty of Physics, University of Warsaw, Warsaw, Poland*
[*]*ktrajan@physics.iitd.ac.in*

We show that using a three waveguide directional coupler with appropriate waveguide dimensions and poling period it is possible to achieve high dimensional modal entanglement through type II spontaneous parametric down conversion process in a periodically poled lithium niobate substrate.

Introduction

Quantum states with higher dimensional entanglement provide larger information capacity and increased noise threshold in comparison to entangled system in two dimensions. In the literature several ways have been proposed to generate higher dimensional entanglement using orbital angular momentum (OAM) of photons [1], time- bin entanglement etc. In this paper, we propose a device for the generation of high dimensional entanglement using the modal basis in a three waveguide directional coupler.

Theory

Consider a directional coupler consisting of three identical single mode waveguides such that it supports three normal guided modes referred to as 0, 1 and 2. Using an adiabatic evolution we excite the *H*-polarized fundamental symmetric pump mode which due to parity conservation can only down convert to following pairs of modes of signal and idler of orthogonal polarization: $H_{s0}V_{i0}$; $H_{s1}V_{i1}$; $H_{s0}V_{i2}$; $H_{s2}V_{i0}$ and $H_{s2}V_{i2}$, where H and V correspond to horizontal and vertical polarization states, subscripts s and i correspond to signal and idler and the integer corresponds to the mode number. In order to achieve higher dimensional entangled photon pairs, we need to properly design the waveguides and their separation so that three of the above mentioned processes occur with the same probability. In order to show that this is possible, we choose the following three process: $H_{s0}V_{i0}$; $H_{s1}V_{i1}$ and $H_{s2}V_{i2}$. In such a case the output is expected to be an entangled state given by: $|\psi\rangle = C_1|H_{s0},V_{i0}\rangle + C_2|H_{s1},V_{i1}\rangle + C_3|H_{s2},V_{i2}\rangle$, where, C_1, C_2 and C_3 are constants which are determined by the field overlap integral and the phase matching function. The output state will be maximally entangled if the values of coefficients C_1, C_2 and C_3 becomes equal.

Result

As an example we consider type II SPDC in a three waveguide directional coupler with waveguides of width 6 μm, depth 7 μm, and separated by 6 μm and having a poling period Λ = 6.92 μm in a $LiNbO_3$ substrate (Fig.1 (a)). In such a case a single grating can lead to all the three processes with almost equal overlap integrals. Figure 1(b) shows the variation of efficiency with signal wavelength and as can be seen it is possible to generate high dimension mode entangled state by using a narrow band wavelength filter at the specific wavelength of 1350 nm.

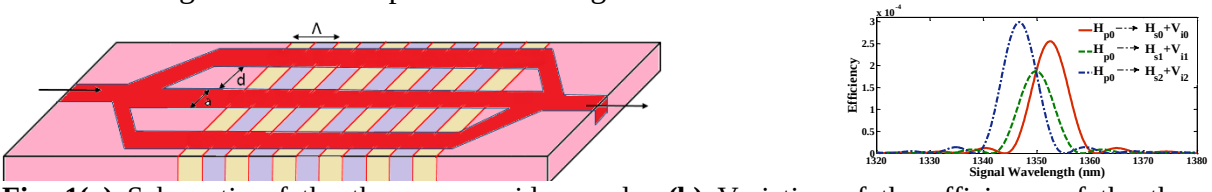

Fig. 1(a) Schematic of the three waveguide coupler **(b)** Variation of the efficiency of the three down conversion processes versus signal wavelength.

References

[1] Alois Mair, Alipasha Vaziri, Gregor Weihs, and Anton Zeilinger, Nature **412**, 313 - 316 (2001).

SESSION 6

Photonic Crystals and Nanostructures

Photonic Control of Thermal Radiation Leading To Radative Cooling

Shanhui Fan[1,*], Aaswath Raman[1], Linxiao Zhu[1], Marc Anoma[1], and Eden Rephaeli[1]
[1]*Ginzton Laboratory, Stanford University, Stanford, CA 94305*
*shanhui@stanford.edu

We discuss some of our latest work of designing photonic structures for the control of thermal radiation. We show that such control leads to new application opportunities, including daytime radiative cooling and solar cell cooling.

Introduction

The earth atmosphere is transparent in the wavelength range between 8-13 micron. This range coincides with the peak emission of thermal body at room temperature. A properly designed photonic structure can therefore be used to achieve radiative cooling, leading to the possibility for exploiting the cold universe as a thermodynamic resource [1].

Summary

Here we present recent results from two experiments. In the first experiment [2], we show that by designing a photonic structure that reflects most of the sunlight, while having strong thermal emission in the 8-13 micron window, we can achieve daytime radiative cooling, through which the structure, through sky access, lowers its temperature below that of the ambient, in an entire passive manner. In the second experiment, we show that related concepts can be used to cool a silicon solar absorber without affecting its solar absorption [3].

Results

Fig. 1. Daytime radiative cooler in a roof top experiment.

Conclusion

The cold universe represents an enormous thermodynamic resource that has been under-exploited. Photonic structure design represents the key in using such resource for energy applications.

References

[1] E. Rephaeli, A. Raman, and S. Fan, "Ultrabroadband photonic structures to achieve high-performance daytime radiative cooling", Nano Letters, vol. 13, pp. 1457-1461 (2013).

[2] A. P. Raman, M. A. Anoma, L. Zhu, E. Rephaeli, and S. Fan, "Passive radiative cooling below ambient air temperature under direct sunlight", Nature, vol. 515, pp. 540-544 (2014).

[3] L. Zhu, A. Raman and S. Fan, "Radiative cooling of solar absorbers using a photonic crystal functioning as a visibly transparent thermal blackbody" (submitted).

Simulation of high-speed nanophotonic modulators based on electrical and two-photon absorption injection

S.N. Kaunga-Nyirenda[1*], H.K. Dias[1], S. Bull[1], J.J. Lim[1], G. Bellanca[2], and E.C.Larkins[1]

[1] *Electrical Systems & Optics Research Division, University of Nottingham, United Kingdom*

[2] *Department of Engineering, University of Ferrara, Ferrara, Italy*

*simeon.kaunga-nyirenda@nottingham.ac.uk

We present the design and simulation of an ultracompact, high-speed photonic crystal modulator whose operation depends on strong spatio-temporal coupling of the photon and carrier populations. We discuss the dynamics and performance of electro-optic modulators based on electrical and optical injection, respectively.

Summary

Numerical modelling continues to play an important role in the design and development of novel device structures and technologies. Advanced simulation tools are required for the accurate, physics-based simulation of active nanophotonic devices, whose functionality is achieved by the perturbation of the dielectric response function of the material. The dielectric response function is strongly dependent on the electron and hole densities. At the same time, the electron and hole distributions are strongly influenced by the optical fields through stimulated recombination and absorption processes. A self-consistent dynamic simulation tool is required to accurately describe the coupled electronic, thermal and electromagnetic properties of active nanophotonics devices. A dynamic 2D bipolar electrical/thermal solver is bidirectionally coupled to a computationally efficient coupled-mode theory (CMT) model [1] (Fig. 1 far left), which is calibrated by FDTD. The coupled CMT/electrical model has the advantage of being computationally more efficient than an FDTD solver so that longer simulations can be performed, while still sufficient to investigate most important features and faithfully representing its electrical response (including the use of electrical input signals/biases).

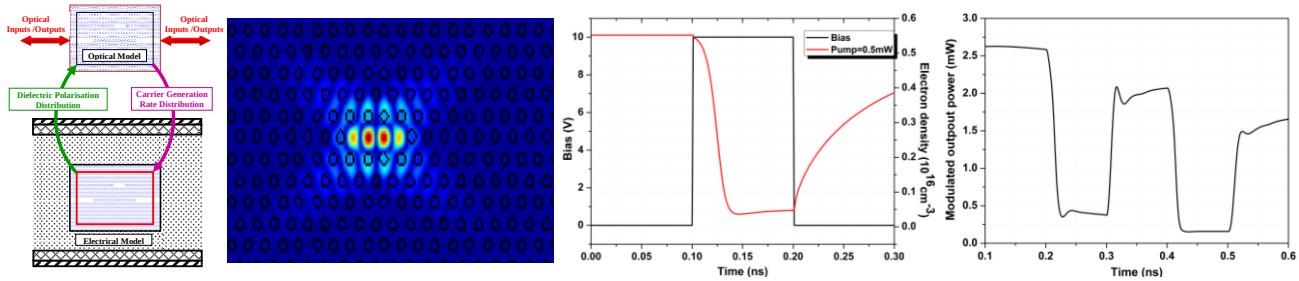

Fig. 1. Far left: Block diagram of coupled electrical/CMT model. Left: Mode profile in L3-PhC cavity from FDTD. Right: Time variation of bias voltage and carrier density. Far right: Modulated output (10 Gb/s bias signal).

Conclusion

We report on the design and simulation of an ultracompact (~50 μm^2) nanophotonic electro-optic modulator capable of high speed modulation (>30 Gbps). We will investigate several performance metrics and compare the performance of electro-optic modulators based on electrical and two-photon absorption injection.

References

[1] H. Dias, S.N. Kaunga-Nyirenda, J.J. Lim, A.J. Phillips and E.C. Larkins, *Modelling the dynamics of a micro-cavity switch*, IET Optoelectronics, 8 (2), 58-63, 2014.

Interrogating Nanoparticles with Focused Doughnut Pulses

T. A. Raybould[1], V. A. Fedotov[1], N. Papasimakis[1,*], I. Youngs[2], N. I. Zheludev[1,3]
[1]*Optoelectronics Research Centre, University of Southampton, Southampton, United Kingdom*
[2]*DSTL, Salisbury, United Kingdom*
[3]*Centre for Disruptive Photonic Technologies, Nanyang Technological University, Singapore*
*np3@orc.soton.ac.uk

We study the propagation properties of space-time localized single-cycle waveforms of toroidal symmetry and report on their light-matter interactions with interfaces and nanoparticles.

Focused doughnut (FD) pulses are part of a family of exact solutions to Maxwell's equations representing localised transmission of finite electromagnetic energy [1,2]. These are single-cycle pulses with toroidal field topology and polynomial energy localisation (Fig.1a) [2]. They exhibit an ultra-broadband frequency spectrum, which varies spatially. In addition, the toroidal topology of the pulse gives rise to significant longitudinal field components that hold potential for particle acceleration [2], but also resemble the field configuration associated with the toroidal dipole moment [3]. Here, we present a computational study of the FD pulse propagation properties and its interactions with dielectric and metallic interfaces, revealing unusual behaviour under reflection. Furthermore, the interactions of FDs with dielectric particles are considered, where the broadband nature and complex field topology of the pulses is expected to control mode excitation. Recent work has demonstrated broad modal excitation within the nanostructures and distinct differences between the interaction with TE and TM pulses (Fig. 1c). Possible experimental realisations of these complex electromagnetic perturbations resulting from the theoretical/computational treatment presented here will be discussed.

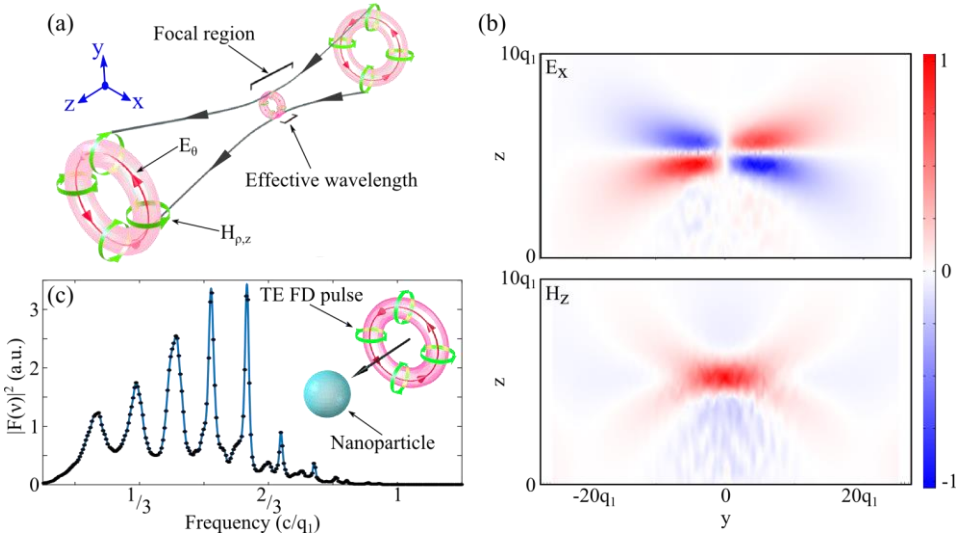

Fig. 1. (a) Illustration of the field topology and focusing properties of a TE FD pulse propagating along the *z*-axes. (b) E_x (upper) and H_z (lower) fields of the FD pulse with q_1 denoting the effective wavelength. (c) Excitation spectrum for a non-dispersive, dielectric nanoparticle (r=q_1) under FD illumination.

References

[1] R. W. Ziolkowski, *Localised transmission of electromagnetic energy*, Phys. Rev. A **39**, 2005 (1989)

[2] R. W. Hellwarth, P. Nouchi, *Focused one-cycle electromagnetic pulses*, Phys. Rev. E **54**, 889 (1993)

[3] T. Kaelberer et al., *Toroidal dipolar response in a metamaterial*, Science **330**, 1510 (2010)

Rigorous retrieval of linear and nonlinear parameters in graphene waveguides

A. Pitilakis[1,*], D. Chatzidimitriou[1], E. E. Kriezis[1]
[1]*Department of Electrical and Computer Engineering, Aristotle University of Thessaloniki, Greece*
*alexpiti@auth.gr

We outline a framework for the electromagnetic modelling of arbitrary cross-section nanophotonic waveguides that comprise both bulk and sheet materials, like graphene, based on the finite element method (FEM). Our formulation is extended to the analysis of third-order nonlinear effects in these waveguides.

Introduction

Graphene is a quasi-2D (sheet) material exhibiting remarkable thermal and electric conductivity with an ample tuning range in the optical and THz bands. Graphene has been successfully utilized in a number of guided-wave components like photodetectors, polarizers and modulators [1] and very recently its nonlinear response has started generating significant interest.

Summary

The optimal representation of a graphene sheet in the context of FEM modelling is effectuated by attributing a complex-valued surface conductivity to appropriate edges (or faces) shared by two surface (or volume) finite elements of the mesh. Furthermore, it is shown that the representation of graphene as a bulk medium of finite sub-nanometre thickness is inappropriate for the modelling of inherently anisotropic, arbitrarily oriented, sheet materials in $\mathbf{R}^3$ vector spaces and further requires substantially increased computational resources to mesh ultra-thin bulk layers. We extend our formulation to provide rigorous expressions for the calculation of the nonlinear parameter (γ) of arbitrary cross-section graphene-comprising waveguides. The third-order nonlinear part of the surface conductivity of sheet materials $\sigma^{(3)}$ complements the nonlinear susceptibility of bulk materials $\chi^{(3)}$ [2] and the contributions of the two nonlinearities to the overall γ are assessed.

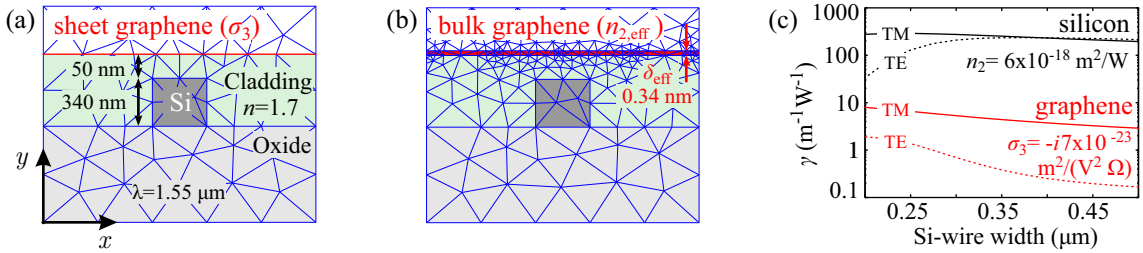

Fig. Sample finite element meshing of a Si-wire waveguide covered with a graphene monolayer, in its (a) sheet and (b) bulk representation. (c) Si-wire and graphene-sheet contributions to the nonlinear parameter.

Overall we provide a robust framework for the FEM modelling of graphene-comprising waveguides, in the linear and nonlinear regime. The natural and superior sheet representation of graphene is employed, thus circumventing the pitfalls of the effective bulk medium approach.

Acknowledgements

This work has been supported by European Union (European Social Fund) and Greek national funds through the Research Funding Program THALES (Project ANEMOS) and by the "IKY Fellowships of Excellence for Postgraduate Studies in Greece – Siemens Programme".

References

[1] M. Liu, X. Yin, X. Zhang, "Double-layer graphene optical modulator," *Nano Lett.*, vol. 12, no. 3, pp. 1482–5, 2012

[2] A. Pitilakis, E. E. Kriezis, "Highly nonlinear hybrid silicon-plasmonic waveguides: analysis and optimization," *J. Opt. Soc. Am. B*, vol. 30, no. 7, pp. 1954–65, 2013

Rod-type Photonic Crystals For Colloidal Quantum Dot Light Coupling

Y. J. Noori[1,*], J. Roberts[1], C. Woodhead[1], M. Young[1], R. J. Young[1]
[1]*Department of Physics, Lancaster University, United Kingdom*
*y.noori@lancaster.ac.uk

We present results from rod-type two-dimensional photonic crystals designed to efficiently couple colloidal quantum dots to semiconductor devices. Moderate Q factors for this type of cavities ensure the light-matter coupling remains in the weak regime, making the structures designed suitable for applications requiring bright quantum light sources.

Introduction

In recent years quantum light has found numerous applications including; quantum communications[1], beating the classical diffraction limit in quantum imaging[2] and minimising cell damage in the microscopy of biological systems.[3] Colloidal quantum dots are versatile sources of quantum light, having physical properties that are easily tuned to the demands of specific applications. It is difficult, however, to efficiently couple light emitted from them into other optoelectronic systems. In this paper, we introduce a rod-type photonic crystal template to couple emission from the dots to III-V semiconductor optoelectronics. The structure is designed to suite GaAs based applications, the 2D supercell contains dielectric rods in a triangular lattice with a cross-sectional radius of $0.18a$, where a is the lattice constant. The rods are surrounded by air, and have a dielectric constant of 12.11. The lattice is found to have a TE bandgap at $f = 0.83c/a$.

Results

Mode simulations of high Q candidate photonic crystal cavities were investigated using FDTD on a large computer cluster. Q-factors over 6000 were found after optimisation, as shown in Figure 1.

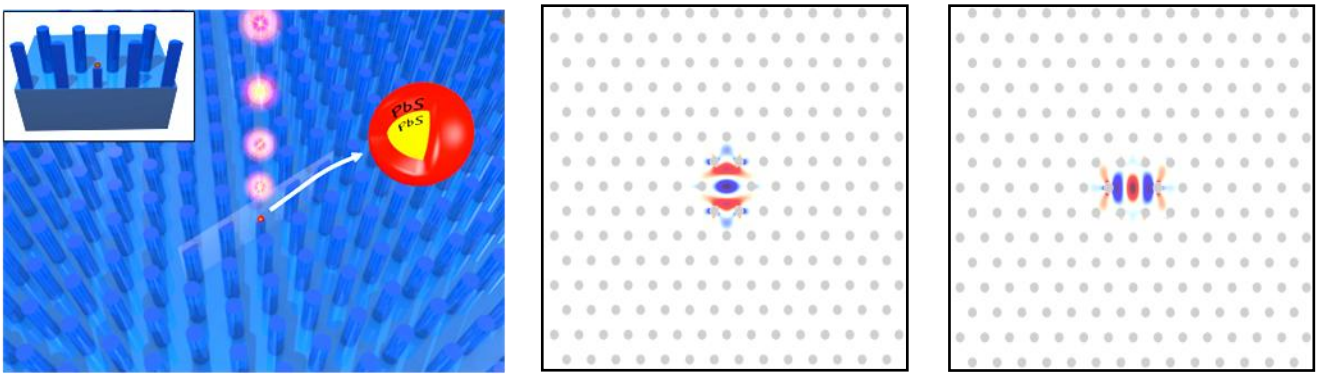

Fig. 1. An illustration of the proposed cavity structure with the simulated E_x and E_y field confinement.

Future Work

Following successful modelling, we have begun fabrication of the photonic crystal templates using e-beam lithography and Inductively Coupled Plasma. Next, colloidal quantum dots will be diluted, to a density designed to deposit a few on the half-height pillar, and then spun on to the template. This will allow coupling of the cavity mode to the emission from the dots, and will represent the first step in designing robust III-V quantum optoelectronic components relying on colloidal dots.

References

[1] N Gisin et al., Reviews of Modern Physics, 74, 145 (2002)
[2] R. M. Stevenson et al., Optics Express 15, 6507 (2007)
[3] V. Giovannetti, S. Lloyd, L. Maccone, Science 306, 1330 (2004)

Photonic and Plasmonic Quasicrystals

F. Mohammed[1,3], A. Quandt[1,2,3]

[1] *School of Physics, University of the Witwatersrand, Johannesburg, South Africa,*
[2] *DST-NRF Centre of Excellence in Strong Materials, University of the Witwatersrand,*
[3] *Materials for Energy Research Group, University of the Witwatersrand, Johannesburg, South Africa.*
faris@aims.ac.za

Abstract

A new numerical tool is introduced that extends the functionality of MPB [1] using perturbation theory. The photonic band structure for a dodecagonal quasicrystal is presented.

Introduction

Photonic Quasicrystals form a new class of materials which exhibit novel properties such as the localization of light [2]. The need for a sophisticated numerical tool to study such properties is essential. We present a simple method that generates quasicrystalline patterns [3] in addition to calculating photonic as well as plasmonic band structures.

Results

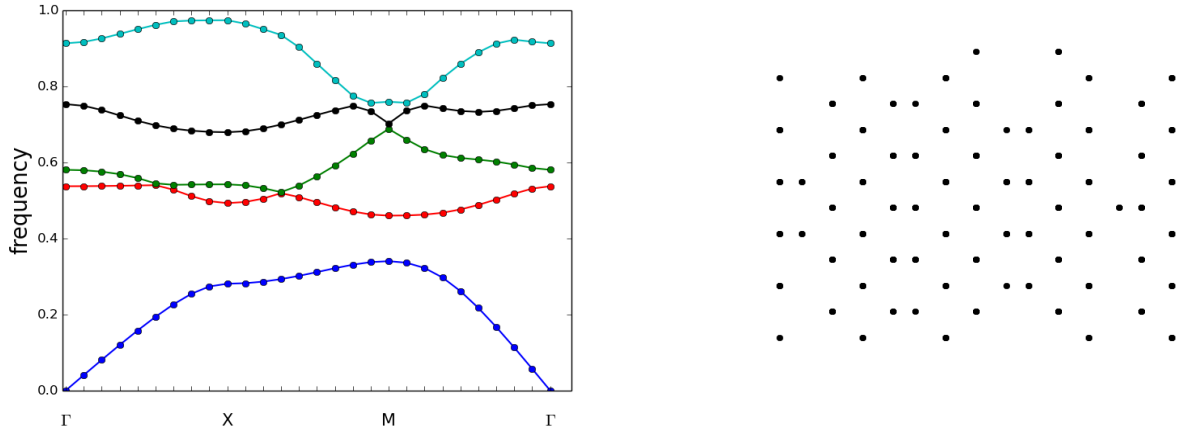

TM modes photonic band structure (left) for a single layer in a quasicrystal with dodecagonal symmetry (right).

Summary

We present a tool that forms a single entry point to a detailed analysis of photonic crystals and quasicrystals. One possible extension of the tool would be the use of dielectric functions which are obtained from ab-initio calculations or any other suitable form. This is under development.

References

[1] Steven G. Johnson and J. D. Joannopoulos, Block-iterative frequency-domain methods for Maxwell's equations in a planewave basis, Optics Express 8, no. 3, 173-190 (2001)
[2] Z. V. Vardeny, A. Nahata and A. Agrawal, Optics of photonic quasicrystals, Nature Photonics, Vol 7, 343
[3] S. I. Ben-Abraham and A. Quandt, Hybrid quasiperiodic-periodic structures constructed by projection in two stages, Acta Cryst. (2007). A63, 177–185.

SESSION 7

Modelling methods for Photonics

Simulation of photonic nanostructures - mixing nonlinear material theories with Maxwell solvers

J. Förstner
[1]*Theoretical Electrical Engineering group, University of Paderborn, Germany*
jens.foerstner@uni-paderborn.de

The progress in miniaturization of nanophotonic structures lead to a variety of fascinating systems, in which both near-field optical effects and quantum mechanics becomes important. A theoretical description is therefore challenging. We combine nonlinear material theories with advanced Maxwell simulation techniques like the Disontinuous Galerkin method to describe such systems.

Introduction

Meta materials, nano antennas, wave guides, micro resonators – the technological improvements of the recent decades made it possible to create photonic structures smaller than the wavelength of the light. Also, by suitable structuring one can influence the quantum mechanical properties of the nanophotonic system, e.g. to modify the energy structure by confining electrons or to enhance non-locality and nonlinearities.
The interplay of both phenomena – near field propagation and material dynamics – leads to vast possibilities in the tailoring for specific requirements of applications but is also a challenge concerning the derivation of consistent theoretical descriptions. In our approach we combine modern numerical techniques with advanced microscopic material theories: For the simulation of the near field light propagation we incorporate vector Maxwell solvers as the Finite Difference/Integral Time Domain (FDTD, FIT) and the Nodal Discontinuous Galerkin Time Domain (DG-TD) method. The nonlinear material dynamics requires advanced theories like the hydrodynamical plasma model or quantum mechanical Bloch equation. With this approach we are able to quantitatively simulate the nonlinear optics of a wide range of nanophotonic structures. As an example, second harmonic generation light emission in arrays of metallic particles will be discussed with a focus on the relevance of inter-particle coupling.

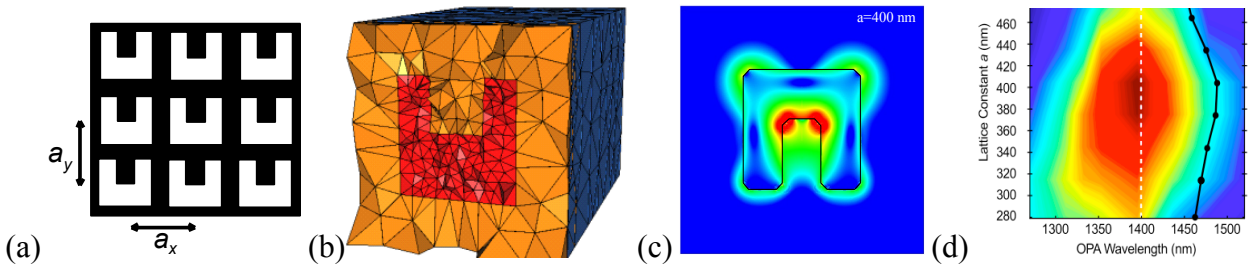

Fig. 1. (a) Considered array of gold split-ring resonators, (b) numerical mesh used in the Discontinuous Galerkin Time Domain method solving Maxwell equations combined with a nonlinear hydrodynamical material model, (c) emitted SHG field, (d) emission spectrum as a function of the lattice distance.

References

[1] S. Linden, F.B.P. Niesler, J. Förstner, Y. Grynko, T. Meier, M. Wegener, *Collective effects in second-harmonic generation from split-ring-resonator arrays*, Phys. Rev. Lett., 109, 015502, 2012

Modelling the coupling of electromagnetic waves to cylindrical waveguides with the Method of Lines

S. F. Helfert

FernUniversität in Hagen, Chair of Micro- and Nanophotonics, Universitätsstr. 27
58084 Hagen, Germany
stefan.helfert@fernuni-hagen.de

In this presentation we show how the coupling of electromagnetic fields to cylindrical wires can be modelled. The analysis is performed with cylindrical coordinates and the fields are expanded into a Fourier series. In this way only a one-dimensional discretization of the cross–section is required.

Introduction

In a recent experiment [1] was shown that Terahertz waves can be excited on a metallic wire via end-fire coupling. Due to different symmetries of the injected field and the wire mode some asymmetry has to be introduced. In this presentation we show how this coupling can be modelled numerically.

Numerical algorithm

For the simulation we used the Method of Lines (MoL see e.g. [2]). In the MoL the derivatives in direction of the cross-section are discretized with finite differences while analytic expressions are used in direction of propagation. Usually, a 2D-discretization is required to examine this three-dimensional problem. Here, however, we utilize that the wire has a cylindrical symmetry. Then, cylindrical coordinates are used and analytic expressions can be applied also for the the φ-dependency of the electric or magnetic field. Thus, the field is written in the following way:

$$F(r,\varphi) = \frac{1}{2}F_{c0}(r) + \sum_m \left(F_{cm}(r)\cos m\varphi + F_{sm}(r)\sin m\varphi\right) \qquad F_{c0}(r) = \frac{1}{\pi}\int_0^{2\pi} F(r,\phi)d\phi \quad (1)$$

With this formulation, the analysis only requires a one-dimensional discretization in radial direction. The important wire mode (Sommerfeld mode) does not depend on φ ($m = 0$). Therefore, we must only consider one element F_{c0}, which is determined as shown.

Numerical results

The developed algorithm was used to examine the coupling of the Terahertz-waves to a metallic wire. Without going into the details, we show the schematic setup in Fig. 1a, where the input field is shifted and tilted relative to the axis of the wire. A typical result for the calculated coupling power is plotted in Fig. 1b. Note, that the maximum occurs for a significant lateral offset (i.e., $\Delta x > 0$) and angular tilt ($\theta > 0$).

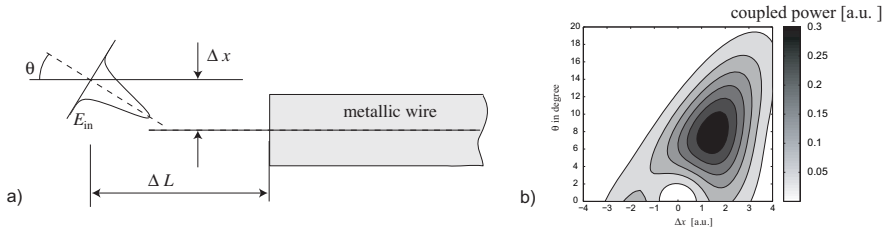

Fig. 1. Coupling an asymmetric field to a metallic wire; a) principle, b) coupled power

References

[1] A. Edelmann, L. Möller, and J. Jahns, *Electron. Lett.*, vol. 49, no. 7, pp. 884–886, 2013.
[2] R. Pregla, *Analysis of Electromagnetic Fields and Waves - The Method of Lines*, Wiley & Sons, Chichester, UK, 2008.

Computing 3-D Diffraction by Finite Difference Split-Step Nonparaxial Method

D. Bhattacharya[1, 2,*], A. Sharma[1]
[1]*Physics Department, Indian Institute of Technology Delhi, New Delhi, India*
[2] *Physics Department, Techno India University, Salt Lake, Kolkata, India*
*debjani112@gmail.com

We present highly accurate simulation of diffraction in 3-D using the finite difference split-step method. It shows better accuracy than the shifted angular spectrum method. Propagation of optical vortices is presented.

Theory and Results

The most widely used methods for simulation of diffraction are the Fresnel method and the angular spectrum method (AS). The Fresnel method cannot compute near-field diffraction and the AS can compute propagation near the source plane only, due to aliasing error of the sampled transfer function. Recently a shifted AS [1] has been proposed for computing both near and far field and off-axis propagation, but has lower accuracy due to use of a band limited function.

Earlier we published a Finite Difference Split-Step Nonparaxial (FDSSNP) method for scalar [2], semivectorial and bidirectional wave propagation in photonic devices. The method is a direct solution of the nonparaxial Helmholtz equation, and can compute nonparaxial, paraxial and also evanescent field propagation very accurately. It uses a higher order finite difference series and analytical matrix diagonalization. To simulate diffraction, the 3-D method [2] has been modified to avoid using block matrix multiplication, reducing memory and increasing computational speed by orders of magnitude. Diffraction over arbitrary distances is computed in a single propagation step,

$$\Phi(z) = \mathbf{P}\Phi(z_0), \quad \Phi = \mathrm{col}\left[\psi \quad \partial\psi/\partial z\right] \text{ and } \mathbf{P}\text{-propagation operator.}$$

In Example 1 original image size is 512×512 points, sampling=$10\mu m\times10\mu m$, $\lambda = 633nm$ [1]. The images are obtained by back propagating the diffracted field at 0.2m to object plane. FDSSNP has much higher accuracy for same and lower window size (Fig. 1) compared to shifted AS. Respective computation times are 7.1s and 2.9s, using MATLAB 7.11 on Intel Core i5, 4GB RAM. In Fig. 2 we show generation and propagation of an optical vortex at various distances from object plane. More results and comparison with experimental data will be presented at the workshop.

Fig. 1. Simulation of diffraction using shifted-AS and 3D FDSSNP.

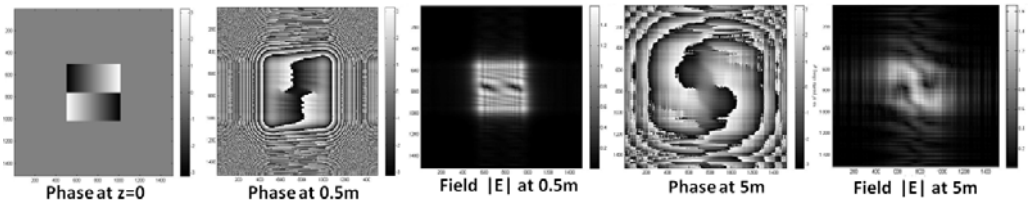

Fig. 2. Optical vortex propagation using 3DFDSSNP. Phase object courtesy Dr. Sanjay Mishra, IRDE, India.

References

[1] T. Shimobaba et al., Computer Physics Communications 183 (2012) 1124–1138
[2] D. Bhattacharya, A. Sharma, OWTNM2007, Copenhagen, Denmark, 2007.

Modified Finite Element Frequency Domain Using Gradient Smoothing Technique

Khaled S. R. Atia[1], A. M. Heikal[2], S. S. A. Obayya[1,*]
[1]*Center for Photonics and Smart Material, Zewail City of Science and Technology, Egypt*
[2]*Department of Electronics and Communication Engineering, Mansoura University, Mansoura, Egypt*
*sobayya@zewailcity.edu.eg

Introduction

The finite element method models complex geometries by discretizing the computational domain into triangular elements. In this paper, a computationally efficient modified finite element frequency domain (SFEFD) is proposed. The presented method has a superior convergence rate. It consumes less time than conventional finite difference frequency domain.

Formulation

Considering a 2D computational domain (Ω). The perfectly matched layer is used to truncate Ω. The gradient smoothing procedure is applied to the weak form of the TM wave equation as follows,

$$\nabla\Phi = \int_{\Omega_s} \frac{1}{A_s} \nabla\Phi d\Omega_s \,, \tag{1}$$

where Φ is the field function and A_s is the area of the smoothing domain (Ω_s). The integration is made over Ω_s which is constructed by simply connect the mid-point of the element to the two end points of each edge.

Results

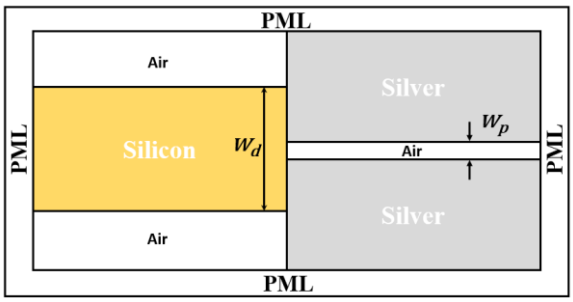

Fig. 1. Schematic diagram of the plasmonic coupler.

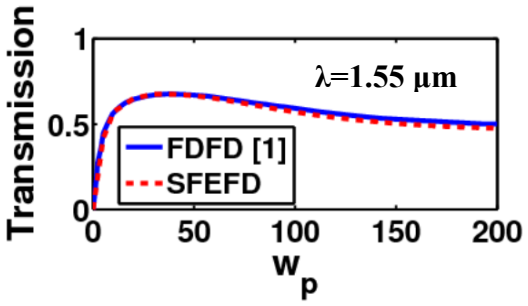

Fig. 2. Efficiency of the plasmonic coupler.

The plasmonic coupler shown in Fig.1 consists of a silicon waveguide of width W_d = 300 nm, and a plasmonic waveguide of gap size W_p varied from 0 to 200 nm. Figure 2 shows the transmission efficiency calculated at different W_p. The refractive index of silicon and silver are 3.47 and 0.409+10.048*i*, respectively. It may be seen an excellent agreement between the results obtained by SFEFD and the FDFD results [1]. The converged results are obtained by less number of unknowns and less computational time than the FDFD.

References

[1] G. Veronis and S. Fan, "Theoretical investigation of compact couplers between dielectric slab waveguides and two-dimensional metal-dielectric-metal plasmonic waveguides," Optics Express, vol. 15, no. 3, Jan 2007.

Reduced Basis Method for Fast Online Solution of Scattering Problems

S. Burger [1,2], M. Hammerschmidt [1], S. Herrmann [1] , J. Pomplun [2], F. Schmidt [1,2],

[1] *Zuse Institute Berlin, Germany*
[2] *JCMwave GmbH, Berlin, Germany*
frank.schmidt@zib.de

We present an adaptive, error controlled reduced basis method for solving parameterized optical scattering problems as they appear in many-query and real time contexts. Application fields are, among others, design and optimization problems of nano-optical devices as well as inverse problems for parameter reconstructions, as they occur, e. g., in optical metrology. The background technology is a finite element modeling of the problem plus parameterizations of materials, geometries and sources.

Reduced basis method

The basic concepts and first applications to nano-optics have been published in [1], [2]. Fig. 1 illustrates a simple situation. Given a geometry with three independent geometrical parameters p_1, p_2, p_3, one one seeks a realization with certain desired properties, here a phase-balanced throughput through the two openings. To this end, a large number of solutions with different parameter settings has to be performed. The reduced basis method offers an elegant approach. It is assumed that the solution process can be split into an online and an offline part. In the *offline step* the reduced basis is built self-adaptively by solving the underlying Maxwells equations rigorously several times. The full model is then projected onto the reduced basis spanned by these solutions. In the *online step* the assembled reduced system can be solved very quickly and independently on the size of the original problem. The method is efficient if the computational offline costs do not play a prominent role but the online costs for accurate 3D simulations are in the range of a few seconds, which is typically the case.

Algorithmic progress

Methods from the well established field of a posteriori error estimation of finite element methods are applied to guaranty the reliability of the computed output. Extensions with respect to previous publications concerns the inclusion of parameter dependent sources and frequencies.

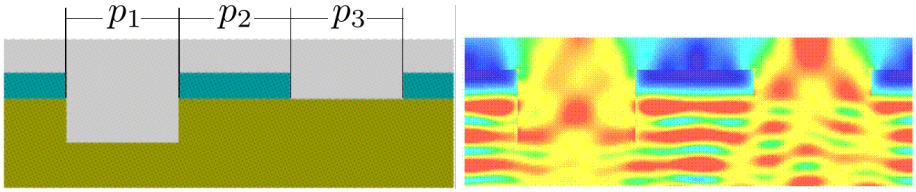

Fig. 1. A simple structure depending on three geometric parameters p_1, p_2, p_3 and the corresponding field. The parameters have to be varied such that the optical field is optimized.

References

[1] J. Pomplun and F. Schmidt. Accelerated a posteriori error estimation for the reduced basis method with application to 3d electromagnetic scattering problems. *SIAM J. Sci. Comput.*, 32:498 – 520, 2010.

[2] J. Pomplun, S. Burger, L. Zschiedrich, and F. Schmidt. Reduced basis method for real-time inverse scatterometry. In *Modelling Aspects in Optical Metrology III*, volume 8083, page 808308, 2011.

SESSION 8

Multiphysics effects in active and functional devices

Fundamental aspects of linear slow light systems

Luc Thévenaz
EPFL Ecole Polytechnique Fédérale de Lausanne ; Institute of Electrical Engineering, SCI-STI-LT Station 11, 1015 Lausanne, Switzerland
*luc.thevenaz@epfl.ch

In a linear slow light system the delaying process is necessarily inducing distortion for fundamental reasons, strictly bounding the maximum delay-bandwidth product to unity. Slowing the light does not directly enhance light-matter interaction, but is a corollary of the intensity enhancement by multiple interferences.

Context

A decade ago slow & fast light has been perceived like a very performing solution to control the timing of an optical signal, offering the yet missing photonics tool for timing control, with the ultimate objective to implement all-optical routers in telecommunications systems. It is essential that the delaying system is linear for such applications, to avoid power- and sequence-dependent timing. It has rapidly been observed that in such systems the delaying process was undermined by massive distortion when the induced fractional delay exceeds 1, i.e. when a light pulse is delayed by more than its nominal width. Experts have rapidly concluded that future all-optical routers won't certainly be based on slow light, for which other applications have been searched. Much hope has been placed in the possibility to enhance light-matter interactions, with some successful demonstrations, but here again it turns out that light slowing is not the essence of this enhancement.

Summary

Like in any linear system the slow light element is described by a transfer function that must ideally realize the perfect delaying function taking the simple following form $\exp(-i\omega\tau)$. This perfect transfer function shows a uniform spectral amplitude response and a linearly varying phase response. Slow light is generated using narrowband spectral resonances, for which amplitude and phase spectral dependences are related by a Hilbert transform, which translates into the Kramers-Kronig relations linking absorption to refractive index. It can be shown that a spectral resonance spanning over a limited spectrum can never simultaneously present a pure flat amplitude response and a pure linear phase response, leading to a distortion that cannot be circumvented.

Recent results have shown that the distortion can be reduced by optimizing the spectral profile of the resonance, but it can never be entirely cancelled, limiting the delay-bandwidth product to a value close to unity. This has been entirely validated by very recent experimental results.

Slow light systems are classified into 2 categories: *material* systems, in which a resonance is induced by a nonlinear interaction and optical pumping and subject to an energy transfer between the lightwave and the optical medium, and *structural* systems, in which the sharp spectral transmission change is induced by a passive structure generating multiple interferences. The most straightforward example of a structural system is the Fabry-Perot resonator.

Tuneable delays can be generated in material slow light systems, by varying the pumping power, which are active systems. Structural systems can normally not be tuned directly, since they are based on passive structures.

It has been proved that material slow light does not enhance light-matter interaction, since the excess energy density resulting from the slowing is actually entirely stored into the optical medium. On the contrary enhancement has been observed using structural slow light, since there is a direct relation between energy density and group velocity and the energy is this time uniquely present in the lightwave. This distinct behaviour proves that this is not the light slowing that strictly causes the interaction enhancement, but the light concentration through wave superposition that results in a higher intensity and has the automatic consequence to slow the group velocity.

Laser gain compact model for photonic integrated circuit (PIC) simulation

V. Pacradouni, J. Klein, V. Donzella, J. Pond*
[1]*Lumerical Solutions, Inc., Vancouver, Canada*
*jpond@lumerical.com

We present a semiconductor laser gain 1D compact model that runs within *INTERCONNECT*, Lumerical's PIC simulator, and self-consistently incorporates the effects of external feedback and resonances, allowing it to be used in the design of hybrid III-V Si-SiO_2 laser chips as well as integrated lasers driving PICs.

Introduction

The growth of silicon photonics has made the use of PICs with integrated lasers and hybrid III-V Si-SiO_2 laser chips more attractive. However, the unavailability of optical isolators for use in such systems, as well the design advantage of incorporating resonances and reflections external to and possibly distant from the gain medium, makes accurate and efficient modeling of laser performance critical to the design process.

Summary

We have developed a model which propagates the complex slowly-varying amplitudes of forward and backward traveling optical modes through the gain medium in the time domain on a 1D grid in the longitudinal direction. The transverse properties of each mode are characterized by scalar quantities such as effective and group index, wave impedance, and mode confinement to the gain region which can be accurately pre-calculated with an eigenmode solver. Frequency and local carrier dependent gain and stochastic spontaneous emission are included using digital filtering, and carrier concentrations are updated based on optical gain, spontaneous emission, and non-radiative recombination rates.

Results

We have obtained results for a Fabry-Perot laser that compare favorably with those presented in [1]. We have also obtained preliminary results, presented in Fig. 1(b), for the laser structure shown in Fig. 1(a), comprised of the same gain medium coupled via a waveguide to a DBR reflector.

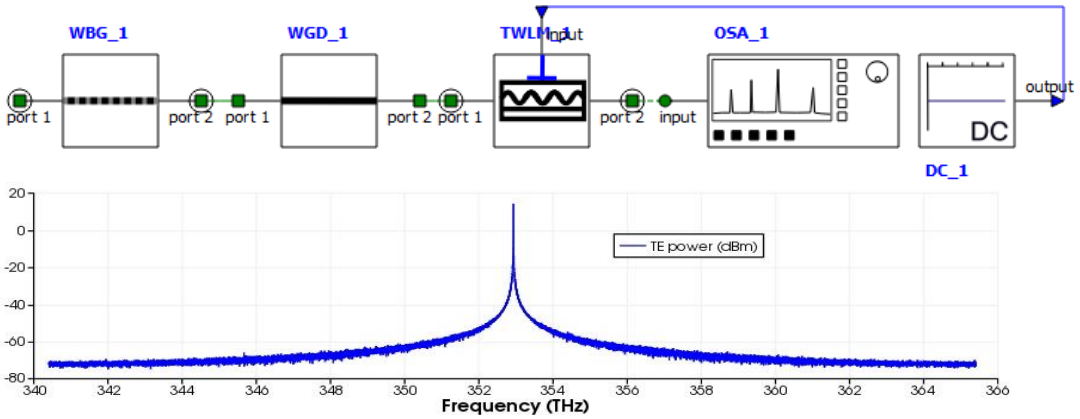

Fig. 1. Simulated DBR laser structure (a) and output spectrum (b)

References

[1] A.J. Lowery, *New dynamic semiconductor laser model based on the transmission-line modelling method*, IEE Proceedings, Vol. 134, Pt. J, No. 5, October 1987.

Diffraction properties of a tailored parity-time (PT) symmetric grating

N. X. A. Rivolta and, B. Maes

Micro- and Nanophotonic Materials Group, Faculty of Science, University of Mons, Belgium
nicolas.rivolta@umons.ac.be

We study the diffraction properties of a parity-time (PT) symmetric transmission grating. The bimodal interferometric operation is altered by the introduction of balanced gain and loss, leading to efficient switching around the symmetry breaking point. In addition, we separately tailor the periodicities of gain and loss to control the mode merging phenomenon.

Loss is usually an unwanted feature in optics, which limits the efficiencies of many applications. However, the concept of PT symmetry (originating from quantum mechanics) allows for a proper use of loss, when it is judiciously combined with gain. PT symmetry already facilitated various interesting and counter-intuitive phenomena, such as optical Bloch oscillations and loss induced lasing.

We numerically examine a diffraction grating (Fig. 1(a)) that was extensively discussed without loss/gain in [1]. By introducing gain and loss (quantified by γ) in the grating we can now uncover its rich transmission characteristics.

We identify different regimes, which are adjusted by the not-often studied longitudinal feedback (see Fig. 1(b) for the direct transmission T_0). The properties are explained by the propagating modes in the structure. Below a critical point (γ =0.23) the grating acts like a Mach-Zehnder interferometer, with a gain-controlled coupling length. Beyond this point there is one mode with gain (due to symmetry breaking), which provides us with lasing resonances.

In further work, we tailor the gain and loss periods separately, providing for more exotic characteristics, which mix various incidence cases and introduce multiple critical points. We explain these phenomena by examining the mode-merging picture in detail.

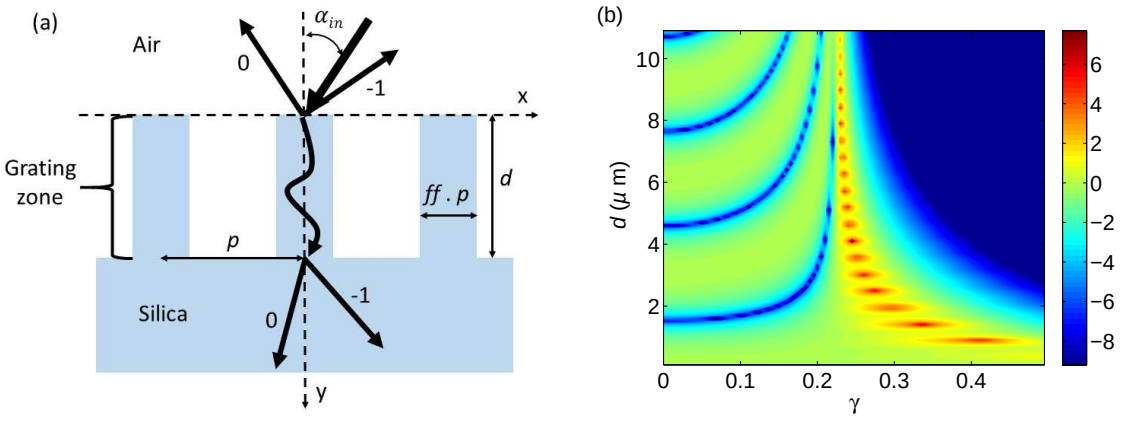

Fig. 1. (a) Diffraction grating with the reflection and transmission orders. (b) Transmitted light (log scale) to T_0 as a function of groove depth d and gain/loss factor γ.

References

[1] T. Clausnitzer, T. Kämpfe, E.-B. Kley, A. Tünnermann, U. Peschel, A. V. Tishchenko and, O. Parriaux, Opt. Express **13**, 10448 (2005).

CST STUDIO SUITE 2015

From Components to Systems. Simulate, Optimize, Synthesize.

From the first steps to the finishing touches, CST STUDIO SUITE® is there for you in your design process. Its tools allow engineers to develop and simulate devices large and small across the frequency spectrum. The powerful solvers in CST STUDIO SUITE 2015 are supplemented by a range of new synthesis and optimization tools, which are integrated directly into the simulation workflow. These can suggest potential starting points for component design, allow these components to be combined into systems, and finally analyze and fine-tune the complete systems.
Even the most complex systems are built up from simple elements. Integrate synthesis into your design process and develop your ideas.

Choose CST STUDIO SUITE – Complete Technology for EM Simulation.

Imaging and Spectroscopy Reimagined!

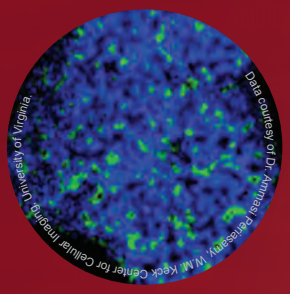

Microspectroscopy • Biomedical Imaging
Plasmonics • LIBS • Raman Hyperspectral Imaging
Carbon Nanotube Research • Singlet Oxygen
Detection Combustion • FLIM
• Small Animal Imaging
• Quantum Imaging

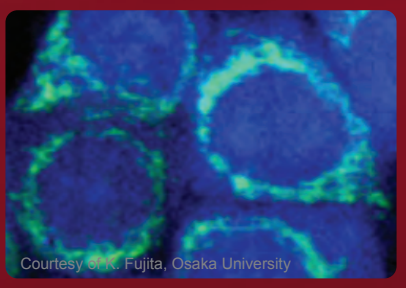

Princeton Instruments

Learn how our innovative products can facilitate your research.
Visit **www.princetoninstruments.com**
or call **+1 609-587-9797**

POSTERS 1

Friday 17th April

Equiangular Spiral Micro-Structured Waveguides in Lithium Niobate

H. Karakuzu, M. Dubov,* S. Boscolo
Aston Institute of Photonic Technologies, Aston University, Birmingham B4 7ET, UK
**m.dubov@aston.ac.uk*

Y. O. Azabi, A. Agrawal
City University London, London EC1V 0HB, UK

Buried, microstructured waveguides with an equiangular spiral geometry, which can be formed in a lithium niobate crystal by direct femtosecond laser writing, are analysed with the full-vectorial finite element method. The guiding properties of such waveguides are presented.

Summary

Micro-structured waveguides (MS WGs) can be fabricated in lithium niobate ($LiNbO_3$) crystals by the method of direct femotsecond (fs) laser inscription using the so-called depressed-index cladding approach [1]. In comparison with MS WGs with an hexagonal geometry, spiral geometries have been recently shown to achieve better confinement of light in much smaller cores [2]. The equiangular spiral (ES) WG design investigated in this paper is adapted from the design reported in [2]. Given the relatively moderate induced refractive index (RI) contrasts that are typical of the direct fs inscription in crystals, enhanced control over the waveguiding properties may be achieved by compact and dense cladding structures made of tracks with different sizes with the smallest tracks at the core-cladding interface. In this study, we used a suitable variation of the track size along each arm of the spiral structure [3], along with the experimentally found dependencies of the track size and the induced RI contrast on the laser pulse energy [1]. The anisotropic WGs were simulated using the COMSOL software. The results presented in Fig. 1 show that the spectral region where the confinement losses (i.e., the losses due to the finite transverse extent of the confining structure) in both ordinary (O) and extraordinary (E) polarisations are acceptably low (below 1 dB/cm) can extend up to a wavelength of 2.5 μm for the example WG structure being characterised. While the ES geometry seems not to be preferable to the conventional hexagonal geometry in terms of extent of the low-loss operational spectral range of the WG [3], the much broader parameter space available for the design of spiral WG structures makes it possible to efficiently tune the modal characteristics of the field in the WG. This may enable a broader range of nonlinear optical device applications with optimised WG performance at the wavelengths of interest.

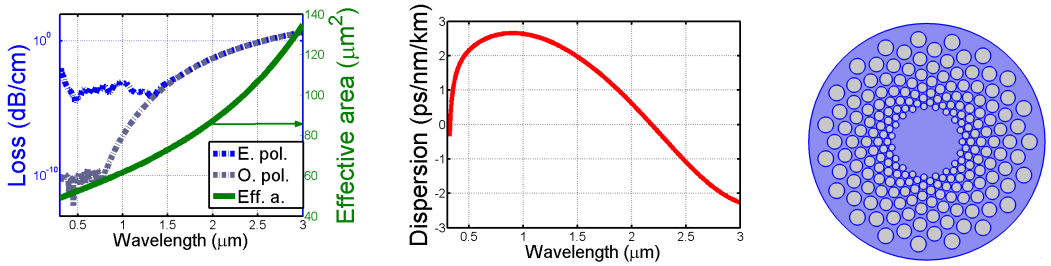

Fig. 1. Confinement loss (left) and WG dispersion (middle) for O and E waves as a function of wavelength for an ES WG with 19 arms and 11 rings (right). Also shown is the variation of the WG effective area with wavelength.

References

[1] M. Dubov, S. Boscolo, D. J. Webb, Opt. Mater. Express **4**, 1708 (2014).
[2] A. Agrawal, N. Kejalakshmy, J. Chen, B. M. A. Rahman, K. T. V. Grattan, Opt. Lett. **33**, 2716 (2008).
[3] H. Karakuzu, M. Dubov, S. Boscolo, L. A. Melnikov, Y. A. Mazhirina, Opt. Mater. Express **4**, 541 (2014).

Mid-infrared supercontinuum generation using dispersion-engineered $Ge_{11.5}As_{24}Se_{64.5}$ chalcogenide rib-waveguide

M. Rezaul Karim* and B. M. A. Rahman
School of Mathematics, Computer Science and Engineering, City University London, United Kingdom
**mohammad.karim.2@*city.ac.uk

A promising design of air-clad $Ge_{11.5}As_{24}Se_{64.5}$ chalcogenide rib-waveguide for supercontinuum (SC) generation is proposed through numerical simulations. It can be used for SC generation with up to 3-octaves bandwidth by pumping at a wavelength of 3100 nm with a peak power of 1 kW.

Introduction

Chalcogenide glasses have emerged as promising nonlinear materials having a number of unique properties that makes them attractive for fabricating planar optical waveguides and using them for applications such as mid-infrared (mid-IR) SC generation and optical sensing.

Summary

Dispersion of a waveguide plays an important role in determining the SC output spectrum along with the position of pump wavelength and peak power applied. By rigorous numerical simulations using our full-vector FE mode-solver, we have optimized our design to obtain the zero-dispersion wavelength (ZDW) with an anomalous dispersion region around the pump wavelength by varying the dimensions of the waveguide, as shown in Fig.1 (a). We have tested accuracy of the modal solutions through Aitken's extrapolation technique and also tested the numerically calculated GVD parameters as describe earlier [1]. We optimized an air-clad $Ge_{11.5}As_{24}Se_{64.5}$ rib-waveguide with MgF_2 glass as its lower cladding and obtained good modal confinement in such structure.

Results

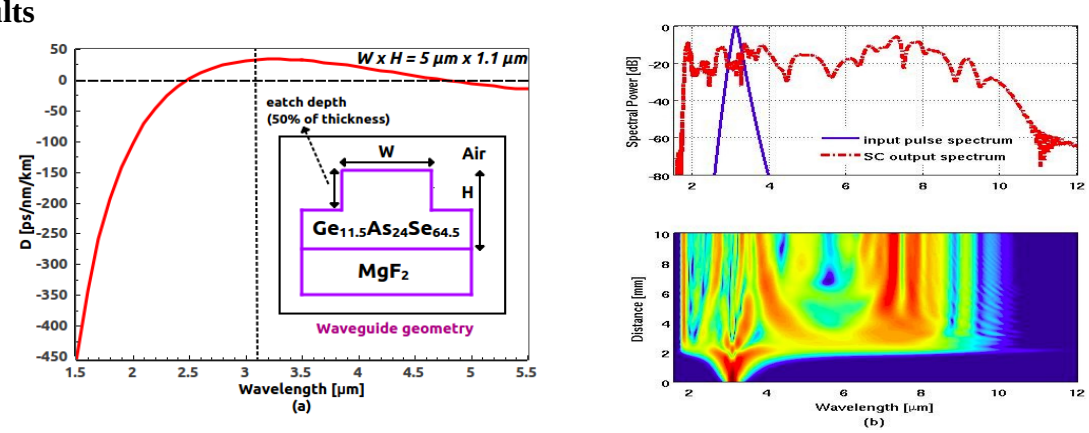

Fig. 1. (a) GVD Curve with waveguide structure as an inset and (b) SC evolution.

Conclusion

An air-clad rib-waveguide by employing MgF_2 glass as its lower cladding is optimized for a pump wavelength of 3100 nm to generate broadband SC in the mid-IR regime, as shown in Fig.1 (b).

References

[1] M. R. Karim, B. M. A. Rahman, and G. P. Agrawal, *Dispersion engineered $Ge_{11.5}As_{24}Se_{64.5}$ nanowire for supercontinuum generation: A parametric study*, Optics Express 22(25), 2014.

Effect of SPR on the attenuation coefficient of an Ormocomp nanowire

Charusluk Viphavakit[1]*, Sakoolkan Boonruang[2], Christos Themistos[1], Michael Komodromos[1], Waleed S. Mohammed[3], and B.M.Azizur Rahman[4]

[1]*Department of Electrical Engineering, Frederick University, Nicosia, 1036, Cyprus*

[2]*Photonics Technology Laboratory, NECTEC, Klong Luang, 10120, Pathumthani, Thailand*

[3]*BU-CROCCS, Bangkok University, Paholyotin Rd., Klong Luang, Pathumthani, Thailand*

[4]*Department of Electrical Engineering, City University London, London, UK*

*charusluk.v@gmail.com

Effect of surface plasmon resonance (SPR) on the attenuation coefficient of an Ormocomp nanowire with non-vertical sidewalls is studied. The attenuation coefficient of ormocomp nanowires is measured to be 0.84 dB/mm at the 595 nm SPR peak.

Summary

The Ormocomp nanowires reported here have been fabricated by using a nano-imprint method. However, during the fabrication process the resulting surface roughness increases the loss coefficient, but this also enhances the sensitivity of the nanowire sensors [1]. However, the effect of the surface roughness is not strong enough to maximize the sensitivity of the nanowires. Therefore, additionally surface plasmon resonance is introduced at the top surface of the nanowires to enhance the sensitivity. A 50 nm thick gold layer is coated on the nanowires using sputtering technique. The ormocomp nanowire has a height of 0.5 μm but with its trapezoidal shape, the top and bottom widths are different, 1.0 μm and 1.5 μm, respectively. The transmittance (*T*) of the light propagating along the nanowire with water-cladding was measured and the attenuation coefficient of the nanowires is extracted by using the Beer-Lambert Law, given in Eq. 1.

$$\alpha_{nw}(\lambda) = \frac{-\alpha_{wg}(\lambda)(L_o - 2L_{tp} - L_{nw}) - 2\alpha_{tp}(\lambda)L_{tp} - \ln(T_{nw})}{L_{nw}} \quad (1)$$

where L_o is 5000 μm, L_{tp} is 270 μm, and L_{nw} is varied from 250 to 2000 μm. The average attenuation coefficient of the feed waveguide and ormocomp nanowire is shown in Fig. 1.

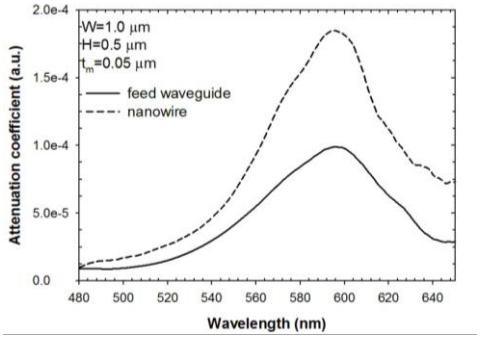

Fig. 1. Variations of attenuation coefficients of the Ormocomp nanowires with wavelength.

The absorption peaks for both feed waveguide and nanowires were observed at the wavelength of 595 nm. The feed waveguide has attenuation coefficient of 0.45 dB/mm which is lower than the absorption coefficient of nanowires which is around 0.84 dB/mm. Therefore, the sensitivity of the narrower nanowires is higher than that of the feed waveguide.

References

[1] C. Viphavakit, *et al.*, *Realization of a polymer nanowire optical transducer by using the nanoimprint technique*, Applied optics, 53(31), 7487-7497 (2014).

Counter-propagating Airy beams interactions in nonlinear media

D. Wolfersberger[1,*], N. Wiersma[1], N. Marsal[1] , M. Sciamanna[1]
[1]*CentraleSupelec – LMOPS EA 4423, 2 Rue Edouard Belin, 57 070 Metz, France*
*delphine.wolfersberger@centralesupelec.fr

We numerically study the interactions of two counter-propagating Airy beams in a photorefractive crystal. By varying the Airy beams' properties and the photorefractive coupling strength, we achieve soliton-like interactions leading to new waveguide structures and to peculiar spatiotemporal dynamics.

Introduction and Motivations

Collisions of counter-propagating (CP) optical beams and spatial optical solitons have been extensively studied in both Kerr and photorefractive (PR) media [1]. In recent years, the self-trapping character of Airy beams in biased nonlinear media has suggested interesting dynamics such as soliton-like behaviors [2]. Although numerical studies have been done using co-propagating Airy beams, only few studies concern the collision of two counter-propagating Airy beams [3].

Numerical modeling

In this paper, we investigate theoretically the interaction of two CP Airy beams in a PR crystal. We inject on each side of the medium a one-dimensional Airy beam with the same deflection directions. By varying the crystal length and the photorefractive coupling strength, we demonstrate new interesting phenomena such as stable counter-propagating off-shooting solitons or peculiar spatiotemporal dynamics (Fig.1.).

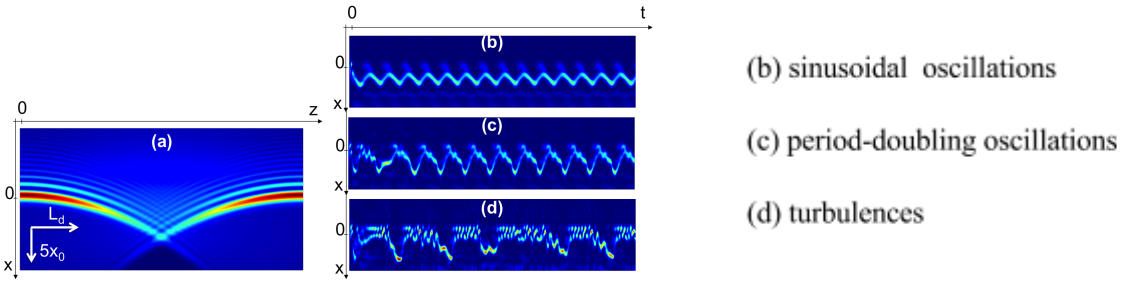

Fig. 1. (a) Initial intensity distribution of two counter-propagating Airy beams along the photorefractive crystal (waist size x_0=10µm, crystal length L=32mm). (b)-(d) Spatiotemporal dynamics of the off-shooting solitons at each output of the crystal for various coupling strength

Conclusion

To conclude the interaction of two CP Airy beams in a photorefractive crystal leads to different waveguide possibilities that are interesting for optical interconnects. We also analyse peculiar spatiotemporal dynamics and show that this system evolves along a chaotic-like route with larger interaction schemes.

References

[1] M. Petrović, M. Belić, C. Denz, Y. Kivshar, *Counterpropagating optical beams and solitons*, Laser & Photonics Rev, **5**, 214-233 (2011).

[2] I. Kaminer, M. Segev, D.N. Christodoulides, *Self-accelerating self-trapped optical beams*, Phys. Rev. Lett. **106**, 213903 (2011).

[3] N. Wiersma, N. Marsal, M. Sciamanna, D. Wolfersberger, *All-optical interconnects using Airy beams*, Optics Letters, **39**, n° 20 (2014).

Fast Finite Element Time Domain with Perforated Mesh

S M Raiyan Kabir*, B. M. A. Rahman
School of Engineering, City University London, United Kingdom
*Raiyan.Kabir.1@city.ac.uk

This paper presents a finite element based technique to solve the electromagnetic time domain problem with perforated mesh faster than conventional Finite Difference Time Domain approach.

Introduction

The Finite Element techniques for solving electromagnetic time-domain problem traditionally perform slower than the Finite difference counterpart, the FDTD method. This is due to formulation of large global matrix, implicit formulation, matrix inversion and use of iterative algorithm. The perforated mesh system based finite element time domain (FETD) method was introduced in [1] and this paper will report much faster simulation performances than the FDTD method while keeping the effective numerical dispersion same.

Summary

The perforated mesh based FETD is an explicit formulation of the Maxwell's equation. It solved the equations directly similar to the FDTD method; however, it uses a dual and coupled perforated mesh system which reduces the number of computation cells by half. It avoids any matrix formulation and performs minimum possible computer operations. With equilateral elements the method shows significant improvement in numerical dispersion over the FDTD method which allows this method to drastically reduce the spatial resolution by keeping the numerical error same. When the resolution reduction is considered with the Intel based Core processor on recent Haswell architecture, the speed of the method surpasses the speed of the FDTD method, as shown in Fig.1.

Results

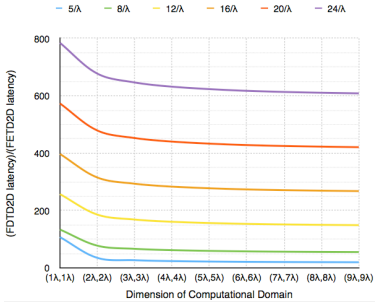

Fig. 1. Theoretical comparison, ratio of FDTD2D latency/FETD2D latency at different FETD resolution

Conclusion

The proposed technique reduces the latency far beyond the FDTD latency. Although the theoretical analysis was performed on equilateral mesh, a close to equilateral mesh should produce similar results and allow faster and more accurate solution of the problem.

References

[1] S. M. R. Kabir, B. Rahman, A. Agrawal, and K. T. V. Grattan, *"Elimination of numerical dispersion from electromagnetic time domain analysis by using resource efficient finite element technique,"* Progress In Electromagnetics Research, vol. 137, pp. 487–512, 2013.

Analysis of a Plasmonic Pole-Absorber Illuminated from a Specific Direction

J. Yamauchi, S. Ohki, H. Nakano
Faculty of Science and Engineering, Hosei University, Tokyo, Japan
shintaro.oki.m3@stu.hosei.ac.jp

A plasmonic pole-absorber is analyzed using the FDTD method based on the cylindrical coordinate system with the periodic boundary condition. It is found that an absorptivity of more than 80 % is obtained over a wavelength range of λ = 500 nm to 1000 nm.

Summary

A broadband omnidirectional light absorber, which is often called an optical black-hole, has received considerable attention [1]. The use of touching subwavelength-sized metal spheres is effective, although the absorption occurs only for a specific polarization. We have proposed a plasmonic pole absorber (so-called black-pole) using a periodic structure and analyzed under the assumption that the pole-absorber is illuminated omnidirectionally [2]. In this work, we consider the case where the pole-absorber is illuminated with a vertically polarized cylindrical wave from a specific direction. Fig. 1 depicts the configuration of the pole-absorber, which is assumed to be placed in free space. The metal is taken to be aluminum whose dispersion property is expressed as the Drude-Lorentz model [3]. Taking into account the periodicity along the z-axis, we only deal with the single cell whose length is $\Lambda = 2r_z$, as shown in Fig. 1(b). The configuration parameters are chosen to be r_ρ = 700 nm, θ_r = 10°, and r_z = 61 nm. Fig. 2 shows the absorptivity as a function of wavelength. The power distribution observed in the contact plane #1 at λ = 750 nm is illustrated in the inset of Fig. 2, in which the incident wave is excited towards the center axis from a position of ρ = 800 nm over ϕ = 45° ∼ 315°. An absorptivity of more than 80 % is obtained over a wavelength range of λ = 500 nm to 1000 nm. In addition, almost no power is evaluated in the transmission region.

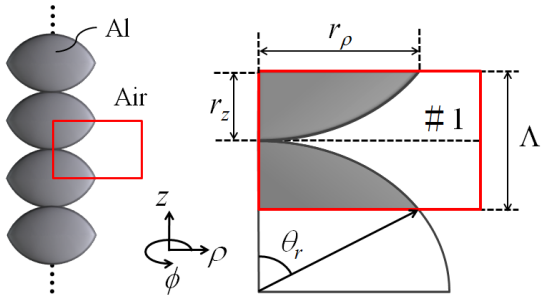

(a) Prespective view (b) Cross-sectional view of the single cell

Fig. 1. Plasmonic pole-absorber.

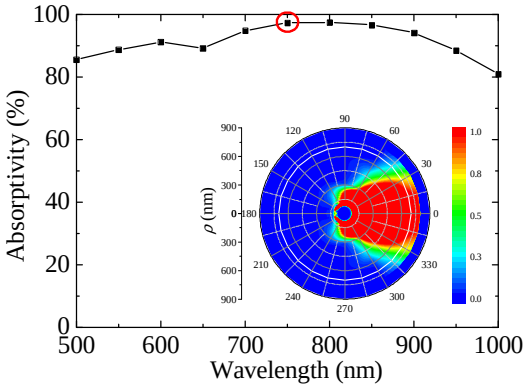

Fig. 2. Absorptivity as a function of wavelength.

References

[1] E. E. Narimanov and A. V. Kildishev, "Optical black hole: Broadband omnidirectional light absorber," Appl. Phys. Lett., vol. 95, 041106, 2009.
[2] J. Yamauchi, Y. Nakagomi, and H. Nakano, "Plasmonic pole-absorber using a periodic structure," *APCAP*, Chiang Mai, T1A2, 2013.
[3] A. Vial, "Implementation of the critical points model in the recursive convolution method for modelling dispersive media with the finite-difference time domain method," J. Opt. A: Pure Appl. Opt., vol. 9, pp. 745-748, 2007.

Gain-Equalization of 3-mode groups using dual-core EDFA

A. Gaur*, V. Rastogi
Department of Physics, Indian Institute of Technology Roorkee, Uttrakhand, India
*ankitagaur.phy@gmail.com

We propose a dual-core few mode erbium doped fiber (FM-EDF) wherein central core is graded index and doped ring core is step-index. The proposed fiber amplifies LP_{11}, LP_{21} and LP_{31} mode groups with more than 20 dB of gain each and less than 0.19 dB differential modal gains (DMG) using LP_{01} as pump mode.

Introduction

Space Division Multiplexing is an attractive regime to enhance capacity of optical communication. FM-EDF is an important component to amplify all the signal mode groups with minimal DMG [1]. In this context, we have proposed a dual-core FM-EDF which provides ≥ 20 dB gain and low DMG.

Fiber Design and Results

The proposed dual-core EDF consists of a central graded-index core and a step-index Er–doped ring core. The mode profiles of the fiber have been calculated by transfer matrix method and their gains have been calculated by using the mathematical model proposed in Ref. [2]. In this study we have considered LP_{11}, LP_{21} and LP_{31} mode groups with 30 μW input power in each mode at 1530 nm-wavelength. The erbium concentration used is $N_0=1\times10^{24}$ m^{-3}. The LP_{01} mode at 980 nm has been used as pump. Variations of gain and DMG with pump power are plotted in Fig. 1.

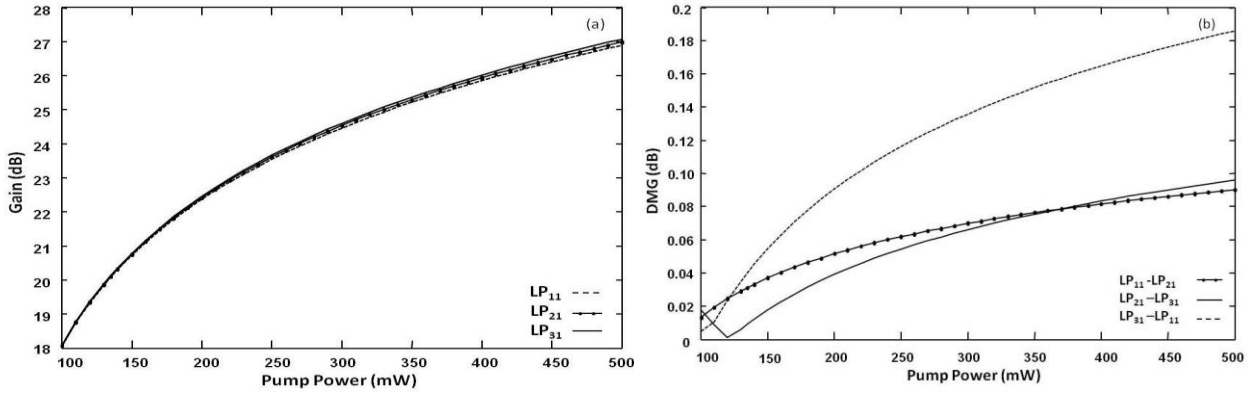

Fig. 1. (a**)** Variation of gain with pump power, **(**b**)** Variation of DMG with pump power.

We could achieve 20 dB gain with less than 0.04 DMG with 135 mW pump power and 28-nm EDF length. The gain could be increased to 27dB with 0.19 dB DMG with a pump power of 500 mW.

Conclusion

The proposed EDF provides 20 dB amplification of 12 modes of LP_{11}, LP_{21} and LP_{31} mode groups with very small DMG and would be useful in SDM optical communication system.

References

[1] Y. Jung, E. L. Lim, Q. Kang, T. C. May-Smith, N. H. L. Wong, R. Standish, F. Poletti, J. K. Sahu, S. U. Alam, D. J. Richardson, *Cladding pumped few-mode EDFA for mode division multiplexed transmission*, Opt. Express 22(23), 29008-29013, 2014

[2] N. Bai, E. Ip, T. Wang, G. Li, *Multimode fiber amplifier with tunable modal gain using a reconfigurable multimode pump*, Opt. Express 19(17), 16601-16611, 2011

Mode mixing in anisotropic metamaterial waveguides

A. Neira[1*], G. A. Wurtz[1], A. V. Zayats[1]
[1]*Department of Physics, King's College London, United Kingdom*
* andres_david.barbosa@kcl.ac.uk

We analyzed numerically the strong coupling between extraordinary and ordinary modes in diagonal anisotropic metamaterial-based waveguides.

Introduction

Anisotropic metamaterials are artificial materials defined by an effective permittivity tensor, whose linear optical properties can be designed through the structure engineering of the composite materials. Using these materials a large variety of complex optical effects have already been shown such as negative refraction, high light-confinement, backward waves, etc. [1]

Analysis and Results

Diagonal anisotropic metamaterials have an effective permittivity tensor[1]:

$$\hat{\varepsilon} = \begin{pmatrix} \varepsilon_x & 0 & 0 \\ 0 & \varepsilon_x & 0 \\ 0 & 0 & \varepsilon_z \end{pmatrix} \quad (1)$$

Where the subindexes x and z indicate the components perpendicular and parallel to the anisotropy axis. Using first order perturbation theory, we demonstrate that the lateral confinement allows the coupling of both extraordinary and ordinary modes. Additionally, in the hyperbolic case (when ε_z and ε_x have different sign), it is shown that the hybrid extraordinary-ordinary mode created through this coupling, exhibits anomalous dispersion. The results obtained are in excellent agreement with the finite element method eigenvalue analysis. Further, we analyze the effects of losses on the hybrid waveguided mode. It is shown that a strong anisotropy in the imaginary part of the permittivity ($\mathrm{im}(\varepsilon_x) \ll \mathrm{im}(\varepsilon_z)$) reduces the coupling between the extraordinary and ordinary modes. This characteristic behavior renders metamaterial waveguides a suitable platform for all-optical switching as this strong anisotropy in the imaginary part can be optically induced readily in plasmonic metamaterials based in metallic nanorod arrays [2]. Indeed this behavior has been used recently for the design of a compact ultrafast all-optical modulator.[3]

References

[1] A. Poddubny, I. Iorsh, P. Belov, and Y. Kivshar, "Hyperbolic metamaterials," *Nature Photonics,* vol. 7, pp. 948-957, 2013.

[2] G. A. Wurtz, Pollard R, Hendren W, G. P. Wiederrecht, D. J. Gosztola, V. A. Podolskiy*, et al.*, "Designed ultrafast optical nonlinearity in a plasmonic nanorod metamaterial enhanced by nonlocality," *Nature Nanotechnology,* vol. 6, pp. 2011.

[3] A. D. Neira, G. A. Wurtz, P. Ginzburg, and A. V. Zayats, "Ultrafast all-optical modulation with hyperbolic metamaterial integrated in Si photonic circuitry," *Optics Express,* vol. 22, pp. 10987-10994, 2014

Mimicking photon propagation through 2-D array by a 1-D array

K. Thyagarajan[1], Surajit Paul[2]
Department of Physics, IIT Delhi, New Delhi 110016, India
[1]ktrajan@physics.iitd.ac.in, [2]surajitpaul26@gmail.com

We show that an appropriately chosen one dimensional waveguide array can mimic photon propagation through a two dimensional waveguide array. This alternative design is attractive since fabrication of one dimensional array is comparatively easier than two dimensional arrays.

Introduction

Quantum random walks have recently been used to emulate various quantum phenomena like Bloch oscillations, Anderson localization, Quantum zeno effect etc. These phenomena can be readily implemented using integrated optical waveguide devices such as 1-D array of optical waveguides. Moreover, many interesting problems such as energy transport in biological systems [1], quantum search algorithms and graph theory [2] require two-dimensional quantum random walk phenomena. A promising way for the emulation of such random walks is to study photon propagation through a two-dimensional array of optical waveguides.

Summary

Here we show that an appropriately designed 1-D waveguide array consisting of a pair of two mode waveguides coupled to a single mode waveguide can be shown to be equivalent to a 2-D array of five single mode waveguides and hence can be used to mimic photon propagation through a 2-D array. This is achieved by using a combination of evanescent coupling and appropriate periodic coupling among the modes of the three waveguides [see Fig. 1(b)]. We show that by an appropriate design, the five normal modes of the 2-D array become equivalent to the five normal modes of the 1-D array. Thus light propagation through either of the structures is described by the same set of equations and thus the 1-D array can completely simulate the 2-D array. Figure 1(c) shows a sample simulation of the photon bunching exhibited in either of the structures.

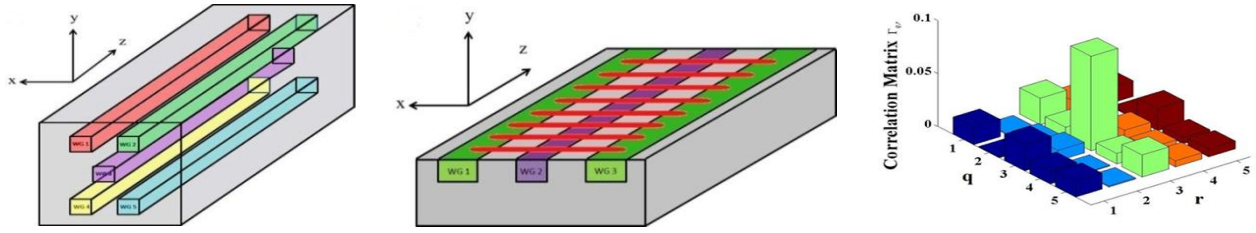

Fig. 1. (a) 2-D array of five identical single mode waveguides, (b) Equivalent 1-D array with a long period grating for periodic coupling. (c) Simulation showing photon bunching phenomenon.

Conclusion

In conclusion, we have shown that a properly designed, easy to realize one-dimensional array consisting of a pair of two mode waveguides coupled to a single mode waveguide via evanescent coupling and periodic coupling among appropriate modes of the waveguides, can be a replacement for a two dimensional array of five identical single mode waveguides and can be used to mimic light propagation including phenomena such as quantum random walk in a 2-D array.

References

[1] M. B. Plenio and S. F. Huelga, *Dephasing-assisted transport: quantum networks and biomolecules*, New J. Phys.10, 113019 (2008).

[2] J. M. Harrison, J. P. Keating, and J. M. Robbins, *Quantum statistics on graphs*, Proc. R. Soc. A 467, 212 (2011).

Graphene based Surface Plasmon Resonance Gas sensor for Terahertz

Amrita Purkayastha and Rajan Jha*
Nanophotonics and Plasmonics Laboratory, School of Basic Sciences, IIT Bhubaneshwar, India
*rjha@iitbbs.ac.in; rajaniitd@gmail.in

Abstract

Surface Plasmon Resonance (SPR) based gas sensor in terahertz with modified Otto configuration based on attenuated total reflection (ATR) technique using doped graphene monolayer is proposed. The sensitivity and detection accuracy (1/FWHM) was found to be 40 deg/RIU and 14.97 deg^{-1} respectively.

Introduction

Conventional SPR sensors at visible and infrared with noble metals like gold and silver suffer from major drawbacks in terms of confinement and tunability of the surface plasmons (SPs) at terahertz. To overcome this problem of poor confinement, graphene, a 2D form of carbon having atoms arranged in honeycomb lattice has shown promising advantages for SP generation in terahertz frequencies [1, 2].

ATR Graphene-Based Configuration

High index coupling prism is used as coupling element. The Otto geometry is modified by replacing the air gap between the graphene monolayer and prism with organic material compatible with terahertz of RI=1.5 as shown in fig1 (a).Its thickness is optimised to give maximum energy transfer. Gaseous analytes are considered as the sensing medium. For quantifying the SPR sensor performance, we use the angular interrogation technique in which the reflectivity of output radiation is measured as a function of incident angle. For our calculation, we use the accurate Transfer Matrix Method (TMM) for analysis of light propagating through the layered structure.

Results and Conclusions

We found that the resonance angle of the SPR curve shifts from 53.23º for the n_d=1.000 to 55.25º for nd=1.050, showing a sensitivity of 40.4 deg/RIU as shown in fig1 (b). Also the detection accuracy of the sensor which is given by (1/FWHM) increases with increasing RI of the gaseous analyte. Such type of gaseous sensors can open a new window for gaseous sensing in terahertz.

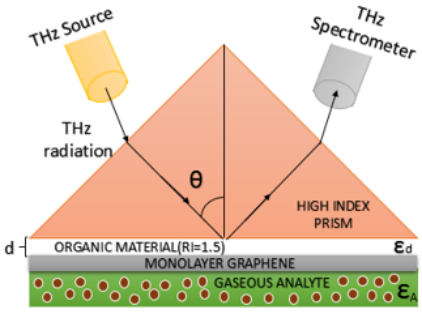

Fig1(a) Proposed Setup

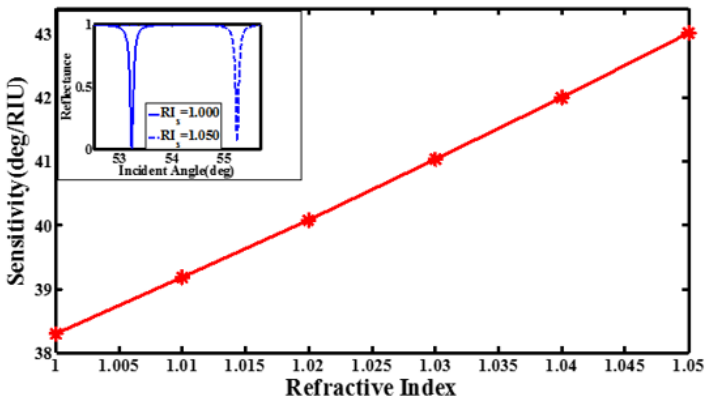

Fig1(b) Variation of Sensitivity with Refractive index

[1] Choon How Gan, Analysis of surface plasmon excitation at terahertz frequencies with highly doped graphene sheets via attenuated total reflection, Appl. Phys. Lett. vol 101,(2012).

[2] P.K. Maharana, P. Padhy, R. Jha, On the field enhancement and performance of an ultra-stable SPR biosensor based on graphene", IEEE Photonics Technology Letters, 25(22), 2156-2159 (2013).

Multi-path propagation in waveguide media: Fading emulation assuming large RC network models with pre-equalization using fractional order models

S. Hadjiloucas[1,*], H. Alyami[1], V. M. Becerra[1], R. J. M. Afonso[2], R. K. H. Galvão[2], K. H. Kienitz[2]
[1]*School of Systems Engineering, The University of Reading, Reading RG6 6AY, United Kingdom*
[2]*Instituto Tecnológico de Aeronáutica, São José dos Campos, SP, 12228-900, Brazil*
[*]s.hadjiloucas@reading.ac.uk

Multi-path propagation in waveguides is modelled assuming a multi-layer three-dimensional RC network with randomly allocated resistors and capacitors to represent the waveguide transmission medium. A pre-equalization procedure that takes into account the capabilities of the transmission source as well as the transmission properties of the medium is developed.

Introduction

Propagation of non-meridional rays in an optical, microwave, or THz waveguide from pulsed coherent sources incur path-dependent distortion manifested as group velocity dispersion. When partially coherent, or incoherent sources are used, additional frequency-selective attenuation may also be observed. We propose a pre-equalization procedure to address these problems; the technique casts the problem within a Mixed Integer Linear Programming (MILP) optimization framework that uses the developed nominal RC network model, to customize the excitation waveform so as to optimize signal fidelity from the transmitter to the receiver minimizing distortions.

Summary

The RC model is casted in state space form and emulates the multi-path propagation process. Its transfer function is of fractional order. The inclusion of source power constraints entails an optimization problem over a non-convex region of possible solutions. This issue poses a difficulty to obtain the optimal solution as most optimization algorithms are designed to search over a convex set of feasible solutions. Therefore, MILP is used instead.

Results

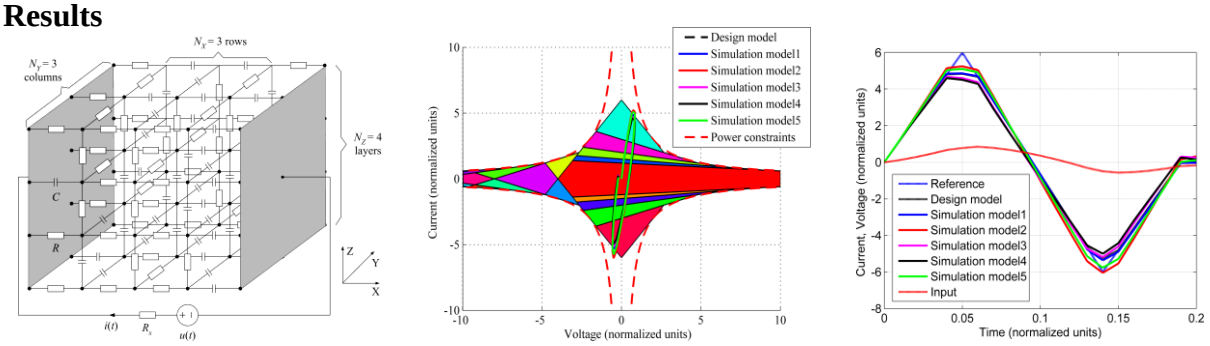

Fig. 1. a) Multi-path propagation analogy assuming proposed 3D-RC model, b) power-constrained trajectories for source modulation over the feasible region and c) different current & voltage pre-equalization plots for 5 different network realizations assuming double-ramp excitation.

Conclusion

The MILP optimization framework enables pre-equalization assuming arbitrary modulation modalities and optimizes signal fidelity from the transmitter to the receiver.

References

[1] S. Hadjiloucas, A. Hashem, V.M. Becerra, and RKH Galvão, *Journal of Physics: Conference Series*: **450** (2013) 012051.

Full-vector modeling of thermally-driven gain competition in Yb-doped large-mode-area photonic-crystal fiber

L. Rosa*, E. Coscelli, F. Poli, A. Cucinotta, S. Selleri
Information Engineering Department, University of Parma, V.le G.P. Usberti 181/A, I-43124 Parma, Italy
*LRosa@ieee.org

A new model to study gain competition in high-power fiber amplifiers is proposed, which accounts for the full-vector nature of the propagating modes and thermal effects on core overlap. Model tests on a Yb-doped large-pitch photonic-crystal fiber show a successful analysis of gain competition.

Introduction

Currently, power scaling of fiber lasers is limited by mode instabilities, which appear beyond a certain power threshold due to power transfer between guided modes [1,2,3]. Though its cause has to be clarified, it is commonly attributed to a thermally-driven refractive index gradient in the cross-section due to quantum-defect core heating. High-Order Modes (HOMs) not guided in the cold fiber, can be significantly confined into the core by high-power pumping, thereby jeopardizing the output beam quality. To pursue robust single-mode guiding in Yb-doped fibers under severe heat load, it is necessary to thoroughly analyze the amplification process, taking into account the gain competition between the Fundamental Mode (FM) and the most detrimental HOMs. To this aim, a new model, based on the Finite Element Method (FEM) has been developed, which accounts for the full-vector nature of the propagating modes and the change in their overlap with the doped core caused by the heat load, showing gain competition effects.

FEM Model and Results

Light propagation is modeled by solving the rate equations along the fiber segments, with heat load given by the quantum defect fraction of the absorbed pump power. The thermally-driven refractive index change on each segment is given by solving the steady-state heat equation on the fiber transverse plane. The propagating modes are then calculated by a FEM full-vector solver, obtaining the heat-dependent doped core overlap. Tests performed on a Large Pitch Fiber (LPF) are shown in Fig. 1: notice in Fig. 1(a) the effective index change of the FM and the first two HOMs along the fiber. Fig. 1(b) depicts the power evolution of the modes, showing the gain competition between FM, HOM1, and HOM2, with gain of 15.5, 4.9, and 6.5 dB at input power of 5, 0.5, and 0.5 W, respectively. Finally, Fig. 1(c) reports the behavior of the guided mode overlap on the doped core along the fiber, showing that the heat load value determines the most detrimental HOM.

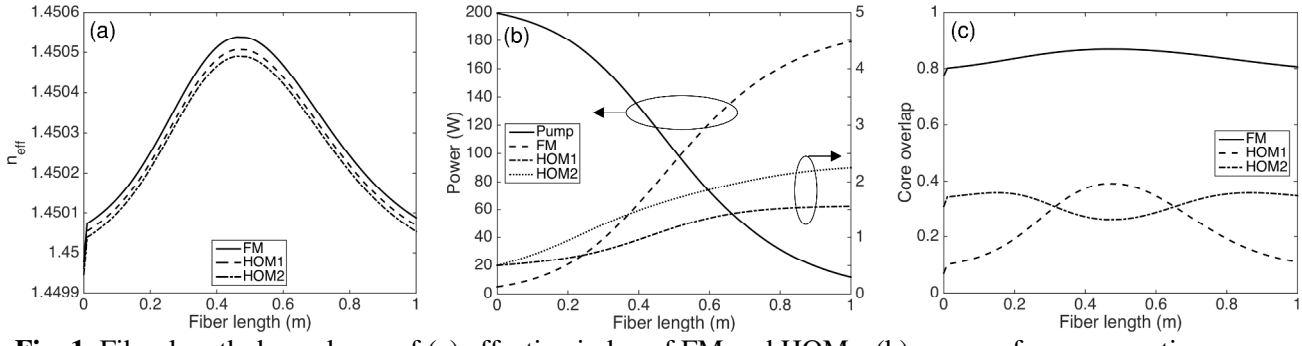

Fig. 1. Fiber length dependence of (a) effective index of FM and HOMs, (b) power of co-propagating pump and fiber modes, and (c) overlap of FM and HOMs with the doped fiber core.

References

[1] Eidam et al., Opt. Express **19**, 13218–13224, 2011
[2] Smith and Smith, Opt. Express **19**, 10180–10192, 2011
[3] Hansen et al., Opt. Express **19**, 23965–23980, 2011

Counter-circular-polarization Characteristics of a Quarter-wave Plate Using a Triangular Hole Array in a Metallic Plate

J. Yamauchi, Y. Takagi, H. Nakano

Faculty of Science and Engineering, Hosei University, Tokyo, Japan

yuhei.takagi.t6@stu.hosei.ac.jp

A quarter-wave plate using a triangular hole array in a metallic plate is analyzed by the FDTD method with the periodic boundary condition. The wave plate exhibits counter-circular-polarization characteristics, i.e., the incident light can be changed from linear to right- or left-handed circular polarization at different wavelengths.

Summary

Considerable interest has been directed towards thin wave plates, which include the application of surface plasmon polaritons[1,2]. We have proposed and analyzed a quarter-wave plate using a triangular hole array in a metallic plate[3]. Fig. 1 schematically illustrates the proposed configuration. Triangular-shaped holes are periodically made in an Ag plate. Owing to the generation of the surface plasmon polaritons, symmetric (first) and asymmetric (second) modes are excited in the triangular aperture. Since the two orthogonal modes have a phase difference of $90°$ or $-90°$, the incident light can be changed from linear to right- (RCP) or left-handed circular polarization (LCP) in different wavelength bands. Fig. 2 shows the transmittance, the polarization rotation angle θ, and the ellipticity as a function of wavelength. It is found that the plate acts as an efficient polarization converter at specific wavelengths. In particular, RCP whose ellipticity is more than 0.7 (less than 3 dB) is obtained over a wide wavelength range of 1.46 to 1.51 μm, while LCP whose ellipticity is less than -0.7 is achieved over a narrow wavelength range of 1.10 to 1.11 μm. The transmittance at λ = 1.11 μm is 78 $\%$, which is higher than 57 $\%$ at λ = 1.48 μm.

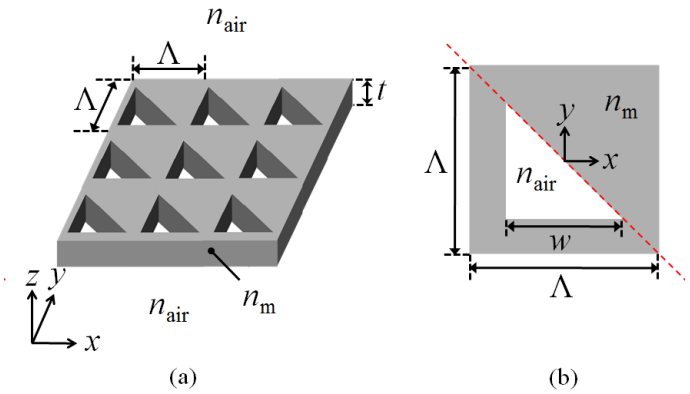

Fig. 1. Configuration. (a) Perspective view. (b) Top view of the unit cell.

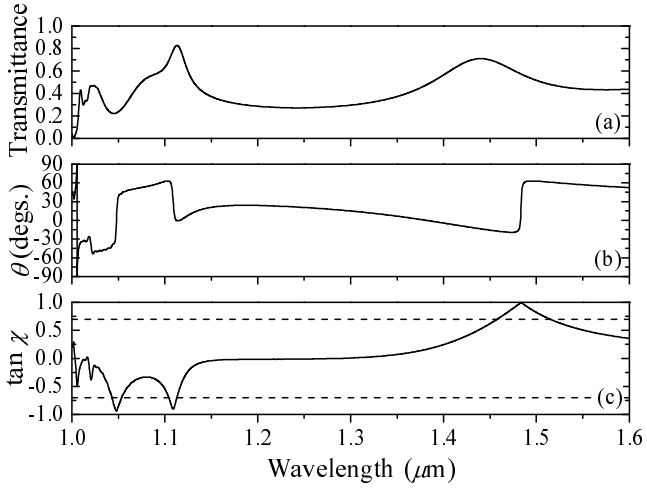

Fig. 2. Wavelength characteristics. (a)Transmittance. (b)Rotation angle. (c)Ellipticity.

References

[1] A. Roberts and L. Lin, "Plasmonic quarter-wave plate," *Opt. Lett.*, vol. 37, no. 11, pp. 1820-1822, 2012.

[2] B. Yang, W.-M. Ye, X.-D. Yuan, Z.-H. Zhu, and C. Zeng, "Design of ultrathin plasmonic quarter-wave plate based on period coupling," *Opt. Lett.*, vol. 38, no. 5, pp. 679-681, 2013.

[3] J. Yamauchi, R. Taniguchi, Y. Takagi, and H. Nakano, "Quarer-wave plates consisting of subwavelength triangular hole arrays," in *Integ. Photon. Res.*, JT3A.22, 2014.

A Polarization Converter Using a Curvilinearly Tapered Waveguide

Y. Nito, S. Fujimura, J. Yamauchi, H. Nakano

Faculty of Science and Engineering, Hosei University, Tokyo, Japan
shunya.fujimura.64@stu.hosei.ac.jp

A mode-evolution-based polarization converter on an SiO_2 substrate is analyzed by the BPM. The use of a curvilinearly tapered core leads to an extinction ratio of more than 15 dB with a device length of 100 μm, over a wide wavelength range from 1.3 μm to 1.7 μm.

Summary

A curvilinearly tapered core is introduced into a mode-evolution-based polarization converter [1] on an SiO_2 substrate with the intention of designing a compact structure [2]. The waveguide treated in this study is illustrated in Fig. 1, where the expression to determine the lower core width is also presented. Consideration is first given to the effective indices of the first and second eigenmodes in a linearly tapered structure (r = 1) as a function of propagation distance. The eigenmode analysis reveals that the introduction of a curvilinear taper (r = 2) widens a hybrid-mode region, where the difference in the effective indices between the two modes is small with subsequent sufficient polarization conversion [2]. We next investigate the polarization conversion behavior using the propagating beam analysis. As expected, the use of the curvilinear taper improves the conversion efficiency, allowing a short device length of 100 μm. However, the conversion efficiency is still low because of remaining ripples due to the polarization recoupling. To prevent the polarization recoupling, we partially remove the upper core at $z > 82$ μm. As shown in Fig. 2, this strategy leads to an extinction ratio of > 15 dB with a conversion length of 100 μm over a wide spectral range from 1.3 μm to 1.7 μm.

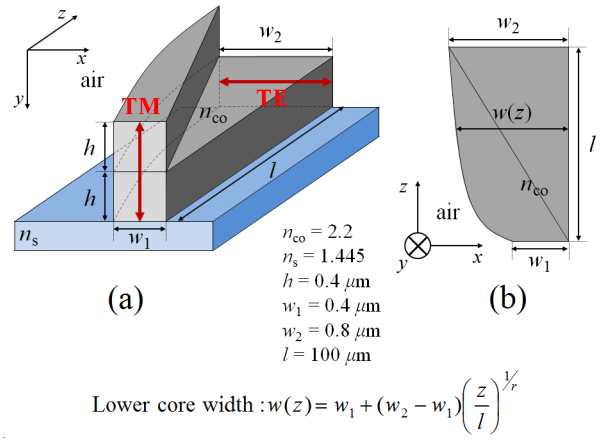

Fig. 1. A curvilinearly tapered polarization converter on an SiO_2 substrate. (a) Perspective view and (b) top view.

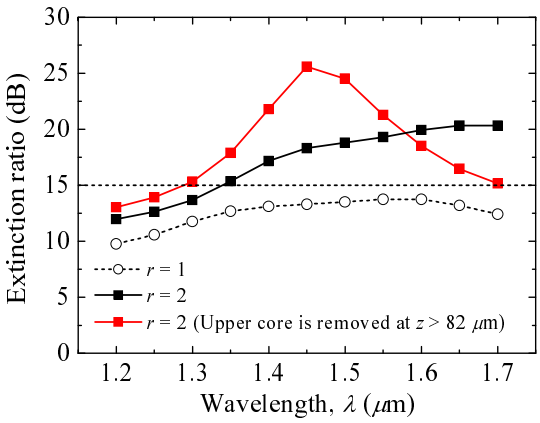

Fig. 2. Wavelength characteristics.

References

[1] M. R. Watts and H. A. Haus, "Integrated mode-evolution-based polarization rotators," *Opt. Lett.*, vol. 23, no. 2, pp. 138-140, Jan. 2005.

[2] Y. Nito, J. Shibayama, J. Yamauchi, and H. Nakano, "Full-vectorial beam-propagation methods based on a fundamental scheme–Design of a short polarization converter," *J. Lightw. Technol.*, vol. 32, no. 21, pp. 4111-4118, Nov. 2014.

Power Budget Analysis for Waveguide-Enhanced Raman Spectroscopy

Zilong Wang[1*], Michalis N. Zervas[1], Philip N. Bartlett[2], James S. Wilkinson[1]
[1]*Optoelectronics Research Centre, University of Southampton, United Kingdom*
[2]*School of Chemistry, University of Southampton, United Kingdom*
*zw1e09@soton.ac.uk

Waveguide-enhanced Raman spectroscopy (WERS) represents an attractive form of enhanced analytical technique for surface chemistry. Comparisons of surface enhanced spectroscopies are hampered by ill-defined enhancement factors. In this work, a full power budget analysis, incorporating dielectric waveguide optimization, is presented for WERS as an approach towards defining a rigorous performance measure.

Introduction

Surface-enhanced Raman Spectroscopy (SERS) is a powerful tool for chemical analysis which can suffer from poor repeatability due to the sensitive nature of plasmonic interactions. Waveguide-enhanced Raman spectroscopy (WERS) is emerging as a competitive analytical tool which avoids nanostructured noble metal surfaces but which potentially provides comparable surface enhancements in a sensorised format [1,2]. Comparison of these approaches suffers from ill-defined definitions of surface enhancement. We present a power budget analysis of WERS, relating the received power in a Raman emission line to the incident pump laser power, using waveguide surface intensity and Raman cross-section, allowing WERS optimisation and clear comparison of surface-enhanced techniques.

Results

Simulations were made for 1mW power per 1mm width at 633nm travelling in a Ta_2O_5 waveguide (n≈2.1) on silica (n≈1.46) with an air superstrate. The modes of the waveguide structure have been solved using a complex transfer matrix approach. The core thickness has been optimised in order to achieve the highest surface intensity at this wavelength as shown in Fig 1 for the fundamental mode in TM polarisation. Comparisons show that for a $1mm^2$ area of illumination the waveguide yields a 1000-fold increase in surface intensity compared with direct illumination of a surface with the same power.

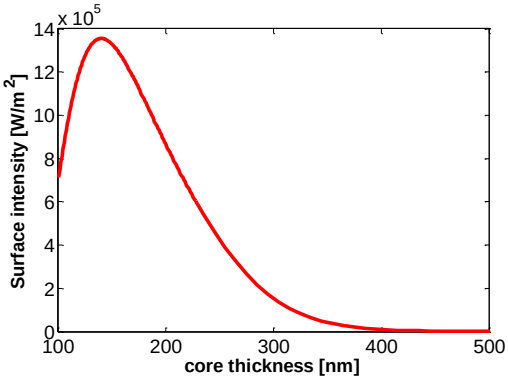

Fig 1. Waveguide surface intensity

A power budget analysis is then employed to determine the power (per unit surface area) emitted in a specific Raman line for unit power in the waveguide. In the case of a semi-infinite toluene superstrate for the waveguide optimized in Fig 1, the emitted power in the $1000cm^{-1}$ line gives a Raman power of 1.1fW. This methodology, which will be extended to waveguide collection as well as excitation, allows unambiguous comparison of Raman configurations. In SERS, factors of 10^6 enhancement are achieved through similar (factor 1000) enhancements for both excitation and emission. Waveguide collection (as opposed to normal collection) of Raman signals in WERS can be expected to achieve similar efficiencies to SERS, without the losses inherent in metal structures.

Summary

Waveguide-enhanced Raman spectroscopy offers advantages over SERS in terms of repeatability and robustness if similar signal enhancements can be achieved. SERS and WERS need rigorous methods to aid comparison. Here a power-budget analysis for WERS is proposed, which can readily be extended to other configurations, and detailed examples will be given of numerically derived enhancement factors.

This research was funded by ERC grant no. 291216 Wideband Integrated Photonics for Accessible Biomedical Diagnostics

References

[1] A. Dhakal et al., *Evanescent excitation and collection of spontaneous Raman spectra using silicon nitride nanophotonic waveguides*, Opt. Lett., 2014, 39, 4025-4028.

[2] J.S. Kanger *et al*, *Waveguide Raman Spectroscopy of Thin Polymer Layers and Monolayers of Biomolecules Using High Refractive Index Waveguides.*, J. Phy. Chem., 1996, 100, 3288-3292.

Characteristics of Twist Induced Phase Deviation through a Distinct Dual-mode-fiber in a Sagnac Loop

Saba N. Khan[1], Sudip Kr. Chatterjee[1], Partha Roy Chaudhuri[1,*]
[1]*Deaprtment of Physics, Indian Institute of Technology, Kharagpur, India*
**roycp@phy.iitkgp.ernet.in*

Abstract: We demonstrate experimentally and discuss theoretically a method to vary the position of transmission peak over a wide dynamic range through a Sagnac interferometer (SI) employed with elasto-optically induced linear and circular birefringence(s) towards measurement of twist.

Torsion is one of the most important parameter for security monitoring of building, bridges, and other infrastructures [**1**]. In the recent past, several highly sensitive fiber-optic twist sensor employing high-birefringent (Hi-Bi) fiber, advance microstructured fiber, fiber Bragg grating emerged out as a promising candidate [2]. Though extremely sensitive all of these sensing configurations are operational over a narrow dynamic range. In this contribution, we present a prototype of *highly-sensitive tunable torsion measuring device* covering a wide-dynamic range (0° to 700°) employing a Sagnac interferometer (SI) possessing distinct dual-mode fiber (DMF) segment in the loop (See **Fig.1**). The wide-range tunability is attained by the application of variable transverse-stress over a small segment (~1.5 cm) of Sagnac loop. In this work, we thoroughly investigated and analyzed the transmission behavior of a SI with stress assisted induced linear birefringence and twist (~5 cm) induced circular birefringence in the loop. Theoretically, the electric field at the transmitting port of a SI is evaluated as:

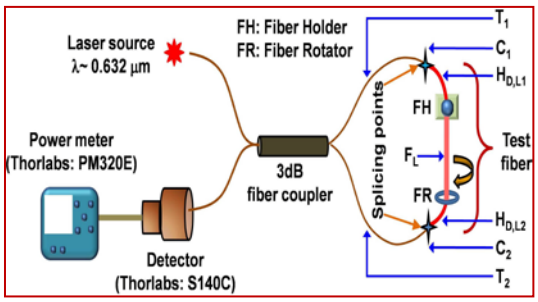

Fig.1. Schematic of SI used for twist-measurement.

$$\begin{pmatrix} E_{out,x} \\ E_{out,y} \end{pmatrix} = \begin{pmatrix} (2\alpha-1)J_{xx} & (1-\alpha)J_{xy}+\alpha J_{yx} \\ -\alpha J_{xy}-(1-\alpha)J_{yx} & (1-2\alpha)J_{yy} \end{pmatrix} \begin{pmatrix} E_{in,x} \\ E_{in,y} \end{pmatrix}; \quad where \; J = \begin{cases} T_1.C_1.F_L.C_2.T_2 & for \;\; SMF \\ T_1 C_1 H_{D,L_1} F_L H_{D,L_2} C_2 T_2 & for \;\; DMF \end{cases}$$

where α is the intensity coupling coefficient of coupler, '*J*' is the Jones matrix of loop and is equal to the product of the transmission matrix of elements constituting the loop (Fig.1). It was observed (theoretically and experimentally) that the influence of the twist is intimately linked with inherent linear birefringence that is present in the Sagnac loop. The shifting of the highest peak in the Transmittance curve was found to be a signature of induced linear birefringence (Transverse-stress) while the intensity variation along the highest peak measures the applied twist. Moreover, the incorporation of DMF in the loop provides additional parameters - the excitation coefficient and length of the DMF segment to tune the transmission response over a wide range. Fig.2 shows the transmission characteristics of distinct twisted fiber segments (SMF/DMF/Hi-Bi). It is interesting to note that the Sagnac loop comprising of Hi-Bi fiber segment is nonresponsive under weak-twist regime (<300°) owing to the dominating high inherent linear birefringence (~10^{-4}). The theoretical analysis is in good agreement with our experimental results and gave the first indication of how to proceed in the experiment. The finer experimental details, underlying physics, involved calculation and governing equation would be presented in detail in the workshop.

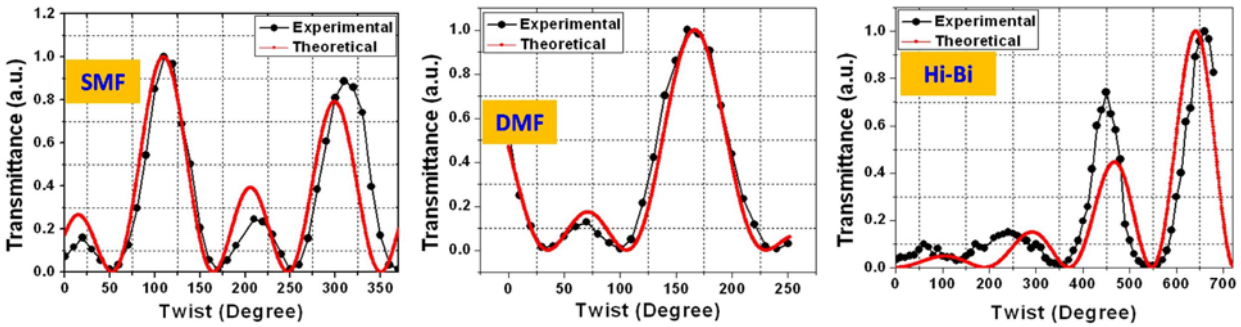

Fig.2. Theoretical and experimental plots for transmission characteristics of (a) SMF (b) DMF (c) Hi-Bi in SI

References

[1] R. Ulrich and A. Simon, "Polarization optics of twisted single mode fibers", Appl. Opt. **18**, 2241-2251 (1979).
[2] H. Liang, M. Sun, Y. Jin, "Twist sensor based on Sagnac single-mode optic fiber interferometer", Optik **124**, 6676-6678 (2013).

Detection of Low Magnetic Field using Fiber Optic Cantilever Technique

Somarpita Pradhan[1], Partha Roy Chaudhuri[1]*
[1]*Department of Physics, Indian Institute of Technology Kharagpur-721302, India*
*roycp@phy.iitkgp.ernet.in

Abstract: Cobalt-doped nickel-ferrite nanoparticles coated optical fiber is used to detect magnetic field as low as 2.0mT utilizing fiber-beam-cantilever technique. Also, a theoretical approach is developed to calculate magnetic properties such as magnetization of the probe sample using the experimental results.

Introduction

Attention in optical fiber based magnetic field sensors [1] has widely increased during the last few years. However, the main challenging task for designing such sensors is to choose proper magnetic probe material. In this work, we have prepared cobalt-doped nickel ferrite ($Ni_{0.97}Co_{0.03}Fe_2O_4$) nanoparticles as probe sample for sensing magnetic field using fiber beam cantilever technique.

Experimental Details and Results

Cobalt-doped nickel ferrite sample was prepared by sol-gel method. These nanoparticles coated optical fibers were used for magnetic field detection utilizing a fiber beam cantilever method (Fig. 1(a)). Variation of fiber-to-fiber transmitted power actually conveyed the signature of magnetic field in the vicinity. Sensitivity was increased by incorporating etched coated fiber tip with diameter 55μm ±5μm in the experimental set up. Experimental results are shown in Fig. 1(b), 1(c).

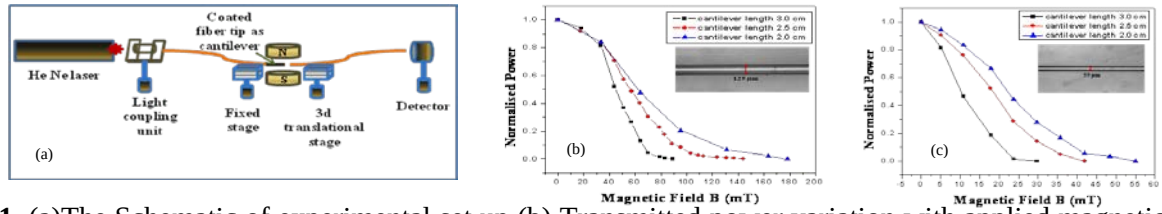

Fig. 1. (a)The Schematic of experimental set up (b) Transmitted power variation with applied magnetic field using normal single mode fiber (SMF) (c) using etched SMF

Theoretical Approach

Variation of transmitted power (T) with applied external magnetic field due to transverse misalignment (d) between two optical fibers that are represented by Gaussian fundamental modes with spot sizes w_1 and w_2 can be modeled [2] by using the equation (1).

$$T = \left(\frac{2w_1 w_2}{w_1^2 + w_2^2} \right)^2 e^{-\frac{2d^2}{w_1^2 + w_2^2}} \quad (1)$$

Deflection of the detection fiber at different magnetic field is calculated which is actually incorporated into the basic torque (τ_m) equation (equation (2)) in a constant magnetic field (H_t) [3] to calculate magnetization (M) and other magnetic properties of the probe sample.

$$\tau_m = V_m M \times H_t \quad (2)$$

Conclusion

Magnetic field as low as ***2.0 mT*** was detected reproducibly using etched optical fiber tips. Finally, a theoretical approach was developed to calculate magnetic properties of the probe sample using the experimental results.

References

[1] H. Wang *et al.*, *Magnetic field sensing based on singlemode–multimode–singlemode fiber structures using magnetic fluids as cladding*, Opt. Lett. 38, 3765-3768, 2013

[2] A. Ghatak, K. Thyagarajan, *Introduction To Fiber Optics*, Cambridge University Press, Reprint 2011

[3] R. Adhikari *et al.*, *The cantilever beam magnetometer: a simple teaching tool for characterization*, Am. J. Phys. 80, 225–231, 2012

Wavelength Characteristics of a Waveguide Polarization Converter with Sidewall-Roughness

J. Yamauchi, T. Takada, H. Nakano

Faculty of Science and Engineering, Hosei University, Tokyo, Japan
takumi.takada.e3@stu.hosei.ac.jp

A polarization converter with sidewall roughness is analyzed by the imaginary-distance BPM based on Yee's mesh and the FDTD method. Regardless of the presence of the sidewall roughness, an extinction ratio of more than 15dB is obtained over a wavelength range of 1.35 μm to 1.55 μm, with an insertion loss of less than 1dB.

Summary

Several converters using an asymmetric waveguide have been proposed and investigated[1][2]. These converters are based on beating of two orthogonal modes. A large difference in the propagation constants of these modes, requiring a strongly guiding waveguide, is necessary to achieve a short conversion length. Note that a strongly guiding waveguide often suffers from the sidewall roughness caused by the imperfection of lithography and etching processes. In this work, we analyze a waveguide polarization converter with sidewall roughness. Fig. 1 shows the configuration, in which a silicon core is located on an SiO_2 substrate. The roughness is assumed to independently occur in each sidewall and the standard deviation σ is chosen to be 5.0 nm. The presence of the substrate leads to a rectangular defect section of $\gamma_H / \gamma_V \simeq 0.85$, even when the square core is employed. The wavelength characteristics of the extinction ratio and the insertion loss are presented in Fig. 2, in which the result obtained for σ = 0 nm is also shown for comparison. It is found that even when the sidewall roughness is taken into account, an extinction ratio of more than 15dB is achieved over a wavelength range of 1.35 μm to 1.55 μm, with the insertion loss being a value of less than 1dB.

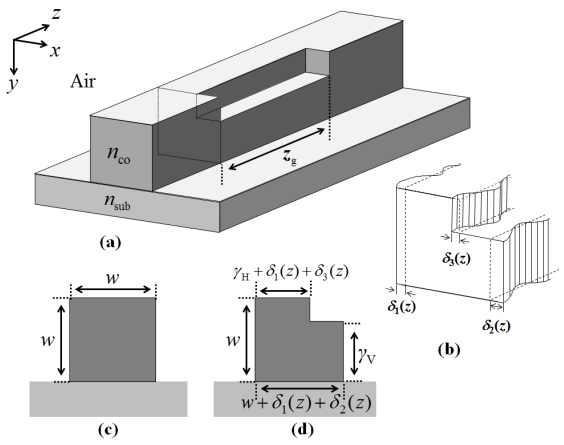

Fig. 1. Configuration. (a) Perspective view. (b) Enlarged view of conversion waveguide. (c) Input waveguide. (d) Conversion waveguide.

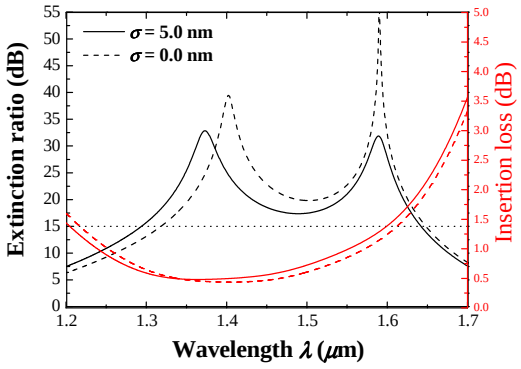

Fig. 2. Extinction ratio and insertion loss as a function of wavelength.

References

[1] Y. Shani, R. Alferness, T. Koch, U. Koren, M. Oron, B. I. Miller, and M.G. Young, "Polarization rotation in asymmetric periodic loaded rib waveguide," *Appl. Phys. lett.*, vol. 59, no. 11, pp. 1278-1280, Sep. 1991.

[2] Y. Wakabayashi, T. Hashimoto, J. Yamauchi, and H. Nakano, "Short waveguide polarization converter operating over a wide wavelength range," *J. Lightw. Technol.*, vol. 31, no. 10, pp. 1544-1550, May 2013.

Purcell effect of asymmetric dipole source distributions in nanowire resonators

K. Filonenko [1], L. Duggen [1], J. Adam [1], M. Willatzen [2]

[1] *Mads Clausen Institute, Syddansk Universitet, Alsion 2, DK-6400 Sønderborg, Denmark*
[2] *Department of Photonics Engineering, Technical University of Denmark, DTU Fotonik, Building 345 West, DK-2800 Kongens Lyngby, Denmark*
filonenko@mci.sdu.dk

We present a model for plasmonic nanowire resonators in combination with non-axisymmetric source distributions. We numerically investigate the Purcell effect for plasmonic metal nanowire modes in varying environments and compare the results to semi-analytic theory.

Summary

Metal nanowire resonators allow subwavelength mode confinement, resulting in a strong Purcell effect [1]. This implies an enhanced emitter-nanowire coupling, potentially useful for quantum information purposes [2]. Recent progress in fabrication of plasmonic nanowire lasers [3] requires reliable approaches in studying resonators, where the metal nanowire is an essential constitutive element [4]. An approach, capable of treating finite-length nanowires together with axisymmetrically distributed emitters, was reported in [5]. In particular nanolaser configurations, however, one needs to treat asymmetric source distributions, such as a single quantum dot placed at an arbitrary distance from the nanowire axis. Here, we investigate the Purcell effect of asymmetric source distributions in proximity to the metal nanowire in two configurations: a metal cylinder truncated by perfectly conducting (PEC) mirrors, and a finite metal cylinder in free-space. In order to evaluate the Purcell factor, we precalculate the mode eigenvalues using Comsol Multiphysics (see Fig. 1 for an example). We compare the eigenfrequency and Purcell factor values calculated numerically with a semi-analytic theory to further analyze the impact of the emitters asymmetry and of the nanowire finite length.

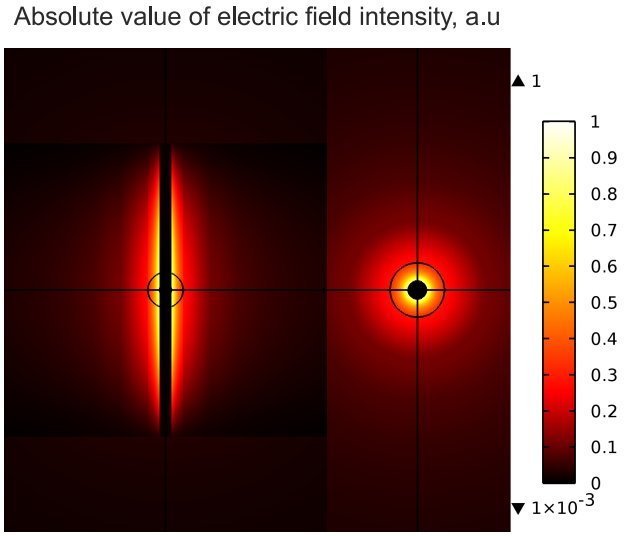

Figure 1. Fundamental plasmonic mode of a finite gold cylindrical nanowire (radius 10 nm, length 500 nm) truncated by PEC plates, with eigenfrequency $\omega = 2.819117e14 + 6.76228e12i$. Dielectric permitivity is calculated from the Drude model $\epsilon_2 = 1 - \omega_p^2/(\omega^2 + i\omega\gamma)$ with $\omega_p = 1.26 \cdot 10^{16}\mathrm{s}^{-1}$ and $\gamma = 1.41 \cdot 10^{14}\mathrm{s}^{-1}$.

References

[1] K. J. Russell, T.-L. Liu, S. Cui, and E. L. Hu, Nat. Photonics, **6**, 459 (2012).
[2] D. E. Chang, A. S. Srensen, P. R. Hemmer, and M. D. Lukin, Phys. Rev. B, **76**, 035420 (2007).
[3] R.-M. Ma, R. F. Oulton, V. J. Sorger, and X. Zhang, Laser Photonics Rev., **7**, 1 (2013).
[4] X. Wu, Y. Xiao, C. Meng, X. Zhang, Sh. Yu, et al., Nano Lett., **13**, 5654 (2013).
[5] C. Sauvan, J. P. Hugonin, I. S. Maksymov, and P. Lalanne, Phys. Rev. Lett., **110**, 237401 (2013).

Optimization of textured Si solar cell with array of hut-like micro pillars

F. J. Cabrera-España*, B. M. A. Rahman and A. Agrawal

School of Mathematics, Computer Science and Engineering, City University London

Francisco.cabrera-espana.1@city.ac.uk

In this paper, we present the simulation results of a hut-like array of micro pillars pattern for silicon solar cells. The Reflectance reduces when increasing the angle between substrate and base of the micro pillars.

Summary

In recent years various texturing patterns have been used to minimize the Reflectance from solar cells such as nano wires [1] and micro pillars (μP) [2]. Here, we present how Reflectance for 1 μm height perfectly vertical μP array can be further reduced. For this purpose, we vary the following simulation parameters: Surface Coverage (SC), cap (vertical section of the μP, see Fig.1) and ϑ (angle between substrate and μP, see Fig.1). This simulation is run for $\text{height} = 1\mu\text{m}$, $\text{cap} = 0.2\mu\text{m}$ and $\text{SC} = 30 - 50\%$.

Results

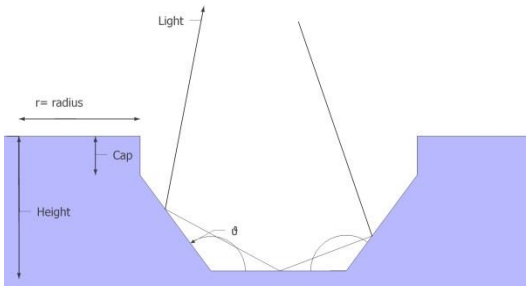

Fig.1 Schematic of hut-like micro pillar

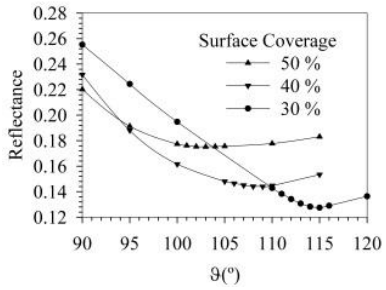

Fig.2 Angular performance $\text{height} = 1\,\mu\text{m}$ & $\text{cap} = 0.2\,\mu\text{m}$

From Fig. 2 we can see the ϑ variation from perfectly vertical (i.e. 90º) to larger values for the hut-like μP. The Reflectance reduces rapidly as ϑ increases for every SC; reaching a minimum. For further increase of ϑ, the hut-like μPs overlap with each other; leading to higher Reflectance. Another fact to highlight is the low values of SC while implementing the hut-like pattern provide a better Reflectance than the optimum SC for perfectly vertical micro pillars [3]. This is due to a more efficient light trapping in the hut-like pattern which enables a larger portion of the incoming light to be re-utilised.

Conclusion

The Reflectance reduces when placing hut-like μP array on top of the substrate instead of the perfectly vertical μP array. This improvement is due to a more efficient light trapping in the hut-like μP.

References

[1] E. Garnet and P. Yang (2010) *Light trapping in Silicon Nanowire Solar cell*, Nano letter, Vol. 10, 1082-1087.

[2] J. Shin *et al.* (2012) *Experimental study of design parameters in Silicon Micropillar Array Solar Cells produced by Soft lithography and metal-assisted chemical etching*, IEEE Journal of photovoltaics, Vol. 2, No. 2, 129.

[3] F. J. Cabrera-Espana, B. M. A. Rahman, A. Agrawal (2014) *Study of optical properties of textured Si solar cell with micro pillar,* OWTNM 2014, Nice, France.

Accurate and efficient arrayed waveguide grating simulations for InP membranes

B. Gargallo [1], Y. Jiao [2], P. Muñoz [1], J. van der Tol [2], X. Leijtens [2]
[1] *iTEAM Research Institute, Universitat Politècnica de València, Valencia, Spain*
[2] *COBRA Research Institute, Eindhoven University of Technology, Eindhoven, The Netherlands*
bergarja@iteam.upv.es

We analyze the Arrayed Waveguide Grating (AWG) response on indium phosphide (InP) membranes on silicon (IMOS) technology. The model is based on an analytical approach [1] that provides a better accuracy than the Gaussian approximation for similar simulation times.

Introduction

The IMOS photonic integration technique, based on the use of an indium phosphide membrane on top of a silicon chip, has advantages such as the possibility of integrating active and passive devices with approximately the same dimensions as silicon on insulator (SOI) technologies [2]. The cross-section consists of a silicon substrate, a 1850 nm height layer of silicon dioxide and the InP membrane (300 nm height) where the waveguides will be fabricated.

Design and simulation

Simulating AWGs with such high index contrast (HIC) is very difficult, due to the lack of an efficient numerical method where analytical approximations are still valid. In this work, we successfully developed an analytical method that can simulate the AWG accurately in a few seconds. The main idea is to reduce the 3D waveguide to a 2D waveguide applying the effective index method. Then, the field profile can be approximated as cosine and exponential functions. This method is not usually suitable for HIC structures, but in our case the use of shallow waveguides as inputs/outputs, where the approximation holds, enables us to apply it. For this reason, all the approximations used in [1] are still valid and the analytical model is applicable. As a comparison, Fig. 1 shows the real field profile obtained from a commercial software using the Film Mode Matching (FMM) method and the approximated field. An example of simulation using this analytical model is shown in Fig. 2. The comparison between simulations using the real profile and the analytical approach shows a very good match.

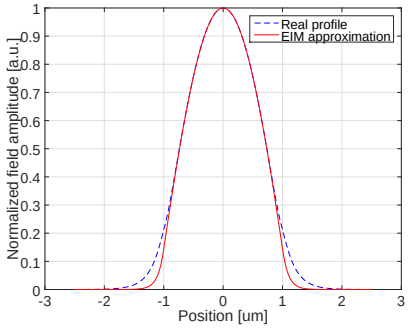

Fig. 1.: Field profile approximation

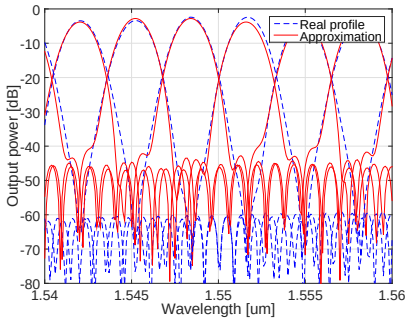

Fig.2.: Comparison between simulations

In conclusion, the analytical model provided in [1] is suitable for IMOS AWGs when using shallow waveguides as input/outputs, obtaining a good approach in a few seconds.

References

[1] E. Kleijn et al., *New analytical arrayed waveguide grating model,* J. Lightw. Technol. 31(20), 2013.
[2] J. van der Tol et al., *Photonic integration in indium-phosphide membranes on silicon (IMOS),* Proc. SPIE 8988, Paper 89880M, 2014.

Optimization of an Integrated Mach-Zehnder interferometer using the Fisher Information

N. Raicevic[1,2], A. Maluckov[1], J. Petrovic[1]

[1]*Institute of Nuclear Sciences Vinca, University of Belgrade, Belgrade, Serbia*
[2]*School of Electrical Engineering, University of Belgrade, Belgrade, Serbia*
**nevenar@vin.bg.ac.rs*

In this paper, a new approach to design of integrated Mach-Zehnder interferometers as sensors of fluid concentration is presented.Sensitivity estimation and optimization of the interferometer are based on calculation of the Fisher information.

Introduction

Integrated Mach-Zehnder interferometers (MZI) have been widely used in sensing and quantum optics. Interferometer sensitivity is defined as the smallest phase change that can be detected and is determined by the fringe slope and the measurement error. However, due to the uncertainty underlying quantum mechanics, quantum optics often uses statistical approach based on Fisher information (FI). Here, we explore application ofFI to classical MZI sensor and its optimization.

Summary

Changes in a fluid concentration cause changes in its refractive index and, hence, the index profile of an optical guide immersed in the fluid. The consequent modulation of the effective refractive index of the propagating mode is converted in the change in theintensity at the output of a MZI. The sensor sensitivity is calculated with respect to the refractive index of fluid n_F, thus keeping the consideration independent of the type of fluid.

The FIis a local probability measure of obtaining a system parameter from the data measured at the output [1]. For the MZI considered here, it is defined via a conditional probability function $p(I|n_F)$ that describes probability to obtain the output intensity I conditioned by n_F,$FI(n_F) = \int \frac{1}{p(I|n_F)} (\frac{dp(I|n_F)}{dn_F})^2 \, dI$. In a classical power measurement p has the normal distribution with the intensity variance given bythe detector precision.The maximum of FIgives the ultimate measurement sensitivity known as the Cramer-Rao bound,$\delta n_F = 1/\sqrt{FI_{max}}$,[1]. Therefore, the aim of the sensor design is to maximize the FI.

Results

The MZI intensity output is calculated numerically from the superposition of the eigenmodes of the test and reference waveguide for a range of n_F. It is used to determine the sensitivity both via the FI and standard definition $\delta n_F = \delta I/(dI/dn_F)$. The excellent agreement of the two corroborates our approach. FI was further used to obtain the waveguide profile that renders the maximum sensitivity.

Conclusion

Is it shown how the Fisher information can be defined and used as a measure of sensitivity of a classical integrated MZI. This result provides a tool for the measurement sensitivity estimation in classical optics that relates it to the approaches used to determine sensitivity scaling with the number of photons in quantum optics.

References

[1] B. R. Frieden, Science from Fisher information: A unification, Cambridge Univ. Press, 2004

Fiber based Plasmonic Sensor using Graphene oxide encapsulated Au-nanoparticles

Jeeban Kumar Nayak[1], Rajan Jha[1,*]
[1]*Nanophotonics and Plasmonics Laboratory, School of Basic Sciences, IIT Bhubaneswar, Odisha, India*
*rjha@iitbbs.ac.in,rajaniitd@gmail.com

Fiber sensor based on graphene oxide encapsulated Au nanoparticles has been reported. Here, the red shift of 10 nm has been observed for Au-nanoparticles encapsulated with 1 nm thick graphene oxide.

Introduction

Owing to the unique properties of graphene and its oxide, it has recently emerged as a novel class of 2D carbon-based nanomaterials. Encapsulating gold nanoparticles in graphene oxide shells has been used as novel gene vector [1]. However, here we have studied the effect of Graphene Oxide Encapsulated Gold nanoparticles (GOE-Au NPs) on the performance of fiber based plasmonic sensor. Fig.1 shows the proposed set up, where fiber cladding of 1 cm length can be removed from the centre through chemical etching. At the cladding removal site, GOE-Au NPs can be deposited. Light can be launched at one end of the fiber with proper optics and the absorbance spectrum can be studied at the other end of the fiber.

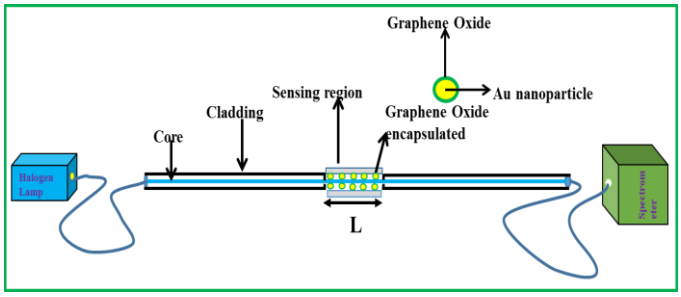

Fig. 1. The Proposed Set up.

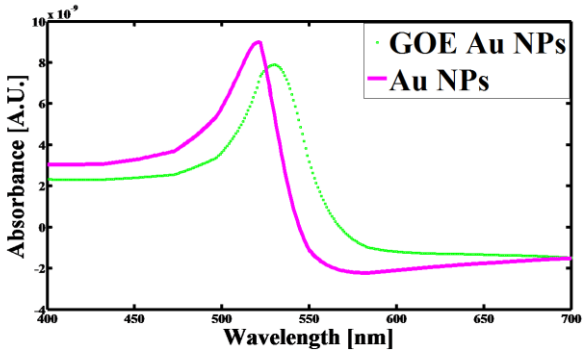

Fig.2. The variation of absorbance with wavelength for GOE-AuNPs and Au NPs.

Results

Fig.2 shows the variation of absorbance with wavelength for two cases, one deposited with Au NPs and other with GOE-Au NPs. It has been observed by introducing graphene oxide of thickness 1 nm around the Au NPs of dia. 40 nm, the peak absorbance value decreases due to the damping effect of surface plasmons. Also, we found that the resonance wavelength shift from 520nm (only gold nanoparticles) to 530 nm after encapsulate gold nanoparticles with graphene oxide as the resonance condition satisfied at higher wavelength.

Conclusion

Fiber based Surface plasmon resonance (SPR) using graphene oxide encapsulated Au nanoparticles has been studied. By encapsulating Au nanoparticles with 1 nm thick graphene oxide, the red shift of 10 nm has been observed. With changing the refractive index in the sensing region, the sensor can be used as refractive index sensor.

References

[1] Cheng Xu, et.al. Encapsulating *Gold Nanoparticles or Nanorods in Graphene Oxide Shells as a Novel Gene Vector*, ACP Appl. Mater. Interfaces 5, 2715-2724, 2013.

Travelling Wave Model Approach for Longitudinal Multimode Dynamics in Multi-Section Lasers

A. Pérez-Serrano[1,*], M. Vilera[1], J. Javaloyes[2], J.M.G. Tijero[1], I. Esquivias[1], S. Balle[2,3]

[1]*CEMDATIC-ETSI Telecomunicación, Universidad Politécnica de Madrid (UPM), 28040 Madrid, Spain*

[2]*Departament de Física, Universitat de les Illes Balears (UIB), 07122 Palma de Mallorca, Spain*

[3]*Institut Mediterrani d'Estudis Avançats, IMEDEA (CSIC-UIB), 07190 Esporles, Spain*

*antonio.perez.serrano@upm.es

We investigate the previously observed longitudinal multimode dynamics of a multi-section master oscillator power amplifier device by means of a travelling wave model that incorporates coupled cavities and thermal effects. We discuss their appearance and dependence on geometrical factors and temperature.

Master Oscillator Power Amplifiers (MOPAs) are devices suitable for applications requiring high brightness light sources. Monolithically integrated MOPAs usually comprise two sections: an index guided single lateral mode waveguide section acting as a Master Oscillator (MO) (in our case a Distributed Feedback laser (DFB)) and a gain-guided Power Amplifier (PA) section. Ideally, the single lateral and longitudinal mode generated by the MO is injected into the PA section where it undergoes free diffraction and amplification keeping its initial beam quality. However, MOPAs often exhibit instabilities that have been attributed to a combination of thermal effects and the residual reflectance at the amplifier front facet, which leads to the coupling of the MO modes and the modes of the full MOPA cavity [1].

In this contribution, we numerically investigate the different dynamical regimes previously observed in a MOPA emitting at 1.5 μm [2]. The theoretical framework is a Travelling Wave Model (TWM) [3] that naturally includes spatial effects (such as spatial hole burning and coupled-cavity effects) and multimode dynamics. Thermal effects are included by considering the optical response of the Quantum Well active medium within the quasi-equilibrium approximation at finite temperature [4], with a phenomenological description of the redshift of the gain peak and the changes in the background material refractive index by means of self- and cross-heating coefficients for both sections. Fig. 1 shows the simulated evolution of the optical spectra (a) and the Radio-Frequency (RF) spectra (b) as a function of the PA current while keeping the MO current constant at a value slightly above the threshold. The great variety of dynamical regimes appearing under these conditions include: emission at the Bragg wavelength, emission at the gain peak and self-pulsations. We discuss the appearance of these dynamical regimes and their dependences on the geometrical factors and temperature via numerical simulations, in comparison with our previous experimental results [2]. In addition, we perform a semi-analytical modal analysis of the TWM for such devices in order to get a deeper physical insight [5].

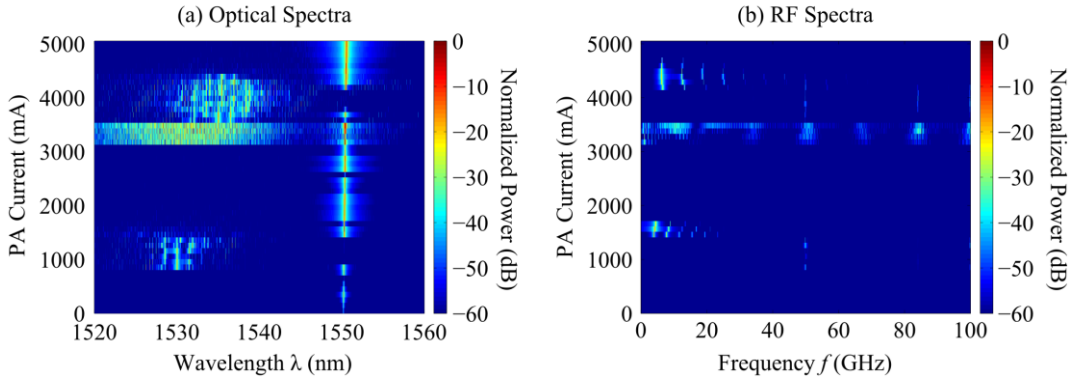

Fig. 1. Numerical simulation of the evolution of the optical and RF spectra as a function of the PA current.

References

[1] Spreemann et al. *IEEE J. Quantum Electron.* **45**, 609 (2009)
[2] Vilera et al. *submitted to IEEE Photon J.*
[3] Javaloyes and Balle, *IEEE J. Quantum Electron.* **45**, 431 (2009)
[4] Javaloyes and Balle, *IEEE J. Quantum Electron.* **48**, 1519 (2012).
[5] Pérez-Serrano et al., *Phys. Rev. A* **89**, 023818 (2014).

Transmission Spectra in a Multilayer Photonic Structure

E.L. Albuquerque*, U.L. Fulco and M.S. Vasconcelos
Department of Biophysics, UFRN, 59072-970, Natal-RN, Brazil
e-mail: eudenilson@gmail.com

In this work we investigate the transmission spectra of a light beam normally incident from a transparent medium into a multilayer photonic structure composed of SiO2 / metamaterial layers arranged in a quasiperiodical fashion, which follows the Fibonacci (FB) substitutional sequences.

Introduction

Materials simultaneously possessing negative magnetic permeability and electric permittivity are physically permissible and would exhibit a negative refractive index [1]. They were coined as left-handed materials (LHM) because they support backward waves, for which the electric field ***E***, the magnetic field ***H***, and the Poynting vector ***S*** form a left-handed triplet. Besides, the group velocity of wave propagation in such media is opposite to its phase velocity, making the perfect lens possible. Periodic multilayered structures containing these materials can be considered as a sequence of perfect lenses with unique transmittance or reflectance properties in the Bragg regime [2]. On the other hand, the discovery of quasiperiodic structures has fired up this field, giving rise to many practical applications (for a review see Ref. 3).

Results

The optical transmission spectrum for the 9th-generation (55-layer) quasiperiodic FB sequence, as a function of the reduced frequency $\Omega=\omega/\omega_0$, ω_0 being the midgap frequency, is depicted in Fig. 1(a). The transmission spectrum presents a unique mirror symmetrical profile around the midgap frequency $\Omega = 1$ (the midgap frequency of a periodic quarter-wavelength multilayer). Besides the structure is transparent at the reduced frequencies $\Omega = 0.898$ and $\Omega = 1.101$, as we can see in Fig. 1(b), forming two broad peaks, also distributed symmetrically around $\Omega = 1$. Furthermore, the transmission spectrum has a scaling property with respect to the generation number of the FB sequence, within a symmetrical interval around $\Omega = 1$.

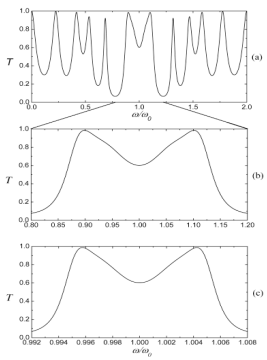

To understand this scaling property, consider Fig. 1(b), which shows the optical transmission spectrum of Fig. 1(a) for the range $0.80 < \Omega < 1.20$. This spectrum is the same, as shown in Fig. 1(c), to the one representing the 15th-generation quasiperiodic FB sequence (i.e. it has been recovered after six Fibonacci generations), for the range of frequency reduced by a scale factor approximately equal to 25, characterizing a six-cycle self-similar behavior with respect to the generation number of the Fibonacci sequence.

Fig. 1: Transmission spectra of a light beam into a FB photonic structure.

Acknowledgement: The authors want to acknowledge the Brazilian Research Agencies CNPq and CAPES.

References

[1] V.G. Veselago, *Sov. Phys. Usp.* **10,** 509 (1968).
[2] M.S. Vasconcelos, P.W. Mauriz, and E.L. Albuquerque, *Phys. Lett. A* **373**, 496 (2009)
[3] E.L. Albuquerque and M.G. Cottam, *Phys. Rep.* **376,** 225 (2003).

Dynamics of decelerating pulses at a dielectric layer

A. Nerkh[1,*], D. Zolotariov[1], O. Kuryzheva[1] and T. Benson[2]
[1] *Kharkov National University of Radio Electronics, 14 Lenin Ave., Kharkov, 61166, UKRAINE*
[2] *George Green Institute for Electromagnetics Research, University of Nottingham, University Park, Nottingham, NG7 2RD, UK*

* nerukh@gmail.com

Time dependent electromagnetic pulses propagating with deceleration along the dominant propagation direction and passing a dielectric layer is investigated in the 1D+T case. Consideration is made by using an integral equation in paraxial approximation and the symmetric Green's function.

Introduction

An approach which considers a problem when electromagnetic pulses are generated by an external source is given without making any assumptions on the temporal dependence of the field but with assumption of the paraxial approximation. It provides a physically natural picture of the phenomenon, allows to avoid a problem of backward flow of time and has a clear physical meaning being free of exotic corollaries [1]. The construction of the decelerating Airy pulse and the Gaussian is given.

Summary

The problem is described by the integral equation in paraxial approximation by using the symmetric Green's function. The results are presented in Fig. 1 where comparison of the reflected wave and the transmitted one (both in red) with the initial wave (blue) is shown**.**

Results

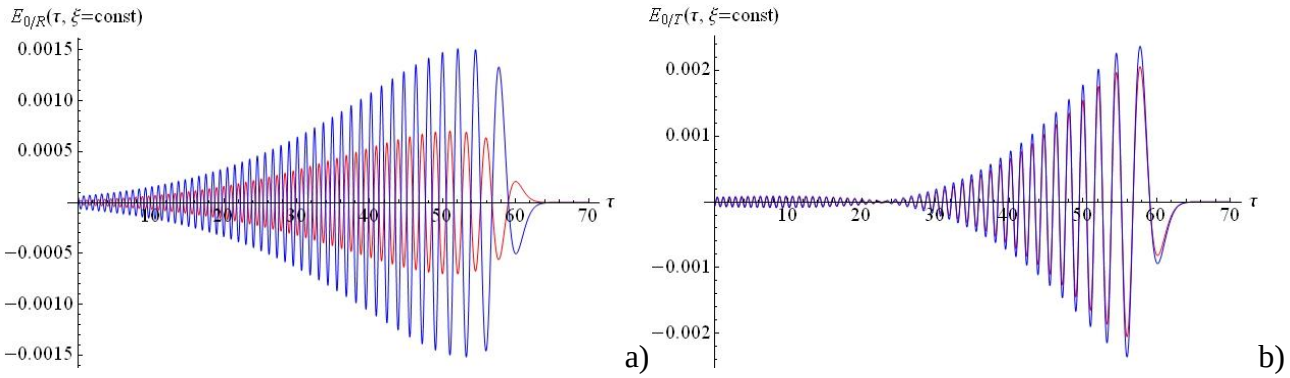

Fig. 1. Comparison of the reflected wave (a) and the transmitted one (b) with the initial wave which is given in blue.

Conclusion

The interaction of the time dependent Airy and Gauss pulses with a dielectric layer is considered by a method of the integral equation in paraxial approximation. It is shown that the corresponding reflected and transmitted pulses propagate in time with deceleration.

References

[1] I. Kaminer, Y. Lumer, M. Segev, D.N. Christodoulides, Causality effects on accelerating light pulses, Optics Express, vol. 19, No 23, 23132-23139 (2011).

A Switchable Figure Eight Fiber Laser Based on Inter-Modal Beating By Means of Non-Adiabatic Microfiber

A. A. Jasim[1,*], M. Dernaika[1], S.W. Harun[1], H. Ahmad[1]
[1] *Photonics Research Centre (PRC), University of Malaya, 50603 Kuala Lumpur, Malaysia*
*jasim@um.edu.my

Switchable multi-wavelength figure eight fiber laser effect of multi-mode interference is proposed by incorporating a tapered non-adiabatic microfiber in a Sagnac loop mirror. The proposed laser generated single longitudinal modes having a 3 dB line-width of less than 0.16 pm with an optical signal-to-noise ratio of 58 dB at 82 mW pumping power. Moreover, nonlinear polarization rotation and strain switching mechanisms are demonstrated for generating single, dual and triple wavelength over more than 20 nm span.

Introduction

Switchable fiber lasers have been developed intensively over the last ten years as it allows a fast switching from single wavelength to dual and multiple wavelength operation with very high speed while maintain high stability and reliability. Recent designs accomplished switchable and tunable multi wavelength fiber laser with single longitudinal mode (SLM) output using a distributed mirror and configurable filter mirror design and achieved a switchable wavelengths with a 50 and 100 GHz spacing [1].

Summary

An experimental demonstration of a novel design of multi-wavelength switchable figure eight fiber laser based multi-mode interference that used a tapered non-adiabatic microfiber of 70 mm length and 2 μm diameter as a comb filter. The design was able to generate single, dual and triple longitudinal modes. Two mechanisms of nonlinear polarization rotation and straining are used for switching wavelength over a range of 20 nm span as shows in figure 1.

Results

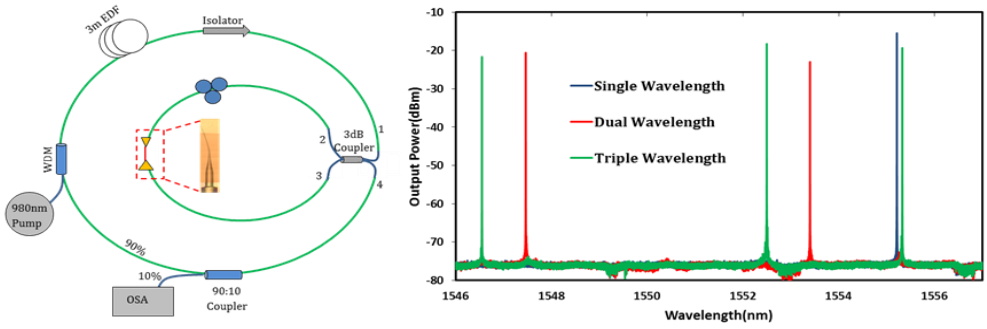

Fig. 1. The experimental setup of the proposed figure eight laser besides the generated of the single, dual and triple wavelength.

Conclusion

The proposed laser generated single longitudinal modes with an OSNR of 58 dB at 82 mW pumping power with a 3 dB linewidth of at most 0.16 pm. Two mechanisms, nonlinear polarization rotation and straining, were demonstrated as enabling efficient generation of single, dual and triple wavelengths.

References

[1] V. DeMiguel-Soto, M. Bravo, and M. Lopez-Amo, *Fully switchable multiwavelength fiber laser assisted by a random mirror*, Optics Letters, vol. 39, 2014.

Effect of Filling the Surface Texture with Metamaterial on Spoof Surface Plasmon Dispersion

T. Gric[1,2,3*], J. Pistora[3], M. Cada[1,3]

[1] *Dalhousie University, Halifax, Canada;* [2] *Semiconductor Physics Institute, Center for Physical Sciences and Technology, Vilnius, Lithuania;* [3] *Center for Nanotechnologies, Technical University of Ostrava, the Czech Republic*

*Tatjana.Gric@dal.ca

Herein we investigate a conducting film with holes filled with a metamaterial, we find that the surface texture and geometry can significantly influence the dispersion.

Introduction

In this work, we deal with an influence of the surface geometry and arrangement on spoof surface plasmon polaritons (SPP) dispersion in more detail and note that the material inside the fundamental unit can play a major role. The present study may have a significant contribution to the design of novel types of materials

Results

A dielectric dispersion relation for a conducting film with two-dimensional (2-D) periodic rectangular holes has already been derived in [1]. Let us assume that holes are filled with a metamaterial [2]. Fig. 1 shows the dispersion curves for spoof SPPs on corrugated surfaces with different lattice constants D=200, 300, 400 nm. The groove parameters are a=b=150 nm for all cases.

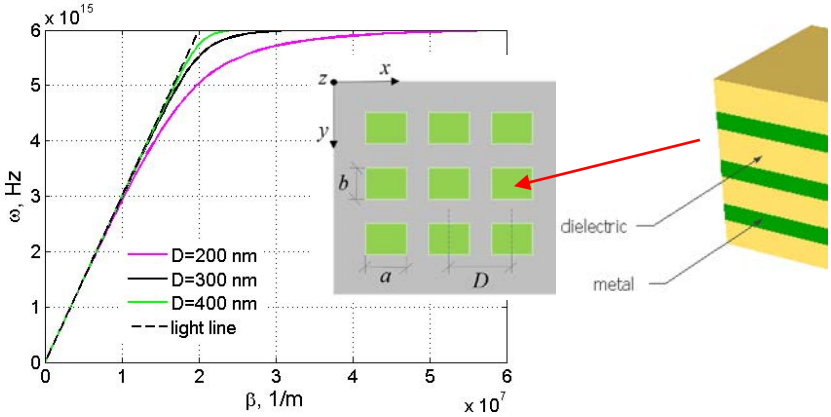

Figure 1. Dispersion relations of spoof SPPs for different lattice constants.

Conclusion

A method for analyzing spoof SPPs on a structured surface has been presented. Compared to the previous works, our approach enables us to investigate a conducting film with holes filled with a metamaterial since it takes into account its permittivity.

References

[1] S.-H. Yang, P. R. Bandaru, *Effect of surface texture and geometry on spoof surface plasmon dispersion*, Opt. Eng. 47(2), 029001 (2008).

[2] V. M. Agranovich, V. E. Kravtsov, *Notes on crystal optics of superlattices*, Solid State Commun. 55, 85–90 (1985).

Effect of wavelength and graphene layers on the SPR sensitivity

K. Bhavsar and R. Prabhu*
IDEAS Research Institute, Robert Gordon University, Aberdeen, United Kingdom
*r.prabhu@rgu.ac.uk

This paper reports study on the effect of wavelength and graphene layers on the sensitivity of the surface plasmon resonance (SPR) sensor. Results have suggested that increase in the wavelength of light decreases the sensitivity, while increasing the number of graphene layers increases the sensitivity of the SPR sensor.

Introduction

Graphene, a single layer of carbon atoms arranged in honeycomb structure, is emerging as the most popular material of the decade which is under intense research. Recently, there have been few reports on using the graphene on thin metal film based SPR sensor in order to improve the sensitivity [1]. But, the role of wavelength on the sensitivity of the graphene based SPR sensors has not been investigated. Herein, we report Matlab based investigations on wavelength effect on the sensitivity of graphene based SPR sensor and relative sensitivity enhancement with increase in graphene layers.

Results and discussions

Reflectivity of the p-polarized incident light has been calculated using the N-layer model for a most common Kretschmann configuration. Sensitivity analysis has been carried out for a change in refractive index unit (RIU = 0.005) using 50 nm gold film coated on high refractive index (SF11) prism at 633 nm. To analyze the effect of graphene layers, reflectivity calculations have been carried out for multi-layers of graphene. Sensitivity enhancement over the conventional SPR ($\Delta S_{RIU}^{L}/S_{RIU}^{0}$) have been calculated for different wavelengths with increasing the number of graphene layers, L = 1 to 10, as shown in fig.1. Results have shown that with increase in the number of graphene layers sensitivity increases while increase in the wavelength cause reduction in sensitivity.

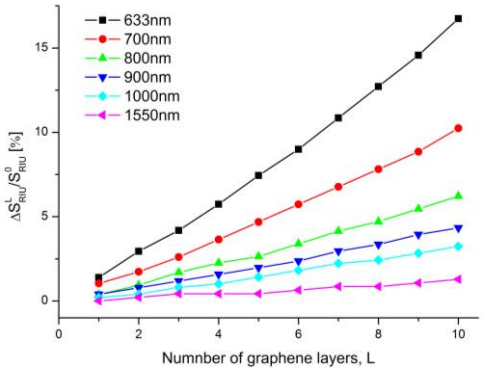

Fig. 1. SPR sensitivity enhancement as a function of graphene layers at different wavelengths.

Conclusion

Effect of wavelength and relative sensitivity enhancement over conventional SPR sensor have been investigated and found that increase in wavelength reduces the sensitivity, while increase in the number of graphene layers enhances the sensitivity of the graphene based SPR sensors. These investigations have opened up new possibilities for highly sensitive biomolecular interactions studies.

References

[1] J. A. Kim, J. Kang et al. *Journal of Nanoscience and Nanotechnology* **12,** 5381-5385 (2012).

Modelling of Polarization and Wavelength Insensitive Single Mode Al_2O_3 Rib Waveguides for Active and Passive Applications

M.Demirtaş[1*], A.Özden[2], F.Ay[1]
[1]*Anadolu University, Department of Electrical and Electronics Engineering, Eskişehir, Turkey*
[2]*Anadolu University, Department of Material Science and Engineering, Eskişehir, Turkey*
*m_demirtas@anadolu.edu.tr

A single mode, polarization and wavelength insensitive a-Al_2O_3 rib waveguide on thermal oxide with optimized confinement factor and mode size was modelled for applications at telecommunication wavelengths at the range of 1.48 – 1.61 µm.

Introduction

Amorphous Al_2O_3 (a-Al_2O_3) is an interesting candidate for waveguide application due to its relatively high refractive index which allows high optical confinement. This in turn paves the way for small-footprint micro-photonic devices [1]. Another attractive property of a-Al_2O_3 based waveguides stems from the fact that large amounts of rare-earth ions can be homogeneously doped into a-Al_2O_3 and thus is of interest for realization of integrated optical amplifiers such as active waveguides [2].

Summary

In this study, Beam Propagation Method (BPM) is used to determine single mode, polarization and wavelength insensitive operation region. Effect of rib width and etch depth for a fixed waveguide height is investigated with a mode solver program. Simulation range of etch depth and rib width dimensions ranges from 0 to 0.5 µm and 0 to 10 µm, respectively. This range of parameters has been specifically chosen in accordance with the growth capabilities of Atomic Layer Deposition (ALD) tool, which is intended to be used for realization of the devices.

Results

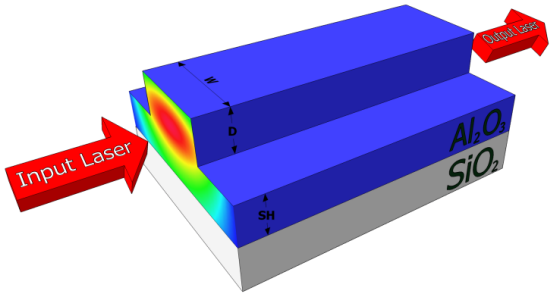

Fig.1. Schematic of a-Al_2O_3 waveguide structure

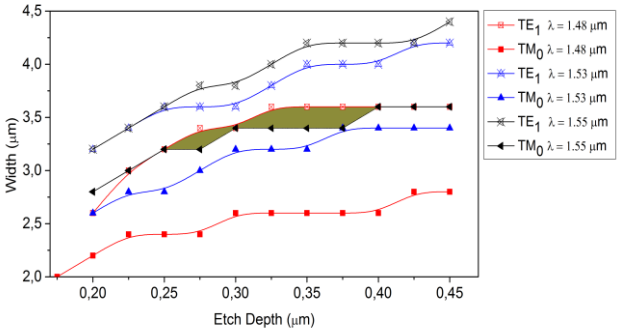

Fig.2. Simulation results

Optimized waveguide structure is given in Fig.1. W, D and SH represents waveguide rib width, etch depth and slab height, respectively. In Fig.2, green filled area demonstrates the region where indicated wavelengths are single mode for both polarizations and have no birefringence.

Conclusion

In this paper, we investigate the effects of the wavelength, polarization, rib width, and etch depth on waveguide mode characteristics. As a result, polarization and wavelength independent single mode design range is identified and a novel TE mode selective filter design is suggested.

References

[1] M. K. Smith, G. A. Acket, C. J. Vaan Der Laan, *Al_2O_3 Films for Integrated Optics*, Thin Solid Films (138), 171-181, The Netherlands, 1986.

[2] K.Wörhoff, J.D.B. Bradley, F.Ay, M. Pollnau, *Low-Loss Al_2O_3 Waveguides for Active Integrated Optics*, OSA, Conference on Lasers and Electro-Optics, Baltimore, Maryland United States, 2007.

Advanced bifurcation analysis of a laser diode with phase-conjugate feedback

M. Sciamanna [1], E. Mercier [1], A. Karsaklian dal Bosco [1], M. Virte [1], L. Weicker [1], D. Wolfersberger [1]

[1] *CentraleSupélec, OPTEL and LMOPS lab. (CentraleSupélec-Université de Lorraine), Metz, France*
marc.sciamanna@centralesupelec.fr

The richness and complexity of laser diode nonlinear dynamics is here revisited in the context of a phase-conjugate optical feedback. The combination of mathematical and numerical analysis with experiment provides new insight into the underlying bifurcations and brings new perspectives into this 30-years old problem.

Introduction-A laser diode behaves dynamically like a damped nonlinear oscillator showing so-called relaxation oscillations. However there exist configurations including external optical feedback for which these oscillations become un-damped leading to self-pulsation and chaos [1]. This problem has been traditionally addressed in the context of conventional optical feedback (from an external mirror). However applications have driven a resurgent interest in analyzing configurations such as phase-conjugate optical feedback where the reflected field is dynamically filtered and self-aligned.

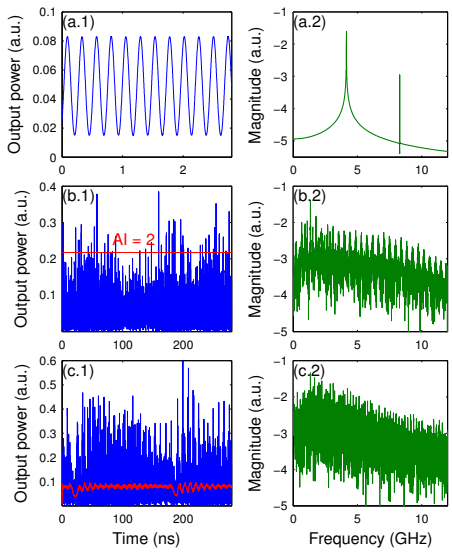

Fig. 1. Numerical results. (a) super-harmonic self-pulsation. (b) extreme events in chaotic dynamics. (c) chaotic low-frequency fluctuations.

Results - Phase-conjugation is achieved experimentally using four-wave mixing in a SPS photorefractive crystal [2]. The laser diode is an edge-emitting laser emitting at 852 nm. We model the laser system using modified Lang-Kobayashi rate equations [3]. Figure 1 shows qualitatively different dynamics observed numerically and then confirmed experimentally when increasing the external-cavity length (left: time-trace, right: power spectrum). In (a) the laser diode shows self-pulsation at a harmonic frequency of the external cavity (called external-cavity mode solution or ECM). The case (b) shows a chaotic dynamics with high intensity pulses that overcome the threshold for so-called extreme events ('AI' or abnormality index equals 2). In (c) the chaotic pulses now show a greater contribution of low-frequency dynamics as typical for so-called low-frequency fluctuations (LFF). We shall discuss how these different dynamics bifurcate from the ECM and then analyze the impact of the laser and feedback parameters.

References

[1] M. Virte, K. Panajotov, H. Thienpont, M. Sciamanna, *Deterministic polarization chaos from a laser diode,* Nat. Photonics 7, 60-65 (2013).

[2] A. Karsaklian dal Bosco, D. Wolfersberger, M. Sciamanna, *Super-harmonic self-pulsations from a time-delayed phase-conjugate optical system,* Appl. Phys. Lett. 105, 081101 (2014).

[3] E. Mercier, D. Wolfersberger, M. Sciamanna, *Bifurcation to chaotic low-frequency fluctuations in a laser diode with phase-conjugate feedback,* Opt. Lett. 39, 4021-4024 (2014).

Investigation of Confinement Losses in Photonic Crystal Fibre

J. Johny*, R. Prabhu, W.K. Fung
Ideas Research Institute, School of Engineering, Robert Gordon University, Aberdeen, United Kingdom
*j.johny@rgu.ac.uk, r.prabhu@rgu.ac.uk, w.k.fung@rgu.ac.uk

An investigation of confinement losses in liquid crystal filled Photonic Crystal Fiber (PCF) with different number of air hole rings was conducted. The hexagonal solid core PCF with liquid crystals has been designed using COMSOL MULTIPHYSICS software.

Introduction

Liquid crystal PCFs are opening new perspectives in optical telecommunication, all- optical switching and sensing applications [1]. It is important to develop approaches to reduce losses occurring within the core of the PCF, so that the Signal to Noise Ratio (SNR) is improved and thereby the transmission and sensing range of the fiber can also be increased. Confinement loss is the leakage of power from the core into the cladding.

Summary and Results

Confinement loss depends on the number of rings and it decreases with increase in number of rings. As the number of rings is increased, light confinement increases and confinement losses also gets reduced. In our analysis, the four ring structure showed minimum confinement loss, because the field leakage was negligible.

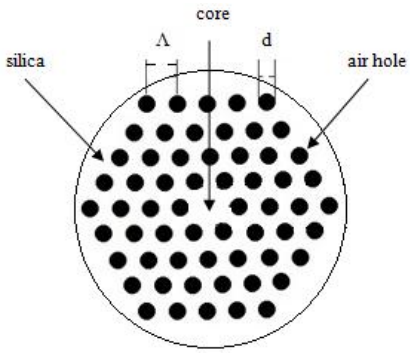

Fig. 1. Cross section of liquid crystal PCF

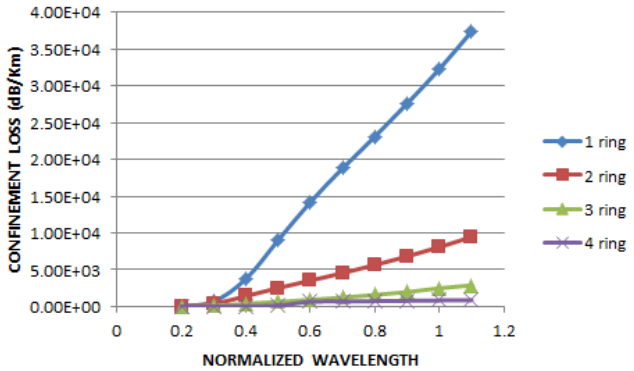

Fig. 2. Confinement loss vs normalized wavelength.

Fig. 1 shows the cross section of the designed four ring liquid crystal PCF, where pitch (Λ) is the hole to hole spacing and d is the diameter of the air hole. Refractive index of background material, silica is taken as 1.45 and the airhole is infiltrated with liquid crystal having index value 1.522. Fig. 2 shows the variation of confinement loss (L) with respect to normalized wavelength (λ/Λ) for a liquid crystal filled PCF with d/Λ=0.5, Λ=2μm, d=1 μm for different number of air hole rings in the cladding. For small values of d/Λ, the resulting loss can be large unless a sufficiently large number of air holes are introduced in the PCF core.

Conclusion

From the current investigation, it was found that confinement loss is a strong function of number of rings employed in the cladding. The greater the confinement, the lesser will be the confinement loss. Further investigations will be carried out by varying the air hole size, shape and distribution for improving the SNR.

References

[1] Wolinski T, Szaniawska K, Ertman S, Lesiak P, Domanski A, Dabrowski R, et al. Influence of temperature and electrical fields on propagation properties of photonic liquid-crystal fibres. *Measurement Science and Technology.* 2006; 17(5):985.

Modelling the optical properties of mixed ionic and electronic conductors (MIECs) with reversible ion intercalation

F. Morichetti[1], L. Lüken[2], F. Berkemeier[2], G. Schmitz[3], H.-D. Wiemhöfer[2], and A. Melloni[1,*]
[1]*Dipartimento di Elettronica, Informazione e Bioingegneria, Politecnico di Milano, Milano, Italy*
[2]*Institute of Materials Physics, University of Münster, Münster, Germany*
[3]*Institute of Materials Science, University of Stuttgart, Stuttgart, Germany*
[4]*Institute of Inorganic and Analytical Chemistry, University of Münster, Münster, Germany*
*andrea.melloni@polimi.it

We propose a Lorentz-oscillator-based model to describe the change of the optical properties of ion-intercalated mixed ionic and electronic conductors (MIECs) in the visible and near-IR wavelength range.

In mixed ionic and electronic conductors (MIECs), intercalation of mobile ions and coupled changes of electron concentration can be reversibly controlled by an applied voltage between suitable contact materials. This is usually accompanied by a non-volatile and reversible change of the optical properties. Many transition metals based MIECs (Ta_2O_5, WO_3, and V_2O_5) can intercalate ions and exhibit also good transparency in the near-IR range, thus making them good candidates for many optical applications. In this work, we analyze the physical mechanisms responsible for the change of the real (n) and imaginary (k) part of MIECs upon ion-intercalation. Our results show that the *free-charge* Drude model conventionally employed for modeling carrier injection/depletion effects in covalently-bonded crystal (e.g. Si and InP, often referred to as Soref equations [1]) does not apply to MIECs.

In ion-intercalated MIECs, Coulomb interaction between conduction electrons and lattice ions (Fig. 1a) results in a strong electron-phonon coupling (*polaron* particle). Polaron effects can be described by the Lorentz oscillator model, where conduction charges are assumed to be *bounded* to the crystal atoms. The complex dielectric constant ε is given by

$$\varepsilon = \varepsilon_s + \frac{\omega_p^2}{j\omega/\tau + \omega_0^2 - \omega^2}, \qquad (1)$$

where ε_s is the static dielectric constant, $\omega_p=(Nq^2/\varepsilon_0 m^*)^{1/2}$ is the plasma frequency (N ion intercalation density, q electron charge, ε_0 vacuum permittivity, m^* polaron effective mass), τ and $\omega_0 = 2\pi c/\lambda_0$ are polaron relaxation time and resonant frequency. Fig. 1 shows a comparison between experimental data reported in the literature [2] and theoretical models for (b) Δk and (c) Δn in a Li-intercalated WO_3 film with N=1.47·10^{21} cm^{-3}, demonstrating the accuracy of the bound charge model across the entire visible/near-IR range. Around ω_0 ($\omega_0 << 1/\tau$), simple relations can be derived

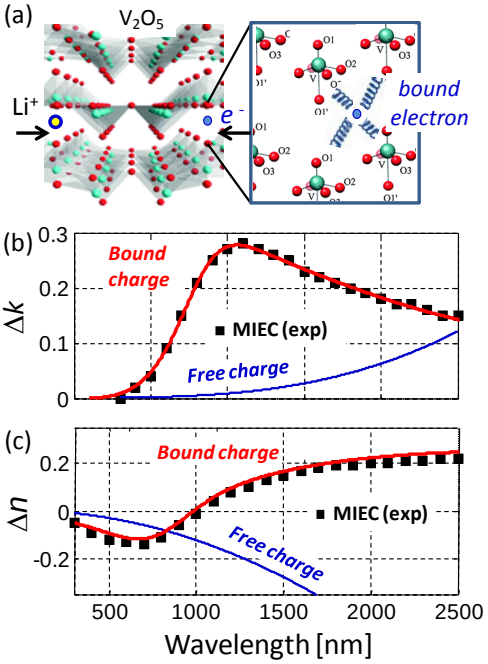

Fig. 1. (a) Schematic picture of ion-intercalation in MIEC; comparison between experimental data (squares) [2] and models for Li-intercalated WO_3: *free-charge* (blue) and *bound-charge* (red) model for (b) Δn and (c) Δk.

$$\Delta n = \frac{\mu^2 m^*}{2n\varepsilon_0}\frac{\lambda^2 - \lambda_0^2}{\lambda_0^2}\Delta N, \qquad (2)$$

$$\Delta k = \frac{\omega_p^2 \tau}{2n\omega} = \frac{q\mu\lambda}{4\pi n\varepsilon_0 c}\Delta N, \qquad (3)$$

representing the analogous of the free-carrier Soref equations for ion-intercalated MIECs. The validity of the model has been demonstrated also for other material compounds (V_2O_5, $LiCoO_2$).

[1] R. A. Soref, *et al.*, IEEE J. Quant. Electron. **23**, 123 (1987).
[2] K. von Rottkay, *et. al.*, Thin Solid Films **306,** 10 (1997).

POSTERS 2

Saturday 18th April

Diffraction Suppression and Soliton Formation in Binary Plasmonic Lattices

Yao Kou* and Jens Förstner
Department of Electrical Engineering, University of Paderborn, Warburger Str. 100, 33098 Paderborn, Germany
* yao.kou@uni-paderborn.de

Introduction

New types of plasmonic solitons are studied under a binary metal-dielectric lattice. We find that the transverse lattice modulation greatly suppresses discrete diffraction and decreases the required nonlinearity to support these subwavelength solitons.

Summary

Plasmonic solitons have received an increasing attention in the recent years, due to its fundamental and practical interest in nonlinear optics and nanophotonics [1,2]. The space localization of these solitons is not restricted by the diffraction limit. However, due to the strong discrete diffraction, giant nonlinear refractive index is usually required, which create a barrier on their experimental realization.

Here we consider the existence of solitons in a binary-modulated plasmonic lattices. Under a suitable modulation depth, we observe significant diffraction suppression, accompanied by the generation of a transmission gap inside the fundamental band. Figure 1(a) shows a plasmonic soliton supported by the binary lattice. Compared with its counterpart in the uniform lattice, one sees that the soliton size can be deeply compressed with a reduced power and nonlinearity level, as shown in Fig 1(b). We also reveal the existence of photonic-plasmonic vector solitons in such binary lattice, whose mutual trapping behavior is determined by the originating band of the plasmonic component.

Results

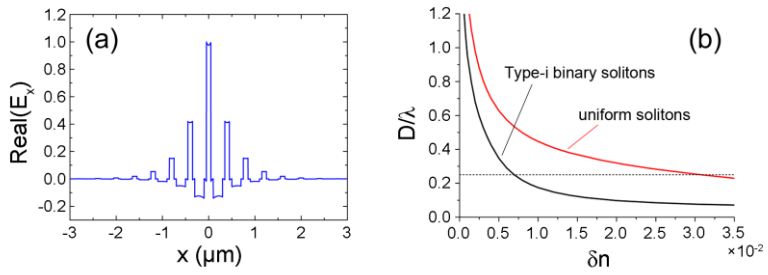

Fig. 1. (a) Normalized electric field profile of Type-i plasmonic solitons. (b) Soliton effective diameter D *vs.* nonlinear refractive index δn, for Type-i binary solitons and uniform solitons.

Conclusion

We show significant diffraction suppression and ultra-small solitons in binary plasmonic lattices.

References

[1] Y. Liu, G. Bartal, D. A. Genov, and X. Zhang, Phys. Rev. Lett. 99, 153901 (2007).

[2] Y. Kou, F. Ye, and X. Chen, Opt. Lett. 38, 1271 (2013).

Efficient Optical Modeling of Graphene

R.B. Armenta, J. Niegemann, J. Pond*, A. Reid
Lumerical Solutions Inc.
*jpond@lumerical.com

An efficient numerical approach for modeling graphene within the FDTD algorithm is presented here. By introducing graphene as a 2D conductive surface within a 3D FDTD discretization, we show that the properties of graphene can be accurately modeled without resorting to very fine grids.

Motivation and Approach

Simulating graphene using a 3D permittivity (or conductivity) is computationally inefficient because graphene is usually a thin material layer with a thickness as small as one atom. Our method introduces graphene as a 2D conductive surface within a 3D FDTD grid and avoids the need for small mesh sizes. It is able to accurately account for the full dispersion of graphene at arbitrary temperature and chemical potential, including both intra-band and inter-band effects. As an example, consider the slotted graphene waveguide geometry described in Fig. 1 (left). The structure, originally introduced in [1], is excited with the mode shown in Fig. 1 (right).

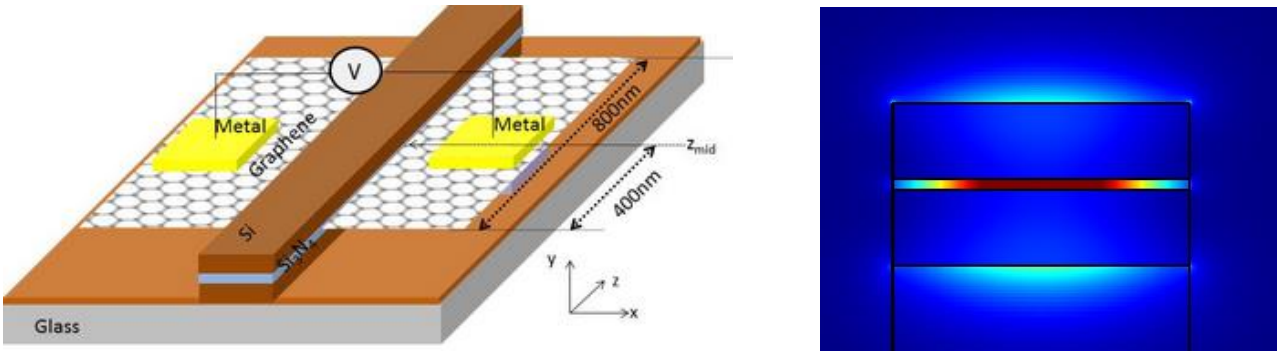

Fig. 1. Slotted graphene waveguide geometry (left) excited at λ=1550nm with the shown mode (right).

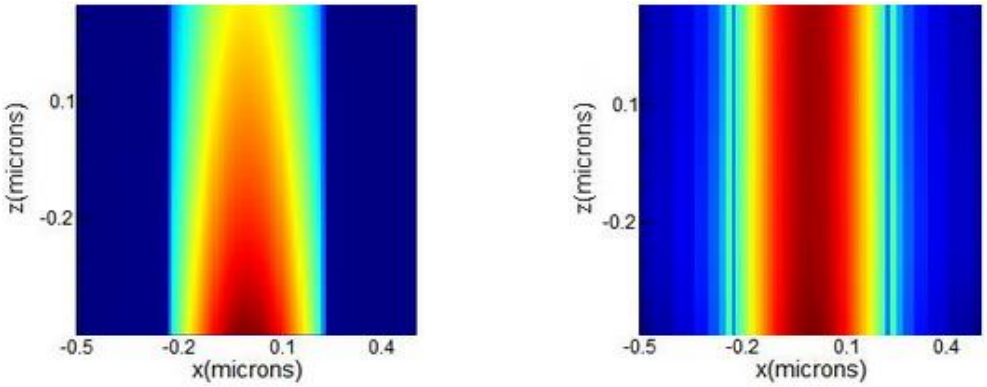

Fig. 2. Electric field amplitude along the propagation axis (z) with (left) and without (right) a bias voltage.

Conclusion

Our approach can accurately simulate the properties of graphene, and obtain good agreement with significantly less efficient 3D effective permittivity based methods.

References

[1] Z. Lu and W. Zhao, "Nanoscale electro-optic modulators based on graphene-slot waveguides," *J. Opt. Soc. Am. B* vol. 29, pp. 1490-1496 (2012).

Analysis of modal spectrum and associated thresholds of a silver-strip plasmonic nanolaser as a novel light emitter

O.V. Shapoval*, A.I. Nosich
Laboratory of Micro and Nano-Optics, Institute of Radio-Physics and Electronics NASU
*olga.v.shapoval@gmail.com

An electromagnetic analysis of modal spectrum and associated thresholds of a silver-strip plasmonic nanolaser as a novel light emitter has been presented.

Problem formulation and basic ideas

Progress in the understanding of the resonance phenomena able to concentrate the electromagnetic-wave power at the nanoscale opens ways to miniaturize various devices important for advanced photonic, optoelectronic and sensing applications. One of such devices is the plasmon-assisted nanolaser. The first demonstration of this effect was published in 2009 in [1], where the lasing was achieved in a random solution of gold nanospheres covered with dye-doped silica shells. Other groups have studied the lasing in periodic arrays of nanoparticles immersed into an active layer [2]. Potential applications of such devices are numerous, and they can include the sensing of refractive index changes, through the measurements of the emission wavelength.

We consider a thin silver nanostrip (of the complex refractive index $\nu_{Ag} = \varepsilon_{Ag}^{1/2}(\lambda)$) placed into an active circular cylinder (shell) with complex-valued refractive-index $\nu = \alpha - i\gamma$, where $\alpha > 0$ is the real-valued refractive-index and $\gamma > 0$ is the bulk material gain. This core-shell structure is immersed into the host medium of another refractive index, for example, air. Assuming the lasing-mode frequency to be real-valued and following [3], we formulate the lasing eigenvalue problem (LEP) in terms of pairs of real positive numbers (λ_s, γ_s), where λ_s is the wavelength and γ_s is the associated threshold value of material gain in the cylinder, introduced as imaginary part of the bulk refractive index. Due to the inherent two-fold symmetry, all modes split into four independent classes of symmetry with respect to the *x* and *y*-axes: *x-even/y-even case* (EE), *x-even/y-odd case* (EO), *x-odd/y-odd case* (OO), and *x-odd/y-even case* (OE) and using generalized boundary conditions and Nystrom-type discretization [4] derive to four independent characteristic equations, $\det|\mathbf{A}^{i,j}(\lambda,\gamma)| = 0$ for each class of symmetry (*i*,*j* = E,O), and find their roots (λ_s, γ_s) numerically.

Some of the preliminary results for such ab initio modeling of the EO-class lasing modes and corresponding relief of the $\det|\mathbf{A}^{EO}(\lambda,\gamma)|$ as a function of the wavelength and threshold gains, together with near-field portraits are shown in Fig. 1.

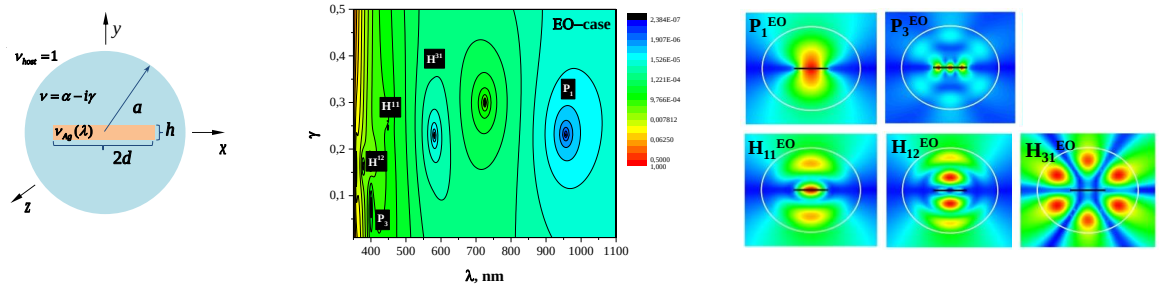

Fig. 1. Nanolaser geometry. Relief of the $\det|\mathbf{A}^{EO}(\lambda,\gamma)|$ of the modes of EO-class symmetry for strip of *d* = 100 nm, *h* = 20 nm ,*a* = 300 nm. Near-field portraits for the H-polarized lasing modes of a nanostrip laser.

References

[1] M. A. Noginov, *et al.*, *Nature*, **460**, pp. 1110–1112, 2009.
[2] A. H. Schokker, A. F. Koenderink, arXiv:1409.7293v1 [physics.optics] 25 Sep 2014
[3] E.I. Smotrova, V.O. Byelobrov, et al., *IEEE J. Quant. Electron.*, **47**, 1, pp. 20-30, 2011.
[4] O.V. Shapoval, R. Sauleau, A.I. Nosich, *IEEE Trans. Nanotechnol.*, **12**, 3, pp. 442-449, 2013.

Numerical Investigation of a Fiber Grating Coupler on SOI for SDM

B. Wohlfeil[1,*], S. Burger[1], F. Schmidt[1], C. Stamatiadis[2], L. Zimmermann[3], K. Petermann[2]
[1]*Zuse Institut Berlin, Takustraße 7, D-14195 Berlin*
[2]*TU Berlin, Institut für Hochfrequenztechnik/Photonics, Einsteinufer 25, D-10587 Berlin*
[3]*IHP GmbH, Im Technologiepark 25, D-15232 Frankfurt (Oder)*
*wohlfeil@zib.de

A numerical investigation of a two dimensional integrated fiber grating coupler capable of exciting several LP fiber modes in both TE and TM polarization is presented. Simulation results and an assessment of the numerical complexity of the 3D, fully vectorial finite element model of the device are shown.

Introduction

To satisfy the ever growing demand in bandwidth in optical communication systems, much research has been focused recently on the exploitation of the last remaining degree of freedom - space. Spatial Division Multiplexing (SDM) potentially offers a manifold increase in bandwidth by means of multi-core or multi-mode transmission. However, generating and detecting multiple spatial distributions of light efficiently is a difficult and cost intensive endeavor. Therefore an integrated solution to this problem is an attractive alternative, when it comes to low cost and high bandwidth transmission systems. We propose an integrated fiber grating coupler on the Silicon On Insulator (SOI) platform, that is capable of exciting and detecting the LP_{01}, $LP_{11,a}$, $LP_{11,b}$ and $LP_{21,a}$ fiber modes in two orthogonal polarizations at the same time and independently of each other.

Concept

The device is based on a two dimensional fiber grating coupler with four input arms (c.f. Fig. 1), of which each carries either the fundamental waveguide mode TE_{00} or the first higher order mode TE_{10}. If the fields on opposing input arms are in phase, the resulting scattered field will exhibit a plane phase in longitudinal direction, while in case of a phase shift of $\Delta\varphi = 180°$, two opposing phases are created. The field in lateral direction is controlled by the use of either the TE_{00} mode for a plane phase front or TE_{10} mode for a lateral phase shift of 180°. The polarization of the resulting field is regulated by means of two orthogonal pairs of input waveguides.

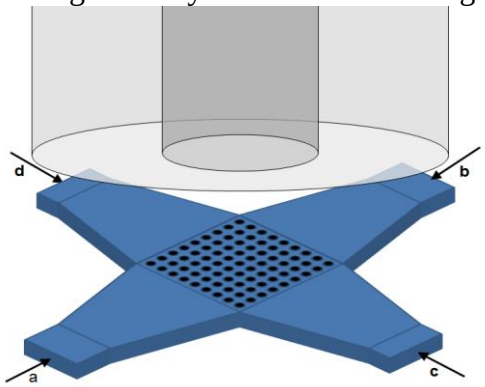

In_1	In_2	Mode	$\Delta\varphi$	Out	Pol.
a	b	TE_{00}	0°	LP_{01}	E_x
a	b	TE_{00}	180°	$LP_{11,b}$	E_x
c	d	TE_{00}	0°	LP_{01}	E_y
c	d	TE_{00}	180°	$LP_{11,b}$	E_y
a	B	TE_{10}	0°	$LP_{11,a}$	E_x
a	B	TE_{10}	180°	$LP_{21,a}$	E_x
c	D	TE_{10}	0°	$LP_{11,a}$	E_y
c	D	TE_{10}	180°	$LP_{21,a}$	E_y

Fig. 1. Schematic of the device and a table of all excitable modes.

Fully three dimensional finite element simulations of the device show an overall coupling efficiency of approximately 3dB at the center wavelength of $\lambda = 1.55\mu m$, while maintaining a low cross-talk and low mode dependent loss.

Acknowledgement

This work has been funded by the German Research Foundation DFG through SFB 787.

Numerical Investigation of the Photon-Extraction Efficiency for InGaAs/GaAs Quantum Dots in Microlens-Mirror Structures

B. Wohlfeil[1,*], S. Burger[1], F. Schmidt[1], S. Rodt[2], S. Reitzenstein[2]
[1]*Zuse Institut Berlin, Takustraße 7, D-14195 Berlin*
[2]*TU Berlin, Institut für Festkörperphysik, Hardenbergstr. 36, D-10623 Berlin*
*wohlfeil@zib.de

A numerical investigation of the optical properties of quantum-dot single-photon-emitters is presented. Monolithic microlenses of various shapes and back reflectors are compared with respect to the emission characteristics as a function of the numerical aperture of the light-collection optics.

Introduction

The reliable generation of single photons is crucial for secure quantum communication channels as well as studies of entangled photon pairs. Semiconductor quantum dots (QDs) have proven to be an excellent alternative to the widely used attenuated lasers, showing very high quantum efficiencies and high emission rates. Being compatible with standard semiconductor manufacturing processes, QD single-photon emitters can be produced in large quantities with low cost. For the deployment in quantum communication channels the photon-extraction efficiency is an important figure of merit, as it determines the obtainable bit rate of the channel. Therefore a deep understanding of the impact of device geometry and performance-enhancing measures can yield great benefit.

Device modeling

Due to the highly complex nature of the structure (cf. Fig. 1), very precise simulations are required to obtain an accurate model of the device. The fully-vectorial finite-element solver JCMsuite is employed to obtain a realistic representation of the electromagnetic field in near- and far-field regimes. The high-refractive-index-contrast material system of the GaAs based single photon emitter at the operation wavelength of $\lambda = 935$nm demands a high degree of numerical accuracy, which would not be obtainable by approximative methods. Although the device itself exhibits a rotational symmetry (cf. Fig. 1), the quntum-dot source, which is represented by a dipole, prohibits a simplification to two dimensions. Since next to the photon-extraction efficiency, the electromagnetic field in the far-field region is of interest (e.g. when considering coupling to fibers or other optics), the near- and far-field distribution needs to be modeled in an open enviroment using adaptive transparent-boundary conditions (PMLs) for scattering into homogeneous (air) and structured (DBR / substrate) media. A numerical study is conducted to obtain optimal lens and back reflector designs, using an accurate finite-element model of the large-scale device in an open environment.

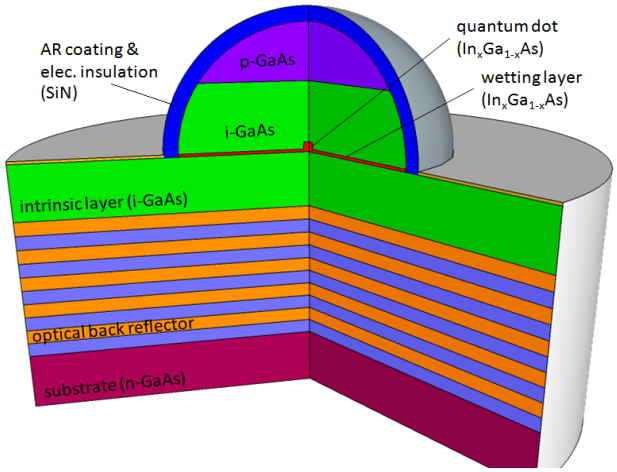

Fig. 1. Cross-sectional schematic of the QD SPE

Acknowledgement

This work has been funded by the German Research Foundation DFG through Collaborative Research Center SFB 787.

Modified Grating for High Absorption Enhancement Thin Film Solar Cell

Muhammad H. Muhammad [1] , Mohamed F. O. Hameed [1,2], S. S. A. Obayya [1*]
[1] *Centre for Photonics and Smart Materials, Zewail City of Science and Technology, Egypt.*
[2]*Faculty of Engineering, Mansoura University, Mansoura, Egypt.*
[*]sobayya@zewailcity.edu.eg

In this paper, a novel design of grating thin film solar cell is investigated and analysed using 3D finite difference time domain method. The suggested design has a modified rectangular grating with hydrogenated amorphous silicon (a-Si:H) as an active material. The aim of our work is to maximize the absorption enhancement of thin film solar cell by using a modified grating design in the active layer. Therefore, the effects of the structure geometrical parameters on the absorption are investigated. The numerical results show that 72% absorption improvement is achieved over the conventional thin film solar cell.

Design and Numerical Results

Figure 1(a) shows cross section of the suggested thin film solar cell for high absorption enhancement. The proposed design is based on modified grating through the active layer to enhance the light absorption. Fig. 1(b) shows the absorption of the active layer for the reported design, conventional thin film solar cell [1] with and without rectangular grating. It is evident from this figure that the absorption % of the suggested design is greater than those of conventional designs. The numerical results show that our design offers 5% and 72% absorption improvement over the conventional thin film solar cell with and without rectangular grating, respectively.

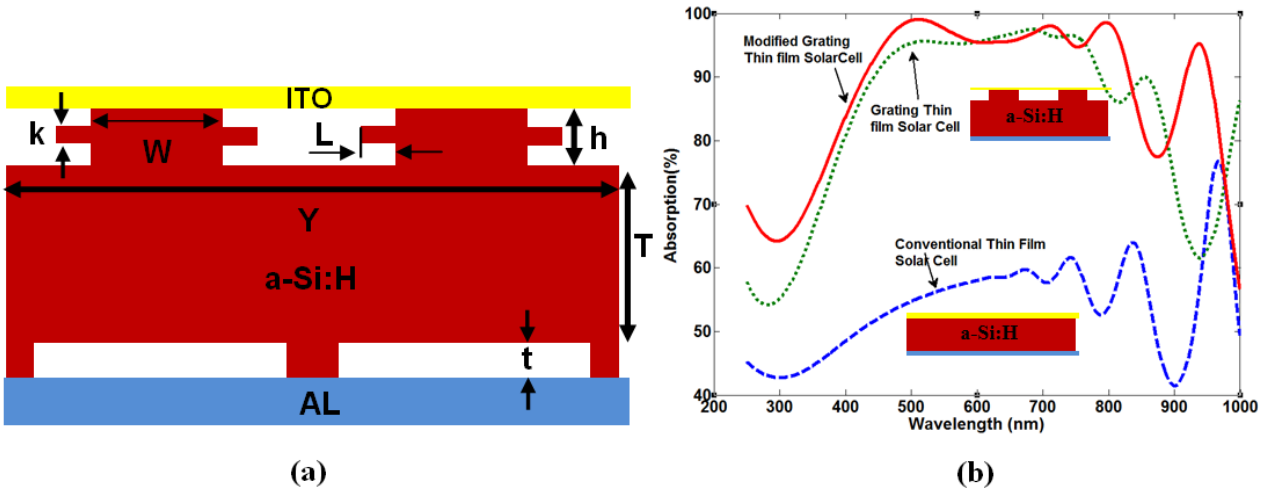

Fig.1 (a) 2D schematic diagram of the proposed modified grating thin film solar cell. (b) Spectral absorption of the a-Si:H photo-active layer as a function of the wavelength at different types of thin film solar cell.

References

[1] C. S. Schuster *et al.*, "*Dual gratings for enhanced light trapping in thin-film solar cells by a layer-transfer technique*," Optics Express, 21, A433-A438 (2013).

Semi-vectorial Sinc-Galerkin Method with Domain Decomposition for Optical Waveguides Analysis

A. A. El-Mohsen [1], A. M. Heikal [1, 2] and S. S. A. Obayya [1*]
[1] *Centre for Photonics and Smart Materials, Zewail City of Science and Technology*
Sheikh Zayed District, 6th of October City, Giza, Egypt,
[2] *Department of Electronics and Communication Engineering*
Mansoura University, Mansoura, 35516, Egypt
*sobayya@zewailcity.edu.eg

In this paper, a novel numerical method based on the sinc-Galerkin method with domain decomposition is proposed. The field components are expanded by a suitable set of sinc basis function. Patching of subdomains is done by imposing the continuity of longitudinal field components E_z and H_z. The proposed method overcomes the problem of unphysical field reflections since basis are defined for the entire outer domains i.e. no PMLs are required.

Mathematical Formulation

The wave equations used in each subdomain for $\boldsymbol{H_x}$ and $\boldsymbol{H_y}$ are as follows:

$$\nabla^2 H_\tau + k_0^2 \left(n^2 - n_{eff}^2\right) H_\tau = 0,\ \tau = x, y, \tag{1}$$

where $n_{eff} = \beta / k_0$ is the mode effective index, and β is the propagation constant.

The field components $\boldsymbol{H_x}$ or $\boldsymbol{H_y}$ are expanded in each subdomain k as follows:

$$H_\tau^{(k)} = \sum_{i=-M}^{N} \sum_{j=-M}^{N} c_{ij}^{(\tau)} S_i^{(k)}(x) S_j^{(k)}(y),\ \tau = x, y, \tag{2}$$

$$S_k(\tau) = \frac{\sin\left[\left(\pi / h_\tau\right)\left(\varphi_\tau^{(k)} - k h_\tau\right)\right]}{\left(\pi / h_\tau\right)\left(\varphi_\tau^{(k)} - k h_\tau\right)},\ \tau = x, y, \tag{3}$$

where $\varphi_\tau^{(k)}$ is a suitable conformal map for each subdomain k.

Numerical Results

A standard rib waveguide structure whose cross section is shown in Fig. 1 will be analyzed. The rib width, W, is 2.0 µm, the rib height, H= 1.1 μm, and the outer slab depth, D = 0.2 μm, and the operating wavelength is 1.55 µm. The refractive indices of the guiding, n_c, and substrate, n_s, regions are 3.44 and 3.34, respectively. The values of the effective index for fundamental quasi-TE and quasi-TM modes reported in table 1 compared with those obtained using the multi-domain spectral collocation method [1]. The results are in good agreement.

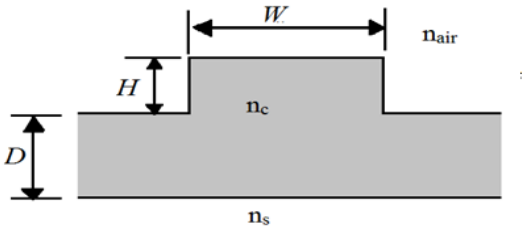

Fig. 1. Schematic diagram of the rib waveguide structure.

Table 1: Effective indices for rib wavguide obtained by sinc-Galerkin and multi-domain spectral method

	Quasi-TE	Quasi-TM
Sinc-Galerkin	3.38876	3.38756
MD spectral [1]	3.38871	3.38785

References

[1] Alharbi, F., J. C. Scott, Multi-domain spectral method for modal analysis of optical waveguide, *Opt. Quant.* Electron., Vol. 41, No.8, 583-597, 2009.

Optimization of Gold Nanorod Arrays for SERS analysis of CTCs

J. Calderón[1,*], M. I. Gómez[1], D. Hill[1]
[1]*Group of Solid Spectroscopy, Material Science Institute, University of Valencia, Spain*
*jonathan.calderon@uv.es

We report on the modelling, using the Finite Element Method (FEM), of gold nanorod arrays for the Surface Enhanced Raman Spectroscopy (SERS) analysis of circulating tumour cells (CTCs). An enhancement factor of approximately 10^9 is achieved at a wavelength of 785nm for optimal design parameters.

Introduction

The enumeration of CTCs is a promising approach for early detection and frequent monitoring of cancer. Through the engineering of nanostructured substrates, targeted CTCs can be directly identified using SERS.

Summary

When gold is conveniently nanostructured, field enhancements large enough to overcome the low molecular Raman cross-section of adsorbed molecules enable their detection, such as for CTC biomarkers and even single molecules. Here, we report on the modelling of arrays of gold nanorod on silica substrates for SERS analysis. Using FEM, the Localized Surface Plasmon Resonance (LSPR) characteristics of the arrays[1] are calculated, in order to investigate their potential as SERS substrates. Averaging the electric field in a volume around each nanorod, provides an estimation of its suitability for SERS. Their geometrical parameters (size, aspect ratio, pitch distances and different substrates) are then optimized for an excitation wavelength of 785 nm (a common line in Near IR Raman spectroscopy).

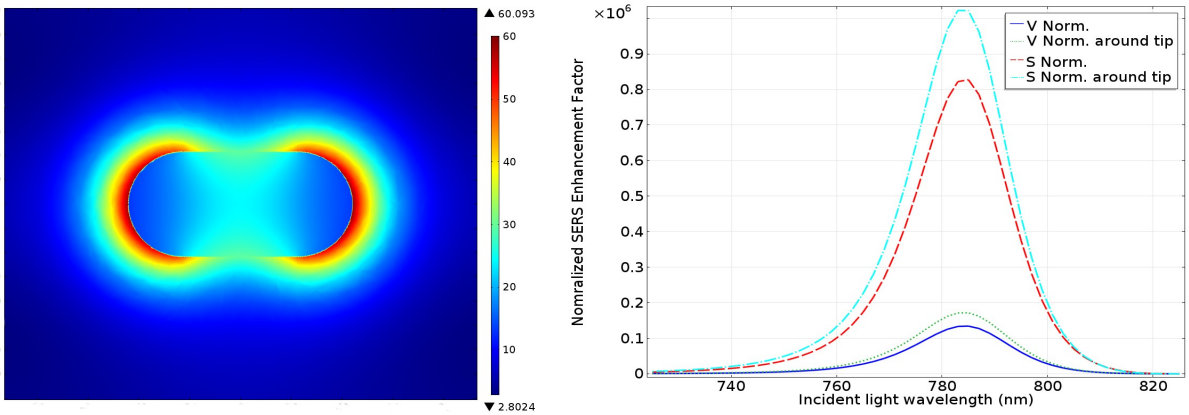

Fig. 1. Calculated electric field around a gold nanorod 50 nm wide with an aspect ratio 1.9 (**left figure**), the normalized enhancement factor for an array of these nanorods (horizontal pitch = 110 nm, vertical pitch = 180 nm) on a silica substrate covered with a 15 nm layer of ITO (**right figure**).

This optimization corresponds to enhancement factors of more than 10^7, corresponding to electric fields ~60 times greater than the incident field, once the design parameters are moderated from the consideration of fabrication limitations. The tuning of the pitch distances for the arrays of nanorods provides a substantial increase of this factor (~10^3) over isolated nanorods.

References

[1] D. Weber et al, *Longitudinal and transverse coupling in infrared gold nanoantenna arrays: long range versus short range interaction regimes*, Opt. Express, OSA, 2011, Vol 19 (16)

Acousto-optical Interaction in Ge-doped Silica Planar Optical Waveguide

M. M. Rahman*, B. M. A. Rahman
Dept. of Electrical and Electronic Engineering, City University London, United Kingdom
**mohammed.rahman.5@city.ac.uk*

A full-vectorial finite element based approach, exploiting structural symmetry, is used to find light-sound interactions between the fundamental quasi-TE optical mode and fundamental and higher order transverse acoustic modes in a Ge-doped planar silica waveguide.

Summary
Stimulated Brillouin scattering (SBS) is a nonlinear process of acousto-optical interaction that can limit optical power delivery, but can also be exploited for optical sensing. Recently, we have developed a full-vectorial acoustic code [1] and here we report light-sound interactions in a planar silica guide. The height and width of the core are taken as 3 μm and 6 μm, respectively and core is doped with 10% Ge to increase both the optical and acoustic indices to ensure that optical mode is guided at the operating wavelength of λ_o = 1550 nm. This waveguide supports higher order longitudinal and shear acoustic modes. Variations of the phase velocities with the acoustic frequency for the several shear modes are shown in Fig. 1. The dominant H_Y field profile of the quasi-TE mode is similar to that of the dominant U_X vector profile of the U^X_{11} acoustic mode, and their overlap was significantly high as shown by a blue curve in Fig.2 (left hand scale). On the other hand, overlap of this H_Y profile with the non-dominant profiles of the fundamental acoustic modes, with odd symmetry will cancel out and the acousto-optical interactions would be negligible. The overlap of the optical field with the higher order transverse U^X_{31} mode is also carried out and found to be below 5%, shown by the green curve (right hand scale). However, it should be noted that although overlap of U_X profile for the U^X_{21} mode with the optical field is zero as the former has odd symmetry, but its non-dominant U_Z profile may have a considerable overlap, as this have an even symmetry. It is observed to have near 20% overlap, shown by a red curve (right-hand scale). So, to study complex light-sound interaction in optical waveguides, non-dominant components should also be considered by using full-vectorial acoustic and optical modal approaches, as presented here.

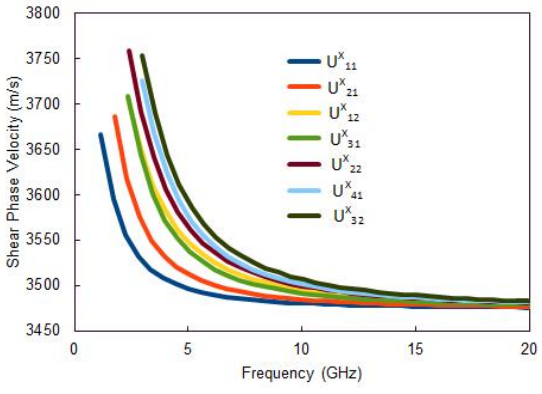

Fig. 1. Variations of the phase velocities with the acoustic frequencies for the shear modes.

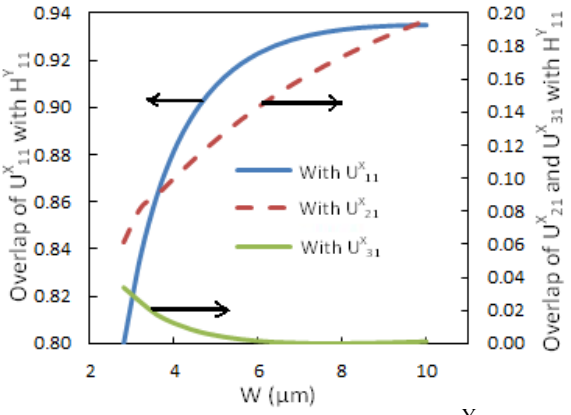

Fig. 2. Variations of overlap of the H^Y_{11} mode with U^X_{11}, U^X_{21} and U^X_{31} modes with the guide width

References

[1] B.M.A. Rahman, *et al.*, Applied Optics, pp.6797, Oct. 2014.

Modelling of microbending loss in optical fibres

X.Q. Jin*, D.C. O'Brien, and F.P. Payne
Department of Engineering Science, University of Oxford, United Kingdom
*xianqing.jin@eng.ox.ac.uk

We present an analytical model for microbending in optical fibres. Using our model together with the beam propagation method (BPM) we have investigated microbending loss in four different types of optical fibre.

Introduction

Microbending in optical fibres results from high-frequency random perturbations of the fibre core along the fibre axis, as illustrated in Fig. 1(a) and is an important cause of loss in many optical fibres [1]. To investigate microbending-induced loss, an analytic function is proposed for the random perturbations which is used in numerical simulations using the beam propagation method.

Model and Results

For an ideally straight optical fibre, the refractive index profile $n=n_0(x, y)$ is constant along the propagation direction. In the presence of random perturbations of the fibre axis the refractive index profile can be expressed as $n=n_0(x-f(z), y)$ where $f(z)$ describes the random perturbation of the fibre core. In general, the random function f is described by an auto-correlation function R and associated power spectral density $\widetilde{R}(\omega)$. Assuming an exponential auto-correlation function R, $f(z)$ can be written as a sum of sinusoids as follows:

$$f(z)=\sum_{k=1}^{N} 2\sqrt{\omega_0 \widetilde{R}(k\omega_0)}\cos(k\omega_0 z+\phi_k) \qquad \widetilde{R}(\omega)=\frac{\sigma^2 L_c}{\pi(1+\omega^2 L_c{}^2)}$$

where L_c and σ are correlation length and standard deviation of f, respectively. ϕ_k is a uniformly distributed random phase, $N = 64L/(2\pi L_c)$ and $\omega_0 = 2\pi/L$ where L is the fibre length. The random function f was used to calculate microbending loss using a beam propagation program with transparent boundary conditions for: (1) a single mode fibre (SMF), (2) a few-mode fibre (FMF) with 3 modes, (3) a multimode fibre (MMF) with 55 modes and (4) a ring-core fibre (RCF) with 13 azimuthal modes, as shown in Fig. 1(b). Fig. 1(c,d) shows the microbending loss calculated for each of these fibres ($L=40L_c$) at a wavelength of 1550nm. For SMF, the microbending loss agrees well with theoretical values calculated in [1], indicating the validity of the proposed model. The microbending loss of each fibre increases with increasing standard deviation σ or decreasing correlation length L_c as expected. It is interesting to note that the RCF and SMF suffer nearly equal loss, whilst the microbending loss of FMF is about two orders of magnitude lower than SMF.

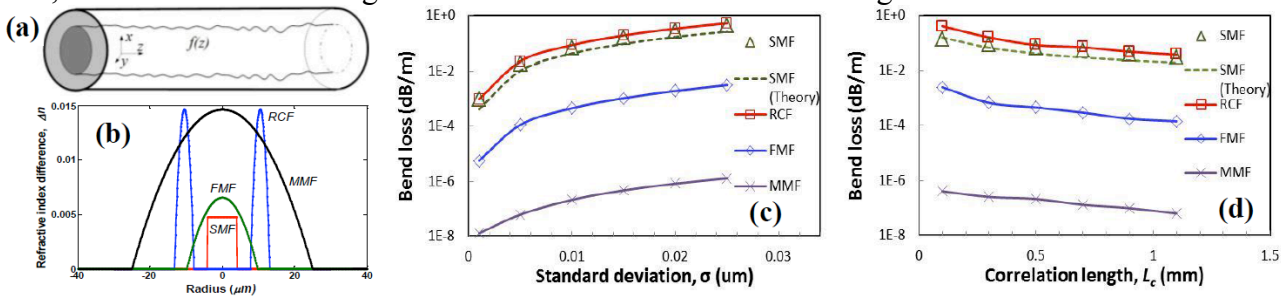

Fig. 1. (a) Random perturbation of fibre core, (b) Refractive index profiles of four different types of optical fibres, (c,d) Microbending loss versus σ (L_c: *0.5mm*) or L_c (σ:*0.01*μm).

References

[1] D. Marcuse, *Microdeformation losses of single-mode fibers*, Applied Optics, 23, 1082 (1984)

1D Glass Bragg grating analysis for integrated Raman pump filtering in the visible

A. Morand* and P. Benech
[1]*IMEP-LAHC, Université Genoble Alpes/CNRS, Grenoble, France*
*morand@minatec.inpg.fr

1D Glass Bragg grating is modelized using both a Bloch-mode computation and the AFMM[1]. Thanks by the Redheffer star product, finite length grating with high number periods are characterized. We demonstrate a 2mm length grating is enough long as integrated Raman optical pump notch filter.

Introduction

The Raman spectroscopy is a very accurate, non-destructive method to characterize the molecular composition of a material, based on an optical frequency shift propagating in a sample under test. A lot of research are focused on mobile and low cost device to realize this kind of analysis. High resolution spectrometer is then necessary to analyze the scattering signal after eliminating the optical pump. SWIFTS[1] is a high spectral resolution spectrometer using glass integrated optic waveguide with low confinement. In order to implement this spectrometer in a Raman spectroscopy device, it is suggested to insert a Bragg grating in the glass chip to play the role of the optical pump notch filter. There is of course constraint of size. We modelize this filter in this paper taking in to account the balance between performances and size.

Summary

The glass waveguides realized for the SWIFTS is monomode at the optical pump wavelength (532nm or 785nm). The grating is realized by etching the surface of the glass at a specific depth with an approximatively square shape and a duty cycle around 50%. Firstly, an infinite grating is considered to calculate the Bragg resonant wavelength using a Bloch-mode computation of one-dimensional grating waveguides[2]. Secondly, to analyze the finite length of the grating, the Aperiodic Fourier Modal Method is used. Long grating is calculated using the Redheffer star product[3] in order to reduce the number matrix used to modelize the grating. High minimum transmission is reached under 30dB for 2mm length and a bandwidth of 0.1nm. In the following figure, the transmission is shown for etched depth of 500nm and for different waveguide length.

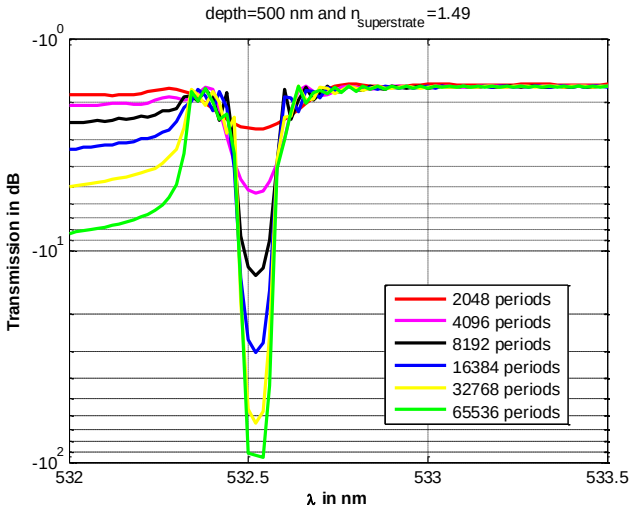

References

[1] F. Thomas et al, "*High performance high-speed spectrum analysis of laser sources with SWIFTS technology*", Proceeding of SPIE Volume 8992, 2014.

[2] Q. Cao, P. Lalanne and J-P. Hugonin, *"Stable and efficient Bloch-mode computational method for one-dimensional grating waveguides"*, JOSA A (19), 335-338, 2002.

[3] R. C. Rumpf, *"Improved formulation of scattering matrices for semi-analytical methods that is consistent with convention"*, PIER B (35), 241-261, 2011.

Design Methodology for Metal Clad Polarizer in SOI Waveguides

Shivani Sital[1,*], Enakshi Khular Sharma[1]

[1]*Department of Electronic Science, University of Delhi South Campus, New Delhi-110021, India.*

[*]*shivanisital18@gmail.com*

We here give a specific design methodology for design of metal clad waveguide polarizers and validate it on a design of a polarizer in SOI configuration.

Metal clad waveguide polarizers in various configurations have been proposed for suppressing the TM polarization [1-3]. However, optimal design for such polarizers is usually based on parametric simulations. We here give a specific design methodology for design of metal clad waveguide polarizer (Fig.1a) based on phase matching between the guided TM waveguide mode of the dielectric waveguide (Fig.1b) and surface plasmonic TM mode supported at the metal-dielectric interface (Fig.1c). The design steps are validated by design of metal clad polarizer in SOI configuration at $\lambda_0 = 1550\text{nm}$ shown in Fig.1a. The design criteria explicitly shows the necessity

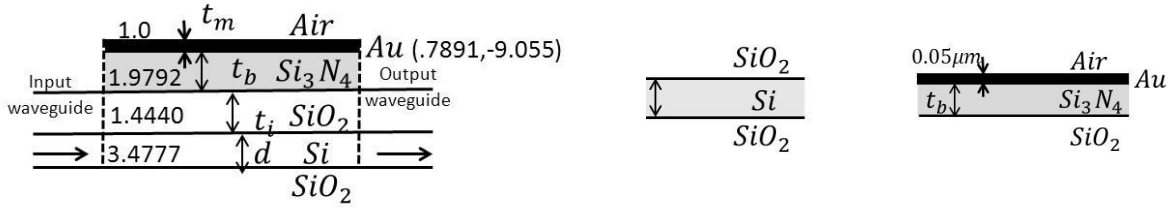

(a) (b) (c)

Fig1.a) Polarizer in SOI configuration, b) Dielectric waveguide, c) Plasmonic waveguide.

of a 'thin' high index buffer layer, chosen to be silicon nitride, between metal and cladding layer to obtain a phase matched mode of the dielectric waveguide which is well guided. The thickness of the high index buffer layer is defined by the criteria that the plasmonic waveguide supports only one TM mode ($t_b < 550\text{nm}$).We chose $t_b = 500\text{nm}$, to obtain the TM effective index as (1.9939,-0.0160), and the corresponding thickness, $d = 212.6\text{nm}$ for phase matching. The resulting polarizer section supports one TE mode (which is identical to that of the input/output waveguides) and two TM modes [with effective indices n_{e1}= (1.9968, -0.0053), n_{e2}= (1.9914, -.01075)]. The length of the polarizing section is defined by the coupling length required to couple the TM waveguide mode to the resonant plasmonic mode and can be evaluated as $l = \frac{\lambda_0}{2Re(n_{e1}-n_{e2})} = 0.14\text{mm}$. This length depends on the thickness of the cladding insulator layer. We have chosen it as $t_i = 500\text{nm}$.

The designed slab waveguide configurations can now be converted to the ridge waveguide configuration by choosing an appropriate width of the ridge so as to support single TE/TM mode along the transverse direction. Our calculation shows that at the width of 320nm the input/output ridge waveguides support one TE and TM mode while the polarizer section supports two TM modes.

References

[1] M. Saini, Enakshi K. Sharma, *Strong effect of output coupling on the performance of metal-clad waveguide polarizers,*Vol. 20,No.4,365-367,Optics Letters ,1995.

[2] M.Z.Alam, J.S. Aitchison and M. Mojahedi, *Compact and silicon-on-insulator-compatible hybrid plasmonic TE-pass polarizer*, Vol. 37, No. 1, 55-57, Optics Letter, 2012.

Design of compact polarization splitter using silicon nanowires

S. Soudi* and B. M. A. Rahman
School of Engineering, City University London, United Kingdom
**Sasan.Soudi.1*@city.ac.uk

Design of an ultra-compact polarization splitter based on silicon-on-insulator platform is presented by using a full-vectorial finite element method.

Introduction

TE/TM polarization splitters are important integrated components for polarization diversity optical systems. Here design optimization of a compact optical polarizer is presented by exploiting the polarization dependent coupling lengths of high-index contrast waveguides.

Summary

The polarization splitter proposed here is a very compact design by using two coupled identical nanowires which can be fabricated by using the mature CMOS technology. A full-vectorial Finite Element method (VFEM) [1] in used to calculate the coupling lengths for the two polarized modes.

Results

From the modal solutions, the coupling length Ratio (L_c^y /L_c^x) for the TM and TE polarizations are calculated and shown its variation with the waveguide width in Fig.1 (a) for three different guide heights. It can be observed that as width of the guides increase, this Ratio also increases and it is possible to obtain an optimum Ratio of 2. For H=280 nm, this is obtained when waveguide width is 311 nm and with separation distance 150 nm the device length equal to 5.235 μm, where most of the TE and TM polarized modes will couple to two separate ports. Effect of the width variation on the device performance is shown in Fig. 1(b).

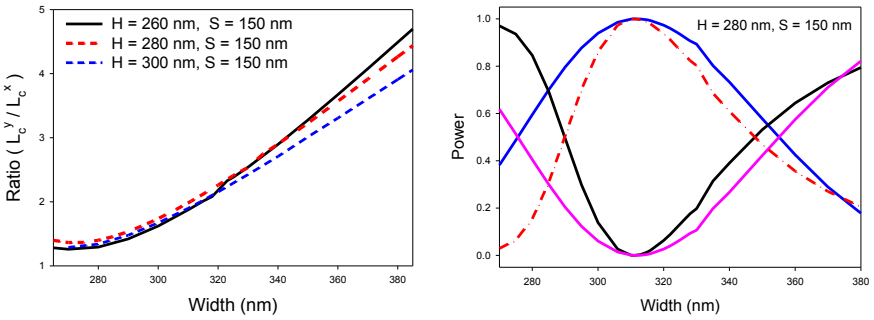

Fig. 1. (a) Variation of the coupling length ratios with the waveguide width for different heights (b) Variation of the power coupling for different waveguide width for H = 280 nm.

Conclusion

Accurate modal solutions of a directional coupler are obtained to design a compact polarization splitter and its expected performance is shown by using rigorous numerical simulations.

Reference

[1] B. M. A Rahman and J. B. Davies, "Finite element solution of integrated optical waveguides." *J. Lightwave Technol* 6, 52-57 (1998).

Tunable Mid-IR Fiber-Optic Parametric Sources

S. P. Singh[1], V. Mishra[1], S. K. Varshney[2,*]

[1]*Department of Physics*

[2]*Department of Electronics and Electrical Communication Engineering,*
Indian Institute of Technology, Kharagpur 721 302, India

**skvarshney@ece.iitkgp.ernet.in*

Coherent radiations in mid-IR region is of great interest due to their variety of applications, mainly spectroscopy, atmospheric sensing and molecular finger printing regimes. Since last few years, efforts are being made to generate broadly tunable mid-IR radiations (2-5 μm, 6-14 μm). We have suggested a potential way to obtain a broadly tunable optical parametric amplifier in a CCOF [1-4]. The tunability feature in the device appears due to infiltration of thermo-optic liquid into air-holes (or capillary) of CCOF. The variation in the temperature of the device, changes the refractive index of the capillary which further modifies the waveguide dispersion. we numerically demonstrated that thermo-optic liquid filled capillary-assisted chalcogenide optical fibers are useful in generating mid-IR tunable parametric frequencies. It was found that it is possible to generate new radiations with varying line widths symmetric to the pump frequency. We have emphasized that in case of fiber with three zero dispersion wavelengths and high nonlinearity, the phase-matching curves cannot be approximated only with group-velocity dispersion when the pump is in the anomalous dispersion region. The sixth-order dispersion parameter plays a crucial role in the generation of narrow gain peaks over the mid-IR region. The various temperature-dependent phase matching topologies, which are only possible with different fiber structures, are quite important as one need not to fabricate different fiber structures with very precise control over parameters as reported in [5]. Our proposed scheme overcomes this difficulty of precise and controlled fabrication process. The fabrication of capillary-assisted silica or chalcogenide optical fibers is well understood and established. Figure 1 shows the cross-section of the capillary-assisted chalcogenide optical fiber, generation of tunable line widths signals for different change in temperatures, and the phase-matching map at room temperature. Fig. 1c explains the temperature-dependent phase-matching gain dynamics . Several radiations can be generated over 2-6 μm, using only single pump in a 50-cm long CCOF.

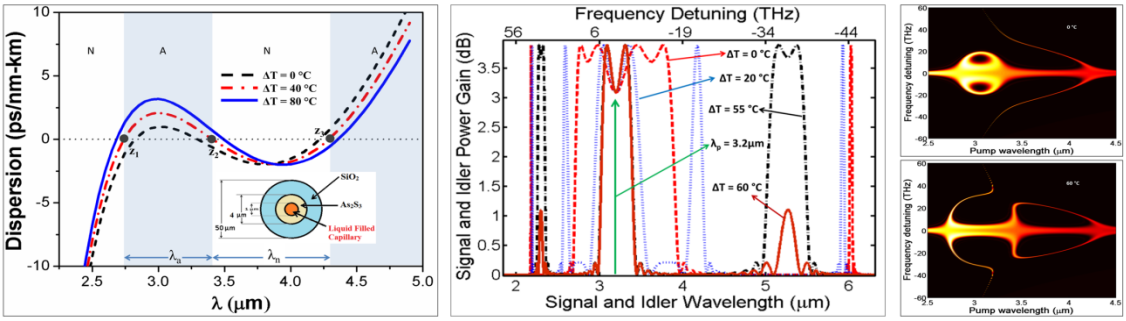

Figure 1: Dispersion characteristics at different temperatures of CCOF (inset) is shown in the LHS of the figure, middle figure shows the OPA gain and RHS of the figure shows the phase-matching characteristics at ΔT = 0 °C and 60°C, where color represents the OPA gain.

References:

1. B. J. Eggleton, B. Luther-Davies, and K. Richardson, "Chalcogenide photonics," *Nature photonics* 5, 141-148 (2011).
2. J. S. Sanghera, L. B. Shaw and I. D. Aggarwal, "Chalcogenide glass-fiber-based mid-IR sources and applications," *IEEE J. Sel. Topics Quantum Electron.*, vol. 15,114-119 (2009).
3. S. P. Singh, V. Mishra and S. K. Varshney, "Continuous-wave pumped, tunable mid-infrared fiber-optic parametric sources," *JOSA B* 31, 2786-2791 (2014).
4. S. P. Singh, V. Mishra, P. K. Datta and S. K. Varshney, "Dispersion Engineered Capillary-Assisted Chalcogenide Optical Fiber Based Mid-IR Parametric Sources," *Journal of Lightwave Technology*, 33, 55-61 (2015).
5. S. P. Stark, F. Biancalana, A. Podlipensky and P. St. J.Russell, "Nonlinear wavelength conversion in photonic crystal fibers with three zero-dispersion points," *Phy. Rev.* A 83, 023808 (2011).

Photon control by multi-periodic binary grating waveguides: A coupled-mode theory approach

J. Adam [1], H. Lüder [2], M. Gerken [2]

[1] *Mads Clausen Institute, University of Southern Denmark, Alsion 2, DK-6400 Sønderborg, Denmark*
[2] *Institute of Electrical and Information Engineering, Christian-Albrechts-Universität zu Kiel, Kaiserstr. 2, D-24143 Kiel, Germany*
jostadam@mci.sdu.dk

We present a coupled-mode theory (CMT) approach for the description of the modal behavior of planar waveguides with binary corrugations, created by the superposition of multiple binary gratings with varying pitches and fill factors. We present inter-modal coupling results for both, bound and radiating states.

Summary

In order to control the photon emission from thin-film devices, high-index layer structuring is frequently used to increase guided light outcoupling efficiency. Multi-periodic nanostructures, yielded by a logical disjunction of multiple binary gratings, have recently been proposed to achieve simultaneous control over multiple spectral resonance positions and relative intensities [1]. The experimental findings were theoretically backed up by a rigorous coupled-wave analysis (RCWA, [2]) approach, yielding the leaky modes' complex propagation constants and diffraction efficiencies. This approach, however, can only lead to quantitative results outside the device's band gaps, since only radiative propagation loss is calculated.n order to provide more physical and quantitative insight to grating-induced waveguide losses, we implemented a coupled-mode theory (CMT, [3]) approach for the semi-analytical treatment of the corrugated waveguides modal behavior. In this contribution, we present guided-to-guided as well as guided-to-radiation mode coupling in multi-periodic binary grating waveguides.

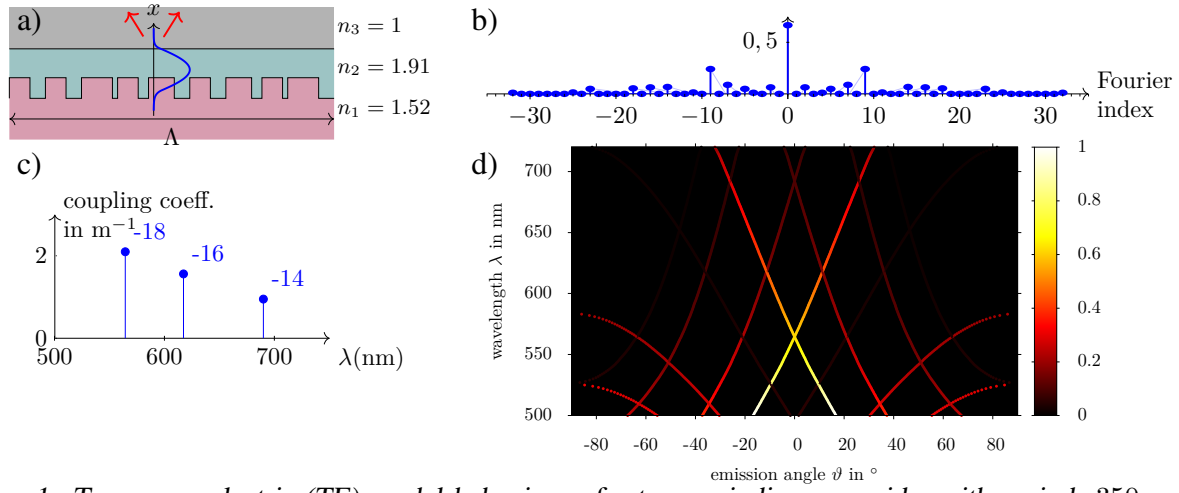

Figure 1: Transverse-electric (TE) modal behaviour of a two-periodic waveguide, with periods 350 nm *and* 450 nm*; a) geometry sketch and* TE_0 *mode profile, b) Fourier index moduli for the two-periodic grating, c)* TE_0 *to* TE_{-0} *mode-coupling coefficients, d) normalized* TE_0 *to radiation-mode coupling coefficients.*

The authors gratefully acknowledge financial support by the European Research Council, grant number 307800.

References

[1] K. Kluge, J. Adam, N. Barie, P.-J. Jakobs, M. Guttmann, M. Gerken, Opt. Express **22**(S5):A1363 (2014).
[2] M. Moharam, E. Grann, D. Pommet, and T. Gaylord, J. Opt. Soc. Am. A, **12**(5):1068 (1995).
[3] S. M. Norton, T. Erdogan, and G. M. Morris, J. Opt. Soc. Am. A, **14**(3):629 (1997).

Coupled Electromagnetic –Thermal Model for Plasmonic Waveguides

Ahmed Elkalsh[1]*, Ana Vukovic[1], Phillip D. Sewell[1], Trevor M. Benson[1]
[1]*The George Green Institute for Electromagnetics Research, University of Nottingham, UK, NG7 2RD,*
*eexae10@nottingham.ac.uk

The temperature distribution in a silicon nanotip focusing device with a plasmonic tip is modelled using a coupled electromagnetic-thermal model based on the Transmission Line Modelling (TLM) method. The model shows excellent agreement with measured results taken from the literature.

Introduction

Plasmon waveguides are important components for the nanoscale manipulation of light. The large ohmic losses of noble metals at optical frequencies inevitably give rise to Joule heating, thus opening a new avenue for the nanoscale control of temperature. Several methods including the Boundary Element Method and the Discrete Dipole approximation method [1] exist for modelling steady state thermodynamics. However, modelling transient thermal behaviour is more difficult. In this paper we model the thermal heating of a silicon nanotip focusing device using a time domain numerical method, where the feedback from the electromagnetic (EM) model to the thermal one is enforced on regular time-intervals. In this coupled model, optical field evolution is modelled using the EM TLM method where the metallic tip is described using a plasma model. The EM power loss is then used as a heat source for the thermal TLM method [2] to model temperature distribution.

Results

The dimensions of the silicon nanotip focusing device are taken from [3] and modelled using the two-dimensional coupled thermal-EM TLM method. The waveguide is excited with a fundamental TM mode of amplitude 10mA/m, at a wavelength of $1.55\mu m$. The Joule heating in the metal was considered to be the only heat source as silicon optical losses are negligible at this optical frequency. The EM field distribution and temperature profile the model within time frame ≅200ps are shown in Fig.1 (a, b) respectively. Our modelling results agree very well with experimental ones from [3].

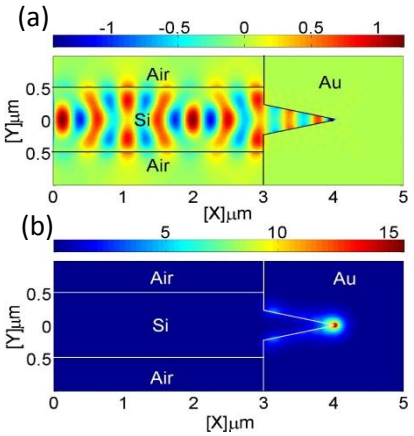

Fig. 1. (a) Electric field [V/m], (b) Temperature Δt $[C^o]$

References

[1] G. Baffou and R. Quidant, "Thermo-plasmonics: using metallic nanostructures as nano-sources of heat," *Laser Photon. Rev.*, vol. 7, no. 2, pp. 171–187, Mar. 2013.

[2] C. Christopoulos, *The Transmission-Line Modeling Method TLM*,. Piscataway,NJ: IEEE press, 1995.

[3] B. Desiatov, I. Goykhman, and U. Levy, "Direct temperature mapping of nanoscale plasmonic devices.," *Nano Lett.*, vol. 14, no. 2, pp. 648–52, Feb. 2014.

Modelling Multiphysics Effects in Optical Components

A. Grinenko[1,*]

[1]*COMSOL Ltd., Cambridge, United Kingdom*

**alon.grinenko*@comsol.com

Following a brief discussion on multiphysics modelling requirements in modern optical components, we shall review the range of coupled physical effects that can be resolved along with the optical wave propagation in COMSOL Multiphysics® finite element modelling package.

Introduction

Optical components are engaged in most modern high-tech electronic devices in retail, communications, space and defense industries. They are required to perform within narrow margins while often being exposed to a range of adverse conditions in harsh operating environments that may inhibit their performance and life cycle. In most cases the designers would be concerned with thermal and mechanical side-effects which can also be expressed in optical elements embedded in integrated circuits. Some of these operate at RF frequencies and generate large amounts of heat. Some external loads can also be inherited during the manufacturing process or constitute the principle underlying the device functionality, for example in sensors.

Incorporating the effects of environmental loads in the design process of optical components can be a laborious task, both due to the physics involved and the ranges of parameters that have to be considered for optimisation. This makes the physical prototyping approach prohibitively expensive and time consuming. In addition, some of the operating conditions can be very hard or even hazardous to reproduce in laboratory. This suggests that a software tool with an integrated multiphysics capabilities for modelling optical devices would spur the efficiency of design process.

Overview

In this presentation we shall introduce the COMSOL Multiphysics® finite element modelling package, point out the features that enable efficient modelling of standard optical applications, and demonstrate the capabilities of the tool in the analysis of thermal, mechanical and electrical loading effects. We shall consider the examples of:

- Parasitic birefringence resulting from a thermally induced stress due to a mismatch in thermal expansion produced after annealing at high temperatures;
- Mach-Zehnder modulator, device in which optical field is modulated by an RF signal;
- Simulation of a thermally integrated photonic system architecture. This architecture will be used in new laser devices and harnesses thermoelectric effects for cooling.

Finally, we shall discuss the new multiphysics interface introduced in the latest release of COMSOL Multiphysics® that enables modelling of optoelectronic devices. It allows the systems of governing drift-diffusion equations of semiconductors and optical wave equations to be solved simultaneously.

PIC Tunable Double Outputs Coupler in MDM system

Weifeng Jiang, Xiaohan Sun*, Na Dong, Chao Pan, Ningfeng Bai and Xu Liu

National Research Center for Optical Sensing/Communications Integrated Networking
Department of Electronics Engineering, Southeast University, Nanjing 210096, P.R. China

*xhsun@seu.edu.cn

Introduction

Optical coupler is one of key devices used in optical interconnect for constructing optical communication system [1], especially as the special device for optical cross-connect (OXC). Electro-optic (EO) effect or Thermo-optic (TO) effect are used to realize tunable optical couplers. Usually, a large device length is required due to slight change of the refractive index caused by them. In this paper, we demonstrate the tunable double outputs coupler based on the mode selection MMI by adjusting the small lateral displacement at the fiber-waveguide interface precisely.

Summary

The schematic of the coupler is shown in Fig. 1. It consists of a 1×4 coupler and a taper fiber. The separation distance between the axis of the taper fiber and input waveguide is Δx, which can be adjusted to control the switching sates of the tunable coupler. When the Δx = 0, only the guide mode can be excited in the input waveguide as shown in Fig. 1(A). When the Δx ≠ 0, the lightwave oscillates along the input waveguide due to the interference of the guided mode with quasi-guided modes, in which quasi-guided modes are generated at the fiber-waveguide interface as shown in Fig. 1(B). The switching characteristics for the tunable coupler is analyzed by 2D-FD-BPM. The tunable coupler chips can be obtained by using SoS technology.

Results

The tunable coupler chip is tested experimentally. By adjusting the lateral displacement between the taper fiber and the input waveguide, we can get near-field output mode patterns of the coupler with low crosstalk and high extinction ratio corresponding shown in Fig. 1(C).

Conclusion

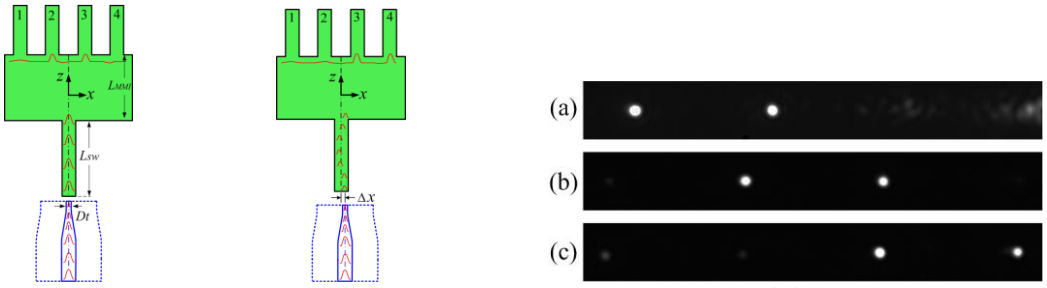

(A) (B) (C)

Fig. 1. Schematic diagram of the tunable coupler and its operation at (A) central excitation (Δ*x*=0); (B) lateral displacement excitation (Δ*x*≠0); (C) Near-field output mode patterns of the tunable coupler with (a) Δx = -2μm; (b) Δx = 0μm; (c) Δx = 2μm.

A tunable double outputs coupler based on the mode selective multimode interference (MMI) is presented which can be implemented by adjusting the exciting location at the input waveguide facet and integrated as the core PIC devices applied in the mode division multiplexing (MDM) systems.

References

[1] Z. Y. Zhang, et al., "Widely tunable grating-assisted heterogeneous silicon nitride/polymer waveguide coupler," Opt. Lett., vol. 39, no. 1, pp. 162-165, Jan. 2014.

Surface Plasmon Resonance Liquid Crystal Photonic Crystal Fiber Temperature Sensor

Mohamed Farhat O. Hameed[1,2], Shaimaa I. H. Azzam[1,2], S. S. A. Obayya[1*]

[1]*Centre for Photonics and Smart Materials, Zewail City of Science and Technology, Egypt.*

[2]*Faculty of Engineering, Mansoura University, Mansoura, Egypt.*

sobayya@zewailcity.edu.eg

High sensitive surface plasmon resonance temperature sensor based on photonic crystal fiber (PCF) is reported and analyzed. The suggested PCF sensor has a central large core infiltrated with temperature dependent nematic liquid crystal (NLC) material. The effects of the structure geometrical parameters, NLC rotation angle φ, and temperature on the sensor performance are studied. The simulation results are obtained using full vectorial finite element method. The proposed sensor is simple for fabrication and can achieve an average sensitivity of 0.77 nm/^{o}C over temperature range from 20 ^{o}C to 50^{o}C.

Design and Numerical Results

Figure 1(a) shows cross section of the suggested silica liquid crystal PCF surface plasmon resonance (LC-PCF SPR) sensor. The cladding air holes of diameter d are arranged in a triangular lattice with a hole pitch Λ. In addition, the air holes of the first ring are replaced by a central hole of diameter D coated by a gold layer of thickness t. Moreover, the central hole is filled with NLC of type E7. Figure 1(b) shows the loss spectra of the quasi TE core mode at φ=0^{o}, and quasi TM core mode at φ=90^{o} at different temperatures, 20^{o}C, 30^{o}C, 40^{o}C, and 50^{o}C. It is revealed from this figure that the shift in the resonance wavelength increases with increasing the temperature. The shift in the resonance wavelength is equal to 5 nm, 6 nm, 12 nm corresponding to temperature intervals [20^{o}C-30^{o}C], [30^{o}C-40^{o}C], and [40^{o}C-50^{o}C] and hence sensitivities of 0.5, 0.6, and 1.2 nm/^{o}C, respectively are achieved. Therefore, the proposed sensor has an average sensitivity of 0.77 nm/^{o}C which is superior to sensitivity of 0.35 nm/^{o}C of temperature sensors with ethanol [1] and to that of [2] with 0.2 nm/^{o}C with almost the same fabrication complexity.

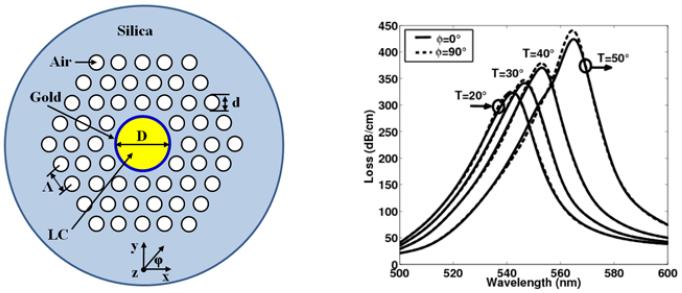

(a) (b)

Fig. 1(a) Cross section of the suggested PCF SPR sensor (b) Confinement loss spectra of the quasi TE mode at φ=0^{o} and quasi TM mode at φ=90^{o} of the LC-PCF core guided mode at different temperatures

References

[1] W. Qian *et al.*, "*Temperature sensing based on ethanol-filled photonic crystal fiber modal interferometer*," Sensors Journal, IEEE, 12(8), 2593-2597(2012).

[2] Y. Peng, *et al.*, "*Simulation of a Surface Plasmon Resonance Based on Photonic Crystal Fiber Temperature Sensor,*" Cross Strait Quad-Regional Radio Science and Wireless Technology Conference, 1, 274 – 277 (2011)

Efficient O – band superluminescent diode with wide optical bandwidth and high power

M. Z. M. Khan, H. H. Alhashim, T. K. Ng, and B. S. Ooi*

Photonics Laboratory, Computer, Electrical and Mathematical Sciences and Engineering Division,

King Abdullah University of Science and Technology (KAUST), Thuwal-239556900, Saudi Arabia.
*boon.ooi@kaust.edu.sa

An InGaAsP/InP multiple quantum well (MQW) superluminescent diode (SLD) is reported emitting at ~1300 nm with simultaneous achievement of high power >70 mW, record broad emission bandwidth of ~117 nm, and exhibiting a wall plug efficiency (WPE) of ~6.8%.

SLDs in the 1300 nm range are highly attractive in the biomedical imaging applications such as optical coherent tomography (OCT) whose resolution and penetration depth is dependent on the optical source bandwidth and power, respectively. Currently, this wavelength window is dominated by InAs/GaAs quantum dot based SLDs with already reported power and optical bandwidth values in few tens to 100 mW and few tens to 350 nm, respectively [1]. However, on MQW based active region SLDs, the results are comparatively inferior with demonstrated ~100 mW power and ~80 nm bandwidth separately. Achievement of simultaneous broad -3 dB amplified spontaneous emission (ASE) bandwidth and high power form MQW SLDs is the subject of this work.

Fig. 1 shows the room temperature output power–current (L-I) characteristic of 7° tilted configuration InGaAsP/InP MQW SLD under pulsed operation. A super linear characteristic is evident with total measured output power (2 facets) of >70 mW. Evolution of ASE spectra at different current injections showed a -3dB bandwidth of >100 nm for ≥0.2 A and reaching a maximum of 117 nm at 1.0 A. The corresponding average spectral power density at this injection is ~0.6 mW/nm and centered at ~1300 nm. The device displayed a coherence length in air of 9.8 µm and maximum external quantum efficiency and WPE of ~13% and ~6.8%, respectively. This achievement is attributed to the active region engineering and exploiting dispersive ground state and excited state emissions of the quantum wells.

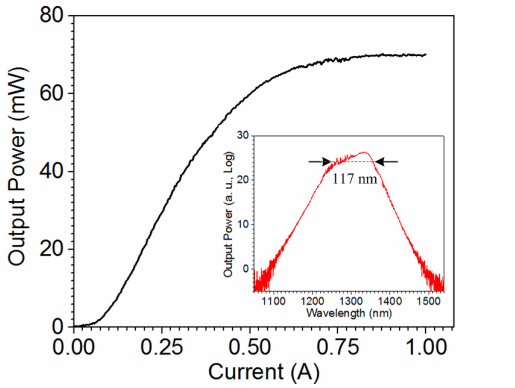

Fig. 1. Room temperature L-I characteristics of the InGaAsP/InP MQW SLD and the inset shows the emission bandwidth at 1.0A.

In conclusion, a small footprint, InGaAsP/InP MQW SLD is demonstrated with 117 nm emission bandwidth and 70 mW output power covering O – band.

References

[1] Z. Zhang, R. Hogg, X. Lv, and Z. Wang, "Self-assembled quantum-dot superluminescent light-emitting diodes," *Advances in Optics and Photonics,* vol. 2, pp. 201-228, 2010.

Coupling mechanisms and field confinement in a hybrid plasmonic-photonic crystal resonator for enhanced optical trapping

M. Mossayebi[1*], A. Parini[2], A. J. Wright[1], M. Somekh1[1,3], E. C. Larkins[1], G. Bellanca[2]
[1]*Electrical Systems and Optics Division, University of Nottingham, United Kingdom*
[2]*Department of Engineering, University of Ferrara, Ferrara, Italy*
[3]*Department of Electronic and Information Engineering, Hong Kong Polytechnic University, Kowloon, Hong Kong, China*
*eexmm30@nottingham.ac.uk

We present a structure combing a photonic crystal cavity with a plasmonic bowtie nanoantenna producing spectral confinement and field enhancement for optical trapping. We will discuss coupling mechanisms and field enhancements in relation to spectral detuning, cavity design, structure geometry and excitation field.

Introduction

Optical traps have a range of applications in the biological sciences, physics, chemistry and material science. True confinement of nano-sized biological objects is difficult, often requiring a higher laser power which can lead to photodamage. Optical resonators and plasmonic structures have been used to resonantly enhance the field and improve optical trapping efficiency. Plasmonic resonators produce very high spatial confinement, but their high radiative loss results in low resonant field enhancement ($Q < 10$). On the other hand, Fabry-Perot, ring and photonic crystal (PhC) based resonators have greater resonant enhancement ($Q \sim 500$ - 10,000). PhC resonators are particularly interesting for optical trapping due to their high Q-factor and small size. However, the fields in PhC resonators are largely confined within the plane of the dielectric so that surface trapping relies on the comparatively weak evanescent field above the dielectric. Zhang *et al.* recently reported a hybrid laser based on an L7 PhC cavity and a plasmonic bowtie nanoantenna (BNA) showing that the BNA strongly influences the fields in the PhC.[1] In this paper, we use finite-difference time-domain (FDTD) method to numerically investigate the coupling of an L3-PhC cavity with a gold BNA.

Methodology and Results

The device structure (Fig.1 Left) is a gold BNA positioned on top of an L3-PhC cavity to couple to its fundamental mode. A benzocyclobutene layer (which fills the holes of the PhC) is used for planarization above the PhC and acts as a support for the BNA. A polystyrene sphere immersed in water is included to represent the particle to be trapped.

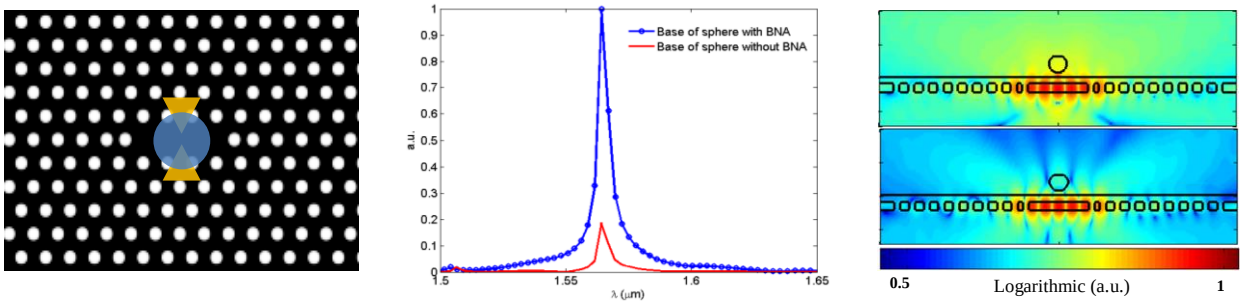

Fig. 1 Left: Top view of the simulated structure. Center: Electric field enhancement at the base of the particle. Right: Pattern of the electric field intensity with (top) and without (bottom) the BNA.

Summary

We show numerically that a hybrid plasmonic-PhC resonator (Fig.1 Left) enhances the trapping field by an order of magnitude (Fig.1 Center). The presence of the BNA improves the coupling between the cavity and the trapped particle and spatially localizes the optical field (Fig.1 Right).

References

[1] T. Zhang, *et al.*, *Plasmonic-photonic crystal coupled nanolaser,* Nanotechnology **25** 315201, 2014

Vertical Mode Expansion Method for Scattering of Light by Nanocylinders

Xun Lu *, Ya Yan Lu

Department of Mathematics, City University of Hong Kong, Kowloon, Hong Kong
xunlu2-c@my.cityu.edu.hk

In this work, the vertical mode expansion method (VMEM) is extended to study optical scattering of coupled nanocylinders. The coupling properties for both metallic and dielectric nanocylinders are rigorously studied.

Introduction

In [1], a vertical mode expansion method (VMEM) was developed to study the extraordinary optical transmission phenomenon. Here, we extend the VMEM to study optical properties of interacting nanoparticles. The obtained results confirm the accuracy of the numerical method, in addition, the coupling properties between the nanocylinders are analyzed in detail.

Method and Results

In VMEM, the electromagnetic field is expanded in 1D vertical modes with "coefficients" satisfying 2D Helmholtz equations. The method requires the so-called Dirichlet-to-Neumann (DtN) maps for 2D Helmholtz equations on the boundaries of related domains. In this work, we construct the DtN maps using cylindrical wave expansions. The method efficiently reduces 3D problems to 2D problems.

Fig. 1 shows the scattering cross section of a metallic dimer as a function of the gap between the two nanocylinders. The gold nanocylider has a constant diameter $d = 150nm$ and height $h = 17nm$. The optical constant of the gold is taken from [2]. The refractive index of the surrounding medium is 1.25. With decreasing interparticle gap, the surface plasmon resonance shows a redshift or a blueshift depending on the polarization of the incident wave. The results obtained from our calculations agree well with the experimental measurements in [3].

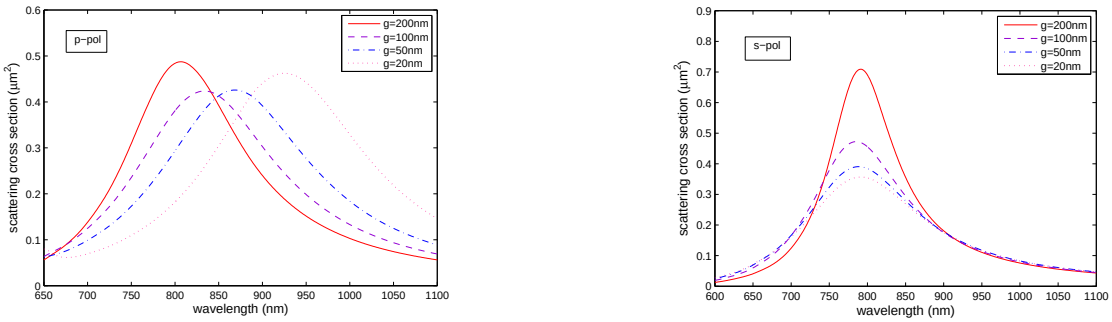

Fig.1 Scattering cross section of a nanocylinder dimer with a gap varying from 200 nm to 20 nm.

References

[1] X. Lu, H. Shi, and Y. Y. Lu, *"Vertical mode expansion method for transmission of light through a single circular hole in a slab," J. Opt. Soc. Am. A, vol. 31, pp. 293-300, 2014*

[2] P. B. Johnson, R. W. Christy, *"Optical constants of the noble metals," Phys. Rev. B, vol. 6, pp. 4370-4379, 1972*

[3] W. Rechberger et al. *"Optical properties of two interacting gold nanoparticles," Opt. Commun., vol. 220, pp. 137-141, 2003*

Floquet-Bloch Analysis of Hill Equation with Analytically Solvable Potentials

S. Caffrey and G.V. Morozov

Scottish Universities Physics Alliance (SUPA), Institute of Advanced Technologies, University of the West of Scotland, Paisley PA1 2BE, Scotland, UK
stuart.caffrey@uws.ac.uk

Wave propagation in nondissipative one-dimensional potentials is studied via Floquet-Bloch functions. Band structures of such systems are investigated for analytically solvable cases of continuous and piecewise continuous (binary or sawtooth) potentials. Special attention is given to the incipient bands (vanishing gaps).

Introduction

Physical phenomena involving either temporal or spatial periodic variations are described by Hill's equation

$$\frac{d^2\Psi(z)}{dz^2} + Q(z)\Psi(z) = 0\,, \quad Q(z) = Q(z+d)\,, \tag{1}$$

where $Q(z)$ is a continuous (piecewise continuous), periodic, real or complex valued function of the real variable z with period d. This equation occurs in many areas of physics including quadrupole field modeling, electron transportation in a crystal lattice and propagating optic waves in photonic crystals. Floquet theory encapsulates solutions of Hill's equation (1) in terms of two Bloch waves satisfying the relation $F_{1,2}(z+d) = \rho_{1,2}F_{1,2}(z)$, where $\rho_{1,2}$ are generally non-zero, complex constants. However at certain special points the Bloch waves coincide, and another function is needed to complete the general solution of Eq. (1).

Objectives

The first objective is to find Floquet-Bloch solutions for analytically solvable Hill equations for both piecewise and piecewise continuous potentials. This includes both binary and sawtooth crystals (piecewise continuous case) as well as two example of continuous potentials, see Refs. [1][2][3]. We demonstrate the construction of the Floquet-Bloch solutions from any two linearly independent continuously differentiable solutions known on at least a single period $0 < z < d$, see Ref. [4]. The second objective is to analyze the band structure of those four potentials from a unified standpoint. Finally we examine typical behaviour of Floquet-Bloch functions in the regions of a band structure identified as allowed bands, bandgaps, bandedges and incipient bands (vanishing gaps).

References

[1] Wu S. M. and Shih C. C., *Construction of Solvable Hill Equations,* Phys. Rev. A **32**, 3736-3738 (1985).
[2] Takayama K., *Note on solvable Hill equations,* Phys. Rev. A **34**, 4408-4410 (1986).
[3] Morozov G. V. and Sprung D. W. L., *Band Structure Analysis of Solvable Hill Equations with Continuous Potential,* J. Opt. Soc. to be published (2015).
[4] Morozov G. V. and Sprung D. W. L., *Floquet-Bloch Waves in One-Dimensional Photonic Crystals,* Europhys. Lett. **96**, 54005 (2011).

Nano-Porous Silicon Waveguides for Optical Sensors

T. Hutter[1,*], S.R. Elliott[1], N. Bamiedakis[2]

[1]*Department of Chemistry, University of Cambridge, United Kingdom*

[2]*Engineering Department, University of Cambridge, United Kingdom*

* tf269@cam.ac.uk

Optical waveguides made from nano-porous materials are of interest for sensing applications. Most literature describes buried waveguides, whereas rib structure has benefits of increased sensitivity due to larger exposed area. In this paper we present some basic simulation studies on single mode porous silicon rib waveguides.

Introduction

Porous silicon (pSi) waveguides have a strong potential for use as optical sensors as they offer high sensitivity owing to their nano-porous structure, which can be functionalized with appropriate dyes so that the optical properties of the waveguide change in the presence of specific analytes. Different waveguide sensors can be produced using such technology, however, the majority of the literature utilises buried pSi waveguides [1,2]. In this paper, we propose the use of rib pSi waveguides for sensing applications, as those can offer increased sensitivity and faster response times due to larger exposed surface area. We present basic simulation studies which will enable the design of more complicated devices such as MZI or microrings.

Simulation

The pSi waveguides are composed of a low porosity (high refractive index) core on a higher porosity (lower refractive index) cladding. The finite-element method (COMSOL) is used to study modes of waveguides made of a 62% porous silica core and 68% porous silica cladding on silicon. The core and cladding layers are 1 µm thick as well as the waveguide width. The refractive index of the porous layers is calculated using Bruggeman effective medium approximation at a 980 nm.

Results

The modes of the rib waveguide as a function of rib height are presented, as well as the effect due to small changes in the refractive index of the surrounding medium (n_{medium}) assuming that this change is either only outside the waveguide (corresponding to non-porous waveguide) or inside the porous voids of the waveguide.

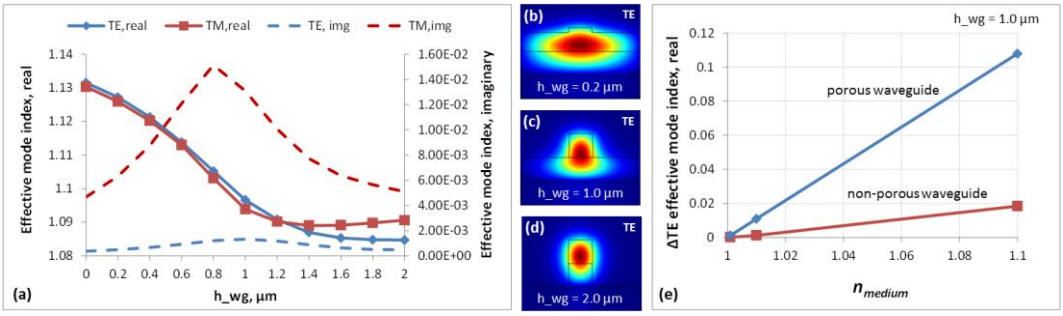

Fig. 1. (a) Effective mode indices for various rib heights; TE mode distribution for rib height of (b) 0.2, (c) 1 and (d) 2 µm; (e) change in the TE effective mode index for different n_{medium}.

Conclusion

The modes of rib waveguide were studied, and also the effect of small change in the n_{medium} showed clear advantage of using porous waveguide for sensing compared to non-porous waveguide.

References

[1] F.H. Arrand et al., *Novel liquid sensor based on porous silicon optical waveguides*, IEEE Photonics Technology Letters, 10 (10), 1998.

[2] J. Charrier et al., *Optical study of porous silicon buried waveguides fabricated from p-type silicon*, Materials Science in Semiconductor Processing 3, 357, 2000.

Square-Lattice Index-Guiding Microstructured Optical Fibers: An Analytical Field Model

Dinesh Kumar Sharma[1,2], Anurag Sharma[1,*] and Saurabh Mani Tripathi[2]
[1]*Department of Physics, Indian Institute of Technology Delhi, New Delhi-110016, India*
[2]*Department of Physics, Indian Institute of Technology Kanpur, Kanpur-208016, India*
*dk81.dineshkumar@gmail.com, *asharma@physics.iitd.ac.in, smt@iitk.ac.in*

We study using an analytical field model the light guiding properties of index-guiding microstructured optical fibres (MOFs) with square-lattice of circular voids or air-holes in the photonic crystal cladding. Comparison with available numerical simulation results based on finite element method has been included.

Introduction

Microstructured optical fibers (usually referred as holey fibers) constitute a class of optical fibers having periodic array of voids running along its entire length [1]. Bouk *et al.* have been investigated the solid core MOFs with square-lattice of voids in the transverse cross-section [2]. We present here an improved analytical field model to simulate the modal properties of index-guiding square-lattice MOFs and demonstrate its accuracy.

Summary

We have improved our recently developed field model [3] for obtaining better accuracy in the results by adding an additional term in the modal field. Thus, we consider four circular rings around the central missing single air-hole (core) in the MOF geometry and two rings of lobes in the modal field associated with four-fold rotational symmetry; thus, we set up the following field:

$$\Psi(r,\varphi) = e^{-\alpha r^2} - Ae^{-\alpha_1 (r-\sigma\Lambda)^2}\left(1+\cos 4\varphi\right) - Be^{-\alpha_2 \left(r-\eta\Lambda\sqrt{2}\right)^2}\left(1-\cos 4\varphi\right) \qquad (1)$$

where $A, \alpha, \alpha_1, \sigma, B, \alpha_2$ and η are the unknown field parameters; and Λ is the pitch (center-to-center separation). We use the variational techniques for scalar modes to obtain the optimized values of these unknown parameters and the propagation constant of the fundamental mode [4].

Results

Using our improved field model we have evaluated the effective indices for an MOF with $d/\Lambda = 0.5$ and the pitch of $\Lambda = 2.0$ μm. The refractive index of the background material (silica) is calculated from the Sellmeier relation. The variation of effective indices of the fundamental mode as a function of wavelength is shown in Fig. 1, where we have included the results of numerical simulation based on FEM as well as those obtained by Ghosh *et al*. [5]. Our results are matching well to FEM values, reflecting the strength of our analytical field model. Further work is in progress.

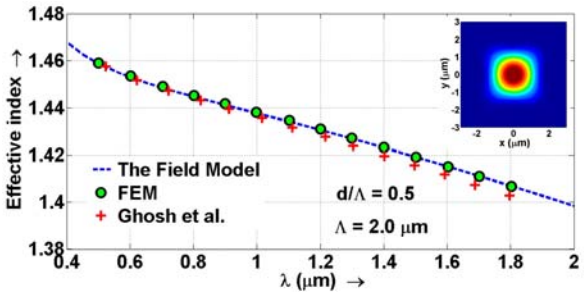

Fig. 1. Effective index as a function of wavelength (inset shows near-field intensity at λ = 1.55 μm, reflecting the 4-fold symmetry of the lattice pattern).

The present work was partially supported by an INSPIRE grant (grant number IFA13-PH-69) of the DST, Ministry of Science & Technology, Govt. of India.

References

[1] P.St. J. Russell, *J. Lightwave Technol.*, **24**, 4729 (2006).
[2] A.H. Bouk, A. Cucinotta, F. Poli, and S. Selleri, *Opt. Exp.*, **12**, 941 (2004).
[3] D.K. Sharma and A. Sharma, *Photonics 2014*, **S5A.15**, OSA (2014).
[4] A. Sharma and H. Chauhan, *OQE*, **41**, 235 (2009); also *OWTNM 2009*; *OWTNM 2012*
[5] D. Ghosh, S. Roy, and S.K. Bhadra, *J. Mod. Opt.*, **57**, 607 (2010).

Approximate Modal Analysis of Dielectric-loaded Surface Plasmon Polariton Waveguide on Metal Strip of Finite Width

K. Gehlot [1,2], A. Sharma [1],
[1] *Indian Institute of Technology Delhi, New Delhi, India*
[2] *University of Rajasthan, Jaipur, India*
[1]*gehlot.kanchan@gmail.com*, [2]*asharma@physics.iitd.ac.in*

The efficiency and the applicability of the Semi-vector optimal variational method (SV-VOPT) to complex surface plasmon polariton (SPP) waveguides is investigated. An example of dielectric loaded SPP waveguide formed on gold strip of finite width is presented.

Summary

The effective index method (EIM) provides fast and efficient tool for the modal analysis of optical waveguides. However, the EIM has limitations when applied to more complex waveguide structures [1]. Recently, we developed a semi-analytical approximate method, SV-VOPT method, which works very well for the dielectric [2] and the SPP waveguides [3]. In present paper, we apply the SV-VOPT method to a practical dielectric loaded SPP (DLSPP) waveguide structure, which is formed on gold layer of finite thickness (inset of Fig 1(a)). The EIM does not take into account the finite width of the gold layer, hence cannot predict modal characteristics for such waveguides, specifically for smaller widths of the gold layer. The converged results of the SV-VOPT method for the DLSPP waveguide

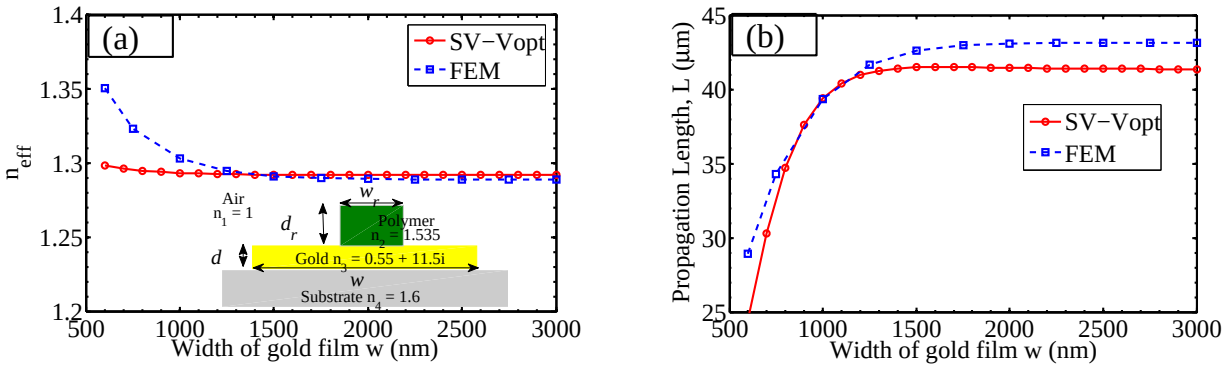

Fig. 1. Variation of n_{eff} and L with width of gold layer w. $d_r = w_r = 600nm$, $d = 100nm$, $\lambda = 1550nm$.

are obtained in 4-5 iterations. The variation of the mode effective index, $n_{eff} = \mathrm{Re}(\beta/k)$, and the propagation length, $L = 1/2\mathrm{Im}(\beta)$, with the width of gold layer w, are shown in Figs. 1(a) and 1(b). The results obtained by the SV-VOPT method agree well with the results of the finite element method (*FemSIM* by Rsoft). Detailed analysis and results will be reported later.

References

[1] J. Grandidier et. al., *Appl. Phys. Lett.*, **96**, 063105 (2010).
[2] K. Gehlot, A. Sharma, *Opt. Express* **21**, 9807-9812 (2013).
[3] K. Gehlot, A. Sharma, *OWTNM-2014*, Nice, France (2014).

Plasmon-polaritons in Photonic Crystals

U.L. Fulco*, E.L. Albuquerque, and L.R. da Silva
Department of Biophysics, UFRN, 59072-970, Natal-RN, Brazil
e-mail: umbertofulco@gmail.com

In this work we investigate the polaritonic band gap spectra, which arise from the propagation of a plasmon-polariton excitation in quasiperiodic multilayer structures of Fibonacci type, forming a photonic crystal, using a theoretical model based on a transfer matrix treatment.

Introduction

When the electromagnetic radiation propagating through a polarizable dielectric or magnetic crystal excites some internal degrees of freedom of the crystal, it gives rise to a hybrid (or mixed) modes called polaritons. Specifically, in the case of an electron plasma, such excitation will have both a photon and a plasmon component, whose resultant mode, the plasmon-polariton, may have either a very strong photon or a very strong plasmon component [1].

Results

The plasmon-polariton dispersion relation is obtained by solving the electromagnetic wave equation for *p*-polarized electromagnetic mode, within the layers A and B of the multilayer structure, yielding cos(QL) = (1/2)Tr(T), where Q is the Bloch wavevector and L is the size of the multilayer. Also, Tr(T) means the trace of the transfer matrix T, which relates the electromagnetic field amplitudes of a layer in cell *n* to the equivalent one in cell *n*-1. The pass (stop) bands are then obtained when the absolute value of the right-hand side of the above equation is less (bigger) than one. This can be seen in Fig. 1, considering the dispersion curves corresponding to a fixed Bloch wavevector Q and a ratio $d_B/d_{A=}2.69$, with d_A (d_B) being the thickness of layer A (B), defined in the region where the average index of refraction of the multilayer vanishes, the so-called zero-<η> photonic region [2].

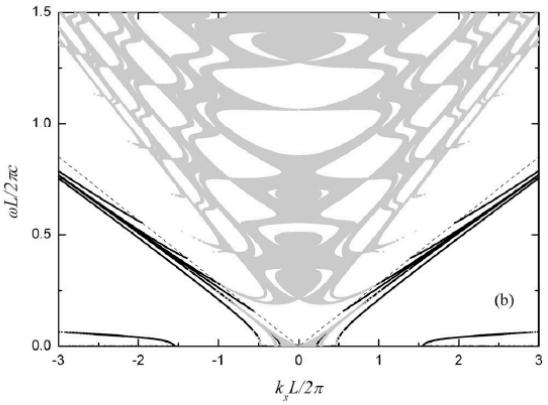

Fig. 1: Plasmon-polariton dispersion relation in a photonic structure zero-<η> photonic region.

Acknowledgement: The authors want to thank financial support of the Brazilian Research Agencies CNPq and CAPES.

References

[1] E.L. Albuquerque and M.G. Cottam, *Phys. Rep.* **376,** 225 (2003).
[2] F.F. de Medeiros and E.L. Albuquerque, *J. Phys.: Condens. Matter* 18, 8737 (2006).

WGM Microrod Laser Fabricated by pulsed CO_2 Laser Micromilling

Shahab Bakhtiari Gorajoobi*, Ganapathy Senthil Murugan, Michalis N. Zervas

Optoelectronics Research Centre, University of Southampton, Southampton, SO17 1BJ, UK

*sbg1u12@soton.ac.uk

Fabrication of high Q milled microrod resonators using a pulsed CO_2 laser, directly on Yb^{3+}-doped fibers, is demonstrated. Evanescently pumped WGM microlaser with ~9μW output power has been achieved.

Introduction

Whispering Gallery Mode (WGM) microlasers have been of a great interest owing to their low threshold and narrow linewidth lasing due to their high Q and small mode volume. Most of the fabrication methods [1-3] are non-controllable and non-reproducible which rely on fiber-tip melting, such as microspheres [3, 4] or splicing of small active-fiber stubs [3]. Microresonators are realized by heating up and melting the material using continuous wave CO_2 lasers. We use a method based on pulsed CO_2 laser which enables controllable ablation of fiber surface. We achieved precise control of the cavity length and ablation depth in a very short fabrication time, as a simplified one-step process to form a WGM microresonator from a Yb^{3+}-doped silica fiber.

Fabrication and Results

A sequence of CO_2 laser pulses is focused onto a rotating 240μm-diameter fiber with 200 μm doped core resulting in 20 μm ablation depth. To improve the surface roughness of the milled edges the structure was fire-polished by applying controlled electrical arcs (Fig. 1(a) inset). This improved the Q-factor from ~10^{+4} to ~$3\times10^{+6}$, and enabled lasing. A laser diode pump at 974.5 nm wavelength is launched into a 2 μm-diameter tapered fiber in-contact with the resonator and evanescently excites pump WGMs. Figure 1(a) shows the measured signal spectra collected through the same tapered fiber. The total signal power, calculated by summing up all lasing peaks (Fig. 1(b)), shows linear dependency to the launched pump power for the powers above a threshold of ~40 mW (absorption of ~1 mW). The optical-to-optical efficiency with respect to absorbed pump power is ~0.1%.

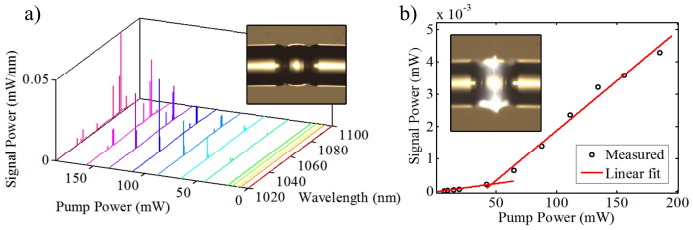

Fig. 1. a) Spectra of signal as a function of launched pump power (inset shows the fabricated microrod resonator), and b) total measured signal as a function of launched pump power (inset shows the light scattered at 70 mW pump power).

Conclusion

With this method, large number of identical microresonators in one-fabrication-step process, can be achieved. The controlled CO_2 exposure results in minimum ablation depths and does not compromise the fiber strength. Therefore, such microresonator structures, with two fiber stems attached naturally to the resonator ends, will enable a variety of future robust sensing applications and tunable telecommunication devices.

References

[1] V. Sandoghdar *et. al.*, Phys. Rev. A 54(3), R1777–R1780 (1996).
[2] G. S. Murugan *et. al.*, Opt. Lett. 36, 73–75 (2011).
[3] G. S. Murugan *et. al.*, Proc. SPIE 8960, 896018 (2014).
[4] C. Grivas *et. al.*, Nat. Commun. 4, 2376 (2013).

Lasing Threshold of Plasmon Mode of Silver Nanowire Grating Embedded in a Partially Active Dielectric Slab

V. Byelobrov
Lab. of Micro and Nano-Optics, IRE NASU, Kharkiv, Ukraine
volodia.byelobrov@gmail.com

Dielectric slab with an embedded grating of silver infinite circular nanowires is investigated for the scattering and lasing eigenvalue problems. In the last, due to added active coating of the nanowires the lasing thresholds were derived and compared for the plasmon and grating resonances.

Summary

A grating of silver nanowires in a free space is an interesting structure in Optics as it combines two phenomena, the grating resonances emerging for a periodic structure and plasmon resonances based on the effects appearing on the surface of noble metal. However for implementation of such structure in a real device, it is necessary to embed it in a dielectric material. According to the surface nature of plasmon resonances, the eigenfield intensifies on the outer boundary of noble metal. Thus each nanowire is coated with active media within the slab to make overlapping of the active region by the high field more efficient. Here is considered a dielectric slab Fig.1 (left) with refractive index ν=1.1 that low value is chosen to track the plasmon resonance as it is very sensitive for physical parameters of hosting media. The value of dielectric function for silver nanowires is taken from [1]. Firstly, the scattering problem of normal incident plane wave in the H-polarization is solved using rigorous mathematical approach. Then using similar method and conception of negative absorption (or adding "activity") [2] in terms of lasing eigenvalues problem we can derive a pair of desired values, namely, lasing threshold γ (imaginary part of the active region refractive index) and lasing frequency that is close to resonance frequency in the scattering problem.

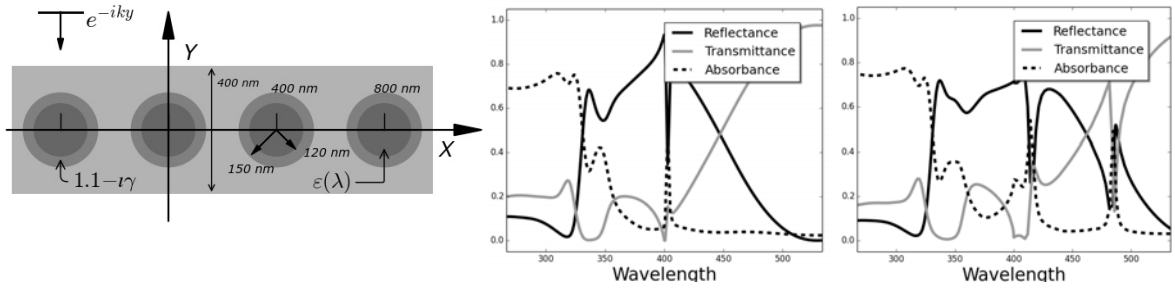

Fig. 1. The sketch of structure geometry (left), reflectance, transmittance, and absorbance for silver grating in a free space ν=1.0(centre) and in a dielectric slab ν=1.1(right)

Fig.1 (centre), the values of reflectivity, shows a wide band of high reflectance that is constructed from two resonances, plasmon one λ≈348nm and grating one λ≈400nm. The shape of the band is essentially affected by the presence of hosting media even (Fig.1 right). However if we add "activity" in the coating of nanowires, the LEP yields following results for plasmon resonance λ=359.153, γ=0.39 and for the grating one λ=400.002, γ=0.275. That values show that the plasmon resonance has a higher lasing threshold, or in other words, requires higher "pumping" to illuminate.

References

[1] P.B. Johnson, R.W. Christy, "*Optical constants of the noble metals*," *Phys. Rev.*, vol. 6, pp. 4370-4379, 1972.

[2] E.I. Smotrova, etc," *Optical theorem helps understand thresholds of lasing in microcavities with active regions*," *IEEE J. Quantum Electronics*, vol. 47, no 1, pp. 20-30, 2011.

Finite Element and FDTD Characterizations of Light Propagation through Lossy Insect Ommatidia

M. Enayet Rahman*, B. M. A. Rahman
School of Engineering, City University London, United Kingdom
***enayet.rahman.1@city.ac.uk**

Numerical solutions of a lossy optical waveguide similar to insect ommatidia have been carried out and reported here by using full-vectorial FEM and FDTD approaches.

Summary
The design of this guide is inspired by similar structures found in insect compound eye [1],[2]. Such a typical insect ommatidia, which is the unit component of the compound eye, can be represented by a 2μm by 2μm guide with n_{core}=1.347 and n_{clad}=1.339. Here it is considered that the core has negligible loss and modal loss is predominantly due to the complex refractive index of the cladding. Both FEM and FDTD approaches are used to find the light propagation at the 550 nm wavelength. Figure 1 shows the confinement factor and guide loss (dB/μm) against loss tangent (tan δ) of the cladding. It can be observed that with increasing tan δ of the cladding, initially modal loss increases, reaches a maximum value and then starts to decrease. It was also observed that with increased material loss value, modal confinement in the core increases. For a highly confined mode, the field is mostly inside the lossless core, which in turn reduces the loss of the guide. Stronger confinement allows closer packing of ommatidia in insect compound eyes. Figure 2 shows the real and imaginary components of the H_y profile of Hy_{11} mode and it can be observed that as the loss value increases, the imaginary part of the field value increases. It was found that the field profile in the cladding is exponentially varying sinusoid instead of exponentially decreasing profile and inside the core follows an exponentially decreasing sinusoidal curve. The exponential term in the core field equation comes from the imaginary part of the cladding refractive index, and this exponential term is responsible for the increment in confinement factor. This guide supports only one mode for wavelength range of 450nm-750nm, with 750nm as the mode cutoff and it supports additional mode in the ultraviolet spectrum.

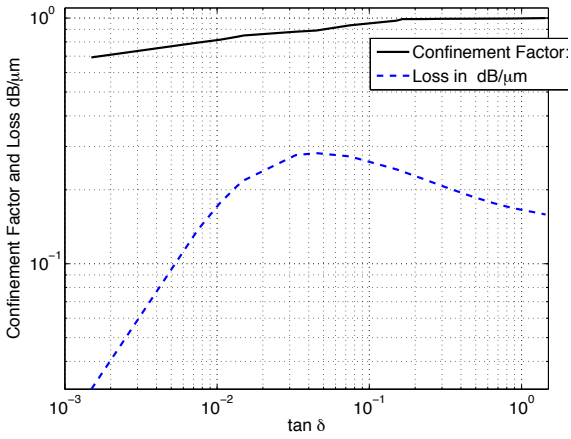

Fig. 1. Confinement factor and Guide loss vs tan δ

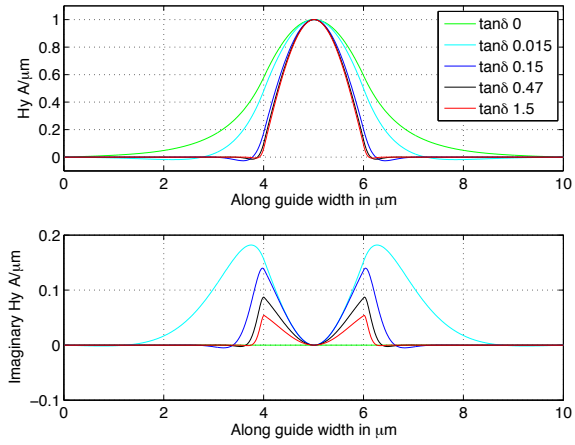

Fig. 2. Hy profile of Hy_{11} mode 2μmX2μm core

References

[1] D. E. Nilsson, M. F. Land, and J. Howard, "Optics of the butterfly eye," Journal of Comparative Physiology A, vol. 162, pp. 341–366, 1988.

In-fibre whispering gallery mode microresonator:

a two-sphere coupled system

K.Kosma[1,], K. Schuster[2], J. Kobelke[2], G. Nikolopoulos[1], S. Pissadakis[1]*

[1]*Institute of Electronic Structure and Laser, Foundation for Research and Technology-Hellas, 70013 Heraklion, Greece*

[2]*Institute of Photonic Technology Jena, Albert-Einstein-Str. 9, 07745 Jena, Germany*

*kosma@iesl.forth.gr

A high optical integration configuration of a microstructured optical fibre infiltrated with two adjacent microspheres placed in one of its capillaries is presented. The optical behavior of the excited coupled cavity under certain conditions is investigated through the analysis of the spectra of the scattered light.

Introduction

Whispering gallery modes result from light trapping inside circular microcavities, while resonating at specific frequencies. Spherical cavities have been successfully integrated in resonator circuits of isolated or coupled systems, operating in lasing, sensing or fluorescence mode [1-4].

Summary

We report on a system of two polystyrene microspheres, which are encapsulated inside the capillary of a collapsed-core microstructured optical fibre in contact to each other, forming a coupled microcavity. Light initially launched to the fibre core from a supercontinuum source, is subsequently coupled to the complex microcavity. The system exhibits resonant whispering-gallery-mode spectra, spanning the whole excitation wavelength range, and recorded from different scattering points of the excited bi-sphere resonator. Change of the spectral patterns and tuneability of the observed resonant modes are shown under external stimulus conditions. Analysis and interpretation of the observations, as well as potential applications are discussed.

Results

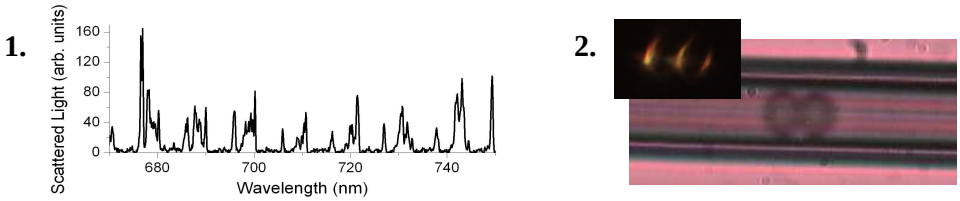

Fig. 1. Resonant spectrum observed after whispering gallery mode excitation in the coupled microspheres.
2. Image of the bi-sphere inside the fiber and the white light scattering observed after excitation.

Fig.1 shows a TE whispering gallery mode spectrum recorded from the point of the cavity in-between the two microspheres (Fig.2). Spectra from other points of the excited bi-sphere are also recorded and analyzed in terms of cross-coupling between the microspheres and mode splitting. Tuneability of the resulted spectral patterns has also been achieved and will be presented on site.

References

[1] S. V. Boriskina Optics Letters **31**, 338 (2006).
[2] O. Svitelskiy, Y. Li, A. Darafsheh, M. Sumetsky, D. Carnegie, E. Rafailov, V. N. Astratov Optics Letters **36**, 2862 (2011).
[3] A. François, K. J. Rowland, T. M. Monro Applied Physics Letters **99**, 141111 (2011).
[4] K. Kosma, G. Zito, K. Schuster, S. Pissadakis Optics Letters **38**, 1301 (2013).

List of Participants

Last name	First name	Email address	Affiliation	
A. El-Mohsen	Amgad	aabdelmohsen@zewailcity.edu.eg	Zewail City for Science and Technology	Egypt
Adam	Jost	jostadam@mci.sdu.dk	The Mads Clausen Institute, University of Southern Denmark	Denmark
Agrawal	Arti	arti.agrawal.1@city.ac.uk	City University London	United Kingdom
Albuquerque	Eudenilson	eudenilson@gmail.com	UFRN	Brazil
Alhashim	Hala H.	hala.alhashim@kaust.edu.sa	King Abdullah University of Science and Technology	Saudi Arabia
Alyami	Hashem	h.m.h.alyami@pgr.reading.ac.uk	University of Reading	United Kingdom
Armenta	Roberto	rarmenta@lumerical.com	Lumerical Solutions Inc.	Canada
Atia	Khaled	katia@zewailcity.edu.eg	Zewail City for Science and Technology	Egypt
Ay	Feridun	feridunay@anadolu.edu.tr	Anadolu Universitesi	Turkey
Azabi	Yousaf O.	yousaf.azabi.1@city.ac.uk	City University London	United Kingdom
Azzam	Shaimaa	sazzam89@gmail.com	Zewail City for Science and Technology	Egypt
Bai	Ningfeng	19550950@qq.com	Southeast University	China
Bakhtiari Gorajoobi	Shahab	sbg1u12@soton.ac.uk	Optoelectronics Research Centre, University of Southampton	United Kingdom
Balle	Salvador	salvador@imedea.uib-csic.es	IMEDEA, CSIC-UIB	Spain
Bamiedakis	Nikos	nb301@cam.ac.uk	University of Cambridge	United Kingdom
Banaszek	Konrad	Konrad.Banaszek@fuw.edu.pl	University of Warsaw	Poland
Barbosa	Andres	pt_finwe@hotmail.com	King's College London	United Kingdom
Bartlett	Philip	P.N.Bartlett@soton.ac.uk	School of Chemistry, University of Southampton	United Kingdom
Becerra	Victor	v.m.becerra@reading.ac.uk	University of Reading	United Kingdom
Bellanca	Gaetano	gaetano.bellanca@unife.it	University of Ferrara	Italy
Benech	Pierre	benech@minatec.inpg.fr	IMEP-LAHC	France
Benson	Trevor	trevor.benson@nottingham.ac.uk	University of Nottingham	United Kingdom
Berkemeier	Frank	Frank.Berkemeier@uni-muenster.de	University of Munster	Germany
Bharadwaj	Divya	divyabharadwaj4@gmail.com	IIT Delhi	India
Bhattacharya	Debjani	debjani112@gmail.com	Techno India University	India
Bhavsar	Kaushalkumar	k.k.bhavsar@rgu.ac.uk	Robert Gordon University	United Kingdom
Boonruang	Sakoolkan	sakoolkan.boonruang@nectec.or.th	Photonics Technology Laboratory, NECTEC	Thailand
Boscolo	Sonia	s.a.boscolo@aston.ac.uk	Aston Institute of Photonic Technologies, Aston University	United Kingdom
Bradley	A. Louise	bradlel@tcd.ie	Trinity College Dublin	Ireland
Bull	Steve	steve.bull@nottingham.ac.uk	University of Nottingham	United Kingdom
Burger	Sven	burger@zib.de	Zuse Institut Berlin	Germany
Byelobrov	Volodymyr	volodia.byelobrov@gmail.com	IRE NASU	Ukraine
Cabrera Espana	Francisco Jose	francisco.cabrera-espana@city.ac.uk	City University London	Spain

Last name	First name	Email address	Affiliation	
Cada	Michael	michael.cada@dal.ca	Dalhousie University	Canada
Caffrey	Stuart	stuart.caffrey@uws.ac.uk	University of the West of Scotland	United Kingdom
Calderon	Jonathan	jonathan.calderon@uv.es	Material Science Institute of the University of Valencia (ICMUV)	Spain
Calzolari	Arrigo	arrigo.calzolari@nano.cnr.it	CNR-NANO Institute of Nanoscience	Italy
Catellani	Alessandra	alessandra.catellani@nano.cnr.it	CNR-NANO Institute of Nanoscience	Italy
Chatterjee	Sudip	skc@phy.iitkgp.ernet.in	IIT KHRAGPUR	India
Chatzidimitriou	Dimitrios	dimitris.chatzidimitriou@gmail.com	Aristotle University of Thessaloniki	Greece
Christopoulos	Thomas	cthomasa@auth.gr	Aristotle University of Thessaloniki	Greece
Coscelli	Enrico	enrico.coscelli@unipr.it	University of Parma	Italy
Creagh	Stephen	stephen.creagh@nottingham.ac.uk	School of Mathematical Sciences, University of Nottingham	United Kingdom
Cucinotta	Annamaria	annamaria.cucinotta@unipr.it	University of Parma	Italy
Da Silva	Luciano	luciano@dfte.ufrn.br	UFRN	Brazil
Dash	Jitendra	jnd10@iitbbs.ac.in	IIT Bhubaneswar	India
Demirtas	Mustafa	m_demirtas@anadolu.edu.tr	Anadolu Universitesi	Turkey
Dias	Hasula	hasula.dias@nottingham.ac.uk	University of Nottingham	United Kingdom
Dong	Na	76831411@qq.com	Southeast University	China
Donzella	Valentina	vdonzella@lumerical.com	Lumerical Solutions, Inc.	Canada
Dubov	Mykhaylo	m.dubov@aston.ac.uk	Aston Institute of Photonic Technologies, Aston University	United Kingdom
Duggen	Lars	duggen@mci.sdu.dk	Mads Clausen Institute, University of Southern Denmark	Denmark
Elkalsh	Ahmed	eexae10@nottingham.ac.uk	University of Nottingham	United Kingdom
Elliott	Stephen R.	sre1@cam.ac.uk	University of Cambridge	United Kingdom
Esquivias	Ignacio	ignacio.esquivias@upm.es	CEMDATIC-ETSIT, Universidad Politecnica de Madrid	Spain
Fedotov	Vassili A.	vaf@orc.soton.ac.uk	Optoelectronics Research Centre and Centre for Photonic Metamaterials, University of Southampton, UK	United Kingdom
Fehrembach	Anne-Laure	anne-laure.fehrembach@fresnel.fr	Institut FRESNEL - Faculte des Sciences de Saint JÃ©rÃ´me	France
Filonenko	Konstantin	filonenko@mci.sdu.dk	Mads Clausen Institute, University of Southern Denmark	Denmark
Foerstner	Jens	foerstner@tet.upb.de	University of Paderborn, Germany	Germany
Fujimura	Shunya	shunya.fujimura.64@stu.hosei.ac.jp	Hosei University	Japan
Fulco	Umberto	umbertofulco@gmail.com	UFRN	Brazil
Fung	Wai Keung	w.k.fung@rgu.ac.uk	Robert Gordon University	United Kingdom
Gargallo	Bernardo	bergarja@iteam.upv.es	iTEAM Research Institute - Universitat PolitÃ¨cnica de ValÃ¨ncia	Spain

Last name	First name	Email address	Affiliation	
Gaur	Ankita	ankitagaur.phy@gmail.com	Indian Institute of Technology Roorkee	India
Gehlot	Kanchan	gehlot.kanchan@gmail.com	Indian Institute of Technology Delhi	India
Gerken	Martina	mge@tf.uni-kiel.de	Institute of Electrical and Information Engineering, Christian-Albrechts-UniversitÃ¤t zu Kiel	Germany
Ginzburg	Pavel	pavel.ginzburg@kcl.ac.uk	King's College London	United Kingdom
Gomez	Maria Isabel	maria.i.gomez@uv.es	Material Science Institute of the University of Valencia (ICMUV)	Spain
Gradoni	Gabriele	gabriele.gradoni@nottingham.ac.uk	University of Nottingham	United Kingdom
Gric	Tatjana	tatjana.gric@dal.ca	Dalhousie University	Canada
Grinenko	Alon	alon@comsol.com	COMSOL Multiphysics	United Kingdom
Hadjiloucas	Sillas	s.hadjiloucas@reading.ac.uk	University of Reasing	United Kingdom
Hameed	Mohamed	mfarahat@zewailcity.edu.eg	Zewail City for Science and Technology	Egypt
Hammer	Manfred	manfred.hammer@uni-paderborn.de	University of Paderborn, Germany	Germany
Hammerschmidt	Martin	hammerschmidt@zib.de	Zuse Institute Berlin	Germany
Heikal	Ahmed	aheikal@zewailcity.edu.eg	Zewail City for Science and Technology	Egypt
Helfert	Stefan	stefan.helfert@fernuni-hagen.de	FernUniversitÃ¤t in Hagen	Germany
Herrmann	Sven	herrmann@zib.de	Zuse Institute Berlin	Germany
Hildebrandt	Andre	hildebrandt@tet.upb.de	University of Paderborn, Germany	Germany
Hill	Daniel	daniel.hill@uv.es	Material Science Institute of the University of Valencia (ICMUV)	United Kingdom
Hutter	Tanya	tf269@cam.ac.uk	University of Cambridge	United Kingdom
Jasim	Ali	jasim@um.edu.my	university of malaya	Malaysia
Javaloyes	Julien	julien.javaloyes@uib.es	Departament de Fisica, Universitat de les Illes Balears	Spain
Jha	Rajan	rjha@iitbbs.ac.in	IIT Bhubaneswar	India
Jiang	Weifeng	903309596@qq.com	Southeast University	China
Jiao	Yuqing	Y.Jiao@tue.nl	COBRA Research Institute - Eindhoven University of Technology	Netherlands
Jin	Xianqing	xianqing.jin@eng.ox.ac.uk	University of Oxford	United Kingdom
Johny	Jincy	j.johny@rgu.ac.uk	Robert Gordon University	United Kingdom
Kabir	S M Raiyan	Raiyan.Kabir.1@city.ac.uk	City University London	United Kingdom
Kailasnath	M	kailas@cusat.ac.in	International School of Photonics	India
Kaliyaperumal	Nakkeeran	k.nakkeeran@abdn.ac.uk	University of Aberdeen	United Kingdom
Karakuzu	Huseyin	karakuzh@aston.ac.uk	Aston Institute of Photonic Technologies, Aston University	United Kingdom
Karanikolas	Vasilios D.	karanikv@tcd.ie	Trinity College Dublin	Greece
Karim	Mohammad	mohammad.karim.2@city.ac.uk	City university London	United Kingdom

Last name	First name	Email address	Affiliation	
Karpinski	Michal	m.karpinski1@physics.ox.ac.uk	University of Oxford	United Kingdom
Karsaklian Dal Bosco	Andreas	andreas.karsakliandalbosco@supelec.fr	CentraleSupÃ©lec	France
Kaunga-Nyirenda	Simeon	simeon.kaunga-nyirenda@nottingham.ac.uk	University of Nottingham	United Kingdom
Khan	Mohammed Zahed Mustafa	mohammedzahed.khan@kaust.edu.sa	KAUST	Saudi Arabia
Khan	Saba	saba04star@gmail.com	IIT KHRAGPUR	India
Khular Sharma	Enakshi	enakshi54@yahoo.co.in	University of Delhi South Campus	India
Kildishev	Alexander	kildishev@purdue.edu	Purdue University	United States
Klein	Jackson	jklein@lumerical.com	Lumerical Solutions, Inc.	Canada
Kobelke	Jens		Institute of Photonic Technology Jena	Germany
Komodromos	Michael	eng.km@frederick.ac.cy	Frederick University	Cyprus
Korotkevich	Alexander	alexkor@math.unm.edu	University of New Mexico	United States
Kosma	Kyriaki	kosma@iesl.forth.gr	Institute of Electronic Structure and Laser, Foundation for Research and Technology-Hellas (IESL-FORTH)	Greece
Kou	Yao	yao.kou@uni-paderborn.de	University of Paderborn	China
Krasavin	Alexey	alexey.krasavin@kcl.ac.uk	King's College London	United Kingdom
Kriezis	Emmanouil	mkriezis@auth.gr	Aristotle University of Thessaloniki	Greece
Kuryzheva	Olga	lyolya.90@bk.ru	Kharkov National University of Radio Electronics	Ukraine
Larkins	Eric	eric.larkins@nottingham.ac.uk	University of Nottingham	United Kingdom
Leijtens	Xaveer	X.J.M.Leijtens@tue.nl	COBRA Research Institute - Eindhoven University of Technology	Netherlands
Lim	Jun	jun.lim@nottingham.ac.uk	University of Nottingham	United Kingdom
Liu	Xu	liuxy@seu.edu.cn	Southeast University	China
Lu	Ya Yan	mayylu@cityu.edu.hk	Department of mathematics, City University of Hong Kong	China
Lu	Xun	xunlu2-c@my.cityu.edu.hk	City University of Hong Kong	Hong Kong
Luder	Hannes	halu@tf.uni-kiel.de	Institute of Electrical and Information Engineering, Christian-Albrechts-UniversitÃ¤t zu Kiel	Germany
Luken	Lea	lea.lueken@uni-muenster.de	University of Munster	Germany
Maes	Bjorn		UMONS	Belgium
Maluckov	Aleksandra	sandram@vin.bg.ac.rs	VinÄ a Institute of Nuclear Sciences	Serbia
Marino	Giuseppe	giuseppe.marino@kcl.ac.uk	King's College London	United Kingdom
Marocico	Cristian A.	MAROCICC@tcd.ie	Trinity College Dublin	Romania
Marsal	Nicolas	nicolas.marsal@centralesupelec.fr	CentraleSupelec - LMOPS	France
May	Alexander	arm103@orc.soton.ac.uk	University of Southampton	United Kingdom
Melloni	Andrea	andrea.melloni@polimi.it	Politecnico di Milano	Italy
Mercier	Emeric	emeric.mercier@centralesupelec.fr	CentraleSupÃ©lec	France
Mishra	Viswatosh	vishwatoshmishra34@gmail.com	IIT Kharagpur	India

Last name	First name	Email address	Affiliation	
Mohammed	Faris	faris@aims.ac.za	University of Witwatersrand	South Africa
Mohammed	Waleed S.	wsoliman@gmail.com	BU-CROCCS, Bangkok University	Thailand
Monti	Tamara	tamara.monti@nottingham.ac.uk	University of Nottingham	United Kingdom
Morand	Alain	morand@minatec.inpg.fr	IMEP-LAHC	France
Morichetti	Francesco	francesco.morichetti@polimi.it	Politecnico di Milano	Italy
Morozov	Gregory	gregory.morozov@uws.ac.uk	University of the West of Scotland	United Kingdom
Mossayebi	Mina	eexmm30@nottingham.ac.uk	University of Nottingham	United Kingdom
Muhammad	Muhammad	mhamdy@zewailcity.edu.eg	Zewail City for Science and Technology	Egypt
Munoz	Pascual	pmunoz@iteam.upv.es	iTEAM Research Institute - Universitat PolitÃ¨cnica de ValÃ¨ncia	Spain
Myslivets	Sergey	sam@iph.krasn.ru	Institute of Physics, Siberian Branch of the Russian Academy of Sciences and Siberian Federal University	Russian Federation
Nakano	Hisamatsu	hymat@hosei.ac.jp	Hosei University	Japan
Natarov	Denys M.	den.natarov@gmail.com	IRE NASU	Ukraine
Nayak	Jeeban	jkn11@iitbbs.ac.in	IIT Bhubaneswar	India
Nerukh	Alexander	nerukh@gmail.com	Kharkov National University of Radio Electronics	Ukraine
Ng	Tien Khee	tienkhee.ng@kaust.edu.sa	King Abdullah University of Science and Technology	Saudi Arabia
Niegemann	Jens	jniegemann@lumerical.com	Lumerical Solutions Inc.	Canada
Nikolopoulos	George	nikolg@iesl.forth.gr	Institute of Electronic Structure and Laser, Foundation for Research and Technology-Hellas (IESL-FORTH)	Greece
Nito	Yuta	nitoron_mail@yahoo.co.jp	Hosei University	Japan
Noori	Yasir	y.noori@lancaster.ac.uk	Lancaster University	United Kingdom
Nosich	Alexander I.	anosich@yahoo.com	Laboratory of Micro and Nano-Optics, Institute of Radio-Physics and Electronics NASU	Ukraine
O'Brien	Dominic	dominic.obrien@eng.ox.ac.uk	University of Oxford	United Kingdom
Obayya	Salah	shassan@zewailcity.edu.eg	Zewail City for Science and Technology	Egypt
Ohki	Shintaro	shintaro.oki.m3@stu.hosei.ac.jp	Hosei University	Japan
Olivier	Nicolas	nicolas.olivier@kcl.ac.uk	King's College London	United Kingdom
Ooi	Boon	boon.ooi@kaust.edu.sa	King Abdullah University of Science & Technology	Saudi Arabia
Ozden	Ayberk	ozden.ayberk@gmail.com	Anadolu Universitesi	Turkey
Pacradouni	Vighen	vpacradouni@lumerical.com	Lumerical Solutions, Inc.	Canada
Pan	Chao	p.c.1987@163.com	Southeast University	China
Papasimakis	Nikitas	np3@orc.soton.ac.uk	University of Southampton	United Kingdom
Parini	Alberto	parini.alberto@gmail.com	University of Ferrara	Italy
Paul	Surajit	surajitpaul26@gmail.com	IIT Delhi	India

Last name	First name	Email address	Affiliation	
Payne	Frank	frank.payne@eng.ox.ac.uk	University of Oxford	United Kingdom
Perez-Serrano	Antonio	antonio.perez.serrano@upm.es	CEMDATIC-ETSIT, Universidad Politecnica de Madrid	Spain
Petermann	Klaus	petermann@tu-berlin.de	TU Berlin	Germany
Petrovic	Jovana	jovanap@vinca.rs	VinÄ a Institute of Nuclear Sciences	Serbia
Phang	Sendy	phang.sendy@gmail.com	George Green Institute for Electromagnetics Research	United Kingdom
Pissadakis	Stavros	pissas@iesl.forth.gr	Institute of Electronic Structure and Laser, Foundation for Research and Technology-Hellas (IESL-FORTH)	Greece
Pistora	Jaromir	jaromir.pistora@vsb.cz	Center for Nanotechnologies, Technical University of Ostrava	Czech Republic
Pitilakis	Alexandros	alexpiti@auth.gr	Aristotle University of Thessaloniki	Greece
Poli	Federica	federica.poli@unipr.it	University of Parma	Italy
Pomplun	Jan	jan.pomplun@jcmwave.com	JCMwave GmbH	Germany
Pond	James	jpond@lumerical.com	Lumerical Solutions, Inc.	Canada
Popov	Evgueni	e.popov@fresnel.fr	Institut FRESNEL - Faculte des Sciences de Saint JÃ©rÃ´me	France
Popov	Alexander	popov@purdue.edu	Purdue University	United States
Prabhu	Radhakrishna	r.prabhu@rgu.ac.uk	Robert Gordon University	United Kingdom
Pradhan	Somarpita	somarpita.lbc@phy.iitkgp.ernet.in	Indian Institute of Technology Kharagpur	India
Purkayastha	Amrita	ap21@iitbbs.ac.in	IIT Bhubaneswar	India
Quandt	Alex	alex.quandt@wits.ac.za	University of Witwatersrand	South Africa
Rahman	Azizur	b.m.a.rahman@city.ac.uk	City university London	United Kingdom
Rahman	M. Enayet	enayet.rahman.1@city.ac.uk	City University London	United Kingdom
Rahman	Mohammed Moseeur	mohammed.rahman.5@city.ac.uk	City University London	United Kingdom
Raicevic	Nevena	nevenar@vinca.rs	VinÄ a Institute of Nuclear Sciences	Serbia
Rassem	Nadege	nadege.rassem@fresnel.fr	Institut FRESNEL - Faculte des Sciences de Saint JÃ©rÃ´me	France
Rastogi	Vipul	vipulfph@gmail.com	Indian Institute of Technology Roorkee	India
Raybould	Tim	T.A.Raybould@soton.ac.uk	University of Southampton	United Kingdom
Reid	Adam	areid@lumerical.com	Lumerical Solutions Inc.	Canada
Reitzenstein	Stephan	stephan.reitzenstein@physik.tu-berlin.de	TU Berlin	Germany
Rivolta	Nicolas	nicolas.rivolta@umons.ac.be	UMONS	Belgium
Rodt	Sven	srodt@physik.tu-berlin.de	TU Berlin	Germany
Rosa	Lorenzo	lrosa@ieee.org	University of Parma	Italy
Roy Chaudhuri	Partha	roycp@phy.iitkgp.ernet.in	Indian Institute of Technology Kharagpur	India
Ruini	Alice	alice.ruini@unimore.it	Universita' di Modena e Reggio Emilia	Italy
Schmidt	Frank	frank.schmidt@zib.de	Zuse Institut Berlin	Germany
Schmitz	Guido	Guido.Schmitz@mp.imw.uni-stuttgart.de	University of Stuttgart	Germany

Last name	First name	Email address	Affiliation	
Schuster	Kay	kay.schuster@ipht-jena.de	Institute of Photonic Technology Jena	Germany
Sciamanna	Marc	marc.sciamanna@centralesupelec.fr	CentraleSupelec - LMOPS	France
Segovia	Paulina	paulina.segovia_olvera@kcl.ac.uk	King's College London	United Kingdom
Selleri	Stefano	stefano.selleri@unipr.it	University of Parma	Italy
Senthil Murugan	Ganapathy	smg@orc.soton.ac.uk	Optoelectronics Research Centre, University of Southampton	United Kingdom
Sewell	Phillip	phillip.sewell@nottingham.ac.uk	George Green Institute for Electromagnetics Research	United Kingdom
Shapoval	Olga V.	olga.v.shapoval@gmail.com	Laboratory of Micro and Nano-Optics, Institute of Radio-Physics and Electronics NASU	Ukraine
Sharma	Anurag	asharma@physics.iitd.ac.in	Indian Institute of Technology Delhi	India
Sharma	Dinesh Kumar	dk81.dineshkumar@gmail.com	Indian Institute of Technology Delhi	India
Sharma	Enakshi Khular	enakshi54@yahoo.co.in	UNIVERSITY OF DELHI SOUTH CAMPUS	India
Shi	Hualiang	shi.hualiang@my.cityu.edu.hk	Department of mathematics, City University of Hong Kong	China
Sinatkas	Georgios	gsinatka@auth.gr	Aristotle University of Thessaloniki	Greece
Singh	Satyapratap	satya0pratap@gmail.comsat	IIT Kharagpur	India
Sital	Shivani	shivanisital18@gmail.com	University of Delhi South Campus	India
Somekh	Mike	mike.somekh@polyu.edu.hk	The Hong Kong Polytechnic University	Hong Kong
Soudi	Sasan	Sasan.Soudi.1@city.ac.uk	City University London	United Kingdom
Stamatiadis	Christos	christos.stamatiadis@tu-berlin.de	TU Berlin	Greece
Sun	Xiaohan	xhsun@seu.edu.cn	Southeast University	China
Takada	Takumi	takumi.takada.e3@stu.hosei.ac.jp	Hosei University	Japan
Takagi	Yuhei	yuhei.takagi.t6@stu.hosei.ac.jp	Hosei University	Japan
Themistos	Christos	c.themistos@cytanet.com.cy	Frederick University	Cyprus
Thyagarajan	Krishna	ktrajan@physics.iitd.ac.in	IIT Delhi	India
Tijero	Jose Manuel G.	jm.g.tijero@upm.es	CEMDATIC-ETSIT, Universidad Politecnica de Madrid	Spain
Tripathi	Suarabh Mani	smt@iitk.ac.in	Indian Institute of Technology Kanpur	India
Tsilipakos	Odysseas	otsilipa@auth.gr	Aristotle University of Thessaloniki	Greece
van der Tol	Jos	J.J.G.M.v.d.Tol@tue.nl	COBRA Research Institute - Eindhoven University of Technology	Netherlands
Varshney	Shailendra	skvarshney_10@yahoo.co.uk	IIT Kharagpur	India
Vasconcelos	M. S.	mvasconcelos@ect.ufrn.br	UFRN	Brazil
Vilera	Mariafernanda	mf.vilera@upm.es	CEMDATIC-ETSIT, Universidad Politecnica de Madrid	Spain
Viphavakit	Charusluk	charusluk.v@gmail.com	Frederick University	Cyprus
Virte	Martin	martin.virte@supelec.fr	CentraleSupÃ©lec	France
Vukovic	Ana	ana.vukovic@nottingham.ac.uk	George Green Institute for Electromagnetics Research	United Kingdom

Last name	First name	Email address	Affiliation	
Wang	Zilong	zw1e09@soton.ac.uk	Optoelectronic Research Centre, University of Southampton	United Kingdom
Weicker	Lionel	lionel.weicker@centralesupelec.fr	CentraleSupÃ©lec	France
Wiemhofer	Hans-Dieter	hdw@uni-muenster.de	University of Munster	Germany
Wiersma	Noemi	noemi.wiersma@centralesupelec.fr	CentraleSupelec - LMOPS	France
Wilkinson	James	jsw@soton.ac.uk	Optoelectronic Research Centre, University of Southampton	United Kingdom
Willatzen	Morten	morwi@fotonik.dtu.dk	Technical University of Denmark	Denmark
Wohlfeil	Benjamin	wohlfeil@zib.de	Zuse Institut Berlin	Germany
Wolfersberger	Delphine	delphine.wolfersberger@centralesupelec.fr	CentraleSupelec - LMOPS	France
Wright	Amanda J.	Amanda.Wright@nottingham.ac.uk	University of Nottingham	United Kingdom
Wurtz	Gregory A.	g.wurtz@kcl.ac.uk	King's College London	United Kingdom
Yamauchi	Junji	j.yma@hosei.ac.jp	Hosei University	Japan
Youngs	Ian	ijyoungs@mail.dstl.gov.uk	DSTL	United Kingdom
Zayats	Anatoly	a.zayats@kcl.ac.uk	King's College London	United Kingdom
Zervas	Michalis	mnz@soton.ac.uk	Optoelectronic Research Centre, University of Southampton	United Kingdom
Zheludev	Nikolay	niz@orc.soton.ac.uk	University of Southampton	United Kingdom
Zimmermann	Lars	lzimmermann@ihp-microelectronics.com	IHP GmbH	Germany
Zinenko	Tatiana L.	tzinenko@yahoo.com	IRE NASU	Ukraine
Zolotariov	Denis	vm@kture.kharkov.ua	Kharkov National University of Radio Electronics	Ukraine

Imaging and Spectroscopy Reimagined!

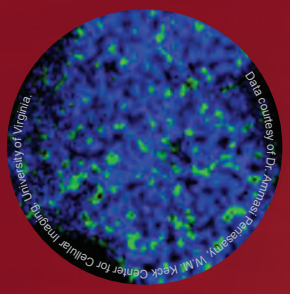

Microspectroscopy • Biomedical Imaging
Plasmonics • LIBS • Raman Hyperspectral Imaging
Carbon Nanotube Research • Singlet Oxygen
Detection Combustion • FLIM
• Small Animal Imaging
• Quantum Imaging

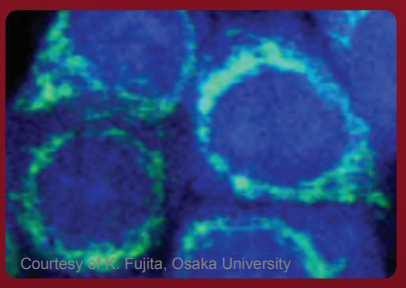

Princeton Instruments

Learn how our innovative products can facilitate your research.
Visit **www.princetoninstruments.com**
or call **+1 609-587-9797**

CST STUDIO SUITE 2015

From Components to Systems. Simulate, Optimize, Synthesize.

From the first steps to the finishing touches, CST STUDIO SUITE® is there for you in your design process. Its tools allow engineers to develop and simulate devices large and small across the frequency spectrum. The powerful solvers in CST STUDIO SUITE 2015 are supplemented by a range of new synthesis and optimization tools, which are integrated directly into the simulation workflow. These can suggest potential starting points for component design, allow these components to be combined into systems, and finally analyze and fine-tune the complete systems.
Even the most complex systems are built up from simple elements. Integrate synthesis into your design process and develop your ideas.

Choose CST STUDIO SUITE – Complete Technology for EM Simulation.

ACKNOWLEDGEMENTS

The organizers thank the following sponsors for their support:

- City University London for funding and use of facilities
- City University Graduate School for funding
- Princeton Instruments for funding
- CST Microwave for funding
- Lumerical for funding and conducting simulation workshop
- Institute of Physics Computational Physics Group for funding
- Institute of Physics Optical Group for funding
- Institute of Physics Quantum Electronics and Photonics Group for funding
- Light Tec for funding
- Fraunhofer UK for funding
- COMSOL for funding
- Huawei for funding
- Optical Society of America for support of student prizes and welcome reception
- Wiley for support of student prizes

Our partners

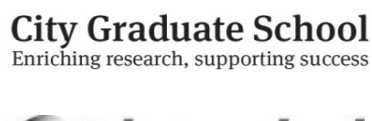

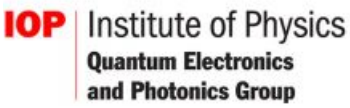

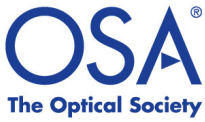

ISBN 978-1-903957-04-2